# Phytochemical and Antimicrobial Studies on Selected Medicinal Plants from The Iraqi Flora: *Citrus grandis*, *Citrus sinensis and Ruta chalepensis*

Shaymaa Hatem Abdullah Al-Majmaie

A Thesis Submitted in Partial Fulfilment of the Requirements of Liverpool John Moores University for the Degree of Doctor of Philosophy

October 2019

# *Dedicated To*

*My greatest mother, the reason of what I have become today.*

*Thanks for your great support and continuous care.*

*My husband, Mohammed, who supports me to achieve my dream. Thank you for your love, wisdom and timeless support.*

*My children, Retaj, Ahmed and Sarah, for your understanding and patience. I love you to the moon and back.*

"NEVER GIVE UP"

# Acknowledgements

First and foremost, praises and thanks to Allah, the Almighty, who enabled me to complete this research work successfully, especially on my difficult days in Liverpool.

This work would not have been possible without the financial support of Iraqi government (Ministry of Higher Education and Scientific Research and Diyala University).

I would like to express my deep and sincere gratitude to my supervisory team, Professor Satyajit D. Sarker, Dr Lutfun Nahar and Professor George P. Sharples for their valuable contributions to the successful implementation of this work. Their patience, motivation, enthusiasm, strong support and immense knowledge throughout the research are greatly appreciated. It was a great privilege and honour to work under their guidance. I am extremely grateful for giving me the opportunity to work with you.

Special thanks to Dr Fyaz Ismail, Dr Mukhlesur Rahman and Dr Sushmita Nath for their encouragements, valuable advice, assistance with the NMR and MS analysis and proofreading.

I am grateful to Dr Khazal Wadi for identification of all the plant species.

I am extending my thanks to Dr Kenneth Ritchie for encouragement, insightful comments and ordering all the research materials.

My sincere thanks to the National Mass Facility Centre (Swansea, UK) and to Dr Nicola Dempster for recording the mass spectra.

I would like to express my deep and sincere gratitude to the staff of the School of Pharmacy and Biomolecular Sciences, particularly, Dr Daniel Graham, Dr Glyn Hobbs, Dr Ismini Nakouti, Dr Jerry Bird and Mr Robert Allen for their technical support during my research work and I am grateful to Dr Omer Hamdi (visitor postdoc) for his precious advice. I am extending my heartfelt thanks to Mrs Angela Lewis for her support and help since my arrival at LJMU.

Dr Afaf Al Gerushi, I gained so much knowledge and experience from you. I will never forget that. Thank you very much for being with me all the time.

I would also like to thank all my colleagues of the Centre for Natural Products Discovery for making an extraordinary workplace in which I was delighted to work everyday. Wish you all the best!

I must express my gratitude to my friends Ms Hiba Jasim, Dr Samar H Thiab, Ms Ruba Bnyan, Ms Hend Abdelrady, Ms Ruqayah Al Ani, Dr Raged Alshabandar and Mrs Ruqaya Sanin for continued support and encouragement especially in my lonely times in Liverpool.

I am extremely grateful to my family my sisters, my aunties and my uncle for their love, prayers, caring my children during my absence. Thanks for being the shoulder I can always depend on.

This thesis is the result of my efforts and sacrifices, as well as from those who love me sincerely.

# Abstract

This study was founded on traditional medicinal information and local traditional uses of three Iraqi medicinal plants from the Rutaceae family, namely, *Citrus grandis* (leaves), *Citrus sinensis* (leaves and peel) and *Ruta chalepensis* (fruits, leaves, stems and roots). A bioassay-guided approach was adopted to study the phytochemicals and antimicrobial activity of these plants. The *n*-hexane, DCM and MeOH extracts of all plants and plant parts, obtained from successive Soxhlet extraction, were assessed for their antimicrobial proprieties using the microtitre resazurin assay involving two Gram-positive bacterial strains, *Micrococcus luteus* and *Staphylococcus aureus*, two Gram-negative strains, *Escherichia coli* and *Pseudomonas aeruginosa* and one fungal strain, *Candida albicans*. The DCM extracts of *C. grandis* (leaves) and *C. sinensis* (leaves) showed notable antimicrobial activity against the microbes used in this study with different MIC values. Both DCM and MeOH extracts of *C. sinensis* (peel) also revealed significant activity. All *R. chalepensis* extracts exhibited antimicrobial activity except for the root extract, which did not show any antimicrobial activity with the maximum concentration of 10 mg/mL. Thirty three compounds including two novel ones, mainly coumarins and flavonoids, were isolated from the active extracts/fractions using a combination of thin layer chromatography (TLC), solid-phase extraction and reversed-phase high-performance liquid chromatography (HPLC). 1D and 2D nuclear magnetic resonance (NMR) and mass spectrometric techniques were employed to identify and confirm the structures of the isolated compounds. Twenty of 33 isolated compounds were evaluated for their anti-MRSA activity against five methicillin-resistant *Staphylococcus aureus* strains (SA1199B, XU212, MRSA340702, EMRSA-15MRSA274819) and the standard strain (ATCC25923). The mechanism of action of six compounds were investigated by scanning electronic microscopic (SEM) method to detect any morphological changes or damage caused by the tested compounds.

This study generated the first phytochemical and antimicrobial report of *R. chalepensis* fruits and Iraqi *C. grandis* leaves. To study the mechanism of action of compounds selected from the resazurin assay, a SEM protocol was developed.

| **Table of contents** | | **page** |
|---|---|---|
| Dedication | | I |
| Acknowledgements | | II |
| Abstract | | III |
| Table of contents | | IV |
| List of abbreviations | | IX |
| List of figures | | XII |
| List of tables | | XVII |
| **Chapter 1** | **Introduction** | **1** |
| 1.1 | Microbial resistance to antibiotics | 1 |
| 1.2 | Traditional uses of medicinal plants to treat infections | 2 |
| 1.3 | Iraqi plants to treat infections | 4 |
| 1.4 | Natural products as antimicrobial agents | 5 |
| 1.4.1 | Plants | 7 |
| 1.4.2 | Microorganism | 9 |
| 1.4.3 | Marine sources | 12 |
| 1.5 | Mechanism of action of antimicrobial natural products | 13 |
| 1.6 | Methods for *in vitro* evaluation of antimicrobial activity | 14 |
| 1.6.1 | Diffusion method | 14 |
| 1.6.2 | Dilution method | 15 |
| 1.7 | Plants used in this study | 17 |
| 1.7.1 | The genus *Ruta* | 19 |
| 1.7.1.1 | *Ruta chalepensis* L. | 19 |
| 1.7.2 | The genus *Citrus* L. | 27 |
| 1.7.2.1 | *Citrus sinensis* L. | 30 |
| 1.7.2.2 | *Citrus grandis* Merr. | 34 |
| 1.8 | Aims and objectives | 38 |
| **Chapter 2** | **Materials and methods** | **39** |
| 2.1 | Plant materials | 39 |
| 2.2 | Materials and reagents for phytochemical studies | 40 |
| 2.3 | Phytochemical work | 41 |
| 2.3.1 | Plant preparation | 41 |
| 2.3.2 | Soxhlet extraction | 41 |
| 2.3.3 | Chromatographic techniques | 42 |
| 2.3.3.1 | Vacuum liquid chromatography (VLC) | 42 |
| 2.3.3.2 | Solid-phase extraction (SPE) | 43 |
| 2.3.3.3 | Thin layer chromatography (TLC) | 44 |

| | | |
|---|---|---|
| 2.3.3.4 | High performance liquid chromatography (HPLC) | 46 |
| 2.3.3 | Isolation of compounds | 49 |
| 2.3.3.1 | Isolation of compounds from *R. chalepensis* fruits | 49 |
| 2.3.3.2 | Isolation of compounds from *R. chalepensis* leaves | 49 |
| 2.3.3.3 | Isolation of compounds from *R. chalepensis* stem | 49 |
| 2.3.3.4 | Isolation of compounds from *C. grandis* leaves | 52 |
| 2.3.3.5 | Isolation of compounds from *C. sinensis* leaves | 52 |
| 2.3.3.6 | Isolation of compounds from *C. sinensis* peels | 53 |
| 2.4 | Identification and characterisation of isolated compounds | 54 |
| 2.4.1 | Nuclear Magnetic Resonance (NMR) spectroscopy | 54 |
| 2.4.1.1 | Proton ($^{1}$H) NMR spectroscopy | 54 |
| 2.4.1.2 | Carbon ($^{13}$C) NMR spectroscopy | 55 |
| 2.4.1.3 | Distortionless Enhancement by Polarisation Transfer (DEPT-135) | 55 |
| 2.4.1.4 | Homonuclear Correlation Spectroscopy (COSY) | 55 |
| 2.4.1.5 | Heteronuclear Single Quantum Coherence Spectroscopy (HSQC) | 56 |
| 2.4.1.6 | Heteronuclear Multiple Bond Correlation (HMBC) | 56 |
| 2.4.2 | Mass spectroscopy (MS) | 63 |
| 2.5 | Antimicrobial study | 63 |
| 2.5.1 | Disk diffusion method | 64 |
| 2.5.2 | Resazurin assay | 64 |
| 2.5.2.1 | Preparation of standard microbial colonies | 64 |
| 2.5.2.2 | Preparation of resazurin solution | 66 |
| 2.5.2.3 | Preparation of tested materials | 66 |
| 2.5.2.4 | Preparation of 96 well plate | 66 |
| 2.5.2.5 | Result interpretation | 66 |
| 2.6 | Determination of bacteriostatic or bactericidal property | 67 |
| **Chapter 3** | **Result and discussion** | **68** |
| 3.1 | *Ruta chalepensis* L. | 68 |
| 3.1.1 | Extraction | 68 |
| 3.1.2 | Preliminary analytical TLC screening | 68 |
| 3.1.3 | Analytical HPLC screening of the MeOH extracts of *R. chalepensis* | 69 |
| 3.1.4 | The antimicrobial screening of extracts of various parts of *R. chalepensis* | 96 |
| 3.1.5 | Chromatographic fractionation of the extracts | 71 |
| 3.1.5.1 | Vacuum liquid chromatography fractionation (VLC) | 71 |
| 3.1.5.2 | Solid-phase extractions (SPE) | 72 |
| 3.1.6 | Screening of *R. chalepensis* fractions for antimicrobial activity | 75 |

| | | |
|---|---|---|
| 3.1.7 | Phytochemistry of *Ruta chalepensis* | 79 |
| 3.1.8 | Isolation compounds from active fractions of *Ruta chalepensis* | 80 |
| 3.1.8.1 | *R. chalepensis* fruit n-hexane fraction 4 | 80 |
| 3.1.8.2 | *R. chalepensis* fruit DCM fraction 7 | 83 |
| 3.1.8.3 | *R. chalepensis* fruit MeOH fraction 2 | 83 |
| 3.1.8.4 | *R. chalepensis* fruit MeOH fraction 3 | 84 |
| 3.1.8.5 | *R. chalepensis* leaves DCM fraction 7 | 85 |
| 3.1.8.6 | *R. chalepensis* leaves MeOH fraction 2 | 85 |
| 3.1.8.7 | *R. chalepensis* leaves MeOH fraction 3 | 87 |
| 3.1.8.8 | *R. chalepensis* stem MeOH fraction 2 | 88 |
| 3.1.8.9 | *R. chalepensis* stem MeOH fraction 3 | 88 |
| 3.1.9 | Characterisation and structure elucidation of isolated compounds | 89 |
| 3.1.9.1 | Structure elucidation of kokusaginine (**99**) | 89 |
| 3.1.9.2 | Structure elucidation of isokokusaginine (**100**) | 91 |
| 3.1.9.3 | Structure elucidation of γ-fagarine (**42**) | 94 |
| 3.1.9.4 | Structure elucidation of skimmianine (**41**) | 97 |
| 3.1.9.5 | Structure elucidation of bergapten (**43**) | 100 |
| 3.1.9.6 | Structure elucidation of isopimpinellin (**44**) | 102 |
| 3.1.9.7 | Structure elucidation of chalepin (**45**) | 104 |
| 3.1.9.8 | Structure elucidation of rutamarin (**47**) | 105 |
| 3.1.9.9 | Structure elucidation of chalepensin (**46**) | 107 |
| 3.1.9.10 | Structure elucidation of imperatorin (**104**) | 111 |
| 3.1.9.11 | Structure elucidation of arborinine (**107**) | 113 |
| 3.1.9.12 | Structure elucidation of ribalinium (**106**) | 117 |
| 3.1.9.13 | Structure elucidation of compound 3′,6-disinapoylsucrose (**108**) | 119 |
| 3.1.9.14 | Structure elucidation of graveoline (**105**) | 120 |
| 3.1.9.15 | Structure elucidation of rutin (**48**) | 122 |
| 3.1.9.16 | Structure elucidation of rutin-3′-methyl ether (**101**) | 124 |
| 3.1.9.17 | Structure elucidation of rutin-7,4′-dimethyl ether (**102**) | 125 |
| 3.1.9.18 | Structure elucidation of 6-hydroxy-rutin 3′-7-dimethyl ether (**103**) | 126 |
| 3.1.9.19 | Structure elucidation of hexadecane (**109**) | 129 |
| 3.1.10 | Antimicrobial activity of the isolated compounds from *R. chalepensis* | 132 |
| 3.1.11 | Discussion | 133 |
| 3.2 | The *Citrus* | 136 |
| 3.2.1 | Extraction | 137 |
| 3.2.2 | Preliminary analytical TLC screening | 137 |

| | | |
|---|---|---|
| 3.2.3 | Analytical HPLC screening for methanolic extracts | 137 |
| 3.2.4 | The antimicrobial screening for *Citrus sinensis* and *Citrus grandis* | 139 |
| 3.2.5 | Chromatographic fractionation of the extracts | 140 |
| 3.2.5.1 | Vacuum liquid chromatography fractionation (VLC). | 140 |
| 3.2.5.2 | Solid-phase extraction (SPE) | 140 |
| 3.2.6 | Screening of *Citrus* fractions for antimicrobial activity | 140 |
| 3.2.7 | Phytochemistry of *Citrus* species | 143 |
| 3.2.8 | Isolation compounds from active fractions of *Citrus* | 144 |
| 3.2.8.1 | *Citrus grandis* leaves DCM extract fraction 7 | 144 |
| 3.2.8.2 | *Citrus sinensis* leaves DCM extract fraction 7 | 145 |
| 3.2.8.3 | *Citrus sinensis* peels DCM extract fraction 6 | 145 |
| 3.2.8.4 | *Citrus sinensis* peels DCM extract fraction 7 | 147 |
| 3.2.8.5 | *Citrus sinensis* peel MeOH extract fraction 2 | 147 |
| 3.2.8.6 | *Citrus sinensis* peels MeOH extract fraction 3 | 147 |
| 3.2.9 | Characterisation and structure elucidation of isolated compounds | 148 |
| 3.2.9.1 | Structure elucidation of 3-methoxynobiletin (**110**) | 148 |
| 3.2.9.2 | Structure elucidation of nobiletin (**57**) | 150 |
| 3.2.9.3 | Structure elucidation of sinensetin (**111**) | 155 |
| 3.2.9.4 | Structure elucidation of 6, 7, 8, 3′,4′-pentamethoxyflavone (**112**) | 155 |
| 3.2.9.5 | Structure elucidation of demethylnobiletin (**113**) | 159 |
| 3.2.9.6 | Structure elucidation of 5-desmethylsinensetin (**114**) | 161 |
| 3.2.9.7 | Structure elucidation of cirsilineol (**115**) | 163 |
| 3.2.9.8 | Structure elucidation of tangeritin (**116**) | 166 |
| 3.2.9.9 | Structure elucidation of tetramethylscutellarein (**117**) | 168 |
| 3.2.9.10 | Structure elucidation of salvigenin (**118**) | 173 |
| 3.2.9.11 | Structure elucidation of hesperidin (**50**) | 174 |
| 3.2.9.12 | Structure elucidation of compound narirutin (**51**) | 176 |
| 3.2.9.13 | Structure elucidation of compound (**119**) | 178 |
| 3.2.10 | Antimicrobial activity of the isolated compounds from *Citrus* species | 182 |
| 3.2.11 | Discussion | 184 |
| **Chapter 4** | **The anti-MRSA activity of isolated compounds** | **187** |
| 4.1 | Methicillin-resistant *Staphylococcus aureus* (MRSA) | 187 |
| 4.2 | Types of MRSA | 189 |
| 4.2.1 | Community-associated MRSA (CA-MRSA) | 190 |
| 4.2.2 | Healthcare-associated MRSA (HA-MRSA) | 190 |
| 4.3 | Treatment of MRSA infections | 190 |
| 4.4 | Natural products with potent anti-MRSA activity | 190 |

| | | |
|---|---|---|
| 4.5 | Materials and methods | 191 |
| 4.5.1 | Tested materials | 191 |
| 4.5.2 | Resistant strains of *Staphylococcus aureus* | 192 |
| 4.5.3 | Materials used for the MRSA assay | 192 |
| 4.5.4 | The anti-MRSA assay | 192 |
| 4.6 | Results and discussion | 194 |
| **Chapter 5** | **Scanning electron microscopic analysis** | **197** |
| 5.1 | What is scanning electron microscope (SEM) | 197 |
| 5.2 | Applications of scanning electron microscope | 197 |
| 5.2.1 | Industrial uses | 197 |
| 5.2.2 | Commercial | 198 |
| 5.2.3 | Research | 198 |
| 5.3 | The use of the scanning electron microscopy (SEM) in microbiology | 198 |
| 5.4 | Materials and methods | 199 |
| 5.5 | Result and discussion | 199 |
| 5.6 | Conclusion | 205 |
| **Chapter 6** | **Conclusion and recommendations** | **206** |
| Refrencess | | 209 |
| Appendix 1 | The numbers and names of the isolated compounds from *Ruta chalepensis* and *Citrus species* | 245 |
| Appendix 2 | HMBC for compounds **47** | 246 |
| Appendix 3 | HMBC for compound **106** | 247 |
| Appendix 4 | HMBC for compound **105** | 248 |
| Appendix 5 | $^{13}$C NMR for compound **48** | 249 |
| Appendix 6 | HMBC for compound **101** | 250 |
| Appendix 7 | List of presentations | 251 |
| Appendic 8 | List of papers during the PhD project | 252 |

## List of abbreviations

| | |
|---|---|
| δ | Chemical shift (ppm) |
| $^{1}$H-NMR | Proton nuclear magnetic resonance |
| $^{13}$C-NMR | Carbon nuclear magnetic resonance |
| 1D | One dimensional |
| 2D | Two dimensional |
| ACN | Acetonitrile |
| ATCC | American Type Cell Culture Collection |
| BC | Before Christ |
| $CD_3OD$ | Methanol deutered |
| $CDCl_3$ | Deuterated chloroform |
| cfu | Colony-forming unit |
| cm | Centimeter |
| COSY | Correlation spectroscopy |
| d | Doublet |
| DCM | Dichloromethane |
| DEPT | Distortionless Enhancement by Polarisation Transfer |
| DMSO | Dimethyl sulfoxide |
| DMSO-$d_6$ | Deuterated dimethyl sulfoxide |
| EtOAc | Ethyl acetate |
| FDA | Food and Drug Administration |
| g | Gram |
| h | Hour |
| HRESIMS | High-resolution electrospray ionisation mass spectrometry |
| HMBC | Heteronuclear multiple bond coherence |
| HPLC | High performance liquid chromatography |
| HSQC | Heteronuclear single quantum coherence |
| Hz | Hertz |
| $IC_{50}$ | Concentration needed to produce 50% of cells inhibition |

| | |
|---|---|
| ICU | Intenstive care unit |
| *J* | Coupling constant |
| km | Kilometre |
| m | Multiplet (for NMR spectrum) |
| *m/z* | Mass to charge ratio |
| MeOH | Methanol |
| mg | Milligram |
| MHz | Mega hertz |
| MIC | Minimum inhibitory concentration |
| min | Minute |
| mL | Milliliter |
| µL | Microliter |
| MS | Mass spectroscopy |
| MRSA | multidrug-resistant *Staphylococcus aureus* |
| MSSA | methicillin-susceptible *Staphylococcus aureus* |
| MHB | Mueller-Hinton broth |
| MTT | 3-( 4,5-dimethyithiazo-2-yl)-2,5-diphenyltetrazolium |
| N/A | No activity |
| NCTC | National Collection types of Culture |
| NMR | Nuclear magnetic resonance |
| ppm | Parts per million |
| prep-HPLC | Preparative high performance liquid chromatography |
| $R_f$ | Retention factor |
| PTLC | Preparative thin layer chromatography |
| s | Singlet |
| SEM | Scanning electron microscope |
| Semi prep-HPLC | Semi preparative high performance liquid chromatography |
| SPE | Solid phase extraction |
| t | Triplet |
| $t_R$ | Retention time |

| | |
|---|---|
| TFA | Trifluoro acetic acid |
| TLC | Thin layer chromatography |
| μg | Microgram |
| μL | Microliter |
| μm | Micromole |
| UV | Ultraviolet |
| UV-DAD | Ultraviolet-diode array detector |
| VLC | Vacuum liquid chromatography |

**List of Figures**:


| No. | Legends | Pages |
|---|---|---|
| 1.1 | New approved drugs (1981-2014) derived from natural products | 6 |
| 1.2 | Structure of Compounds **1**-**8** | 7 |
| 1.3 | Structure of compounds from **9**-**20** | 8 |
| 1.4 | Structures of compounds from **21**-**36** | 10 |
| 1.5 | Structures of compounds **37**-**39** | 14 |
| 1.6 | Disc diffusion method | 16 |
| 1.7 | Dilution method | 16 |
| 1.8 | *Ruta chalepensis* | 19 |
| 1.9 | Structures of compounds **40**-**48** | 23 |
| 1.10 | Structures of compounds **49**-**70** | 28 |
| 1.11 | Structures of compounds **71**-**82** | 32 |
| 1.12 | Structures of compounds **83**-**98** | 35 |
| 2.1 | Iraqi political map | 39 |
| 2.2 | Soxhlet apparatus | 42 |
| 2.3 | Vacuum liquid chromatography (VLC) | 43 |
| 2.4 | Solid-phase extraction (SPE) | 44 |
| 2.5 | Proton ($^{1}$H) NMR experiment | 57 |
| 2.6 | Carbon ($^{13}$C) NMR experiment | 58 |
| 2.7 | DEPT $^{135}$ NMR experiment | 59 |
| 2.8 | COSY NMR experiment | 60 |
| 2.9 | HSQC NMR experiment | 61 |
| 2.10 | HMBC NMR experiment | 62 |
| 3.1 | The TLC plates for *R. chalepensis* extracts | 69 |
| 3.2 | Analytical HPLC results for *R. chalepensis* | 70 |
| 3.3 | TLC analysis of *n*-hexane extracts of *R. chalepensis* | 73 |
| 3.4 | TLC analysis of the DCM extracts of *R. chalepensis* | 73 |
| 3.5 | Isolated compounds from *R. chalepensis* | 79 |
| 3.6 | Analytical TLC (using method **E**) of the VLC fraction 4 of the *n*-hexane extract of *R. chalepensis* fruits | 80 |
| 3.7 | Analytical TLC (using method **I**) of the VLC fractions of *R. chalepensis* fruit fraction 4 | 81 |
| 3.8 | Preparative TLC (using method **K**) of *R. chalepensis* fruit fraction 11 derived from fraction 4 | 81 |
| 3.9 | Preparative-HPLC chromatogram of isolated compounds from *R. chalepensis* fruit DCM extract fraction 7, using method **M** | 83 |
| 3.10 | Preparative-HPLC chromatogram of isolated compounds from *R. chalepensis* fruit MeOH extract fraction 2 using method **L** | 84 |
| 3.11 | Preparative-HPLC chromatogram of isolated compounds from *R. chalepensis* fruit MeOH extract fraction 3, using method **L** | 84 |
| 3.12 | Preparative-HPLC chromatogram of isolated compounds from *R. chalepensis* leaves DCM extract fraction 7, using method **O** | 85 |
| 3.13 | Preparative-HPLC chromatogram of isolated compounds from *R.chalepensis* leaves MeOH extract fractions 2, using method **L** | 86 |

| | | |
|---|---|---|
| 3.14 | Semi-preparative-HPLC chromatogram of purification compounds from RLF2-5, using method **U** | 86 |
| 3.15 | Semi-preparative- HPLC chromatogram of purification compounds from RLF2-7, using method **P** | 87 |
| 3.16 | Preparative-HPLC chromatogram of isolated compounds of *R. chalepensis* leaves MeOH extract fraction 3, using method **L** | 88 |
| 3.17 | Semi -preparative-HPLC Chromatogram of isolated compounds of *R. chalepensis* stem MeOH extract fraction 2, using method **L** | 88 |
| 3.18 | Preparative-HPLC chromatogram of isolated compounds from *R. chalepensis* stem MeOH extract fraction 3, using method **L** | 89 |
| 3.19 | The HRESIMS spectrum of compound **99** | 90 |
| 3.20 | The $^{1}$H NMR (600 MHz, $CDCl_3$) spectrum of compound **99** | 90 |
| 3.21 | The $^{13}$C NMR (150 MHz, $CDCl_3$) spectrum of compound **99** | 91 |
| 3.22 | The HMBC correlations of compound **99** | 91 |
| 3.23 | The HRESIMS spectrum of compound **100** | 92 |
| 3.24 | The $^{1}$H NMR (600 MHz, $CD_3OD$) spectrum of compound **100** | 93 |
| 3.25 | The DEPT NMR (150 MHz, $CD_3OD$) spectrum of compound **100** | 96 |
| 3.26 | The HMBC correlations of compound **100** | 93 |
| 3.27 | The HRESIMS spectrum of compound **42** | 95 |
| 3.28 | $^{1}$H NMR (600 MHz, $CDCl_3$) spectrum of compound **42** | 95 |
| 3.29 | DEPT NMR (150 MHz, $CDCl_3$) spectrum of compound **42** | 96 |
| 3.30 | COSY NMR spectrum of compound **42** | 96 |
| 3.31 | The HMBC correlations of compound **42** | 97 |
| 3.32 | The HRESIMS spectrum of compound **41** | 98 |
| 3.33 | $^{1}$H NMR (600 MHz, $CD_3OD$) spectrum of compound **41** | 98 |
| 3.34 | The $^{13}$C NMR (150 MHz, $CD_3OD$) spectrum of compound **41** | 98 |
| 3.35 | The HRESIMS spectrum of compound **43** | 101 |
| 3.36 | $^{1}$H NMR (600 MHz, $CDCl_3$) spectrum of compound **43** | 101 |
| 3.37 | The $^{13}$C NMR (150 MHz, $CDCl_3$) spectrum of compound **43** | 101 |
| 3.38 | The HMBC correlations of compound **43** | 102 |
| 3.39 | The HRESIMS spectrum of compound **44** | 103 |
| 3.40 | $^{1}$H NMR (600 MHz, $CD_3OD$) spectrum of compound **44** | 103 |
| 3.41 | DEPT NMR (150 MHz, $CD_3OD$) spectrum of compound **44** | 104 |
| 3.42 | The HRESIMS spectrum of compound **45** | 105 |
| 3.43 | $^{1}$H NMR (600 MHz, $CDCl_3$) spectrum of compound **45** | 105 |
| 3.44 | The HRESIMS spectrum of compound **47** | 106 |
| 3.45 | $^{1}$H NMR (600 MHz, $CDCl_3$) spectrum of compound **47** | 107 |
| 3.46 | The HRESIMS spectrum of compound **46** | 108 |
| 3.47 | $^{1}$H NMR (600 MHz, $CDCl_3$) spectrum of compound **46** | 108 |
| 3.48 | The HRESIMS spectrum of compound **104** | 112 |
| 3.49 | $^{1}$H NMR (600 MHz, $CD_3OD$) spectrum of compound **104** | 112 |
| 3.50 | DEPT NMR (150 MHz, $CD_3OD$) spectrum of compound **104** | 112 |
| 3.51 | The HMBC correlations of compound **104** | 113 |
| 3.52 | The HRESIMS spectrum of compound **107** | 115 |
| 3.53 | $^{1}$H NMR (600 MHz, $CHCl_3$) spectrum of compound **107** | 115 |
| 3.54 | $^{13}$C NMR (150 MHz, $CHCl_3$) spectrum of compound **107** | 116 |

| | | |
|---|---|---|
| 3.55 | The HMBC correlations of compound **107** | 116 |
| 3.56 | $^{1}$H NMR (600 MHz, $CDCl_3$) spectrum of compound **106** | 118 |
| 3.57 | $^{13}$C NMR (150 MHz, $CHCl_3$) spectrum of compound **106** | 118 |
| 3.58 | Compound 3',6-disinapoylsucrose (**108**) with numbering atoms | 119 |
| 3.59 | $^{1}$H NMR (600 MHz, $CDCl_3$) spectrum of compound **108** | 120 |
| 3.60 | $^{13}$C NMR (150 MHz, $CDCl_3$) spectrum of compound **108** | 120 |
| 3.61 | The HRESIMS spectrum of compound **105** | 121 |
| 3.62 | $^{1}$H NMR (300 MHz, $CDCl_3$) spectrum of compound **107** | 122 |
| 3.63 | $^{13}$CNMR (75 MHz, $CDCl_3$) spectrum of compound **107** | 122 |
| 3.64 | The HRSEIMS spectrum of compound **48** | 124 |
| 3.65 | $^{1}$H NMR (600 MHz, $CD_3OD$) spectrum of compound **48** | 124 |
| 3.66 | The HRESIMS of spectrum compound **101** | 125 |
| 3.67 | $^{1}$H NMR (150 MHz, $CD_3OD$) spectrum of compound **101** | 125 |
| 3.68 | $^{1}$H NMR (300 MHz, $CDCl_3$) of compound **102** | 126 |
| 3.69 | The HRESIMS of compound **103** | 127 |
| 3.70 | $^{1}$H NMR (600 MHz, $CD_3OD$) of compound **103** | 128 |
| 3.71 | $^{13}$C NMR (150 MHz, $CD_3OD$) of compound **103** | 128 |
| 3.72 | The HMBC correlations of compound **103** | 128 |
| 3.73 | The HRESIMS of compound **109** | 131 |
| 3.74 | $^{1}$H NMR (300 MHz, $CDCl_3$) spectrum of compound **109** | 131 |
| 3.75 | $^{13}$C NMR (75 MHz, $CD_3OD$) spectrum of compound **109** | 132 |
| 3.76 | The TLC plates for *Citrus* extracts | 138 |
| 3.77 | Analytical HPLC chromatogram for MeOH extract of *C. sinensis* leaves | 138 |
| 3.78 | Analytical HPLC chromatogram for MeOH extract of *C. sinensis* peel | 138 |
| 3.79 | Analytical HPLC chromatogram for MeOH extract of *C. grandis* | 138 |
| 3.80 | The analysis TLC for *Citrus* DCM fractions | 141 |
| 3.81 | Isolated compounds from *Citrus* | 144 |
| 3.82 | Preparative-HPLC chromatogram of isolated compounds from *Citrus grandis* leaves DCM extract fraction 7, using method **T** | 145 |
| 3.83 | Preparative-HPLC chromatogram of isolated compounds from *Citrus sinensis* leaves DCM extract fraction 7, using method **N** | 145 |
| 3.84 | Preparative-HPLC chromatogram of isolated compounds from *Citrus sinensis* peel DCM extract fraction 6, using method **S** | 146 |
| 3.85 | Preparative-HPLC chromatogram of isolated compounds from *Citrus sinensis* peel DCM extract fraction 7, using method **T** | 146 |
| 3.86 | Preparative-HPLC chromatogram of isolated compounds from *Citrus sinensis* peel MeOH extract fraction 2, using method **R** | 147 |
| 3.87 | Preparative-HPLC chromatogram of isolated compounds from *Citrus sinensis* peel MeOH extract fraction 3, using method **R** | 147 |
| 3.88 | The HRESIMS spectrum of compound **110** | 149 |
| 3.89 | $^{1}$H NMR (600 MHz, $CDCl_3$) spectrum of compound **110** | 149 |
| 3.90 | $^{13}$C NMR (150 MHz, $CDCl_3$) spectrum of compound **110** | 150 |
| 3.91 | The HMBC correlation of compound **110** | 151 |
| 3.92 | The HRESIMS spectrum of compound **57** | 151 |

| | | |
|---|---|---|
| 3.93 | $^{1}$H NMR (600 MHz, $CDCl_3$) spectrum of compound **57** | 152 |
| 3.94 | $^{13}$C NMR (150 MHz, $CDCl_3$) spectrum of compound **57** | 152 |
| 3.95 | The HMBC correlation compound **57** | 152 |
| 3.96 | The HRESIMS of compound **111** | 154 |
| 3.97 | $^{1}$H NMR (600 MHz, $CDCl_3$) of compound **111** | 154 |
| 3.98 | $^{13}$C NMR (150 MHz, $CDCl_3$) of compound **111** | 155 |
| 3.99 | The HMBC correlation compound **111** | 155 |
| 3.100 | The HRESIMS spectrum of compound **112** | 156 |
| 3.101 | $^{1}$H NMR (600 MHz, $CDCl_3$) spectrum of compound **112** | 157 |
| 3.102 | $^{13}$C NMR (150 MHz, $CDCl_3$) spectrum of compound **112** | 157 |
| 3.103 | The HMBC correlation compound **112** | 157 |
| 3.104 | The HRESIMS spectrum of compound **113** | 160 |
| 3.105 | $^{1}$H NMR (600 MHz, $CDCl_3$) spectrum of compound **113** | 160 |
| 3.106 | $^{13}$C NMR (150 MHz, $CDCl_3$) spectrum of compound **113** | 161 |
| 3.107 | The HRESIMS spectrum of compound **114** | 162 |
| 3.108 | $^{1}$H NMR (600 MHz, $CDCl_3$) spectrum of compound **114** | 162 |
| 3.109 | $^{13}$C NMR (150 MHz, $CDCl_3$) spectrum of compound **114** | 163 |
| 3.110 | The HMBC correlation compound **114** | 163 |
| 3.111 | The HRESIMS spectrum of compound **115** | 164 |
| 3.112 | $^{1}$H NMR (600 MHz, $CDCl_3$) spectrum of compound **115** | 165 |
| 3.113 | $^{13}$C NMR (150 MHz, $CDCl_3$) spectrum of compound **115** | 165 |
| 3.114 | The HMBC correlation compound **115** | 165 |
| 3.115 | The HRESIMS spectrum of compound **116** | 167 |
| 3.116 | $^{1}$H NMR (600 MHz, $CDCl_3$) spectrum of compound **116** | 168 |
| 3.117 | $^{13}$C NMR (150 MHz, $CDCl_3$) spectrum of compound **116** | 168 |
| 3.118 | The HRESIMS spectrum of compound **117** | 169 |
| 3.119 | $^{1}$H NMR (600 MHz, $CDCl_3$) spectrum of compound **117** | 170 |
| 3.120 | $^{13}$C NMR (150 MHz, $CDCl_3$) spectrum of compound **117** | 170 |
| 3.121 | The HMBC correlation compound **117** | 170 |
| 3.122 | The HRESIMS spectrum of compound **118** | 172 |
| 3.123 | $^{1}$H NMR (600 MHz, $CDCl_3$) spectrum of compound **118** | 172 |
| 3.124 | $^{13}$C NMR (150 MHz, $CDCl_3$) spectrum of compound **118** | 173 |
| 3.125 | The HRESIMS spectrum of compound **50** | 175 |
| 3.126 | $^{1}$H NMR (600 MHz, $CDCl_3$) spectrum of compound **50** | 175 |
| 3.127 | $^{13}$C NMR (150 MHz, $CDCl_3$) of compound **50** | 176 |
| 3.128 | $^{1}$H NMR (600 MHz, $CDCl_3$) spectrum of compound **51** | 177 |
| 3.129 | $^{13}$C NMR (150 MHz, $CDCl_3$) spectrum of compound **51** | 177 |
| 3.130 | The HMBC correlation compound **51** | 178 |
| 3.131 | The HRESIMS spectrum of compound **119** | 179 |
| 3.132 | $^{1}$H NMR (600 MHz, $CD_3OD$) spectrum of compound **119** | 180 |
| 3.133 | $^{13}$C NMR (150 MHz, $CD_3OD$) spectrum of compound **119** | 180 |
| 3.134 | HSQC spectra of compound **119** | 181 |
| 3.135 | COSY spectrum of compound **119** | 181 |
| 3.136 | HMBC spectra of compound **119** | 182 |
| 4.1 | Inactivation of Penicillin by β-lactamase enzymes | 187 |
| 4.2 | Structure of methicillin | 188 |

| | | |
|---|---|---|
| 4.3 | Structural similarities and differences in anti-MRSA furanocoumarins **45**-**47** | 194 |
| 4.4 | Structural similarities and differences in anti-MRSA flavonoids **48**, **101** and **103** | 196 |
| 5.1 | Untrated and treated samples of *Candida albicans* | 201 |
| 5.2 | Untrated and treated samples of *Micrococcus luteus* | 201 |
| 5.3 | Untrated and treated samples of *Staphylococcus aureus* | 202 |
| 5.4 | Untrated and treated samples of *Pseudomonas aeruginosa* | 204 |
| 5.5 | Untrated and treated samples of *Escherichia coli* | 204 |

**List of Tables**:


| Table | Titles of the tables | Page |
|---|---|---|
| 1.1 | Worldwide distribution of *Ruta chalepensis* | 21 |
| 1.2 | Compounds identified in essential oils of *R. chalepensis* | 23 |
| 1.3 | Geographical distribution of *Citrus sinensis* | 30 |
| 1.4 | Compounds identified from the essential oils of *Citrus sinensis* | 33 |
| 1.5 | Global distribution of *Citrus grandis* | 34 |
| 1.6 | Compounds identified in essential oils of *Citrus grandis* | 36 |
| 2.1 | Plant used in study | 39 |
| 2.2 | Materials and reagents used in phytochemical work | 40 |
| 2.3 | Methods used in VLC and SPE techniques | 45 |
| 2.4 | Thin layer chromatographic methods | 46 |
| 2.5 | HPLC methods used in the current study | 48 |
| 2.6 | Isolated compounds from *R. chalepensis* fruits | 50 |
| 2.7 | Isolated compounds from *R. chalepensis* leaves | 51 |
| 2.8 | Isolated compounds from *R. chalepensis* stem | 51 |
| 2.9 | Isolated compounds from *C. grandis* | 52 |
| 2.10 | Isolated compounds from *C. sinensis* leaves | 52 |
| 2.11 | Isolated compounds from *C. sinensis* peels | 53 |
| 2.12 | Chemical shifts for deuterated solvents used in this study | 55 |
| 2.13 | Strains, antibiotics, reagents and materials used for antimicrobial activity | 65 |
| 3.1 | Percentage yield of *R. chalepensis* | 68 |
| 3.2 | The MIC values for antibiotics (positive controls) | 70 |
| 3.3 | The minimum inhibitory concentration (MIC) values for crude extracts of *R. chalepensis* | 72 |
| 3.4 | The yields of fractions of the active extracts of various parts of *R. chalepensis* | 74 |
| 3.5 | MIC values (in mg/mL) of *Ruta chalepensis* fruit fractions | 76 |
| 3.6 | MIC values (in mg/mL) of *Ruta chalepensis* leaves fractions | 77 |
| 3.7 | MIC values (in mg/mL) of *Ruta chalepensis* stems fractions | 78 |
| 3.8 | The MIC values of the VLC fractions of *R. chalepensis* fruit fraction 4, and compounds isolated from the active fractions | 82 |
| 3.9 | $^{1}$H NMR (600 MHz) and $^{13}$C NMR data of compounds **41**, **42**, **99**,**100** | 99 |
| 3.10 | $^{1}$H NMR (600 MHz) and $^{13}$C NMR data of compounds **43**-**47** | 109 |
| 3.11 | $^{1}$H NMR (600 MHz) and $^{13}$C NMR data of compound **104** | 113 |
| 3.12 | $^{1}$H NMR (600 MHz) and $^{13}$C NMR data of compound **107** | 116 |
| 3.13 | $^{1}$H NMR (600 MHz) and $^{13}$C NMR data of compound **106** | 118 |
| 3.14 | $^{1}$H NMR (300 MHz) and $^{13}$C NMR data of compound **105** | 123 |
| 3.15 | $^{1}$H NMR data for compounds **48**,**101**-**103** (at 600 MHz in $CD_3OD$, δ in ppm, *J* in Hz) | 129 |
| 3.16 | $^{13}$C NMR data for compounds **48**,**101**-**103** (at 150 MHz in $CD_3OD$) | 130 |
| 3.17 | The MIC for isolated compounds from *R. chalepensis* | 133 |
| 3.18 | Percentage yield of *Citrus* | 137 |
| 3.19 | MIC values (mg/mL) of *Citrus* extracts | 139 |
| 3.20 | The yield of *Citrus* fractions | 141 |

| | | |
|---|---|---|
| 3.21 | The MIC values of DCM fractions for *Citrus* | 142 |
| 3.22 | The MIC (mg/mL) of MeOH extract of *C. sinensis* peels | 143 |
| 3.23 | $^{1}$H NMR (600 MHz) and $^{13}$C NMR data of compounds **57**, **110**, **111**, **112** | 158 |
| 3.24 | $^{1}$H NMR (600 MHz) and $^{13}$C NMR data of compounds **113-115** | 166 |
| 3.25 | $^{1}$H NMR (600 MHz) and $^{13}$C NMR data of compounds **116-118** | 173 |
| 3.26 | $^{1}$H NMR (600 MHz) and $^{13}$C NMR data of compounds **50**, **51**, **119** | 183 |
| 3.27 | The MIC (mg/mL) of isolated compounds from *Citrus* | 184 |
| 4.1 | Materials used in MRSA assay | 192 |
| 4.2 | Anti-MRSA activity of selected compounds isolated in this study | 195 |

# *Chapter 1*
# Introduction

## 1.1. Microbial resistance to antibiotics

Antibiotic resistance is a global problem and is most common in developing countries (Livermore, 2003). According to the World Health Organisation (WHO), every year microbial resistance to antibiotics leads to the deaths of more than 60,000 people worldwide, out of which 77% are children (Moran, 2005).

Microorganisms, particularly bacteria, develop resistance to standard antimicrobial drugs mainly because of clinical, cellular and molecular factors. Instances of misuse, over-prescription of antibiotics have become common practices in developing countries (Burroughs *et al.*, 2003). The unlicensed medicines suppliers, uncontrolled antibiotic sales, and availability of over the counter antibiotics without a prescription, has led to an exponential increase in drug resistance (Ayukekbong *et al.*, 2017). Hospitals are the place of emergence for resistant strains. In the 1930s, military hospitals had reported that *Streptococcus pyogenes* showed resistance to sulphonamide (Levy, 1982). Later in the 1940s, a civilian hospital in London found *Staphylococcus aureus* was resistant to penicillin (Levy and Marshall, 2004) and by 1950, this strain became widespread. In the late 1950s, a new type of microorganism *Shigella dysenteriae* appeared in Japan, which was resistant to antibiotics like chloramphenicol, streptomycin, tetracycline, and sulphonamides (Levy, 1982). In 1972 and 1973, another multidrug-resistant strain of the same bacterial species was identified in Brazil and Vietnam (Goldstein *et al.*, 1986). Generally, every bacterial species has different antibiotic resistance specificity.

Resistant strains increase mortality, morbidity, and cost of treatment (Cosgrove, 2006). In England, successful execution of approximately 4,000,000 operations solely depends on antibiotics, especially for caesarean sections and for women suffering from urinary tract infections (Llor and Bjerrum, 2014; Shallcross *et al.*, 2015). Furthermore, some women need antibiotics during their gestational period to prevent the passage of infection from her body to the newborn child (WHO, 2014). Antimicrobial resistance is causing

hindrance in treatment, and many antibiotics often come with various side effects. Therefore, there is an urgent need to develop new effective antibiotics with fewer side effects and at a lower cost.

### 1.2. Traditional uses of medicinal plants to treat infections

Medicinal plants have been used globally by different civilisations for many centuries to treat diseases, including microbial infections (Ramawat *et al.*, 2009). The Sumerians, from Mesopotamia (Iraq now), in 2600 BC, first mentioned the use of medicinal herbs by writing plant recipes on clay scrolls (Ramawat *et al.*, 2009; Sarker and Nahar, 2012). In most communities, plants play a vital role as food or medicine. Most societies have extensive traditional knowledge of plant usage. However, if these uses are not well documented, successive generations will lose these pieces of information (Hostettmann *et al.*, 2000; Houghton and Mukherjee, 2009). Approximately 400,000 flowering plants have been recorded globally, of which more than 50,000 have been used as medicinal plants (Verpoorte, 2009). These medicinal plants have been used to treat different types of health problems and some probably have an impact on protection from diseases. In addition, the high content of mineral nutrients may enhance the ability of plants to boost the immune system (Kubena and Mcmurray, 1996).

People of developing countries tend to be reported with more cases of infectious diseases due to their life style and often poor living conditions. Their suffering has been exacerbated by infections caused by drug-resistant pathogens and the high cost of treatment (Mondol and Shin, 2014). According to WHO (2008), more than 80% of people in Asia and Africa use medicinal plants as the first choice for their healthcare.

People in India use plants such as, *Achyranthes aspera, Allium cepa, Allium sativum, Aloe vera, Anacardium occidentale, Areca catechu, Azadirachta indica, Bauhinia variegata, Beta vulgaris, Brassica oleracea, Calendula officinalis, Calotropis gigantea, Camellia sinensis, Cannabis sativa, Cassia fistula, Cissampelos pareira, Crocus sativus, Cleome*

*viscosa, Costus speciosus, Curcuma longa, Daucus carota, Echinacea angustifolia, Eucalyptus globulus, Euphorbia spp., Ficus benghalensis, Ficus racemosa, Ixora coccinea, Jatropha gossypifolia, Lavandula officinalis, Lawsonia inermis, Lycopersicon esculentum, Madhuca longifolia, Mangifera indica, Matricaria chamomilla, Mirabilis jalapa, Morinda pubescens, Morus alba, Opuntia dillenii, Plumbago zeylanica, Portulaca oleracea, Pongamia pinnata, Prunus persica, Rosmarinus officinalis, Saraca asoca, Scoparia dulcis, Terminalia bellirica, Thymus vulgaris* and *Vitex altissima*, to treat skin diseases, wounds, and skin cancers. Moreover, Turkish communities use *Rhus coriaria, Echium italicum, Juniperus oxycedrus,* and *Hypericum perforatum* for their anti-infective properties (Yeşilada *et al.*, 1993).

70% of the population of the second most-populous continent Africa still relies on their traditional medication system. They have a widespread use of *Prunus africana* and *Agathosma betulina* to treat urinary tract infections (Hostettmann *et al.*, 2000). Moreover, they use *Pelargonium sidoides* and *Glycyrrhiza glabra* as expectorants, and to treat upper respiratory tract infections. *Securidaca longepedunculata* is one of the common plants used to treat different infections, such as, skin infections, malaria, bilharzias and fever (Hostettmann *et al.*, 2000; Kamsu-Foguem and Foguem, 2014). In addition, *Catharanthus roseus* is utilised as a cancer chemotherapy (Kamsu-Foguem and Foguem, 2014). As a traditional herbal remedy, African people use *Hypoxis hemerocallidea* and *Sutherlandia spp.* as a primary treatment for HIV/AIDS (Mills *et al.*, 2005).

Egyptians use *Centaurium umbellatum Gilib, Azadirachta indica, Alternanthera philoxeroides, Castanospermum australe, Carica papaya, Euphorbia hirta, Kaempferia parviflora* and *Boesenbergia rotunda,* as antipyretics and garlic to treat intestinal worms (Petrovska, 2012; Pigili and Runja, 2014). *Chinese plants such as Artemisia annua, Lycoris radiata, Pyrrosia lingua, Isatis indigotica, Torreya nucifera,* and *Lindera aggregata* can inhibit the SARS-COV enzymes in coronavirus (Lin *et al.*, 2014). In addition, these plants

have been found to be successful in treating atopic eczema in children (Sheehan and Atherton, 1994).

### 1.3 Iraqi plants to treat infections

Iraq, situated in Western Asia, has a unique culture and diverse ecosystem. The country is bounded by Turkey to the north, Iran to the east, Kuwait to the southeast, Saudi Arabia to the south, Jordan to the southwest and Syria to the west. Iraq has disinctive geographical conditions due to the mountains in the north and northeast, and deserts in the southeast with low rainfall. The arid climate of Iraq with subtropical influence is favourable for the growth of particular types of flora, which has prevalent medicinal values. The medicinal plants mentioned in traditional Iraqi medicine is derived from knowledge of their historical usage. There is evidence that, 60,000 years ago, the Neanderthals lived in the equivalent of present-day Iraq. With the considerable advancement in civilisation starting from Sumerian, Babylonian, and Assyrian, the Iraqi people have transferred their folklore of herbal therapeutic information to successive generations (Chakravarty, 1976; Ghazanfar, 1994; Cowan, 1999; Al–Douri, 2014).

In spite of the continuous development of Iraq as a country, people are still dependent on the power of herbs as drinks or poultices for curing infections for their influential therapeutic benefits. Plants such as *Achillea vermicularis, Colutea cilicica, Gentiana olivieri, Potentilla supina* and *Polygonum aviculare* are used to treat helminthinfections, dysentery and diarrhoea. *Aethionema grandiflorum, Agrimonia eupatoria, Allium sativum, Artemisia herba-alba, Cinnamomum zeylanicum, Citrullus colocynthis, Nigella sativa* and *Salvia officinalis* are commonly used to treat bacterial infections. For respiratory infections, *Anthemis nobilis, Allium sativum, Cassia occidentalis, Casuarina equisetifolia, Cordia myxa, Echium italicum, Glycyrrhiza glabra, Lavender angustifolia, Pimpinella anisum* and *Zingiber officinale* are used. In addition, for any gastrointestinal infections, *Ocimum basilicum* is a well-known remedy. Plants like, *Agropyron repens, Ammi majus, Herniaria*

*glabra* and *Jasminum officinale* are used for urinary tract infections. *Ammannia baccifera*, *Caccinia crassifolia, Citrus sinensis, Erodium cicutarium, Ficus carica* and *Fumaria parviflora* are used to treat skin infections. *Clerodendrum inerme* is climed to be a good remedy for venereal infections, *Euphorbia hirta* for parasitic infections, and *Euphorbia tinctoria* for wounds (Molan *et al.*, 2012; Naqishbandi, 2014; Al-Snafi, 2018).

### 1.4 Natural products as antimicrobial agents

Natural products are chemical compounds, which have biological effects and are produced by living organisms in their natural environments (Sarker and Nahar, 2012; Obanla *et al*., 2016). The potential use of highly purifiued natural products as antimicrobial agents dates back to 1929, when Alexander Fleming first reported the production of a bacteria-inhibiting substance in mould, *Penicillium*, later he termed this substance as "penicillin" (**1**). Unfortunately, he could not isolate the substance. Later in 1940, Florey and Chain were able to isolate penicillin and demonstrated its use as a therapeutic agent to treat a large number of bacterial diseases. The period between the 1950s and 1970s was the golden era of discovery of novel antibiotics that led to many new classes of antibiotics being discovered. Between 1981 and 1985, the *Journal of Antibiotics* reported approximately 50 effective compounds per year against pathogenic microorganisms were derived from natural products (Gootz, 1990). After that, 70 out of the 90 currently available antibiotics originated from natural products (Pelaez, 2006). During 2000-2008 more than 300 natural products compounds along with their antimicrobial properties were reported (Saleem *et al.*, 2010). The year 2015 perhaps started a new golden age for natural products research. In this year, Youyou Tu was awarded with the Nobel Prize in Physiology and Medicine for the discovery of artemisinin (**2**) and dihydroartemisinin (**3**), used to treat malaria (Shen, 2015). Antimicrobial agents can be obtained from different sources of natural products like, plants, animals, bacteria, algae and fungi (Gyawali and Ibrahim, 2014; Park, 2015). The number of

approved drugs since 1981 to 2014, derived from natural products in the period 1981 to 2014 is shown in Figure 1.1.

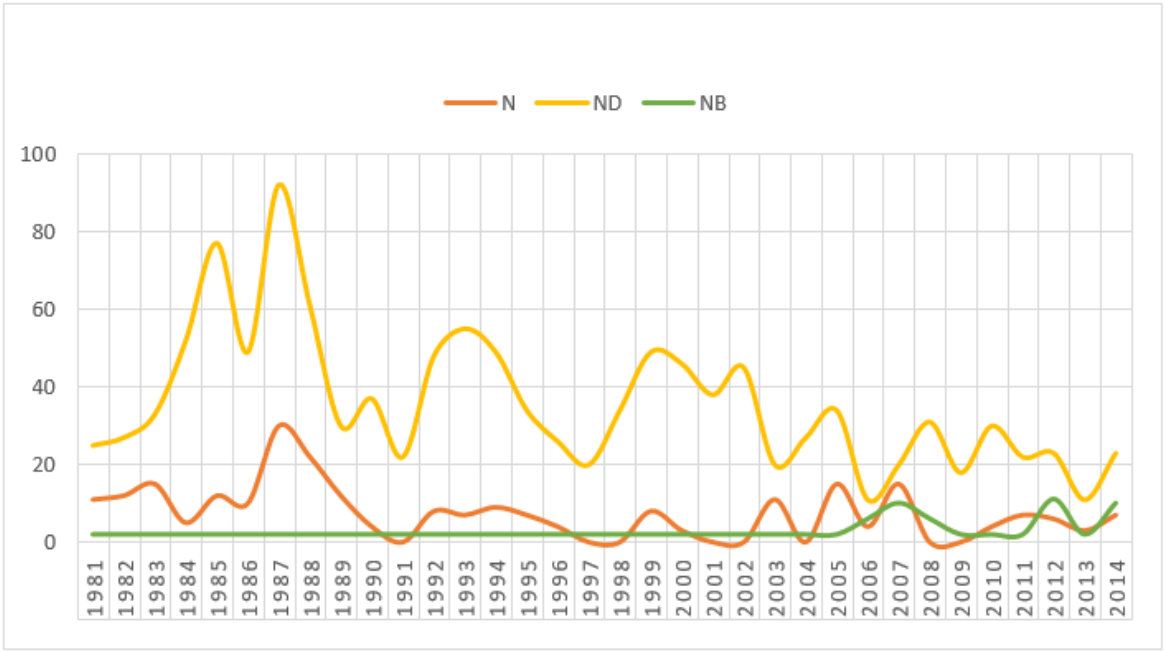


***Figure 1.1**: New approved drugs (1981-2014) derived from natural products*

N: unmodified, semi or totally synthetic compounds, ND: semisynthetic modified natural compounds, NB: botanical drug

In 2015, 70% of novel drugs were from organic resources and out of them 64% were from natural products. The main source of 85% of new approved drugs in 2016 were organic compounds, with a half of them being natural products. In 2017, 87% of the novel drugs approved by the Food and Drug Administration (FDA) were obtained from organic sources, 50% of the active ingredients were natural products such as, ertugliflozin (**4**), deflazacort (**5**) and naldemedine (**6**) (Newman and Cragg, 2016; de la Torre and Albericio, 2018). Until September 2018, 75% of the new authorised drugs are from organic compounds and the active constituent for 50% of them derived from natural products such as cannabidiol (**7**) and sisomicin (**8**) (Figure 1.2).

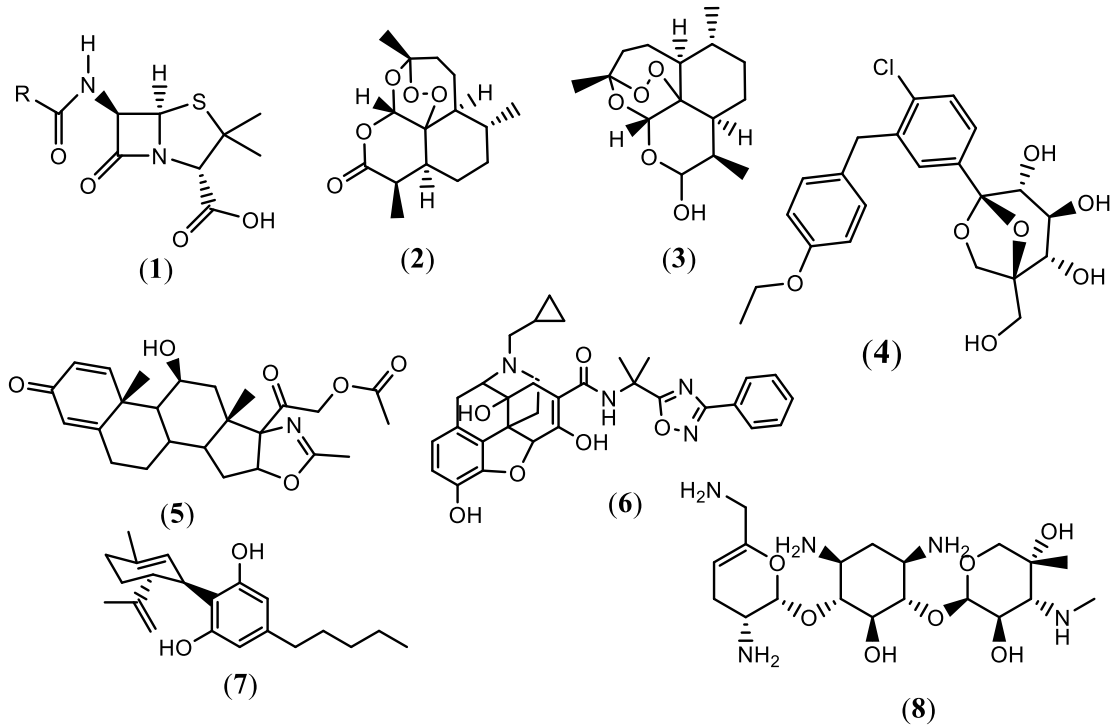


***Figure 1.2**: Structures of compounds **1-8***

Penicillin (**1**), artemisinin (**2**), dihydroartemisinin (**3**), ertugliflozin (**4**), deflazacort (**5**), naldemedine (**6**), cannabidiol (**7**) and sisomicin (**8**)

### 1.4.1 Plants

Higher Plants produce a wide range of secondary metabolites such as coumarins, alkaloids, glycosides, flavonoids, steroids, terpenoids, sugars, saponins, organic acids, phenolics, aliphatic alcohols, aldehydes, ketones, and isoflavonoids etc., many of which can inhibit the growth of microorganisms, heal diseases or promote human health (Sarker and Nahar, 2012; Gyawali and Ibrahim, 2014; Obanla *et al*., 2016).

The majority of researchers are working with the crude extract as phytopharmaceuticals (Iwu *et al.*, 1999). For example, the mustard crude extract showed ntimicrobial activity agansit *E.coli* at 0.01% concentration (Chandual Ahire and khade, 2018) while, the methanolic extract of *Brassica oleracea* (red cabbage) inhibited bacteria *Staphylococcus aureus, Bacillus subtilis* and *Escherichia coli* at MIC 100 mg/mL (Hafidh *et al*., 2018). According to Kumar *et al*. (2014) both of *Syzygium aromaticum* (Clove) and *Allium sativum* (Garlic) revealed antimicrobial effect agansit *Bacillus cereus,*

*Staphylococcus aureus, Salmonella typhi* and *Escherichia coli* at different concentations (1000 ppm, 1500 ppm and 2000 ppm). Some stuides focused on purification of the secondary metabolites and testing their antimicrobial properties (Gyawali and Ibrahim, 2014). According to Shan *et al*. (2007), 46 different plant extracts were found to contain phenolic constituents, which exhibited antibacterial activity against *Bacillus cereus, Listeria monocytogenes, Staphylococcus aureus, Escherichia coli,* and *Salmonella anatum* (Hafidh *et al*., 2011).

The new trends of research are focussing on active compounds (Iwu *et al*., 1999). Important pharmaceutically were isolated from plants include atropine (**9**) from *Atropa belladonna*, salicin (**10**) from *Salix spp.,* caffeine (**11**) from *Coffea arabica,* ephedrine (**12**) from *Ephedra spp.,* quinine (**13**) and quinidine (**14**) from *Cinchona spp*., theobromine (**15**) from *Theobroma cacao,* theophylline (**16**) from *Camellia sinensis,* morphine (**17**) and codeine (**18**) from *Papaver somniferum,* digoxin (**19**) from *Digitalis spp*. and vinblastine (**20**) from *Catharanthus roseus* (Chinou, 2008) (Figure 1.3). The antimicrobial activity of pure compounds is dependent on chemical structure and concentration. Until now, over 30,000 antimicrobial compounds have been isolated from different plants (Gyawali and Ibrahim, 2014). Most of the expectations pointed to an increase in the use of pharmaceuticals derived from plants, even the WHO report has shown international interested in using these as drugs (Verma and Singh, 2008).

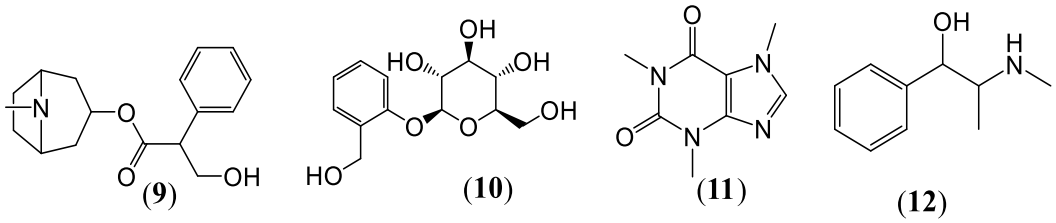


***Figure 1.3****: Structures of compounds from* ***9-20***

Atropine (**9**), salicin (**10**), caffeine (**11**), ephedrine (**12**), quinine (**13**), quinidine (**14**), theobromine (**15**), theophylline (**16**), morphine (**17**), codeine (**18**), digoxin (**19**) and vinblastine (**20)**

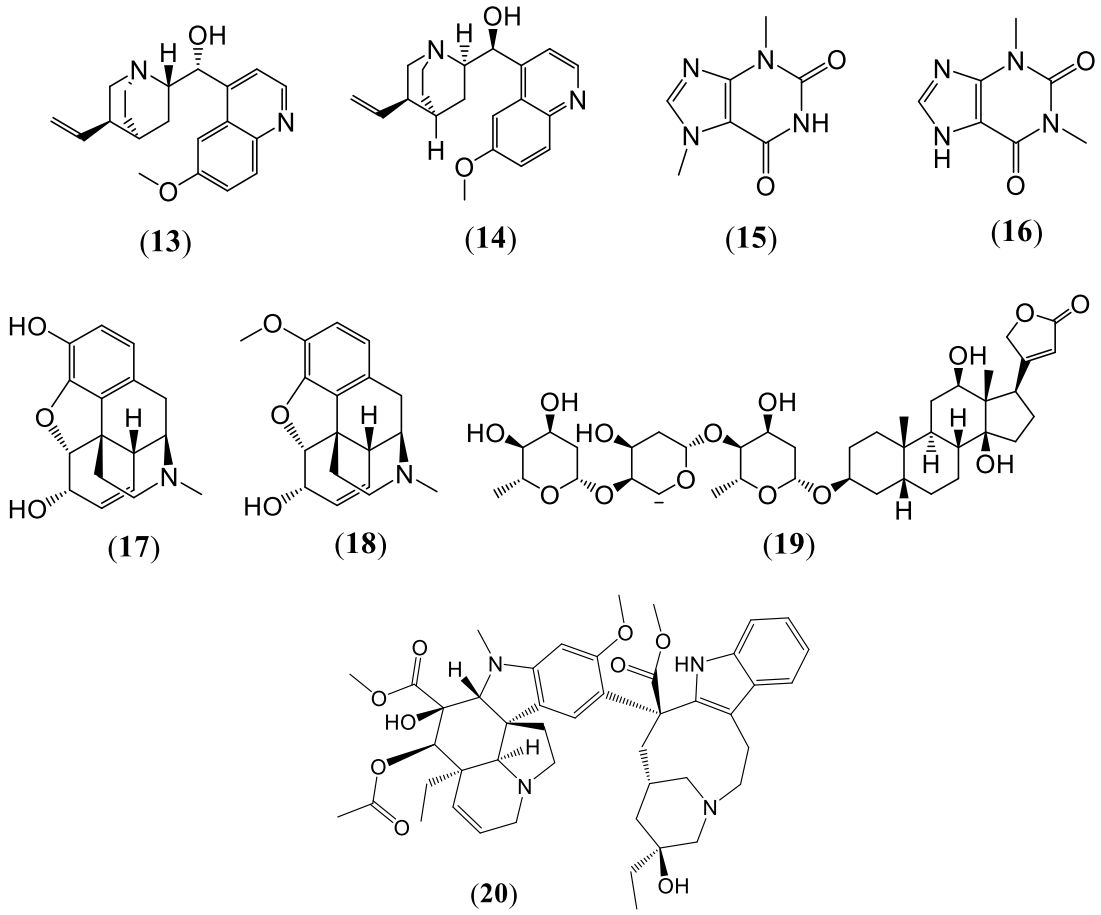


***Figure 1.3****(continued): Structures of compounds from* ***9-20***

Atropine (**9**), salicin (**10**), caffeine (**11**), ephedrine (**12**), quinine (**13**), quinidine (**14**), theobromine (**15**), theophylline (**16**), morphine (**17**), codeine (**18**), digoxin (**19**) and vinblastine (**20)**

### 1.4.2 Microorganisms

Microorganisms, particularly bacteria and fungi, produce secondary metabolites during the stationary phase of growth. These metabolites are a rich source of valuable compounds for use in medicine industry and agriculture (Sultanbawa, 2011; Niu and Tan, 2013). Compounds such as penicillin (**1**), cephalosporin *(***21**), tetracycline *(***22**), chloramphenicol *(***23**), aminoglycosides *(***24**) and macrolides are well known antibiotics (Figure 1.4). The discovery of penicillin followed by innovation of numerable new antibiotics derived from microorganisms include rifamycin (**25**), erythromycin (**26**), chlortetracycline (**27**), streptomycin (**28**), cephalosporin C (**29**), lincomycin *(***30**), vancomycin (**31**), nystatin (**32**), nalidixic acid (**33**), and daunorubicin (**34**) (Figure 1.4). All

of these compounds have a wide range of activities against Gram-positive and Gram-negative bacteria and fungi (Pelaez, 2006; Newman and Cragg, 2007; Dias *et al.*, 2012).

Fungi are a large source of secondary metabolites and novel compounds (Gunatilaka, 2006). These metabolites can have a broad-spectrum of activities against pathogens (Zhang *et al.*, 2006). Taxol (**35**), first discovered from *Taxus brevifolia*, has been isolated from *Pestalotiopsis microspore, Pestalotiopsis guepini, Seimatoantlerium tepuiense*, *Periconia* sp. and *Tubercularia* sp. (Strobel, 2003) (Figure 1.4).

Endophytic bacteria have a broad genetic diversity and are a rich source of natural products with a wide range of biological activities such as Streptomycetes, considered to be the source of up to 80% of the antibiotics (Strobel, 2003; Zhang *et al.*, 2006; De Lima Procópio, 2012). Many researchers have reported antibiotics, antioxidant agents, anticancer compounds, and other biologically active compounds from bacteria. For example celastramycin A (**36**) was purified from *Streptomyces* MaB-QuH-8 (Pullen et al., 2002; Kikuchi et al., 2009; De Lima Procópio, 2012) (Figure 1.4).

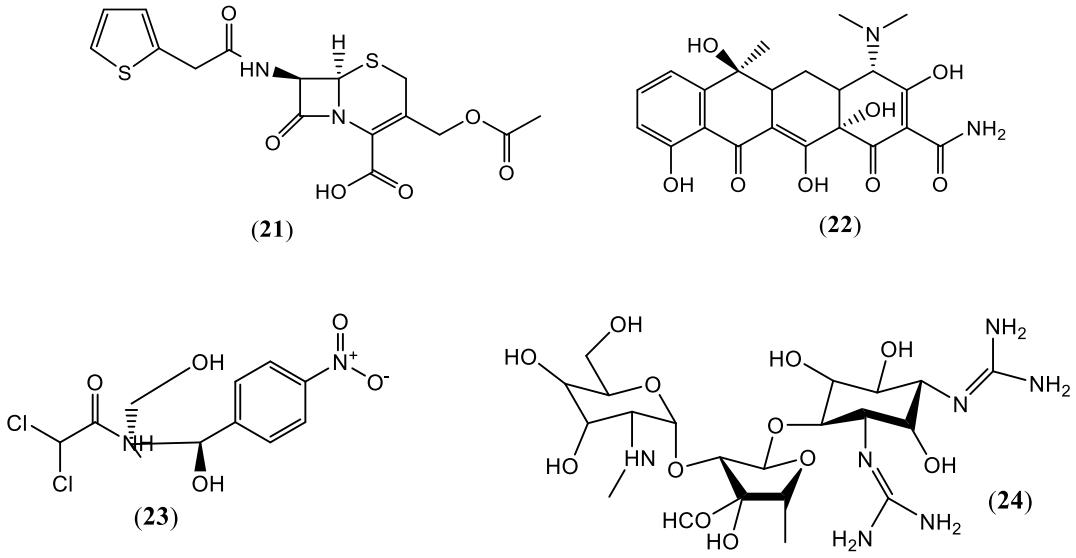


***Figure 1.4**: Structures of compounds from **21-36***

Cephalosporin (**21**), tetracycline (**22**), chloramphenicol (**23**), aminoglycosides (**24**), rifamycin (**25**), erythromycin (**26**), chlortetracycline (**27**), streptomycin (**28**), cephalosporin C (**29**), lincomycin (**30**), vancomycin (**31**), nystatin (**32**), nalidixic acid (**33**), daunorubicin (**34**), taxol (**35**) and adenine (**36)**

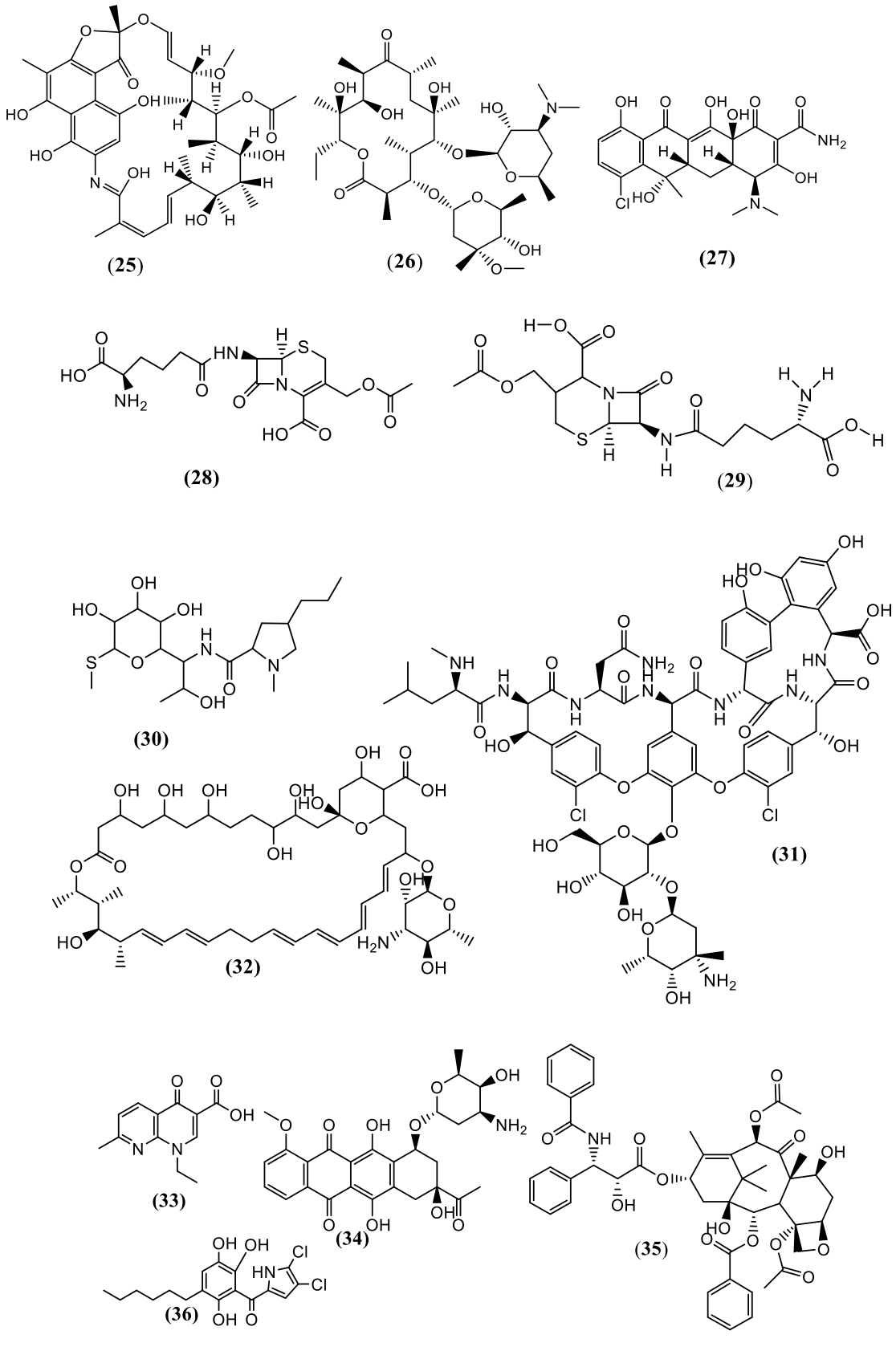


***Figure1.4** (Continued): Structures of compounds from **21-36***

Cephalosporin (**21**), tetracycline (**22**), chloramphenicol (**23**), aminoglycosides (**24**), rifamycin (**25**), erythromycin (**26**), chlortetracycline (**27**), streptomycin (**28**), cephalosporin C (**29**), lincomycin (**30**), vancomycin (**31**), nystatin (**32**), nalidixic acid (**33**), daunorubicin (**34**), taxol (**35**) and adenine (**36**)

In addition, bacteria also produce enzymes and other proteins and enzymes, which have biological activities (Sahai and Manocha, 1993). *Bacillus subtilis* BS-2, for example, produces a thermostable and UV-tolerant antifungal protein (He *et al.*, 2003). It is well established that only a small fraction of microorganisms can be isolated from natural environments using current isolation techniques. Less than 1% of isolated bacteria and 5% of fungal species have ever been described (Patil *et al.*, 2016; Harvey, 2008). There is a need to explore alternative microbial habitats to isolate new microbes with chemical and functional diversity to obtain novel antibiotics (Patil *et al.*, 2016).

### 1.4.3 Marine sources

Discovery of bioactive compounds from marine organisms gained momertam in the middle of the 20$^{th}$ century and every year hundreds of novel compounds are now reported (Sawadogo *et al.*, 2013). Up to 2012, around 8,000 new compounds were reported, and most of there have clamied therapeutic proprieties for different diseases (Sarker and Nahar, 2012). Comparisons between the activity of terrestrial natural products and marine natural products shpws the great superiority of marine products which may be because marine organisms live in a strongly competitive environment for space and nutrition, and are therefore potential sources for detecting new biologically active compounds (Lu *et al.*, 2010; Rahman *et al.*, 2010; Mondol and Shin, 2014). The marine environment is considered particularly valudle place for the variety of organisms (Sawadogo *et al.*, 2013).

Sponges, one of the oldest marine organisms belongs to metazoan phylum, considered to be a key source for pharmacologically active compounds. More than 5000 different compounds have already been discovered from sponges and 800 are documented as antimicrobial agents. Marine sponges are considered to be a major source of new compounds (Laport *et al.*, 2009; Skariyachan *et al.*, 2014). Marine organisms living at a depth of 11 km or more survive stressful conditions in terms of temperature, pressure and light (Sarker and Nahar, 2012). These conditions have contributed to the development of unique metabolites, which are different from those of other organsims. Marine

microorganisms can be a good source of new compounds, which may be a varity of chemical classes including alkaloids, peptides, terpenes, shikimates, polyketides and many of there are uncharacterized (Sarker and Nahar, 2012). Until now, only a few marine microorganisms have been examined for bioactive metabolites.

### 1.5 Mechanism of action of antimicrobial natural products

It is difficult to determine the exact mechanism of actions of natural antimicrobial agents, due to the concurrent occurrence of multiple interactions. Even though, different methods have been adapted to evaluate the mechanism of actions (Gyawali *et al.,* 2014). Studies on the mechanism of actions reveal the basis for the selective toxicity.

- Cell membrane: Some compounds have the ability to distribute membrane function and interact with membrane proteins, causing malformation in construction and functionality (Rimbara, 2012). For example, the Cranberry extract inhibits *S. aureus* by damaging the cell wall (Wu *et al.*, 2008). The Grape seeds and pomegranate polyphenols make a cell surface roughening and formation of blobs on the cell surface (Gyawali *et al.*, 2014)
- pH effects: an increase in proton concentration lowers pH of the substrate. The lower pH prevents intercellular acid molecules dissolving or creates a substrate transfer disorder by altering cell membrane permeability (Davidson *et al.,* 2013).
- Protein synthesis: The organic acids in plant extracts can have effects on the cytoplasmic membrane by interacting with membrane proteins (Gyawali *et al.*, 2014). In addition, the organic acids can be responsible for inhibiting NADH oxidation (Davidson *et al.*, 2013). Inhibition of plasmid conjugation and nucleic material can be caused by organic acids. This effect may not necessarily kill bacteria but could at least cause a decline in a bacterial population. Linoleic acid (**37**) from vegetables inhibits conjugal plasmid F and R388 (Fernandez-Lopez *et al.*, 2005; Jandacek, 2017) (Figure 1.5). Most leaves containing fatty acids and polyketides compounds were identified as specific conjugal inhibitors (Smith and Romesberg, 2007).

- Efflux pumps inhibiton: Proteinaceous transporters found in an organism's outer membrane, function to get rid of accumulated antibiotic molecules (Bay and Turner, 2016).
- The cytoplasmic membrane: Short chain organic acids in plant extracts can interfere with energy metabolism and affect membrane protein (Ricke, 2003). For example, Tea tree oil, which contain 100 terpenes and their related alcohols (Carson, 2002) can destroy the structure of the cytoplasmic membrane for *Escherichia coli* and *Staphylococcus aureus* (Cox *et al.*, 1998).

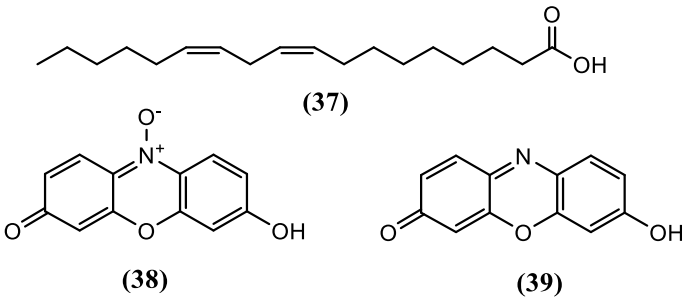


***Figure 1.5****: Structures of compounds* ***37-39***

Linoleic acid (**37**), resazurin (**38**) and resorufin (**39**)

## 1.6 Methods for *in vitro* evaluation of antimicrobial activity

Different methods can be used to assess the *in vitro* antimicrobial activity for various materials including purified phytochemicals or crude natural products extracts and fraction. Often, one method may not be suitable for assessing the antimicrobial activity of different test samples. For example, for non-polar extracts, the diffusion method is not enough to confirm the antimicrobial activity. Many researchers have reported the solid dilution method as more accurate with non-polar extract. In addition, the amount of compound also dictates the researcher may choose a particular method (Houghton and Mukherjee, 2009). Among these methods, the most widely recognised are recorded below.

### 1.6.1 Diffusion method

Diffusion methods are widely used to evaluate the antimicrobial activity of plant extracts. In these methods, microorganisms are inoculated in solid media containing a

reservoir (hole, cylinder or disc) for material testing that means the plant extract will be in direct contact with the microbes through media. After incubation, the diameter of the inhibition zone around the reservoirs (Figure 1.6) is measured. In general, this method is good for primary antimicrobial screening of plant extracts by measuring the minimum inhibition concentration (MIC) (Ayukekbong *et al.*, 2017). When using this method, precautions should be taken not to compare the results between extracts obtained from different studies and to use the same solvent to dissolve the extracts. When using any of the three protocols, it is important to sterilise the sample and choose the suitable methods for extracts depending on solubility. If the extract remains undissolved in water, then the mixing in the whole plate will be the best choice for testing aqueous suspension (Heggers *et al.*, 1987; Thomson *et al.*, 1989; Houghton and Mukherjee, 2009; Balouiri *et al.*, 2016).

### 1.6.2 Dilution method

In this method, a liquid culture medium is inoculated with the target organism and mixed with the plant extract. The suspension is incubated to measure the growth by turbidimetry in comparison with the control without plant extract. This method is most suitable for water-soluble extracts. The "microdilution method" can be used (Houghton and Mukherjee, 2009). This method uses 96-well microtitre plates (Figure 1.7) and the growth of bacteria is determined by turbidity (Kalemba and Kunicka, 2003). Only a small amount of plant extracts is needed for this method and one plate can be used to test many different concentrations. In addition, it is an easy method to determine the MIC (Houghton and Mukherjee, 2009).

Different methods of screening compounds obtained from plant extracts are discussed by Drummond and Waigh (2000), one of these methods is the resazurin assay (milk test), in which a blue compound is used as an indicator for oxidation in the reductase test of milk and as a pH indicator (pink at 3.8, violet at 6.5). Resazurin (**38**) is a metabolic indicator for living cells (O'brien *et al.*, 2000). So far, it has not been clear, where this

reaction occurs within the cell (Sánchez *et al.*, 2002). Researchers have suggested many possibilities on how Resazurin (**38**) is working inside living cells: such as , it can spread to the cell and is reduced to resorufin (**39**), possibly by the influence of several different reductase enzymes in mitochondria, cytosol and microsomes.

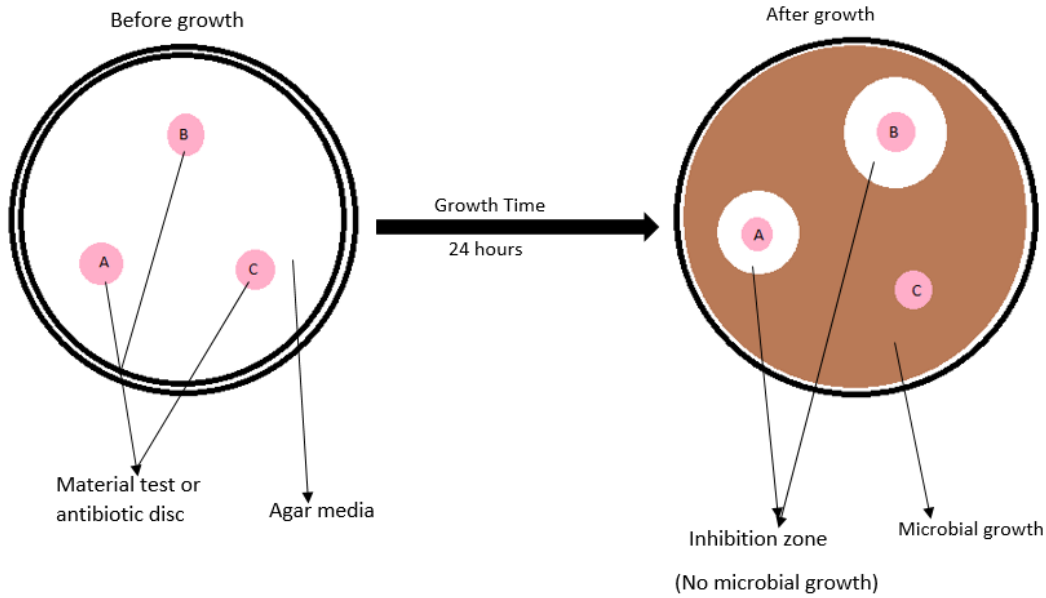


***Figure 1.6**: Disk diffusion method*

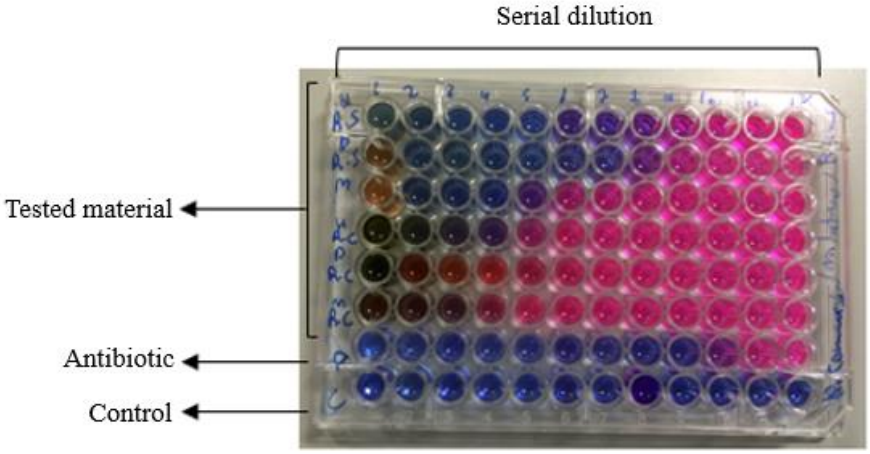


***Figure 1.7**: Dilution method*

The fluorescent resorufin is then distributed from living cells to the surrounding medium (Wu, 2010). A second suggestion is that internal enzymes within cells such as NADH are involved in the interaction, which generates the co-reduction equivalents in this interaction (Riss and Moravec, 2006). Other studies have suggested that the reduction of

resazurin to resorufin may occur on the surface of the plasma membrane, or perhaps in the culture media (Quent *et al.*, 2010). Sarker *et al.* (2007) put forward a resazurin method with new modifications for better accuracy. The first method described by Drummond and Waigh (2000) used incubated microorganisms only, while Sarker *et al.* (2007) measured the incubated microorganisms by spectrophotometer and compared with the Macfarlane standard. This modified resazurin method is simple, sensitive, fast, strong, reliable, and can be successfully used to evaluate the antibacterial properties of natural products.

## 1.7 Plants used in this study

This study included three plants from the Rutaceae family from the Iraqi flora: *Citrus grandis* (leaves), *Citrus sinensis* (leaves and peel) and *Ruta chalepensis* (leaves, stems, flowers and roots). The Rutaceae family is commonly known as "the *Citrus* family". The *Citrus* species are commercially important, and the Rutaceae is the biggest family in the Iraqi flora, comprising around 160 genera and 1700 species (Heywood *et al.*, 2007; Martínez-Pérez *et al.*, 2017). Different types of plants like shrubs, trees, herbs and sometimes climbing or crawling plants come under this family. Most of the Rutaceae members have essential oil in the visible glands of their leaves, flowers, fruits and seeds. Leaves are simple or compound and alternate or opposite; most of the plants in this family have beautiful flowers with bright colours and strong fragrance (Swingle, 1943; Groppo *et al.*, 2008; Tamokou *et al.*, 2017; Saduf *et al.*, 2018). The flowers have long corollas ranging from a few millimetres to several centimetres, and the symmetry pattern of a flower is actinomorphic or zygomorphic. Carpels and stamens are two to many; carpels are free or united and can contain two to many ovaries (Groppo *et al.*, 2008). Fruits can be dry like *Ruta chalepensis* or fleshy like *Citrus sinensis* (Groppo *et al.*, 2008). The species grow in all parts of the world especially in Asia, Australia, South Africa and Africa (Swingle, 1943). This plant family has been used in traditional medicine for treating snakebites, stomatitis, rheumatism, bronchitis and other diseases (Sandjo *et al.*, 2014).

The Rutaceae has been reported to contain 200 different coumarins (Gray and Waterman, 1978). The most economically important genus in the family is *Citrus* (Chase *et al.*, 1999). This family is a good source of alkaloids such as benzylisoquinoline, furquinolines, quinolines, acridones, pyanoquinolines, indole derivatives, imidazoles and oxazoles (Waterman, 1975; Shobana *et al.*, 1989; Groppo *et al.*, 2008), furanocoumarins, furoquinoline alkaloids, phenolics and terpenes (Adamska-Szewczyk *et al.*, 2016), a big range of limonoids (Wang *et al.*, 2009) flavonoids (Koblovská *et al.*, 2008) coumarins and volatile oils. Lots of plants from this family have been used traditionally, for example, the genus *Dictamnus* has been used in traditional Chinese medicine to heal bleeding, rheumatism, itching, hepatitis disease and skin problems (Tang *et al.*, 1999; Wu *et al.*, 1999). Another member of the Rutaceae is *Toddalia asiatica*, in South Africa, it is used to treat malaria, indigestion problems, stomachache, snakebites, and is used in rituals, coughs, influenza, lung diseases, nasal problems, bronchial pains and rheumatism (Adjanohoun *et al.*, 1993; Maundu, 2001; Meyer, 2005; Duraipandiyan *et al.*, 2006; Orwa *et al.*, 2008; Kokwaro, 2009).

A number of scientific reports have been published on the potential medicinal uses of plants belonging to the Rutaceae family; such as the extract of the leaves of *Chloroxylon swietenia*, which has significant anti-inflammatory activity in a rat paw oedema test (Kumar *et al.*, 2006). Another example is *Zanthoxylum chalybeum* extract, which has also shown anti-inflammatory activity (Agyare *et al.*, 2013). Both *Zanthoxylum usambarense* and *Ruta spp*. have antimalarial activity (Agyare *et al.*, 2013). In addition, many members of the Rutaceae family have reports of antimicrobial activity.

Based on reports by Vats *et al.* (2011), the extract of *Murraya koenigii* can inhibit *Staphylococcus aureus*, *Micrococcus luteus*, *Bacillus subtilis*, *Escherichia coli*, *Pseudomonas aeruginosa*, *Candida albicans* and *Aspergillus niger*. During the screening of 172 plant extracts for antimicrobial activity in Puerto Rico, it was found that two species, *Citrus aurantifolia* and *C. auoranotium* were effective (Meléndez and Capriles, 2006). In

another study in Texas, the USA, fruit extract of *C. aurantifolia* acted as an anticancer agent, the result showed that 100 µg/mL of *C. aurantifolia* after 48 h exposure can inhibit growth of colon cancer cells SW-480 up to 78%, by damaging the DNA and expanding the level of caspase-3 (Narang and Jiraungkoorskul, 2016). The Rutaceae members are also known for their antioxidant properties. In a study carried out in India on *Clausena excavate* plant extract the result showed that the plant has high antioxidant activity (Elumalai and Id, 2016).

### 1.7.1 The genus *Ruta*

The genus *Ruta* L. grows in rocky and arid grasslands (Bennaoum and Benhassaini, 2017), contains 14 species of herbs and shrubs that emit green leaves with strong odour and has a bitter taste (Pollio *et al.*, 2008). *Ruta angustifolia, Ruta chalepensis, Ruta graveolens* and *Ruta montana* are some of the bettes known species of this genus.

#### 1.7.1.1 *Ruta chalepensis* L.

*Ruta chalepensis* L., commonly known as "rue or ruda" belongs to the Rutaceae family, and is a perennial herbs and sharbs having wild as well as cultivated forms. This species is characterised by glabrous, alternating bi-pennatisect leaves with narrow oblong-lanceolate or obovate segments and a cymose inflorescence (Figure 1.8). Rue has a strong odour due to the oil glands located in the leaves. The individual yellow flower consists of 4-5 sepals, 4-5 petals, 8-10 stamens and a superior ovary.

***Figure 1.8**: Ruta chalepensis (A: fruits, B: flowers and leaves)*

*Origin and distribution:*

*Ruta chalepensis* is indigenous to the Mediterranean region and Canary Islands. In the tropics, it is cultivated as a potherb or medicinal plant. It has been introduced in several countries, which are listed in the Table 1.1.

*Traditional uses:*

Documented reports suggest various traditional uses of Rue as an anti-inflammatory, analgesic, antipyretic and for uses in rheumatism, nerves disease, neuralgia, dropsy, convulsions and mental disorder. Moreover, it is also used to treat hysteria, colic, headache, eye problems, ear infections, intestinal worms, stomachache, poleaxe, apprehension and intestinal worms (Al-Said *et al.*, 1990; Béjar *et al.*, 2001; Iauk *et al.*, 2004; Alanis *et al.*, 2005; Günaydin and Savci, 2005; Gonzalez-Trujano *et al.*, 2006; Mejri *et al.*, 2010; Ali *et al.*, 2013; Khoury *et al.*, 2014). According to the study of Ali *et al.* (2004), Ruta is one of nineteen Yemeni traditional herbal medicines with known traditional use for Malaria treatment. The results of Günaydin and Savci (2005) however emphasised that *Ruta* causes embryo toxicity in mice and many other harmful effects. In addition, published literature suggest that Ruta is an abortifacient (San Miguel; 2003; Mejri *et al.*, 2010; Martínez-Pérez *et al.*, 2017). The plant is also used as a laxative. In addition to all the above features, *R. chalepensis* is also famous as an insect and lice repellent (Ali *et al.*, 2013; Khoury *et al.*, 2014).

*Veterinary uses:*

Apart from the medicinal usage of *R. chalepensis*, it has an immense claimed effect in farm and poultry animal health. It helps in delivery of sheep, pigs, goat, ewe and cows. Also, it solves digestive problems, joints pain, wounds and acts against parasites. In addition, it is used to kill lice on chickens, and to kill parasites in sheep and pigs. Moreover, it is used to cure earache, eye-ache and to heal the vocal cords in birds (San Miguel, 2003). According to de Sa *et al.* (2000) certain dosages of *R. chalepensis* causes many changes in the placenta and causes disorders in the blood-brain barrier, resulting in embryonic toxicity.

**Table 1.1**: Worldwide distribution of *Ruta chalepensis*

| **Country** | **Reference** |
|---|---|
| Algeria | Dod and Dahmane, 2008; Ferhat *et al.*, 2014; Khourya *et al.*, 2014 |
| America | Gὺnaydin and Savci, 2005; Khoury *et al.*, 2014 |
| Argentina | Zeichen *et al.*,2000; Rustaiyan *et al.*, 2002; Bagchi *et al.*, 2003 |
| Central America | San Miguel, 2003 |
| China | San Miguel,2003; Ferhat *et al.*, 2014; Khoury *et al.*, 2014 |
| Egypt | Ali *et al.*, 2013 |
| Greece | Tzakou and Couladis, 2001; Dod and Dahmane, 2008; Ferhat *et al.*, 2014; Khourya *et al.*, 2014 |
| India | Bagchi *et al.*, 2003; San Miguel, 2003; Dod and Dahmane, 2008; Khoury *et al.*, 2014; Ferhat *et al.*, 2014 |
| Iran | Rustaiyan *et al.*, 2002; Dod and Dahmane, 2008; Rustaiyan *et al.*, 2011; Ferhat *et al.*, 2014; Khourya *et al.*, 2014; Tedone *et al.*, 2014 |
| Iraq | Al-Majmaie *et al.*, 2005 |
| Israel | Ali-Shtayeh and Abu Ghdeib,1999; Landaua *et al.*, 2004 |
| Italy | Ali *et al.*, 2013; Iauk *et al.*, 2014; Tedone *et al.*, 2014 |
| Jordan | Alomary *et al.*, 2013 |
| Latin America | San Miguel, 2003 |
| Lebanon | Khourya *et al.*,2014 |
| Mediterranean area | Ulubelen *et al.*, 1986; Iauk *et al.*, 2014 ; Tedone *et al.*, 2014 |
| Mexico | Ali *et al.*, 2013 |
| Middle east | San Miguel, 2003; Khoury *et al.*, 2014; Bouabidi *et al.*, 2015 |
| Morocco | Uphof,1968; Gὺnaydin and Savci, 2005 |
| North of India | Ferhat *et al.*, 2014 |
| New York | San Miguel, 2003 |
| North California | San Miguel, 2003 |
| North America | Rustaiyan *et al.*, 2002; San Miguel, 2003 |
| North Africa | Khourya *et al.*, 2014 |
| Palestine | Ali-Shtayeh and Abu Ghdeib,1999; Landaua *et al.*, 2004 |
| Portugal | Ferhat *et al.*, 2014 |
| Saudi Aribia | Shah *et al.*, 1991; Rustaiyan *et al.*, 2002; Bagchi *et al.*, 2003; Gὺnaydin and Savci, 2005 |
| Spain | San Miguel, 2003; Khoury *et al.*,2014; Ferhat *et al.*, 2014 |
| Southern Europe | Rustaiyan *et al.*, 2002 |
| Texas | San Miguel, 2003 |
| Tunisia | Mejri *et al.*, 2010; Ferhat *et al.*, 2014; Khourya *et al.*,2014; Tedone *et al.*,2014 |
| Turkey | Ulublen *et al.*,1986; Ulubelen and Terem,1988; Baser *et al.*,1996; Rustaiyan *et al.*, 2002; Bagchi *et al.*, 2003; Gὺnaydin and Savci,2005; Dod and Dahmane, 2008; Ali *et al.*, 2013 |
| Yemen | Alzorekya and Nakahara, 2003; Awadh *et al.*, 2004 |
| Western Atlantic | San Miguel, 2003 |

*Phytochemicals of Ruta chalepensis:*

Previous phytochemical studies on *R. chalepensis* have shown the presence of essential oils (Al-Said *et al.*, 1990; Gonzalez-Trujano *et al.*, 2006; Ali *et al.*, 2013), alkaloids (Al-Said *et al.*, 1990; San Miguel, 2003; Iauk *et al.*, 2004; Khoury *et al.*, 2014) including furoquinoline alkaloids, 5-methoxydictamine (**40**) (Günaydin and Savci, 2005), skimmianine (**41**), quinolone alkaloid, γ-fagarine (**42**), saponins (Al-Said *et al.*, 1990; Ali *et al.*, 2013), sterols, tannins, triterpenes (Gonzalez-Trujano *et al.*, 2006; Ali *et al.*, 2013), coumarins (Khoury *et al.*, 2014) including furanocoumarins, bergapten (**43**) isopimpinellin (**44**) (Ulubelen *et al.*, 1986; Günaydin and Savci, 2005) chalepin (**45**), chalepinsin (**46**) rutamarin (**47**), and the flavonoid rutin (**48**) (Figure 1.9). Additionally, amino acids (de Sa *et al.*, 2000; Iauk *et al.*, 2004; Ali *et al.*, 2013), anthraquinones and various simple phenols (Ali *et al.*, 2013; Khoury *et al.*, 2014) were purified from this species. The essential oils of *Ruta chalepensis* contain many compounds some of which are listed in Table 1.2.

*Bioactivity:*

*Ruta chalepensis* as a repository of numerous compounds motivated the researchers from time to time to investigate the bioactivity of these compounds. It has been reported that the plant possesses antifungal, antibacterial, antimalarial and antiparasitic activities (Mejri *et al.*, 2010; Khoury *et al.*, 2014; Bouabidi *et al.*, 2015). Antitumor (Krayni *et al.*, 2015) and anticancer activity, especially for colon cancer (Tedone *et al.*, 2014), have also been reported. In a study in Italy, fifty-six patients suffering from different stages of colon cancer were treated with an ethanolic extract of *R. chalepensis*. As a result, there was a decrease in disease progression (Acquaviva *et al.*, 2011; Tedone *et al.*, 2014). In Palestine, as a folk medicine, aqueous extracts of 20 plants were evaluated for their antifungal activity, and out of these *R. chalepensis* was one of the most potent plants to inhibit *Microsporum canis*, *Trichophyton mentagrophyte*s and *Trichophyton violaceum* (Ali-Shtayeh and Abu Ghdeib, 1999). Furthermore, according to Alzoreky and Nakahara (2003), in an experiment with the

extracts of 26 plants collected from different countries, *R. chalepensis* was effective in eliminating *E. coli* and *Salmonella infantis*. *Ruta chalepensis* is also effective against *Bacillus subtilis*, but it is less active against *Staphylococcus aureus* and has no activity against *E. coli* (Al-Bakri and Afifi, 2007). During an antibacterial activity study using the disc diffusion method (Perez and Anesini, 1994), it was found that there was no activity against *Salmonella typhii.*

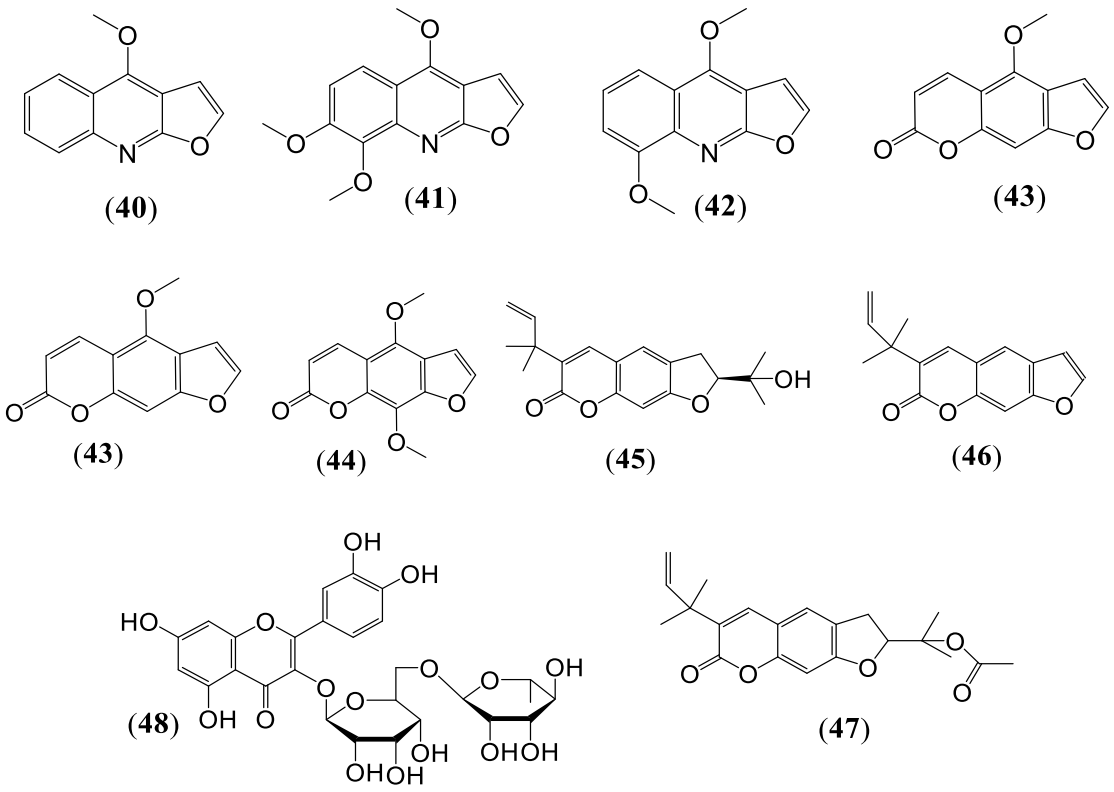


***Figure 1.9****: Structures of compounds* ***40-48***

5-methoxydictamine (**40**), skimmianine (**41**), γ-fagarine (**42**), bergapten (**43**), isopimpinellin (**44**), chalepin (**45**), chalepinsin (**46**), rutamarin (**47**) and rutin (**48**)

**Table 1.2**: Compounds identified in essential oils of *R. chalepensis*

| **Chemical compound** | **Reference** |
|---|---|
| 2-Acetoxytridecane | Ferhat *et al.*, 2014 |
| 2-Acetoxytetradecane | Ferhat *et al.*, 2014 |
| Benzaldehyde | Tzakou and Couladis, 2001: Dob and Dahmane, 2008 |
| (*Z*)-Bisabolene | Tzakou and Couladis, 2001 |
| γ-Bisabolene | Khoury *et al.*, 2014 |
| δ-Cadinene | Bnina *et al.*, 2010; Khoury *et al.*, 2014 |

| | |
|---|---|
| Camphor | Bagchi *et al.*, 2003; Dob and Dahmane, 2008; Bnina *et al.*, 2010; Mejri *et al.*, 2010; Khoury *et al.*, 2014 |
| Carnphene | Tzakou and Couladis, 2001 |
| β-Caryophyllene | Tzakou and Couladis, 2001; Dob and Dahmane, 2008; Bnina *et al.*, 2010; Khoury *et al.*, 2014 |
| Carvacol | Bagchi *et al.*, 2003 |
| Chamazulene | Dob and Dahmane, 2008 |
| 1,8-Cineole | Bnina *et al.*, 2010 |
| *p*-Cymene | Bagchi *et al.*, 2003; Dob and Dahmane, 2008, Bnina *et al.*, 2010 |
| Curcuphenol | Bnina *et al.*, 2010 |
| γ-Decalactone | Tzakou and Couladis, 2001; Dob and Dahmane, 2008 |
| Decanal | Dob and Dahmane, 2008 |
| Decanol | Bnina *et al.*, 2010 |
| 2-Decanol | Rustaiyan *et al.*, 2002; Bagchi *et al.*, 2003; Dob and Dahmane, 2008 |
| 2-Decanone | Rustaiyan *et al.*, 2002; Bagchi *et al.*, 2003; Dob and Dahmane, 2008; Bnina *et al.*, 2010; Mejri *et al.*, 2010; Ali *et al.*, 2013; Khoury *et al.*, 2014; Ferhat *et al.*, 2014 |
| 2-Decyl acetate | Tzakou and Couladis, 2001; Rustaiyan *et al.*, 2002; Bnina *et al.*, 2010; Ali *et al.*, 2013; Khoury *et al.*, 2014 |
| 2-Decanyl acetate | Ferhat *et al.*, 2014 |
| Dodecanol | Tzakou and Couladis, 2001; Bnina *et al.*, 2010; Khoury *et al.*, 2014 |
| 2-Dodecanone | Rustaiyan *et al.*, 2002; Bagchi *et al.*,2003; Dob and Dahmane, 2008; Mejri *et al.*, 2010; Ali *et al.*, 2013; Ferhat *et al.*, 2014; Khoury *et al.*, 2014 |
| Dodecan-3-one | Bagchi *et al.*, 2003; Mejri *et al.*, 2010; Khoury *et al.*, 2014 |
| Elemol | Tzakou and Couladis, 2001; Bagchi *et al.*, 2003; Dob and Dahmane, 2008; Bnina *et al.*, 2010; Khoury *et al.*, 2014 |
| 2-Ethylheptyl acetate | Tzakou and Couladis, 2001 |
| Ethyl linoleate | Dob and Dahmane, 2008 |
| Ethyl octadecanoate | Bnina *et al.*, 2010 |
| 2-Ethyloctyl acetate | Tzakou and Couladis, 2001; Dob and Dahmane, 2008 |
| α-Eudesmol | Bnina *et al.*, 2010; Khoury *et al.*, 2014 |
| β-Eudesmol | Dob and Dahmane, 2008; Bnina *et al.*, 2010 |
| γ−Eudesmol | Dob and Dahmane, 2008; Bnina *et al.*, 2010 |
| (*E*,*E*)-α-Farnesene | Tzakou and Couladis, 2001; Bnina *et al.*, 2010 |
| (*Z*,*E*)-α-Farnesene | Tzakou and Couladis, 2001 |
| Furfural | Dob and Dahmane, 2008 |
| Geijerene | Tzakou and Couladis, 2001; Bagchi *et al.*, 2003; Dob and Dahmane, 2008; Bnina *et al.*, 2010; Ali *et al.*, 2013 |
| Geraniol | Tzakou and Couladis, 2001 |
| Geranyl acetate | Tzakou and Couladis, 2001 |
| Heptanal | Dob and Dahmane, 2008 |

| | |
|---|---|
| Heptan-2-one | Bnina *et al.*, 2010 |
| 2-Heptanol | Dob and Dahmane, 2008 |
| 2-Heptyl acetate | Tzakou and Couladis, 2001; Dob and Dahmane, 2008; Bouabidi *et al.*, 2015 |
| Hexadecanoic acid | Bnina *et al.*, 2010; Khoury *et al.*, 2014 |
| 2-Hexanal | Dob and Dahmane, 2008 |
| (*Z*)-3-Hexanal | Dob and Dahmane, 2008 |
| Hex-3-en-1-ol | Bnina *et al.*, 2010; Khoury *et al.*, 2014 |
| Hex-2-enylacetate | Bnina *et al.*, 2010 |
| Hex-3-enyl acetate | Bnina *et al.*, 2010 |
| α-Humulene | Bnina *et al.*, 2010 |
| β-Ionone | Dob and Dahmane, 2008 |
| Isophytol | Bnina *et al.*, 2010; Khoury *et al.*, 2014 |
| Limonene | Tzakou and Couladis, 2001; Dob and Dahmane, 2008; Bnina *et al.*, 2010; Ali *et al.*, 2013; Khoury *et al.*, 2014 |
| Linalool | Bagchi *et al.*, 2003; Dob and Dahmane, 2008 |
| Mesitylene | Dob and Dahmane, 2008 |
| *p*-Mentha-l,8-diene | Tzakou and Couladis, 2001 |
| Methyl chavicol | Bnina *et al.*, 2010 |
| 2-Methyldecyl acetate | Tzakou and Couladis, 2001; Dob and Dahmane, 2008; Ferhat *et al.*, 2014 |
| 6-Methyl-5-hepten-2-one | Bagchi *et al.*, 2003 |
| Methyl hexadecanonate | Dob and Dahmane, 2008 |
| 10-Methyl-2-undecanone | Ali *et al.*, 2013 |
| 2-Methylnonyl acetate | Tzakou and Couladis, 2001; Dob and Dahmane, 2008 |
| Methyl nonyl ketone | Ferhat *et al.*,2014 |
| Methyl octadecanoate | Bnina *et al.*, 2010 |
| 2-Methoxy-3-isopropyl-5-methylpyrazine | Dob and Dahmane, 2008 |
| Mycrene | Tzakou and Couladis, 2001; Bnina *et al.*, 2010 |
| Naphtalene | Bnina *et al.*, 2010 |
| (*E*)-Nerolidol | Dob and Dahmane, 2008; Bnina *et al.*, 2010 |
| Neryl acetate | Tzakou and Couladis, 2001 |
| Nonan-2-yl | Khoury *et al.*, 2014 |
| Nonyl acetate | Tzakou and Couladis, 2001; Rustaiyan *et al.*, 2002 |
| Nonanal | Tzakou and Couladis, 2001; Dob and Dahmane, 2008; Bnina *et al.*, 2010; Ali *et al.*, 2013; Khoury *et al.*, 2014 |
| 2-Nonanol | Tzakou and Couladis, 2001; Bagchi *et al.*, 2003; Dob and Dahmane, 2008; Bnina *et al.*, 2010; Ali *et al.*, 2013; Khoury *et al.*, 2014 |
| Nonan-3-ol | Bnina *et al.*, 2010 |
| 2-Nonanone | Tzakou and Couladis, 2001; Rustaiyan *et al.*, 2002; Bagchi *et al.*, 2003; Dob and Dahmane, 2008; Bnina *et al.*, 2010; Ali *et al.*, 2013; Ferhat *et al.*, 2014; Khoury *et al.*, 2014 |
| 2-Nonyl acetate | Bagchi *et al.*, 2003; Ali *et al.*, 2013; Ferhat *et al.*, 2014 |

| | |
|---|---|
| (*E*)-β-Ocimene | Dob and Dahmane, 2008; Bnina *et al.*, 2010 |
| (*E*)-*p*-Ocimene | Tzakou and Couladis, 2001 |
| β-Ocirnene | Tzakou and Couladis, 2001 |
| Octanol | Tzakou and Couladis, 2001; Dob and Dahmane, 2008 |
| 2-Octanol | Dob and Dahmane, 2008 |
| 2-Octanone | Rustaiyan *et al.*, 2002; Dob and Dahmane, 2008; Bnina *et al.*, 2010; Khoury *et al.*, 2014 |
| Octyl acetate | Tzakou and Couladis, 2001; Dob and Dahmane, 2008; Bnina *et al.*, 2010; Khoury *et al.*, 2014 |
| 2-Octyl acetate | Dob and Dahmane, 2008; Bnina *et al.*, 2010; Ali *et al.*, 2013 |
| 3-Octyl acetate | Rustaiyan *et al.*, 2002 |
| 3-Odecanone | Dob and Dahmane, 2008 |
| β-Phellandrene | Tzakou and Couladis, 2001; Ferhat *et al.*, 2014 |
| Phenylacetaldehyde | Tzakou and Couladis, 2001; Dob and Dahmane, 2008 |
| Phytol | Ali *et al.*, 2013; Bnina *et al.*, 2010; Khoury *et al.*, 2014 |
| Phytyl acetate | Bnina *et al.*, 2010; Khoury *et al.*, 2014 |
| α-Pinene | Tzakou and Couladis, 2001; Bagchi *et al.*, 2003; Dob and Dahmane, 2008; Bnina *et al.*, 2010; Khoury *et al.*, 2014; Bouabidi *et al.*, 2015 |
| β-Pinene | Tzakou and Couladis, 2001 |
| Pregeijerene | Tzakou and Couladis, 2001; Bnina *et al.*, 2010 |
| Pregeijerene B | Ali *et al.*, 2013 |
| Psoralen | Dob and Dahmane, 2008 |
| Pulegone | Bnina *et al.*, 2010; Mejri *et al.*, 2010 |
| *cis*-Sabinene hydrate | Tzakou and Couladis, 2001; Bnina *et al.*, 2010 |
| α-Terpinene | Tzakou and Couladis, 2001; Dob and Dahmane, 2008 |
| β-Terpinene | Tzakou and Couladis, 2001; Bagchi *et al.*, 2003; Dob and Dahmane, 2008 |
| Terpinolene | Tzakou and Couladis, 2001 |
| α-Terpineol | Tzakou and Couladis, 2001; Dob and Dahmane, 2008 |
| Terpinen-4-ol | Tzakou and Couladis, 2001; Dob and Dahmane, 2008; Bnina *et al.*, 2010; Khoury *et al.*, 2014 |
| Tetradecanol | Bnina *et al.*, 2010 |
| α-Thujene | Tzakou and Couladis, 2001; Dob and Dahmane, 2008 |
| Thymol | Bagchi *et al.*, 2003 |
| 2-Tridecanone | Rustaiyan *et al.*, 2002; Bagchi *et al.*, 2003; Dob and Dahmane, 2008; Bnina *et al.*, 2010; Mejri *et al.*, 2010; Ali *et al.*, 2013; Khoury *et al.*, 2014 |
| 1,2,4-Trimethylbenzene | Dob and Dahmane, 2008 |
| 2-Undecanol | Ali *et al.*, 2013; Dob and Dahmane, 2008 |
| 2-Undecanone | Tzakou and Couladis, 2001; Rustaiyan *et al.*, 2002; Bagchi *et al.*, 2003; Dob and Dahmane, 2008; Mejri *et al.*, 2010; Ali *et al.*, 2013; Bouabidi *et al.*, 2015 |
| 2-Undecanyl acetate | Rustaiyan *et al.*, 2002 |

*Side effects of Ruta chalepensis:*

*Ruta chalepensis* is considered to be one of the dangerous plants, especially in high dosage it may lead to death. Not recommended to use by pregnant or lactating women. It may cause abortion, hyperaemia in the uterus and high oxytocic action (San Miguel, 2003). According to El Sayed *et al.* (2000), *R. chalepensis* causes mutagenicity due to its quinolone alkaloids content.

### 1.7.2 The genus *Citrus* L.

In 1753, Carl Linneaus presented the genus "*Citrus*" to the world (Swingle, 1967). These plants grow in tropical and subtropical areas and in the borderline around the world (The *Citrus* and Date Crop Germplasm Committee, 2004; Sun *et al.*, 2015). The *Citrus* L. has 16 species (Sun *et al.*, 2015), and all of them are trees with a height around 12-30 feet and width ranging between 8-25 feet. The plants have rounded crowns of dark green leaves, which are simple, trifoliate, alternate, and source of essential oils. In addition, *Citrus* has fragrant blossoms (Watson, 1993). This genus is the source of *Citrus* fruits, which has high economical value (The *Citrus* and Date Crop Germplasm Committee, 2004; Sun *et al.*, 2015). Between 2009 and 2010, the world's total production was up to 7.4 million metric tons (Sun *et al.*, 2015).

The plants from the *Citrus* genus have been used in traditional medicine for treating different diseases as an analgesic (Lima *et al.*, 2007; Correa *et al.*, 2016) for us in rheumatism and malaria (Martín *et al.*, 2011). *Citrus* species are reported to have different medicinal, physiological and pharmacological properties, such as antimicrobial (Espina *et al.*, 2011), antioxidant (Goulas and Manganaris, 2012), anticancer (Manthey and Guthrie, 2002; Cirmi *et al.*, 2017) and anti-inflammatory (Menichini *et al.*, 2011). The most important part of the *Citrus* plants is the edible fruit, used for foods, drinks, perfumes, cosmetic, soaps, and in many other aromatic products (Mohammed *et al.*, 2017). *Citrus* natural products are widely perceived as a critical part of the human eating regimen. It is cholesterol free and contains

sodium, vitamin C, folic acid, potassium, flavonoids, coumarins, pectins and dietary fibres (Dugo and Di Giacomo, 2002; Roy *et al.*, 2014).

Phytochemical studies on the genus *Citrus* have shown the presence of essential oils (Gancel *et al.*, 2005), and phenolic compounds (Fejzić and Ćavar, 2014). This genus is considered as a main source of vitamin C (**49**), which provides various health benefits (Zhang *et al.*, 2011). It contains large amounts of polyphenolics, especially flavonoids, such as hesperidin (**50**), narirutin or naringin (**51**), neohesperidin (**52**), eriocitrin (**53**), neoeriocitrin (**54**), rutin (**48**), diosmin (**55**), neoponcirin (**56**), and nobiletin (**57**), which have significant biological activity (Albach *et al.*, 1969; Jourdan *et al.*, 1985; Wang *et al.*, 2007; Zhang *et al.*, 2011) (Figure 1.10). Many other compounds have also been documented from *Citrus* including phenolic acids, β-carotene (**58**), lutein (**59**), lycopene (**60**) cryptoxanthin (**61**) and citric acid (**62**) (Lee *et al.*, 2001; Xu *et al.*, 2006; Kurita *et al.*, 2008). Lycopene is of note for preventing vacuolization in human lens epithelial cells (Mohanty *et al.*, 2002).

In addition, this genus produces hydroxycinnamic acids (**63**), which can inhibit oxidation of low-density lipoprotein, such as caffeic acid (**64**), ferulic acid (**65**), chlorogenic acid (**66**), and *p*-coumaric acid (**67**). In general, *Citrus* fruits are rich in carotenoids, for example, pink fruit has a high concentration of β-carotene (**58**), while other fruits contain high level of lutein (**59)**, cryptoxanthin (**68**), zeaxanthin (**69**), and β-cryptoxanthin (**70**) (Ma *et al.*, 2013) (Figure 1.10).

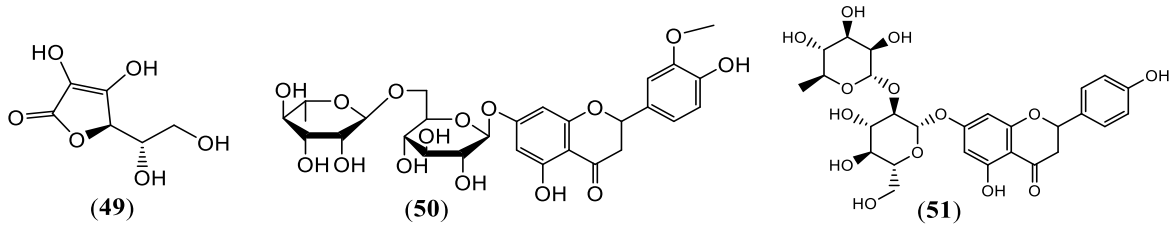


***Figure 1.10**: Structures of compounds **49-70***

Vitamin C (**49**), hesperidin (**50**), narirutin or naringin (**51**), neohesperidin (**52**), eriocitrin (**53**), neoeriocitrin (**54**), diosmin (**55**), neoponcirin (**56**), nobiletin (**57**), β-carotene (**58**), lutein (**59**), lycopene (**60**), cryptoxanthin (**61**), citric acid (**62**), hydroxycinnamic acids (**63**), caffeic acid (**64**), ferulic acid (**65**), chlorogenic acid (**66**), *p*-coumaric acid (**67**), cryptoxanthin (**68**), zeaxanthin (**69**) and β-cryptoxanthin (**70**)

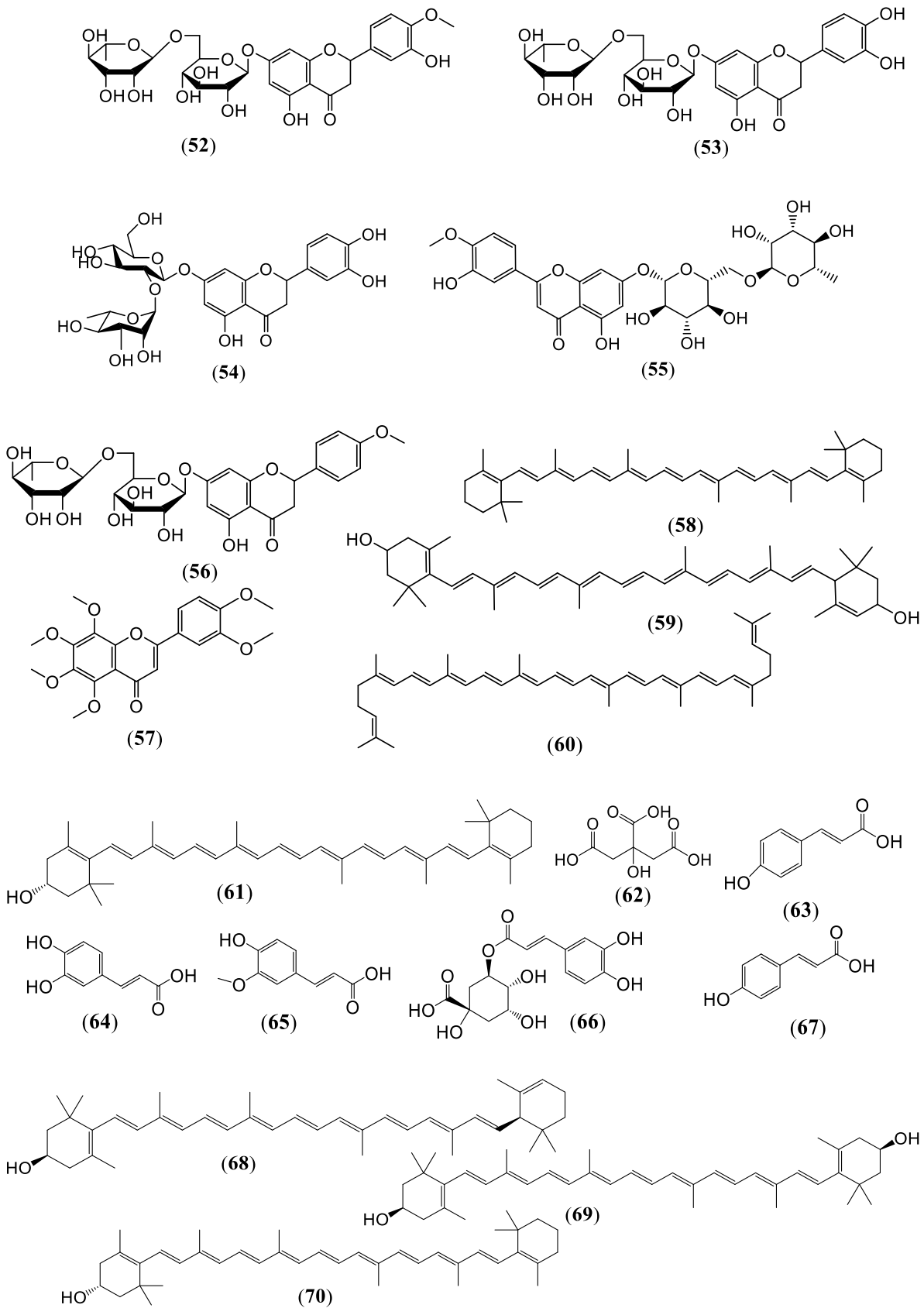


***Figure 1.10** (Continued): Structures of compounds **49-70***

Vitamin C (**49**), hesperidin (**50**), narirutin or naringin (**51**), neohesperidin (**52**), eriocitrin (**53**), neoeriocitrin (**54**), diosmin (**55**), neoponcirin (**56**), nobiletin (**57**), β-carotene (**58**), lutein (**59**), lycopene (**60**), cryptoxanthin (**61**), citric acid (**62**), hydroxycinnamic acids (**63**), caffeic acid (**64**), ferulic acid (**65**), chlorogenic acid (**66**), *p*-coumaric acid (**67**), cryptoxanthin (**68**), zeaxanthin (**69**) and β-cryptoxanthin (**70**)

### 1.7.2.1 *Citrus sinensis* L.

*Citrus sinensis* L. is a common plant in tropical and subtropical parts of the world. It is an evergreen tree growing up to 9-10 meters and have spines on branches. Leaves are elliptical oval to oblong in shape with narrowly winged-petioles measuring 3-5 mm wide, 6.5-15 cm long with an alternate position. The leaves contain oil gland. Axillary flowers include 20-25 yellow stamens and five white petals. The fruit is ball-shaped to oval (6.5 to 9.5 cm wide) and when mature it becomes orange or yellow. Fruits are sweet orange with a solid centre (Flamini *et al.*, 2003; Sharon-Asa *et al.*, 2003; Connell, 2008; Goudeau *et al.*, 2008; Steduto *et al.*, 2012; Ventura *et al.*, 2012).

*Origin and distribution:*

*Citrus sinensis* is a tropical plant; Brazil and the USA are considered as the countries of its origin (Véronique Zech-Matterne (Éditeur), 2018). The plant's geographical distribution is shown in Table 1.3.

**Table 1.3**: Geographical distribution of *Citrus sinensis*

| **Country** | **Reference** |
|---|---|
| Brazil | Kundsen *et al.*, 2011 |
| China | Niu *et al.*, 2009 |
| Czech | Hillebrand *et al.*, 2004; Milind *et al.*, 2012 |
| Germany: | Mirhosseini *et al.* 2008; Naila *et al.*, 2014 |
| India | Hillebrand *et al.*, 2004; Gattuso *et al.*, 2007 |
| Italy | Hillebrand *et al.*, 2004; Gattuso *et al.*, 2007 |
| Iraq | Al-Snafi, 2016 |
| Japan | Matsubara *et al.*, 1991 |
| Mexico | Favela-Hernández *et al.*, 2016 |
| Pakistan | Stöggl *et al.*, 2006; Intekhab and Aslam, 2009; |
| Spain | Kanaze *et al.*, 2009; Barreca *et al.*, 2014 |
| Sweden | Kolhed and Karlberg, 2005 |
| Turkey | Gómez-Ariza *et al.*, 2004; Selli, *et al.*, 2008 |
| USA | Moore *et al.*, 2001; Abbate *et al.*, 2001; Peterson *et al.*, 2006; Saleem *et al.*, 2010 |

*Traditional uses of Citrus sinensis:*

*Citrus sinensis* can be found widely throughout the world as a good source of vitamin C, which is the famous antioxidant compound that actively participates in building the immune system of the person (Etebu and Nwauzoma, 2014). It has been utilised generally to treat sicknesses like stoppage, cramps, colic, bronchitis, tuberculosis, hack, cold and flu, diarrhoea, obesity, menstrual disorder, angina, hypertension, nervousness, depression and stress (Milind and Dev, 2012).

*Phytochemicals of Citrus sinensis*

*Citrus sinensis* is a treasure trove of secondary metabolites and have different biological activities. Several nutritional elements, such as potassium, magnesium, calcium and sodium (Zhao, 2009) have been identified in this species. Major secondary metabolites present in this species are flavonoids, such as kaempferol (**71**) and its derivatives, naringin (**51**), diosmetin (**72**), and daidzein (**73**) (Figure 1.11) (Hillebrand *et al.*, 2004; Gattuso *et al.*, 2007; Favela-Hernández *et al.*, 2016); coumarins like scoparone (**75**), xanthotoxin (**76**), bergapten (**43**), isopimpinellin (**44**), rutamarin (**47**) and triterpene friedelin (**77**) (Figure 1.11) (Gil-Izquierdo *et al.*, 2001; Ribeiro *et al.*, 2008; Dugrand-Judek *et al.*, 2015); carbohydrates, *e.g.,* sucrose (**78**), fructose (**79**), glucose (**80**) and galactose (**81**) (Figure 1.11) (Kolhed *et al.*, 2005); others including steroids, β-sitosterol (**82**), fatty acids (Rani *et al.*, 2009), peptides (Matsubara *et al.*, 1991), carotenoids, such as lutein (**59**) (Aschoff *et al.*, 2015) and essential oils (Gómez-Ariza *et al.*, 2004; Selli *et al.*, 2007). The major components of the essential oils of *C. sinensis* are listed in Table 1.4.

*Bioactivity of Citrus sinensis*

*Citrus sinensis* is known to possess various bioactivities. Different extracts of *C. sinensis* showed a wide range of antibacterial activity against *Escherichia coli, Pseudomonas aeruginosa*, *Staphylococcus aureus* (Kaviya *et al.*, 2011), *Bacillus subtilis* and *Shigella* (Arooj *et al.*, 2014). According to Trovato *et al.* (1996), *C. sinensis* worked as an antifungal agent by inhibiting the growth of *Candida albicans*. The methanolic extract of this plant

successfully demonstrated its ability to inhibit the malaria parasite *Plasmodium falciparum* (Bhat and Surolia, 2001). *C. sinensis* is considered as one of the most potent plants with antioxidant activity and this activity has been proven in various studies (Atrooz, 2009; Barreca *et al.*, 2014; Garcia *et al.*, 2017)**.** In addition, it has claimed anticancer (Xiao *et al.*, 2009), anti-obesity (Cardile *et al.*, 2015), hypocholesterolaemic (Trovato *et al.*, 1996), relaxant, sedative (Lehrner *et al.*, 2000) and anxiolytic activities (Goes *et al.*, 2012). According to Asgary and Keshvari (2013), *C. sinensis* can reduce the risk of cardiovascular problems. Morrow *et al.* (2009) found a relationship between orange and osteoporosis. When they fed oranges to male rats, they showed improved characteristics in bone structure. *C. sinensis* can be a good candidate to use in sun protection products and may protect from skin cancer, because studies proved that they gave protective activity against ultraviolet rays. Moreover, *C. sinensis* has insect repellent activity (Rossi and Palacios, 2013).

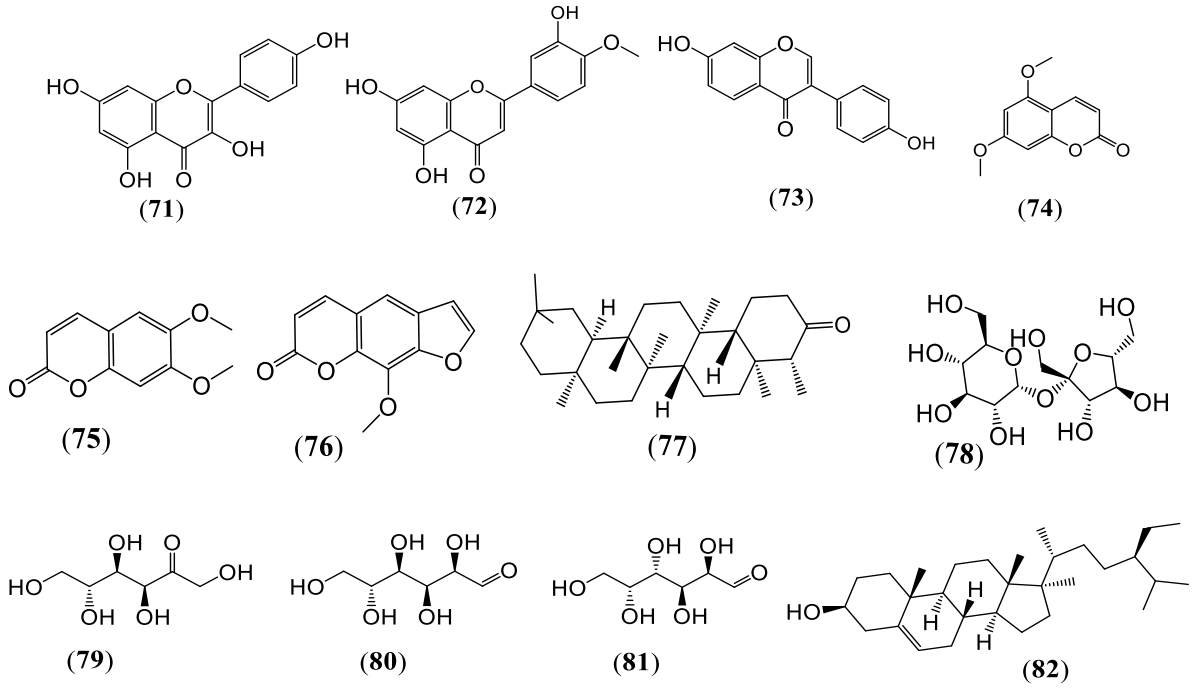


***Figure 1.11**: Structures of compounds **71-82***

Kaempferol (**71**), diosmetin (**72**), daidzein (**73**), limettin (**74**), scoparone (**75**), xanthotoxin (**76**), triterpene friedelin (**77**), sucrose (**78**), fructose (**79**), glucose (**80**), galactose (**81**) and β-sitosterol (**82**)

**Table 1.4**: Compounds identified from the essential oils of *Citrus sinensis*

| **Chemical compounds** | **Reference** |
|---|---|
| 4-Acetyl-1-methylcyclohexene | Selli and Kelebek, 2011 |
| (-)-Carvone | |
| *p*-Coumaric acid | |
| α-Caryophyllene | |
| 3-Carene | |
| Dimethyl trisulfide | |
| Ethyl ethanoate | Gómez-Ariza *et al.*, 2004; Gómez-Ariza *et al.*, 2005; Favela-Hernández *et al.*, 2016 |
| β-Elemene | Selli and Kelebek, 2011 |
| Farnesol | |
| Geraniol | |
| Geranyl acetate | |
| Geranyl pyrophosphate | |
| Guaiacol | |
| Homofuraneol | |
| Limonene | |
| Linalool | Gómez-Ariza *et al.*, 2004 |
| Linalyl acetate | Selli and Kelebek, 2011 |
| Malic acid | |
| 3-Mercapto-2-butanone | |
| Myrecene | |
| *N*-Methyltyramine | |
| 3-Methyl-1-pentanol | |
| Octopamine | |
| 1-Octanol | |
| (*E*)-β-Ocimene | |
| 2-Phenylethanol | |
| α-pinene | |
| Sabinene | |
| Sinensal | |
| Synephrine | |
| Terbutaline | |
| Terpinen-4-ol | |
| α-Terpinene | Gómez-Ariza *et al.*, 2004 |
| γ-Terpinene | Selli and Kelebek, 2011 |
| Tyramine | |
| Valencene | |
| Vanillin | |

### 1.7.2.2 *Citrus grandis* Merr.

*Citrus grandis* is a perennial tree, with a height of around 5-15 m and has , big yellow round pear-shaped fruit of about 15 cm in dimeter. The tree needs around 180-400 days from flowering to the mature fruit stage (Ecocrop, 2018).

*Original and distribution:*

*Citrus grandis* is considered as the first ancestor of all the *Citrus* fruits. It originated in Malaysia and the Malay Archipelago and has tropical distribution (Giovanni and Angelo, 2002). Table 1.5 presents the global distribution of the plant.

**Table 1.5:** Global distribution of *Citrus grandis*

| **Country** | **References** |
|---|---|
| America | Sawamura and Kuriyama, 1988 |
| Bangladesh | Orwa *et al.*, 2009, Singh *et al.*, 2015 |
| Cambodia | Orwa *et al.*, 2009 |
| Chile | Orwa *et al.*, 2009 |
| China | Shih-Chen, 1973; Vinning and Moody, 1997; Zhang and Shaolin, 2000 |
| Haiti | Liogier, 1974 |
| India | Orwa *et al.*, 2009 |
| Indonesia | Orwa *et al.*, 2009 |
| Japan | Mokbel and Hashinaga, 2006 |
| Keyna | Njoroge *et al.*, 2005 |
| Laos | Orwa *et al.*, 2009 |
| Malaysia | Hameed *et al.*, 2008 |
| Philippines | Orwa *et al.*, 2009 |
| South Korea | Lim *et al.*, 2006; Kim *et al.*, 2009 |
| Taiwan | Wu *et al.*,1983; Kuo *et al.*, 2017 |
| Turkey | Steinmetz,1975 |
| Venezuela | Gonzalez *et al.*, 2002 |
| Vietnam | Orwa *et al.*, 2009 |

*Traditional uses of Citrus grandis*

*Citrus grandis* is one of the oldest traditional medicines, which has been used for trating different types of diseases such as oedema, abdominal pain and stomachache. In addition, it is taken orally to prevent or to treat throat pain, fever, anorexia and to cure body

weakness (Rahmatullah *et al.*, 2011). The fruit is used as a cardiac stimulant, antitoxic and to treat stomachache (Arias and Ramón-Laca, 2005). The pulp of *C. grandis* is used as an appetizer (Arias and Ramón-Laca, 2005). The flesh of the fruits is separated from the skin parts and eaten with or without sugar (Lim *et al.*, 2006; Kim *et al.*, 2010). This plant is a part of Chinese medicine for healing cold and to relieve fatigue (Taiping and Shaolin, 2000). In South Korea, leaves are used as a food flavouring and used in making tea (Kim *et al.*, 2010).

*Phytochemicals of Citrus grandis*

Important phytochemical constituents of *C. grandis* are flavonoids (Xi *et al.*, 2014), which are present in high amounts in fruit juice in the form of neohesperidin (**52**), hesperidin (**50**), naringenin (**83**), and naringin (**51**) (Kanes *et al.*, 1993; Kawaii *et al.*, 1999; Xi *et al.*, 2014). In addition, a high level of flavanones, flavones and flavonols are reported to be present in both the free and glycosidic forms (Kanes *et al.*, 1993; Bocco *et al.*, 1998; Kim *et al.*, 2009). On the other hand, most of the studies have mentioned that *C. grandis* contains coumarins and furocoumarins (Kanes *et al.*, 1993; Bocco *et al.*, 1998; Russo *et al.*, 2016). This plant also has sterols and acridone alkaloids, *e.g.*, grandisinine (**84**), prenylcitpressine (**85)**, glycocitrine-I (**86**), citpressine-I (**87**), citrusinine-I (**88**), 5-hydroxynoracronycine (**89**), citracridone-I (**90**), *N*-methylalanine (**91**), preskimmianine (**92**), xanthyletin (**93**), xanthoxyletin (**94**), clausarin (**96**) and *p*-hydroquinone (**97)** (Figure 1.12) (Tian-Shung *et al.*, 1983; Mokbel and Suganuma, 2006). The plant is reported to contain limonoid (**98**) (Boo *et al.*, 2007) and volatile oils (Njoroge *et al.*, 2005) (Table 1.6).

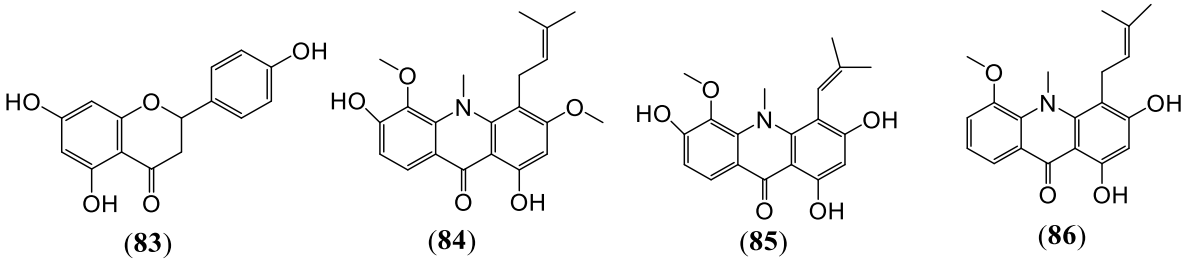


***Figure 1.12**: Structures of compounds **83-98***

Naringenin (**83**), grandisinine (**84**), prenylcitpressine (**85)**, glycocitrine-I (**86**), citpressine-I (**87**), citrusinine-I (**88**), 5-hydroxynoracronycine (**89**), citracridone-I (**90**), *N*-methylalanine (**91**), preskimmianine (**92**), xanthyletin (**93**), xanthoxyletin (**94**), clausarin (**96**), *p*-hydroquinone (**97)** and limonoid (**98**)

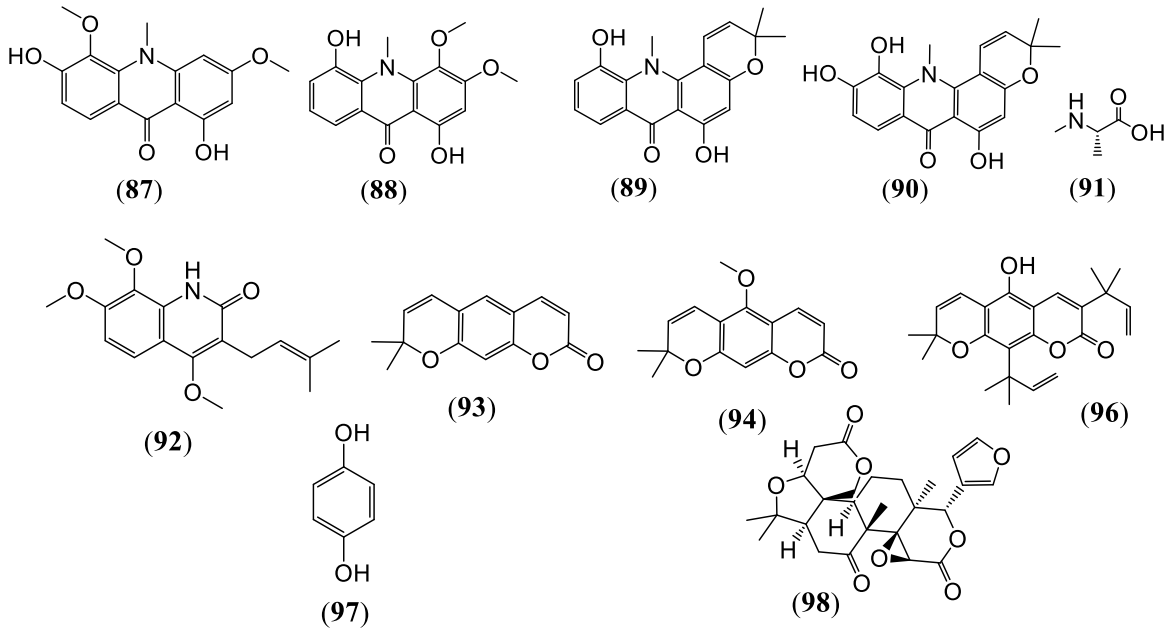


***Figure 1.13*** *(Continued)*: *Structures of compounds* ***83-98***

Naringenin (**83**), grandisinine (**84**), prenylcitpressine (**85)**, glycocitrine-I (**86**), citpressine-I (**87**), citrusinine-I (**88**), 5-hydroxynoracronycine (**89**), citracridone-I (**90**), *N*-methylalanine (**91**), preskimmianine (**92**), xanthyletin (**93**), xanthoxyletin (**94**), clausarin (**96**), *p*-hydroquinone (**97)** and limonoid (**98**)

**Table 1.6**: Compounds identified in essential oils of *Citrus grandis*

| **Compounds *** | **Compounds*** | **Compounds*** |
|---|---|---|
| (*E*)-Carveol | Dodecanal | Neral |
| (*Z*)-Carveol | Elemol | Nerol |
| (*E*)-Carvone | β-Elemene | Nerolidyl acetate |
| (Z)-Carvone | (*E*,*E*)-α-Farnesene | Nonanal |
| Caryophyllene oxide | Geranial | Nonanoic acid |
| *β*-Caryophyllene | Heptyl acetate | α-Pinene |
| (*E*)-Cryophyllene epoxide | Limonene | *β*-Pinene |
| Cedrol | Limonen-10-ol | (*Z*)-Piperitol |
| α-Cedrene | Linalool | Sabinene |
| Citronellal | Linalyl acetate | Sabina ketone |
| α-Copaene | Isothujol | *β*-Sinensal |
| α-Cubebene | Methyl-*N*-methylanthranilate | α- Terpinene |
| Cumin aldehyde | *p*-Mentha-1-en-9-ol | γ-Terpinene |
| Decanal | (*E*)-*p*-2,8-Menthadien-1-ol | α-Terpineol |
| Dihydrocarveol | (*E*)-*p*-Mentha-2,8-dienol | Tetradecenal |

***(Njoroge *et al.*, 2005)**

*Bioactivity of Citrus grandis*

*Citrus grandis* shows potentially useful effects on human health. The antiglycation effect of *C. grandis* extract (0.25-2.00 mg/mL) was approved against fructose-mediated protein oxidation and glycation (Caengprasath *et al.*, 2013) by controlling the blood glucose level of diabetic patients (Kim *et al.*, 2009). Various studies have proven the antioxidant (Lim *et al.*, 2006; Mokbel and Hashinaga, 2006), anti-inflammatory, antimicrobial activity (Kuo *et al.*, 2017) and anticancer activity (Kim *et al.*, 2010). It is also used in cosmetics.

A few studies have focused on the biological effects and chemical composition of *C. grandis* leaves (Kim *et al.*, 2009; Lim *et al.*, 2009). However, the anticancer effect of *C. grandis* fruit giving inhibit ion of human leukaemia cells (U937) was previously reported, and the result obtained indicated the hexane extract inhibited the cancer cells with $IC_{50}$ 60 µg/mL (Lim *et al.*, 2009). Another report showed the anticancer effect of *C. grandis* leaves against human gastric cancer cells (SNU-16), the inhibitory effect of the chloroform extract was $IC_{50}$ 92.15 µg/mL (Yong Moon *et al.*, 2009).

## 1.8 Aims and objectives

The aim of this work was to isolate and characterise the antimicrobial compounds present in three Iraqi medicinal plants from the family Rutaceae: *Citrus grandis*, *Citrus sinensis* and *Ruta chalepensis*. To achieve this aim the following objectives were set:

1. to prepare three types of crude extracts from ground plant material of every plant by successive Soxhlet extraction using the solvents, *n*-hexane, DCM and MeOH;
2. to assess the antimicrobial property of these extracts against various strains of Gram-positive, Gram-negative bacteria and fungi;
3. to follow bioassay-guided fractionation by vacuum liquid chromatography (VLC) and/or solid phase extraction (SPE) leading to the identification of active extracts for isolation of active compounds;

4. to isolate and identify the active compounds using chromatographic and spectroscopic techniques;
5. to determine the minimum inhibitory concentration (MIC) of the active compounds using the resazurin 96-well assay;
6. to carry out anti-MRSA activity testing against various clinical isolates of MRSA strains;
7. to try to understand possible mechanism of actions of active compounds.

# *Chapter 2*

# Materials and Methods

## 2.1 Plant materials

Three Iraqi medicinal plants from the family Rutaceae, *Citrus grandis*, *C. sinensis* and *Ruta chalepensis* (Table 2.1), were selected on the basis of their traditional uses to treat infections, and collected from Diyala, central Iraq at longitude 33.79684° N, and latitude 44.623337° E (Figure 2.1). Plant material were collected in September 2015 and identified in comparison with the voucher specimens held at the National Herbarium of Iraq, where appropriate voucher specimens of this collection were deposited (Table 2.1).

**Table 2.1**: Plant used in study

| Plant name | Voucher number |
|---|---|
| *Citrus grandis* | 15324 |
| *Citrus sinensis* | 6534 |
| *Ruta chalepensis* | 33396 |

***Figure 2.1**: Iraqi political map*

## 2.2. Materials and reagents for phytochemical studies

To carry out the phytochemical analysis of the selected plants, a range of instruments, materials and various chemicals have been used. Table 2.2 summarises instrument, materials and regents for the plant extract preparation and processing.

**Table 2.2**: Materials and reagents used in phytochemical work

| Name | | Details |
|---|---|---|
| **Materials** | Rotary evaporator | Cole-Parmer, UK |
| | Strata C-18-E cartridge | Phenomenex, California-USA |
| | Freeze dryer | Telstar, UK |
| | Silica gel | 60 H, Merck, Germany |
| | Solid phase extraction cartridge | Strata C18-E (55 µm, 70Å), 20 g/60 mL, Giga tubes, Phenomenex, USA |
| | TLC plates | Silica gel on Aluminium foils, Sigma-Aldrich, Germany |
| | Oven | Sciquip, Shrewsbury-UK |
| | UV lamps | Camag, Switzerland |
| | Analytical HPLC | Agilent Technologies, 1200 Infinity Series, Germany<br>Dionex Ultimate 300 diode array detector, Thermo Scientific, Germany. |
| | Preparative HPLC | Agilent Technologies, 1200 Infinity Series, Germany. |
| | Columns | Described in point 2.3.3.4 |
| | Nuclear Magnetic Resonance Spectrometers | Bruker AMX 300 MHz and 600 AMX MHz, Germany |
| **Solvents** | *n*-Hexane | Fisher Scientific, UK |
| | Ethyl acetate (EtOA) | |
| | Dichloromethane (DCM) | |
| | Chloroform ($CHCl_3$) | |
| | Methanol (MeOH), HPLC grade | |
| | Water ($H_2O$), HPLC grade | |
| | Chloroform-$d_3$ ($CDCl_3$) | Cambridge Isotope Laboratories, Inc., USA |
| | Dimethyl sulfoxide-$d_6$ ($C_2D_6OS$) | |
| | Methanol-$d_4$ ($CD_3OD$) | |
| **Reagents** | Anisaldehyde | Sigma-Aldrich, UK |

## 2.3 Phytochemical work

### 2.3.1 Plant preparation

The plant parts were cleaned, sectioned and shade-dried at room temperature. The dried parts were ground in a grinder to prepare the powdered material for Soxhlet extraction.

### 2.3.2 Soxhlet extraction

Extraction of a plant material is the most important initial step in phytochemical and bioactivity processing. Selection of a suitable solvent and extraction technique is necessary to get an optimum extraction yield.

The Soxhlet extraction technique used for extraction of small to moderate volumes of plant materials, consumes less solvent and time. Furthermore, this extraction technique is a continuous extraction which can use solvents of different polarities or mixed solvents. Selection of a suitable solvent and use of reasonable continuous heat is helpful to obtain different types of extracts with high yields (Sarker and Nahar, 2012; Rostagno and Prado, 2013).

Powdered plant material was packed in a thimble made up of filter paper and loaded in the main chamber of a Soxhlet apparatus. The distillation flask filled with an organic solvent was placed on a heating mantle. The Soxhlet chamber along with the condenser was fitted on top of the flask. During each cycle, the chamber gradually filled with warm solvent and after reaching a certain point, the siphon side arm immediately discharges the solvent back down to the distillation flask. The compounds of interest dissolved in that warm solvent were concentrated in the distillation flask (Figure 2.2) (De Castro and Priego-Capote, 2010).

In the present study, the successive extractions were performed using three different solvents of increasing polarity, *viz* ***n***-hexane, DCM and MeOH. Ten cycles were allowed for each extraction. The obtained extracts were concentrated to dryness using a rotary evaporator and stored at 4$^{o}$C for further usage.

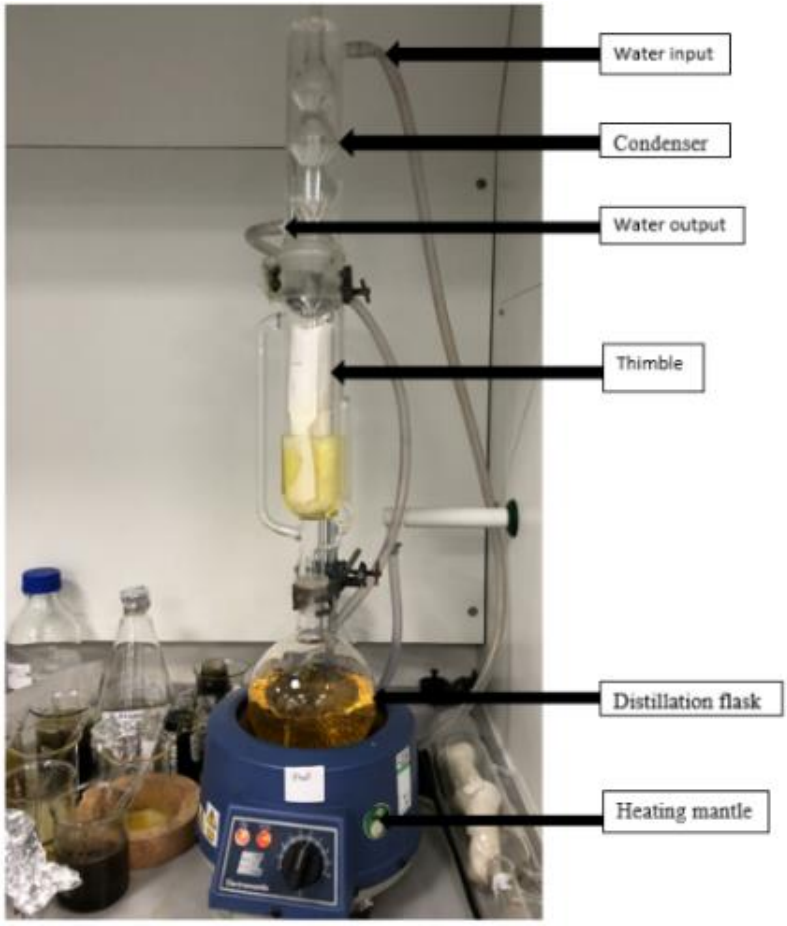


***Figure 2.2**: Soxhlet apparatus*

### 2.3.3 Chromatographic techniques

Chromatography is an analytical technique, which can be used to separate mixture of compounds into individual components. It is used to fractionate a crude extract into different discrete fractions depending on the polarity. Application of a single fractionation technique is usually inadequate for isolation of a single compound from a crude extract. Therefore, different chromatographic techniques were used in this project depending on the polarity of the extracts.

#### 2.3.3.1 Vacuum liquid chromatography (VLC)

Vacuum liquid chromatography (VLC) is a convenient and modified column chromatography method of fractionation on a Silica gel bed as described by Pelletier *et al.* (1986). The VLC method consisted of a sintered glass Buchner filter funnel connected via the flask side arm to a vacuum system (Figure 2.3). The stationary phase on VLC was the

Buchner filter funnel filled with two-thirds of dry silica gel 60H, rinsed with solvent and a vacuum applied to compress the surface and to allow the silica to pack. Selection of eluting solvent usually depends on the solvent that has been used during sample extraction (for example if the sample is a *n*-hexane extract, the rinsing solvent will be *n*-hexane) (Reid and Sarker, 2012). The preparation of sample for the VLC method required the sample to be dissolved in a small amount of the appropriate solvent and then mixed with normal silica gel (70-230 mesh). The mixture was dried and loaded as a uniform thin layer on the top of the funnel. The mobile phase was mixtures of various solvents of increasing polarity and was run under vacuum. The eluted fractions were collected in flasks for further work (Table 2.3). All fractions were evaporated to dryness using a rotary evaporator and analysed by TLC.

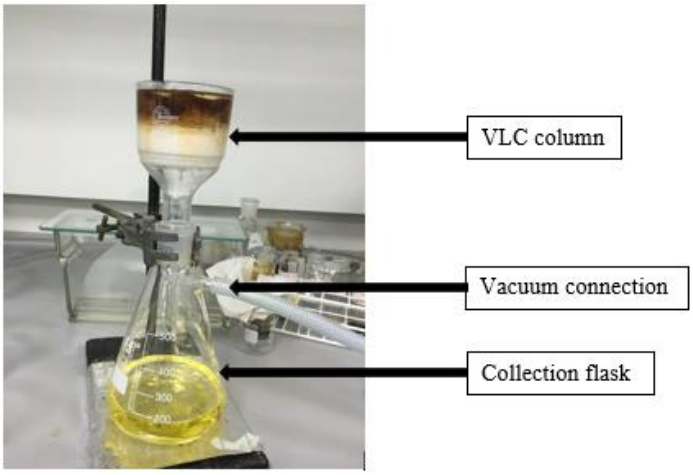


***Figure 2.3**: Vacuum liquid chromatography (VLC)*

### 2.3.3.2 Solid-phase extraction (SPE)

Solid-phase extraction (SPE) is an economical and sometimes automated chromatographic technique used to fractionate liquid mixtures. The SPE technique was very similar to VLC with the only difference being the stationary phase, which was reversed-phase silica ($C_{18}$). Also, in SPE the mobile phase was a mixture of solvents of decreasing polarity (Sarker *et al.*, 2006). Both SPE and VLC operate under vacuum.

A portion of active methanolic extract was dissolved or suspended in 10 mL of 10% MeOH in $H_2O$ and applied to the cartridge, which was previously washed with 50 mL of MeOH and then equilibrated with 100 mL of $H_2O$ sequentially (Figure 2.4). A step gradient protocol was applied with 200 mL of different concentrations of MeOH in water (Table 2.3). Four fractions were collected, dried using a rotary evaporator along with freeze drying and kept for further work (Sarker *et al.*, 2006).

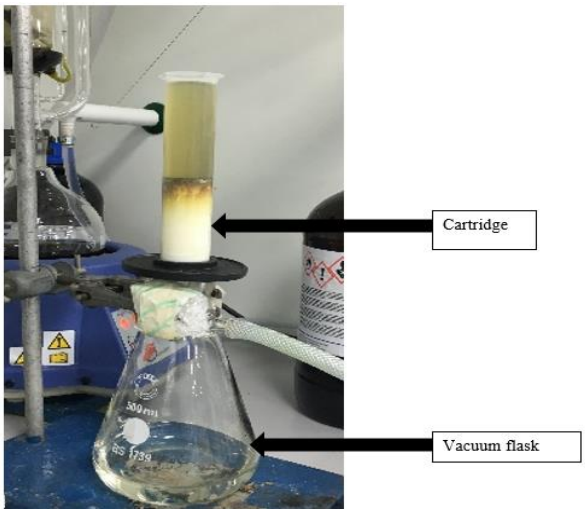


***Figure 2.4**: Solid-phase extraction (SPE)*

### 2.3.3.3 Thin layer chromatography (TLC)

Thin layer chromatography (TLC) is one of the most simple, easy and economical techniques used to determine and monitor compounds during the separation process depending on polarity, absorption and binding to silica. In the current study, this method was used to analyse the secondary metabolites in plant extracts and check the purity of the isolated compounds.

Furthermore, preparative-TLC (PTLC) was applied as an isolation technique for the purification of nonpolar compounds. The TLC plates used in this study were characterised as precoated silica gel 60 $PF_{254}$ aluminium plates with thickness range of 0.5-2.0 mm.

**Table 2.3**: Methods used in VLC and SPE techniques

| **Method** | **Type and method of extracts** | **Fractions** | | | | | | | | | | |
|---|---|---|---|---|---|---|---|---|---|---|---|---|
| | | F1 | F2 | F3 | F4 | F5 | F6 | F7 | F8 | F9 | F10 | F11 |
| **A** | *n*-hexane /VLC | 100% hex | 10% Et/ hex | 20% Et/ hex | 40% Et/ hex | 60% Et/ hex | 80% Et/ hex | 100% Et | _____ | ____ | _____ | _____ |
| **B** | *n*-hexane /VLC | 100% hex | 5% Et/ hex | 10% Et/ hex | 15% Et/ hex | 20% Et/ hex | 50% Et/ hex | 80% Et/ hex | 100% Et | 50% Et/ Ch | 100% Ch | 2% Me/ Ch |
| **C** | DCM/ VLC | 100% Ch | 2% Ch/ Me | 4% Ch/ Me | 6% Ch/ Me | 8% Ch/ Me | 10% Ch/ Me | 20% Ch/ Me | 30% Ch/ Me | ____ | ____ | _____ |
| **D** | MeOH/ SPE | 20% Me/ H | 50% Me/ H | 80% Me/ H | 100% Me | ____ | ____ | _____ | _____ | ____ | ___ | _____ |

hex: *n*-hexane; Me: MeOH, Et: EtOAc; Ch: $CHCl_3$; H: $H_2O$

The processing of a TLC plate involves spotting of the samples on the line around 1.5 cm from the bottom. Then, the plate is transferred to a glass chromatographic chamber containing developing solvent. As the solvent goes up through the TLC plate by the capillary action, the component's spots start developing. In this work, the procedure described above was followed, the TLC plates were dried and visualised under short wave length (254 nm) and long wave length (366 nm) using UV lamps to check the best separation for the target compounds. Anisaldehyde solution (1%) in aqueous $H_2SO_4$ was sprayed over the plate which was then exposed to oven heating at 105 °C for 5 min to detect the spots, which were not detected by UV lights (Gibbons, 2012).

PTLC is a common and most basic method available around the world for compound isolation. This plate can be made from silica, alumina, $C_{18}$ and cellulose, and have thickness range of 0.5-2.0 mm. It should be homogenous to get a good separation. 10-100 mg samples can separated with PTLC (Hostettmann *et al.*, 1986). Table 2.4 below shows the different methods used to analyse and isolate compounds using TLC and PTLC.

**Table 2.4**: Thin layer chromatographic methods

| **Methods** | **Extracts type** | **Mobile phase** |
|---|---|---|
| **E** | *n*-hexane extracts | 10% EtOAc /*n*-hexane |
| **F** | DCM extracts | 5% MeOH/$CHCl_3$ |
| **G** | DCM extract | 100% MeOH |
| **H** | Plant extracts | 100% DCM |
| **I** | RFH4 | 15% EtOAc/*n*-hexane |
| **J** | RFF2-11 | 20 % EtOAc/*n*-hexane |
| **K** | F11 from method B | 25% EtOAc/*n*-hexane |

### 2.3.3.4 High performance liquid chromatography (HPLC)

High performance liquid chromatography (HPLC) is one of the analytical and separation techniques that has been used for determination, separation and purification of compound mixtures.

*Analytical high performance liquid chromatography*

Analytical HPLC was used in this study for detection and preliminary analysis of secondary metabolites in plant extracts and to develop methods for preparative-HPLC. This work was carried out using a Dionex 3000 or an Agilent 1260, both instruments had a binary pump, an autosampler, a column chamber, a degasser and a UV/DAD detector. Before starting, the column was washed with 100% MeOH, 50%-50%, 30%-70% MeOH/water respectively, to wash out all unwanted contaminants tes. The analytical column used in the current study was a Phenomenex Gemini-NX 5 U $C_{18}$ column (150 × 4.6 mm, 5 μm, Phenomenex, USA) or a Hypersil 5 U $C_{18}$ column (150 × 4.6 mm, 5 μm, Phenomenex, USA) and the column temperature was set at 25 °C. The samples were dissolved in MeOH (1 mg/mL) and 10 μL was injected with a flow rate of 1 mL/min and the chromatograms were monitored by variable UV/vis wavelengths between 205 and 366 nm.

*Preparative high performance liquid chromatography*

Reversed-phase preparative HPLC was used for separation and purification of compounds following the developed methods from analytical HPLC. This work was accomplished on an Agilent 1260 infinity series include a binary pump, a degasser, a UV/DAD detector and a column chamber set at on 25ºC. In the case of isolation of compounds from plant extracts, a Phenomenex column LC-18 stainless steel column (150 x 21.2 mm, 5 μm particle size, Phenomenex, USA) was used with a flow rate of 10 mL/min. For the purification of impure compounds or compound mixtures, a Phenomenex semi-preparative column, LC-18 stainless steel (150 x 10 mm, 5 μm particle size, Phenomenex, USA) was used with a flow rate of 2 mL/min. The plant samples were dissolved in MeOH (10 mg/mL) and the HPLC solvents $H_2O$, MeOH, ACN containing 0.1% TFA. Table 2.5 summarizes the developed methods used in HPLC.

**Table 2.5**: HPLC methods used in the current study

| **Methods** | **Description (**All mobile phases containing 0.1% TFA) |
|---|---|
| **L** | Linear gradient 30-100% MeOH in water over 30 min, isocratic 100% MeOH for the next 10 min, linear gradient 100-30% MeOH in water for 5 min, and isocratic 30% MeOH in water for 5 min |
| **M** | Linear gradient 50-80% MeOH in water over 30 min, isocratic 80% MeOH for the next 5 min, linear gradient 80-30% MeOH in water for 5 min, and isocratic 30% MeOH in water for 5 min |
| **N** | Linear gradient 30-100% ACN in water over 30 min, isocratic 100% ACN for the next 5 min, linear gradient 100-30% ACN in water for 5 min, and isocratic 30% MeOH in water for 5 min |
| **O** | Linear gradient 20-80% MeOH in water over 30 min, isocratic 80% MeOH for the next 5 min, linear gradient 80-20% MeOH in water for 5 min, and isocratic 20% MeOH in water for 5 min |
| **P** | Linear gradient 30-100% MeOH in water over 20 min, isocratic 100% MeOH for the next 5 min, linear gradient 100-30% MeOH in water for 5 min, and isocratic 30% MeOH in water for 5 min |
| **Q** | Linear gradient 10-90% ACN in water over 30 min, isocratic 100% ACN for the next 5 min, linear gradient 100-30% ACN in water for 5 min, and isocratic 30% ACN in water for 5 min |
| **R** | Linear gradient 20-80% MeOH in water over 30 min, isocratic 80% MeOH for the next 2 min, linear gradient 80-20% MeOH in water for 2 min, and isocratic 100% MeOH in water for 2min, and isocratic 20% MeOH in water for 5 min |
| **S** | Linear gradient 20-50% ACN in water over 30 min, isocratic 50% ACN for the next 3 min, linear gradient 50-20% ACN in water for 5 min, and isocratic 20% ACN in water for 5 min |
| **T** | Linear gradient 20-80% ACN in water over 30 min, isocratic 80% ACN for the next 5 min, linear gradient 80-20% ACN in water for 5 min, and isocratic 20% ACN in water for 5 min |
| **U** | Linear gradient 30-100% MeOH in water over 18 min, isocratic 100% MeOH for the next 3 min, linear gradient 100-30% MeOH in water for 3 min, and isocratic 30% MeOH in water for 3 min |

### 2.3.3 Isolation of compounds

#### 2.3.3.1 Isolation of compounds from *R. chalepensis* fruits

The dried and ground *R. chalepensis* fruits (206.1 g) were subjected to successive Soxhlet extraction to obtain three extracts, *n*-hexane (9.0 g), DCM (9.37 g) and MeOH (5.36 g). The dried *n*-hexane and DCM extracts were applied to VLC, resulting in seven and eight fractions, respectively, while, the MeOH extract was fractionated by SPE. Active fractions 4 and 11 of the *n*-hexane extract, fraction 7 of the DCM extract, and fractions 2 and 3 of the MeOH extracts were analysed by different chromatographic methods leading to isolation of compounds. Table 2.6 outlines the isolated compounds from the different extracts and fractions from the fruits of *R. chalepensis*.

#### 2.3.3.2 Isolation of compounds from *R. chalepensis* leaves

The leaves of *R. chalepensis* were dried and ground. A portion (293.31 g) of the plant material was subjected to Soxhlet extraction to obtain different extracts, *n*-hexane (9.06 g), DCM (8.18 g) and MeOH (5.33 g). The DCM and MeOH extracts were fractionated using VLC and SPE, respectively. Both fractions 2 and 3 from the MeOH extract along with fraction 7 of the DCM extract were subjected to reversed-phase preparative HPLC to isolate different compounds. Table 2.7 summarizes the isolated compounds from *R. chalepensis* leaves following different methods.

#### 2.3.3.3 Isolation of compounds from *R. chalepensis* stem

To isolate compounds from *R. chalepensis* stem, powdered material (243.3 g) was extracted to obtain three extracts, *n*-hexane (5.4 g), DCM (3.01 g) and MeOH (5.40 g). Only fractions 2 and 3 from the MeOH extract were submitted to reversed-phase preparative-HPLC to isolate the compounds as listed in Table 2.8 with their retention time.

**Table 2.6**: Isolated compounds from *R. chalepensis* fruits

| Extract | Fraction | Methods | $R_f$ value | Retention time ($t_R$) in min | Compounds |
|---|---|---|---|---|---|
| *n*-Hexane | F4 | I | 0.6 | - | **46** |
| | | | 0.5 | - | **47** |
| | F11 | K | 0.20 | - | **42** |
| | | | 0.19 | - | **43** |
| | | | 0.47 | - | **99** |
| DCM | F7 | M | - | 7.19 | **107** |
| | | | - | 10.41 | **105** |
| | | | - | 12.77 | **99** |
| | | | - | 15.15 | **42** |
| | | | - | 18.65 | **41** |
| | | | - | 26.10 | **46** |
| Methanol | F2 | **L** | - | 8.30 | **106** |
| | | | - | 16.02 | **48** |
| | | | - | 16.99 | **101** |
| | | | - | 17.78 | **103** |
| | | | - | 18.64 | **105** |
| | | | - | 21.43 | **44** |
| | | | - | 22.73 | **42** |
| | RFF2-11 | **J** | - | 0.19 | **43** |
| | | | - | 0.47 | **99** |
| | F3 | **L** | - | 18.50 | **48** |
| | | | - | 24.67 | **41** |
| | | | - | 25.15 | **104** |
| | | | - | 26.37 | **46** |
| | | | - | 26.92 | **45** |
| | | | - | 27.94 | **47** |

**Table 2.7**: Isolated compounds from *R. chalepensis* leaves

| Extract | Fraction | Methods | Retention time ($t_R$) | Compounds |
|---|---|---|---|---|
| DCM | F7 | **O** | 13.03 | **105** |
| | | | 14.70 | **99** |
| | | | 20.53 | **107** |
| | | | 24.85 | **45** |
| Methanol | F2 | **L** | 13.34 | **43** |
| | | | 15.73 | **48** |
| | | | 20.41 | **42** |
| | | | 21.28 | **99** |
| | RLF2-5 | **U** | 10.85 | **101** |
| | | | 11.84 | **102** |
| | RLF2-7 | **P** | 10.52 | **48** |
| | | | 11.01 | **100** |
| | | | 14.56 | **105** |
| | F3 | **L** | 12.53 | **48** |
| | | | 16.05 | **105** |
| | | | 17.69 | **43** |
| | | | 18.09 | **99** |
| | | | 19.03 | **42** |
| | | | 20.05 | **107** |
| | | | 23.39 | **45** |
| | | | 24.57 | **46** |

**Table 2.8**: Isolated compounds from *R. chalepensis* stem

| Extract | Fraction | Retention times ($t_R$) | Compounds |
|---|---|---|---|
| Methanol | F2 | 11.56 | **108** |
| | | 12.5 | **48** |
| | | 14.7 | **102** |
| | F3 | 20.64 | **99** |
| | | 21.11 | **42** |
| | | 22.38 | **43** |
| | | 23.01 | **107** |
| | | 27.03 | **45** |
| | | 28.5 | **46** |

### 2.3.3.4 Isolation of compounds from *C. grandis* leaves

The air-dried and powdered leaves (351.0 g) of *C. grandis* were Soxhlet extracted sequentially with solvents of increasing polarity to obtain three extracts, *n*-hexane (5.9 g), DCM (13.5 g) and MeOH (15.9 g). The VLC fractionation of the DCM extract afforded seven fractions. Using the method **T** in reversed-phase preparative-HPLC, six pure compounds were separated from fraction 7 of the DCM extract. Table 2.9 summarizes the separated compounds along with their retention times.

**Table 2.9:** Isolated compounds from *C. grandis*

| Extract | Fraction | Retention time ($t_R$) | Compounds |
|---|---|---|---|
| DCM | F7 | 14.58 | **112** |
| | | 19.00 | **111** |
| | | 20.27 | **115** |
| | | 21.19 | **57** |
| | | 23.93 | **114** |
| | | 28.45 | **50** |

### 2.3.3.5 Isolation of compounds from *C. sinensis* leaves

The air-dried and powdered leaves of *C. sinensis* (194.58 g) were Soxhlet extracted sequentially with solvents of increasing polarity to obtain three extracts, *n*-hexane (6.15 g), DCM (10.2 g) and MeOH (14.3 g). The DCM extract was fractionated using VLC to afford seven fractions. Fraction 7 was subjected to reversed-phase preparative-HPLC using the method **N** to isolate five compounds (Table 2.10).

**Table 2.10:** Isolated compounds from *C. sinensis* leaves

| Extract | Fraction | Retention time ($t_R$) | Compounds |
|---|---|---|---|
| DCM | F7 | 20.39 | **57** |
| | | 21.36 | **114** |
| | | 22.32 | **112** |
| | | 31.61 | **115** |
| | | 33.45 | **50** |

### 2.3.3.6 Isolation of compounds from *C. sinensis* peels

The Soxhlet extraction of the air-dried and ground peels of *C. sinensis* (393.39) produced three extracts, *n*-hexane (7.34 g), DCM (12.7 g) and MeOH (25.17 g). The DCM and the MeOH extracts were fractionated by VLC and SPE, respectively. Fractions 2 and 3 of the MeOH extract and fractions 6 and 7 of the DCM extract were subjected to reversed-phase preparative-HPLC using different methods to isolate various compounds (Table 2.11).

**Table 2.11:** Isolated compounds from *C. sinensis* peels

| **Extract** | **Fractions** | **Methods** | **Retention time ($t_R$)** | **Compounds** |
|---|---|---|---|---|
| DCM | F6 | **S** | 28.28 | **111** |
| | | | 32.00 | **57** |
| | | | 33.21 | **117** |
| | | | 34.35 | **110** |
| | | | 37.03 | **116** |
| | | | 39.84 | **113** |
| | F7 | **T** | 14.01 | **48** |
| | | | 17.70 | **51** |
| | | | 19.74 | **111** |
| | | | 21.75 | **57** |
| | | | 22.42 | **117** |
| | | | 23.03 | **110** |
| | | | 24.33 | **116** |
| MeOH | F2 | **R** | 13.78 | **48** |
| | | | 15.03 | **119** |
| | | | 15.50 | **101** |
| | | | 18.28 | **51** |
| | | | 19.18 | **50** |
| | F3 | **R** | 17.56 | **48** |
| | | | 26.13 | **116** |
| | | | 28.33 | **110** |
| | | | 28.82 | **57** |

## 2.4 Identification and characterisation of isolated compounds

To determine the molecular structures and chemical formula of the isolated compounds in this study, different spectroscopic methods were used, *e.g.*, ultraviolet (UV), Nuclear Magnetic Resonance (NMR) and Mass spectroscopy (MS).

### 2.4.1 Nuclear Magnetic Resonance (NMR) spectroscopy

NMR is a powerful spectroscopic tool that provides information to elucidate chemical structures of compounds. The method involves exposing atomic nuclei of a sample to a magnetic field linked with electromagnetic radiation with specific frequency. By detecting the absorption signals, one can acquire an NMR spectrum (Günther, 2013). Based on these signals, a compound structure can be elucidated. Structure can be confirmed by applying variaous types of NMR experiments 1 dimention (1D) experiments include proton (1H) and carbon (13C) NMR while 2 dimention (2D) NMR experiments include $^{1}$H-$^{1}$H COSY (Correlation Spectroscopy), DEPT 135 (Distortionless Enhancement by Polarization Transfer), HMBC ($^{1}$H-$^{13}$C Heteronuclear Multiple Bond Correlation Spectroscopy) and HSQC ($^{1}$H-$^{13}$C Heteronuclear Single Quantum correlation) (Silverstein and Bassler, 1962; Breitmaier and Sinnema, 1993). The samples were dissolved in appropriate amounts from deuterated solvents and theses solvents were calibrated by specific chemical shifts summarized on Table 2.12. The NMR experiments were performed on a Bruker AMX 300 MHz or AMX 600 MHz.

#### 2.4.1.1 Proton ($^{1}$H) NMR spectroscopy

The $^{1}$H (Figure 2.5) is one of the basic, essential and simple experiments providing important information about H number of protons (signals), chemical shift (measured in ppm), proton neighbour, coupling constant and integration. The different signals of protons indicates protons with different magnetic environments. The signals in chemical shift indicates proton position. The neighbouring ions causes shielding (up field) or deshielding (down field) of the protons, which effects its position in the chemical shift. Spin-spin splitting appears of equivalent hydrogens in a compound; the proton can be a single peak (s)

when there is no equivalent hydrogens otherwise it will be doublet (*dd),* triplet (t) or multipled (m). The coupling constant (*J* value measured in Hz) is the distance value between the doublet, triplet or multiplied protons. Integration indicates number of hydrogens and is presented under the baseline of spectra (Silverstein and Bassler, 1962; Breitmaier and Sinnema, 1993).

**Table 2.12**: Chemical shifts for deuterated solvents used in this study

| Solvents | Chemical shifts δ in ppm | |
|---|---|---|
| | $^{1}H$ | $^{13}C$ |
| Chloroform-*d* ($CDCl_3$) | 7.26 | 77.36 |
| Dimethyl sulfoxide-$d_6$ (DMSO-$d_6$) | 2.5; 3.3 | 39.9 |
| Methanol-$d_4$ ($CD_3OD$) | 3.33 | 49.15 |

### 2.4.1.2 Carbon ($^{13}C$) NMR spectroscopy

The $^{13}C$ NMR (Figure 2.6) is an important experiment to identify all carbon atoms in an organic molecule. This experiment provides the number and types of carbons present in the molecule. The position of the carbon signal by chemical shift helps to identif to which functional groups are connected to carbons. All carbon signals must be in one direction (Silverstein and Bassler, 1962; Breitmaier and Sinnema, 1993).

### 2.4.1.3 Distortionless Enhancement by Polarisation Transfer (DEPT-135)

DEPT carbon (Figure 2.7) distinguishes carbons numbers and full analysis of carbon atoms. The carbon signal of methine (-CH), methyl ($-CH_3$) will be on one side and the methylene ($-CH_2$) be on the other side (Figure 2.7) (Silverstein and Bassler, 1962).

### 2.4.1.4 Homonuclear Correlation Spectroscopy (COSY)

This two-dimensional experiment (2D) (Figure 2.8) includes two proton axes, and the cross plot between them determines their correlation presenting the coupling protons on molecule. Thus, the *HH* COSY indicates the connectivities between *HH* to be *geminal*, *vicinal* or *w*-relationships of the H atoms of a molecular and the associated structural units (Silverstein and Bassler, 1962; Breitmaier and Sinnema, 1993).

#### 2.4.1.5 Heteronuclear Single Quantum Coherence Spectroscopy (HSQC)

HSQC (Figure 2.9) is a two-dimensional experiment (2D) revealing the direct correlation from proton to attached carbon. The HSQC has the $^{1}H$ NMR spectrum on top axis and $^{13}C$ NMR spectrum on side axis. The HSQC identifies protons which are coupled to carbons (Silverstein and Bassler, 1962; Breitmaier and Sinnema, 1993).

#### 2.4.1.6 Heteronuclear Multiple Bond Correlation (HMBC)

HMBC is powerful experiment that shows correlations between carbons and hydrogens that are separated by two or more chemical bonds. HMBC is used to assign the quaternary and carbonyl carbons (Figure 2.10) (Silverstein and Bassler, 1962; Breitmaier and Sinnema, 1993).

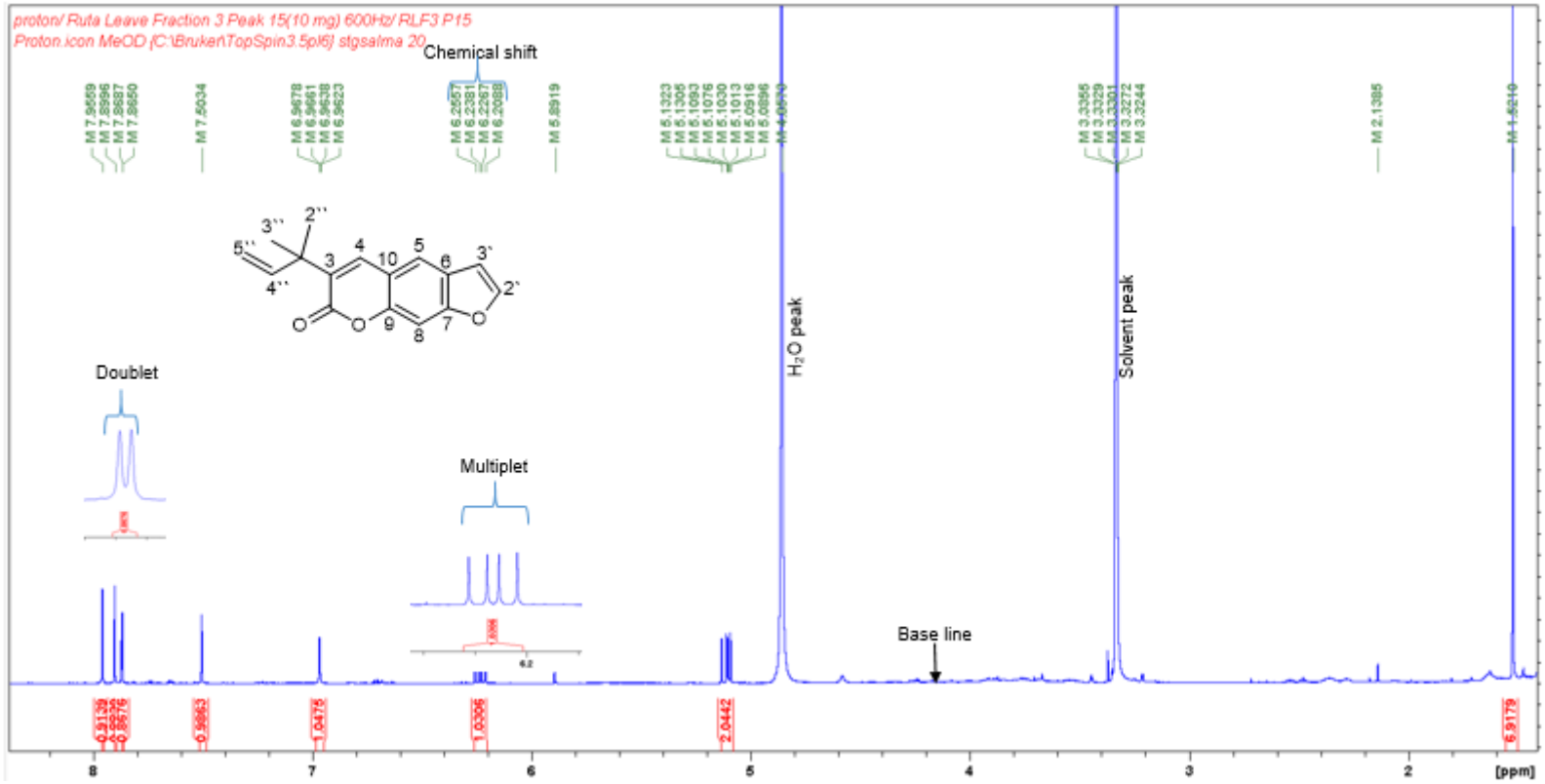


***Figure 2.5**: Proton ($^1H$) NMR experiment*

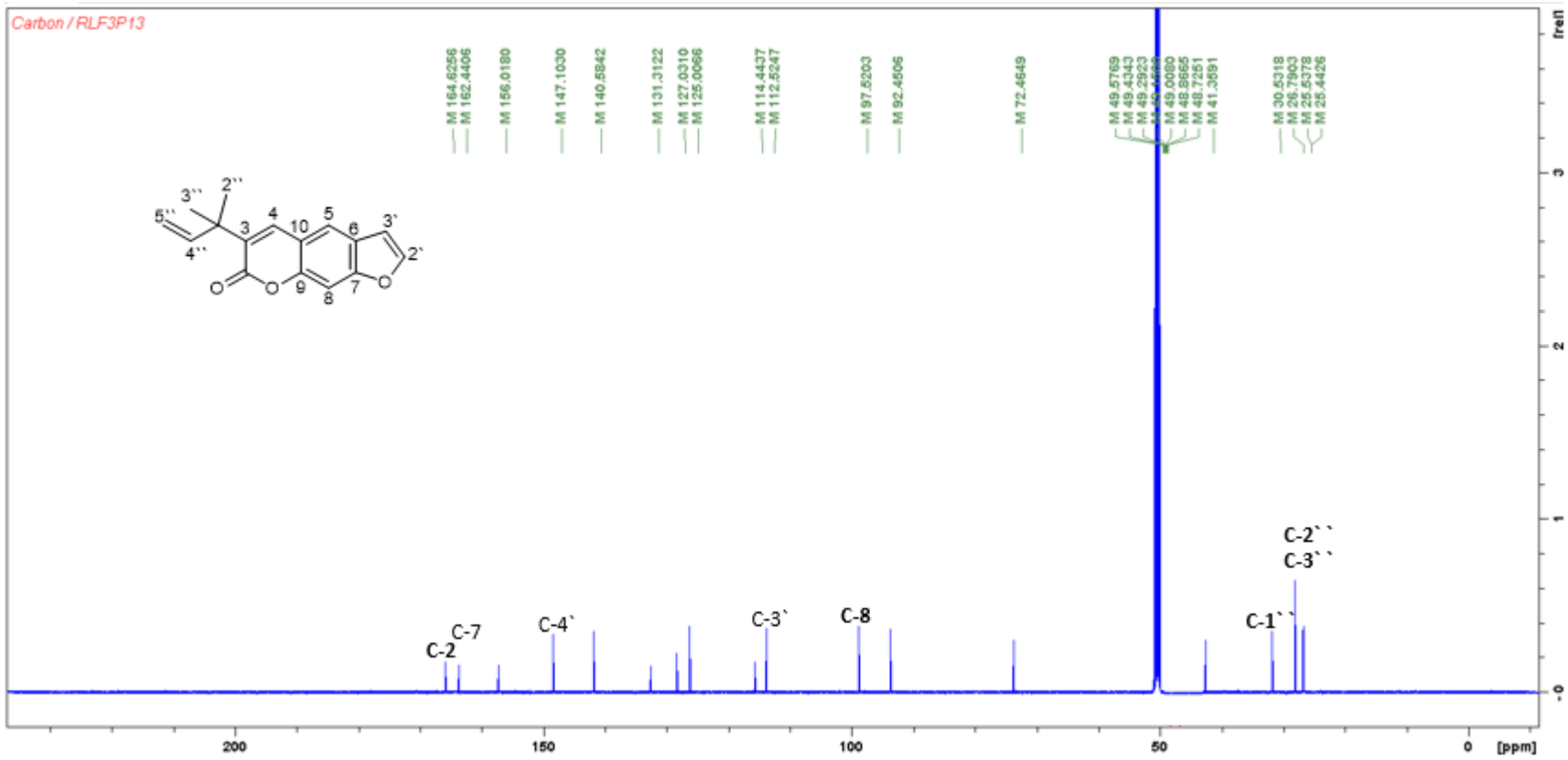


***Figure 2.6**: Carbon ($^{13}C$) NMR experiment*

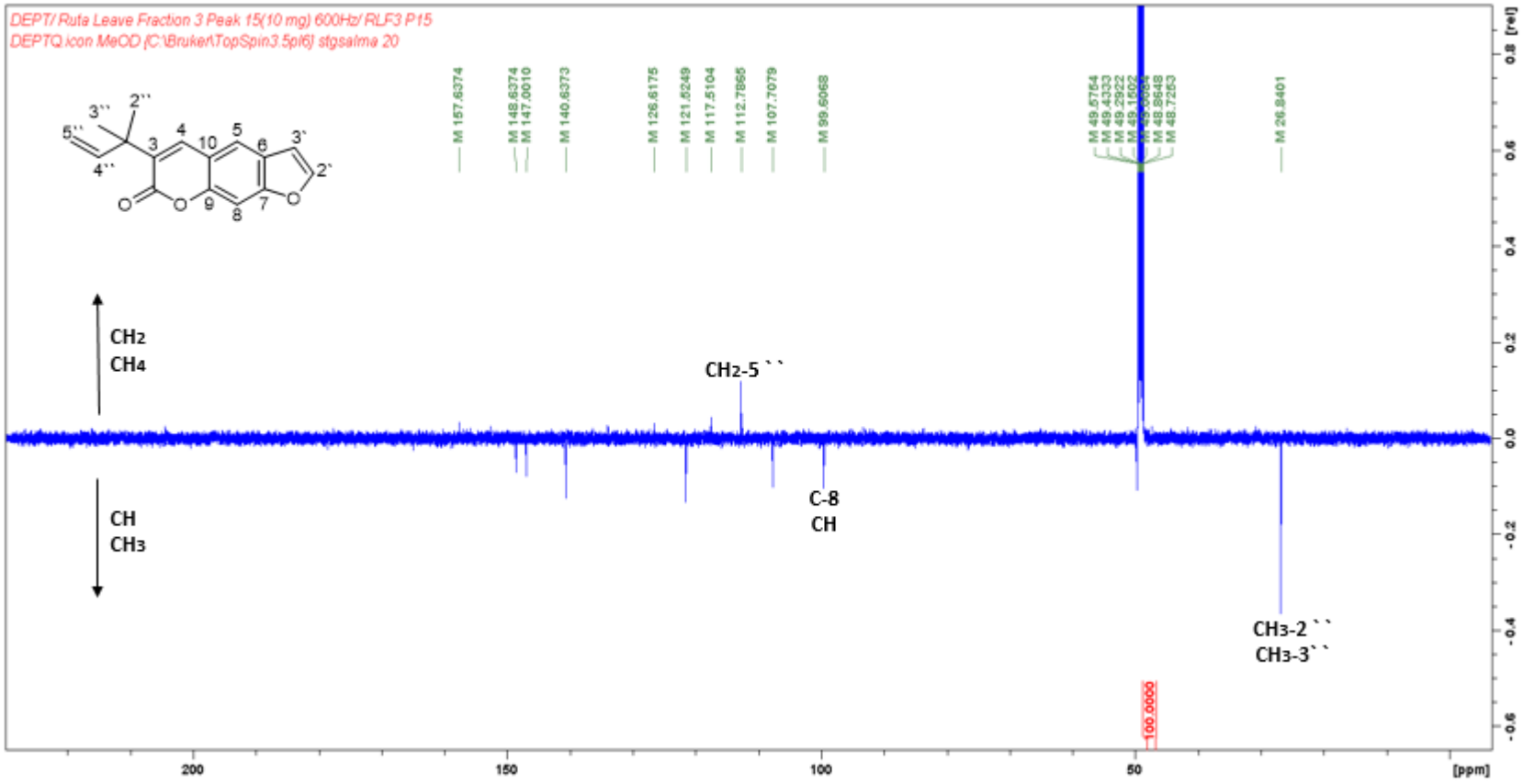


***Figure 2.7**: DEPTQ NMR experiment*

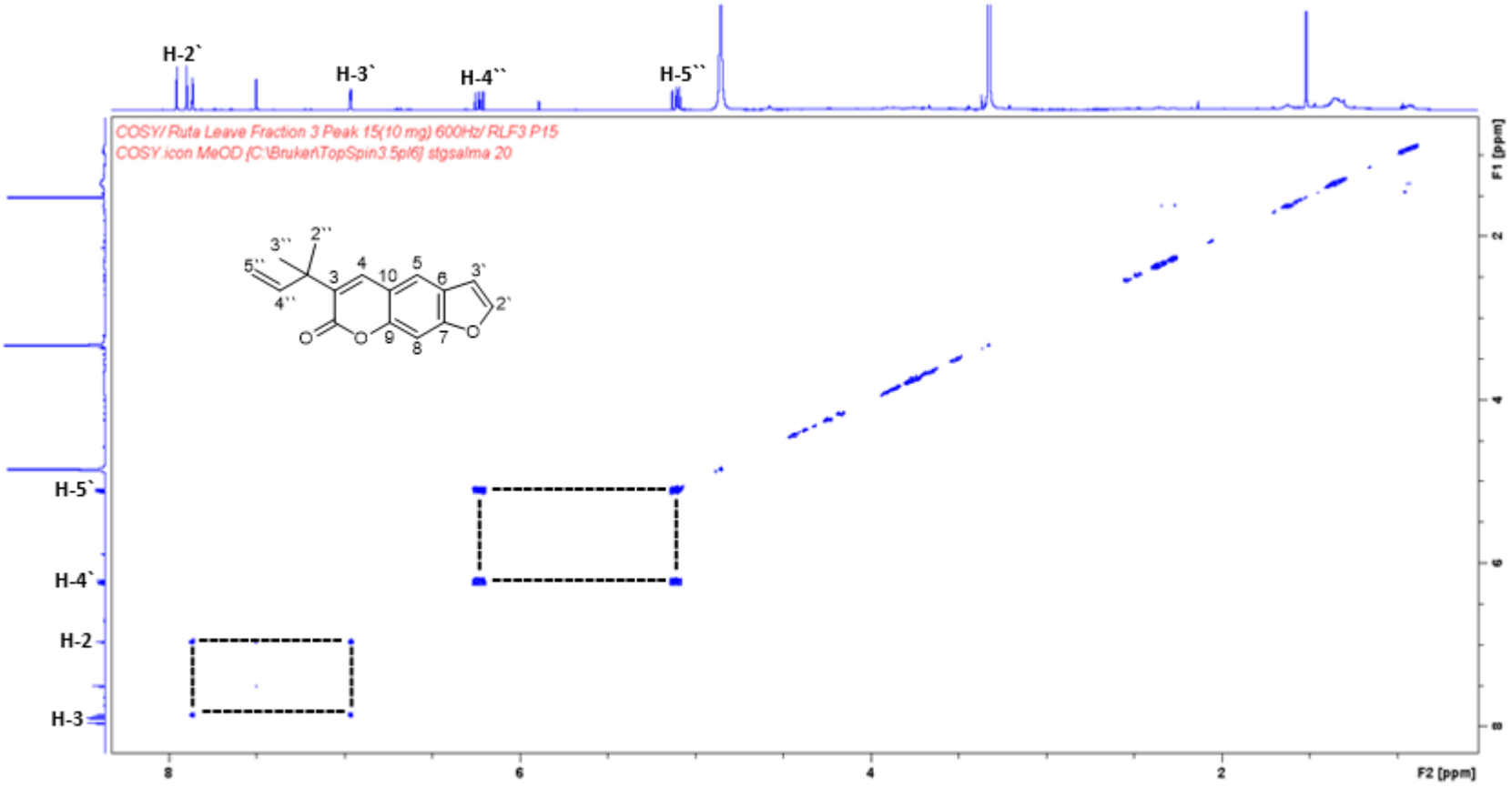


***Figure 2.8**: COSY NMR experiment*

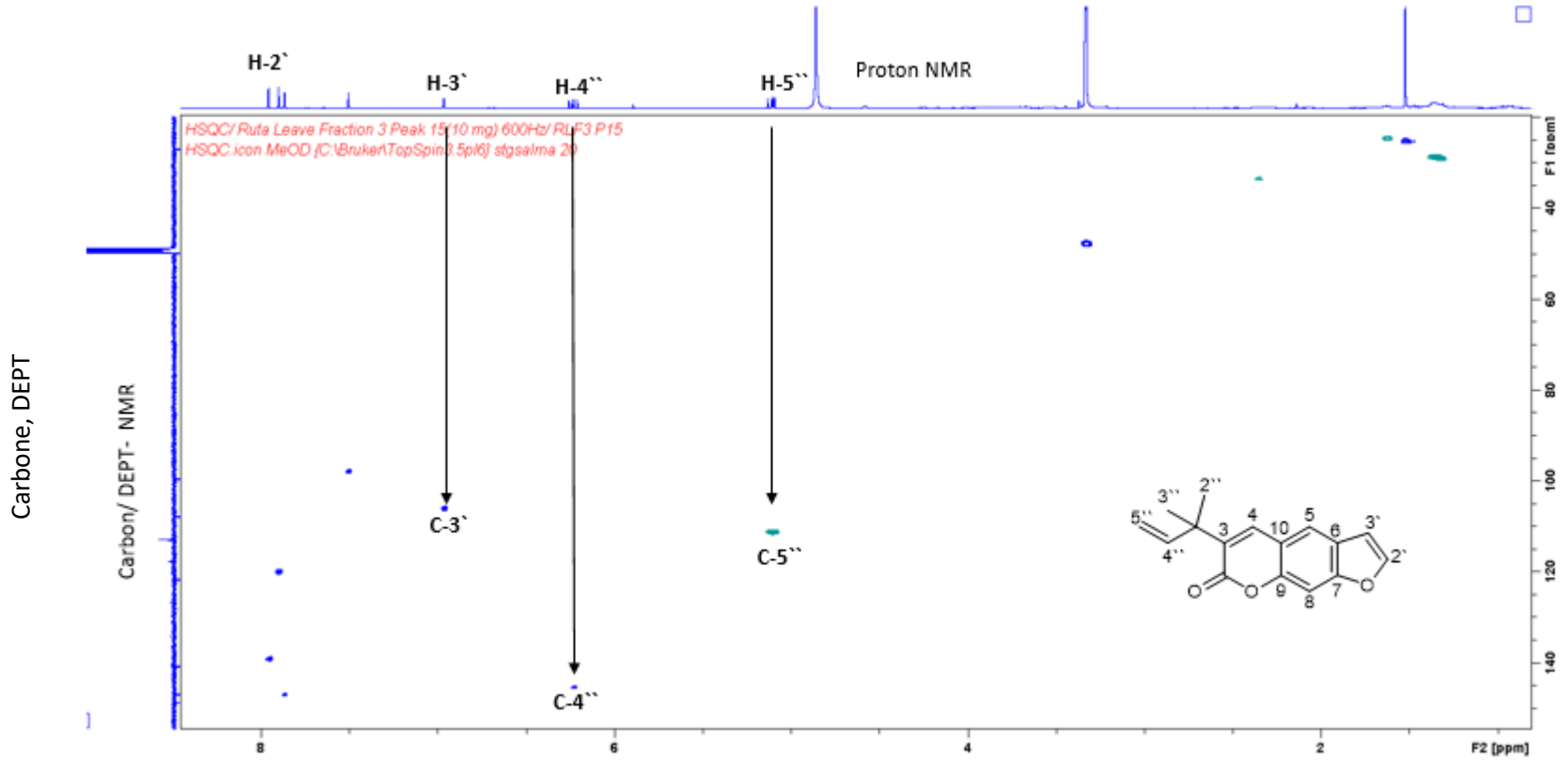


***Figure 2.9**: HSQC NMR experiment*

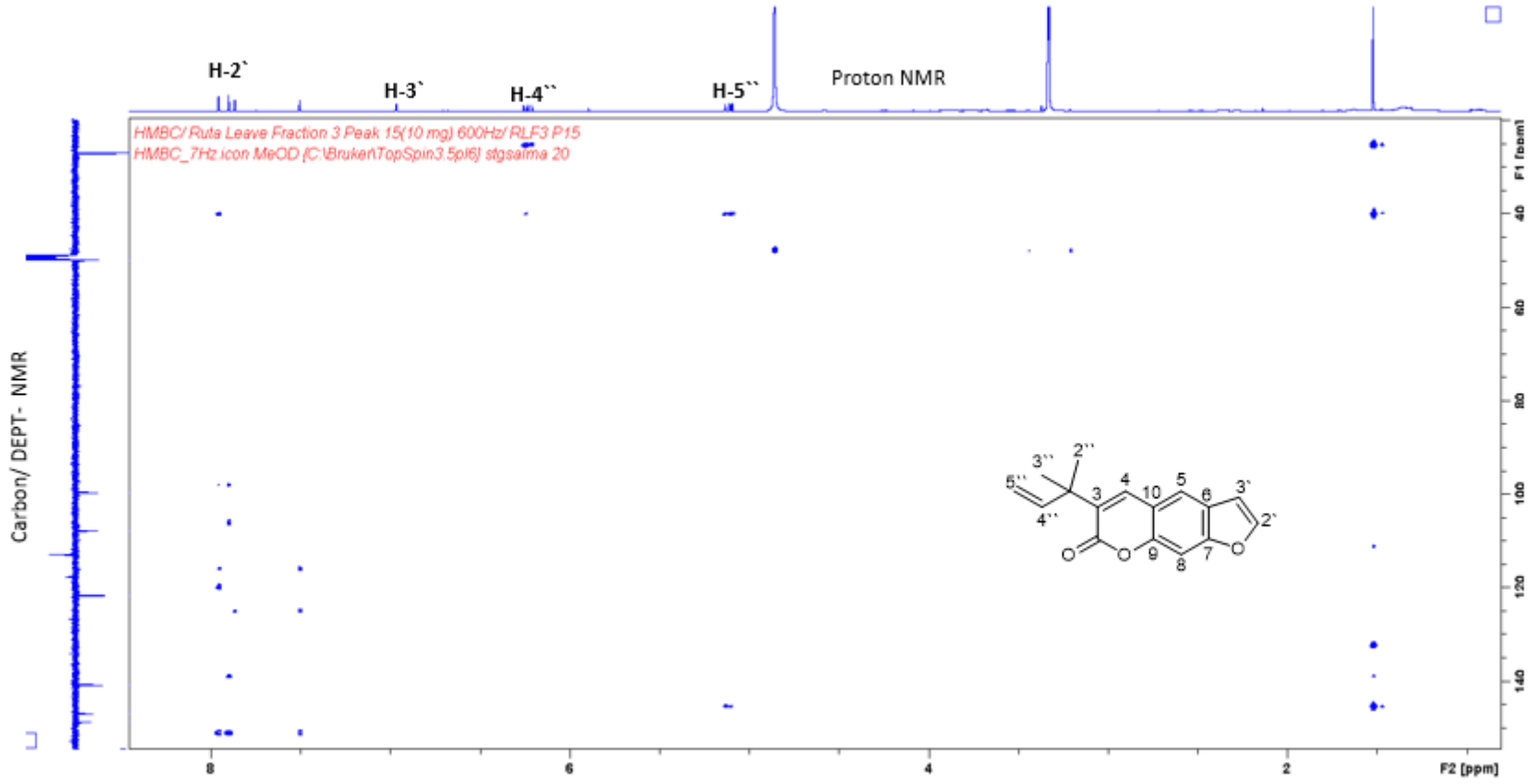


***Figure 2.10**: HMBC NMR experiment*

### 2.4.2 Mass spectroscopy (MS)

Mass spectroscopy is one of the most powerful useful authoritative analytical techniques to determine the molecular weight of compounds and the molecular formula. The MS instrument contains an ion source, mass analyser and a detector operated under high vacuum conditions. The main principle of MS is generates of ions either from organic or from an organic compounds. Each molecular ion undergoes a fragmentation process and, each of these ions are then separated by mass spectrometry depending on the mass ratio to their charge. Then the quantity of each type of ion is measured (Gross, 2017). In this study MS was carried out using High resolution mass spectra (HR MS) by the National Mass Spectrometry Facility (NMSF) (Swansea, UK) on Xevo G2-S ASAP or LTQ Orbitrap XL1 spectrometers. Low and High resolution MS analyses were also obtained at LJMU; HR-MS using Agilent 6200 Series Accurate-Mass Time-of-Flight (TOF) LC/MS using electro spray ionisation (ESI) in positive ion mode connected to an Agilent auto-sampler injection system. The samples were dissolved in MeOH and the mass spectrum was recorded relating to their mass to charge range at 1700 *m/z*. The column temperature was 30ºC.

## 2.5 Antimicrobial study

Various *in vitro* laboratory methods are in use to screen the antimicrobial activity of extracts, fractions and pure compound. In the current study, two of the major phenotypic and sensitive methods were used: disk diffusion method and resazurin assay, for determining the susceptibility of a bacterial isolate. Assessment of the nature of the inhibitory effect (bactericidal or bacteriostatic) and molecular method like methicillin-resistant *Staphylococcus aureus* (MRSA) were applied to establish the direct effect of the antimicrobial agent. All details of the strains with their National Collection types of Culture (NCTC) and American Type Cell Culture Collection (ATCC) number, cultured media, materials and other reagents used in this process are described in Table 2.13. The microbial strains were cultured in nutrient media and all the extracts, fractions and pure compounds

were screened for their potential antimicrobial activity against the selected microbes. A group of antibiotics were used as positive controls.

### 2.5.1 Disk diffusion method

The primarily screening of all extracts were performed using the disk diffusion method, which is one of the common clinical microbiology tests. In this procedure, one single colony from the stock was inoculated in to 100 mL of nutrient broth and incubated overnight at 35 ± 2 °C. After the incubation, microbial strains were adjusted to a McFarland Standard of 0.5 using a Spectrophotometer. Using a micropipette, 200 µL of calibrated nutrient broth was added to a pre-prepared Petri dish with 20 mL agar broth and evenly spread using a swap stick. Disks prepared by filter paper (Whatman, no.1) were cut in circles of 6 mm diameter and sterilized by autoclave. 20 µL from the extract (10 mg/mL) was added to the disk and left to dry for 30 mint in a flow hood or 3h at room temperature. The inoculated disc was placed on the agar surface of the Petri dish and incubated under suitable conditions. In general, the antimicrobial agent is spread in the agar and inhibits the growth of the microorganisms, with the inhibition zone diameters measured by a ruler.

### 2.5.2 Resazurin assay

The modified resazurin test described by Sarker *et al.* (2007) was used to determine the MIC utilising a microtitre-plate. The key feature of this assay is the use of a standard concentration of bacterial suspension. This assay was performed under aseptic conditions.

#### 2.5.2.1 Preparation of standard microbial colonies

The classical method to measure turbidity of microbial strains is to adjust the sample to Macfarland standards at 0.5. In fact, this process is unable to give a standardised number of colony-forming unit (CFU) for all strains due to the difference in optical densities of the different microbe species. In the current study, microbial strains were cultured in 20 mL nutrient agar on Petri dishes and incubated for 12-48 h at 35 °C. Single colonies from incubated plates were transferred to sterilized tubes containing 100 mL nutrient broth and incubate tubes at 35 °C for 24 -48 h. After the incubation, the tubes were centrifuged at 4000 rpm for 5 min. The supernatant was discarded and 20 mL sterile normal saline was added to

the tubes and again centrifuged at the same conditions. Centrifugation was repeated until the supernatant become clear. A spectrophotometer was used at 500 nm to determine the optical density of the bacterial suspension with dilution factor and calculations to obtain a concentration of $5 \times 10^6$ cfu/mL.

**Table 2.13**: Strains, antibiotics, reagents and materials used for antimicrobial activity

| | | | |
|---|---|---|---|
| Microbial strains | Bacterial strain | | NCTC/ ATCC number |
| | Gram-positive | *Micrococcus luteus* | NCTC 7508 |
| | | *Staphylococcus aureus* | NCTC 12981 |
| | Gram-negative | *Escherichia coli* | NCTC12241 |
| | | *Pseudomonas aeruginosa* | NCTC 12903 |
| | | | |
| | Fungal strain | | |
| | *Candida albicans* | | ATCC 90028 |
| | | | |
| Antibiotics | Name | | Product details |
| | Ciprofloxacin | | Sigma-Aldrich, Israel |
| | Nalidixic acid | | Sigma, Germany |
| | Chloramphenicol | | Acros, USA |
| | Gentamicin | | Sigma-Aldrich, USA |
| | Nystatin | | Sigma, Germany |
| | | | |
| Reagents | Nutrient broth | | Sigma-Aldrich, Spain |
| | Agar broth | | |
| | Resazurin sodium salt | | Aldrich, USA |
| | Normal saline prepared from sodium chloride | | Sigma, UK |
| | | | |
| Materials | Spectrophotometer | | BMG Lab Teach, UK |
| | 96 well plate | | Falcon, USA |

#### 2.5.2.2 Preparation of resazurin solution

Resazurin is a blue dye sodium salt. The resazurin solution was prepared by dissolving 1 mg of resazurin in 5 mL of sterile distilled water. A vortex mixer was used to ensure that it was a well-dissolved and homogenous solution. Resazurin was used in this assay as an indicator of cell growth.

#### 2.5.2.3 Preparation of tested materials

The stock concentration was prepared by dissolving the tested materials in 10% (v/v) DMSO or sterilized water. The stock concentration was 10 mg/mL for crude extracts, while 1 mg/mL for the fractions and pure compounds.

#### 2.5.2.4 Preparation of 96 well plates

All wells on 96 plates were filled with 50 µL sterilized normal saline. The test material (100 µL) was added to the first row of the plate and serial dilutions were made using multichannel pipettes by transferring 50 µL. Resazurin (10 µL) was added to all wells and finally 10 µL of bacterial suspension ($5\times10^6$ cfu/mL) was added to each well. To prevent bacterial dehydration, each plate was wrapped loosely with cling film. Every plate contained an antibiotic as a positive control for the bacterial stain, and they were ciprofloxacin, nalidixic acid, gentamacin and chloramphenicol, while for *C. albicanuis*, nystatin was used.

#### 2.5.2.5 Result interpretation

The normal resazurin colour is blue. During incubation, if the test materials inhibited the microorganisms they acquire the resazurin's blue colour, or become purple or colourless, which is considered as a positive result. Whereas, the development of pink colour represents no effect of the test materials on the microbes. The lowest concentration at which the colour change occurs is considered as an MIC (minimum inhibitory concentration) value. The mean of three values were calculated.

## 2.6 Determination of bacteriostatic or bactericidal property

To determine whether the compounds are bacteriostatic or bactericidal, 20 mL nutrient agar were poured in empty Petri dish and incubated at 37°C for 24 h. Under aseptic condition, 100 µL of culture from the rows of MIC in the microtitre plates was transferred to a Petri dish and incubated at 37°C for 24 h. Any microbial regrowth indicated bacteriostatic, and no growth indicated bactericidal activity of the test sample.

# *Chapter 3*

# Results and Discussion

## 3.1 *Ruta chalepensis* L.

### 3.1.1 Extraction

The Soxhlet extraction, sequentially with *n*-hexane, dichloromethane (DCM) and methanol (MeOH), of four different parts of *Ruta chalepensis* afforded three different extracts for each of the plant parts, giving a total of 12 different extracts of varying extraction yields (Table 3.1). The highest percentage yield of extraction of *R. chalepensis* was for the *n*-hexane fruit extract (4.44%), and the lowest percentage was 0.45% for the DCM stem extract.

**Table 3.1**: Percentage yield of *R. chalepensis*

| ***Ruta chalepensis* parts** | **Powder weight (g)** | **Extract type** | **% Yield** |
|---|---|---|---|
| Fruit | 103.05 | *n*-Hexane (RFH) | 4.44 |
| | | DCM (RFD) | 4.05 |
| | | MeOH(RFM) | 5.81 |
| Stem | 81.1 | *n*-Hexane (RSH) | 0.64 |
| | | DCM (RSD) | 0.45 |
| | | MeOH(RSM) | 10.0 |
| Leaves | 97.77 | *n*-Hexane (RLH) | 3.93 |
| | | DCM(RLD) | 2.18 |
| | | MeOH (RLM) | 3.87 |
| Root | 109.89 | *n*-Hexane (RRH) | 2.42 |
| | | DCM (RRD) | 1.50 |
| | | MeOH (RRM) | 2.13 |

### 3.1.2 Preliminary analytical TLC screening

All the *n*-hexane and DCM extracts of *R. chalepensis* parts were subjected to analytical TLC analysis (Suliman, 2018), following the methods **E** and **G** (Figure 3.1). The developed TLC plates were viewed under short (254 nm) and long (366 nm) UV light followed by spraying with anisaldehyde reagent and then heating at 100$^{o}$C for 5 min to reveal various coloured spots (Sarker and Nahar, 2012)

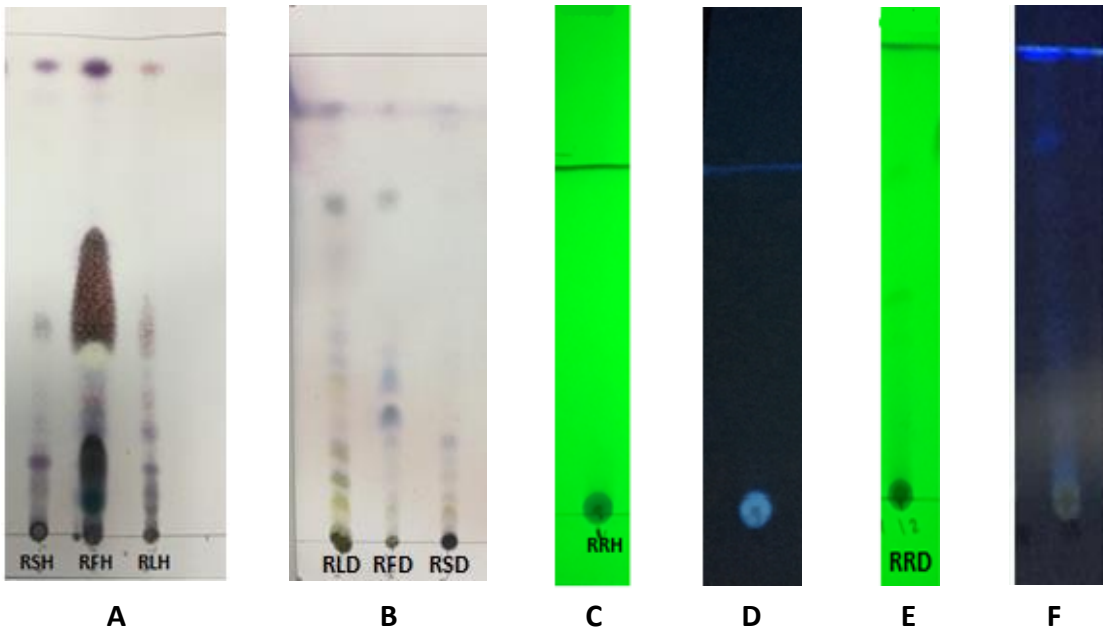


***Figure 3.1**: The TLC plates for R. chalepensis extracts*

*A: TLC plate for n-hexane extract after spraying; B: TLC plate for DCM extract after spraying, C: TLC plate for root n-hexane extract under short UV; D: TLC plate for root n-hexane extract long UV; E: TLC plate for root DCM extract under short UV; F: TLC plate for root n-hexane extract under long UV.*

### 3.1.3 Analytical HPLC screening of the MeOH extracts of *R. chalepensis*

The MeOH extracts of the fruits, leaves and stems of *R. chalepensis* (10 mg/mL) were subjected to Dionex Ultimate 3000 analytical HPLC coupled with a photodiode array detector, while the root extract of *R. chalepensis* (10 mg/ml) was analysed using the analytical Agilent HPLC. Method **L** was used to analyse all the MeOH extracts for 45 min with a volume of injection of 20 µL and a flow rate of 1 mL/min. (Figure 3.2).

### 3.1.4 The antimicrobial screening of extracts of various parts of *R. chalepensis*

The modified microtitre plate assay as described by Sarker *et al.* (2007) was used on this study using four types of bacterial strains, *Escherichia coli* (NCTC 12241), *Pseudomonas aeruginosa* (NCTC 12903), *Micrococcus luteus* (NCTC 7508), *Staphylococcus aureus* (NCTC 12981) and one fungal strain *Candida albicans* (ATCC 90028). A group of antibiotics were used in this assay as positive controls and their MIC values were summarized in Table 3.2, while the negative control was a mixture of nutrient

broth and normal saline. The *n*-hexane, DCM and MeOH extracts of the leaves, stems, fruits and roots of *R. chalepensis* were assessed for antimicrobial proprieties against all these microbial strains. This result revealed that all extracts of the leaves, stems and fruits could inhibit all the microbial strains used in this study with different MIC values (Table 3.3). The *R. chalepensis* root extracts did not show any inhibitory activity, while the MeOH extract of the leaves (RLM) displayed considerable antimicrobial activity against both *C. albicans* and *M. luteus* with an MIC value of 1.95 x $10^{-2}$ mg/mL. Both the DCM extract of the leaves (RLD) and the *n*-hexane extract (RLH) revealed inhibitory activity against *M. luteus* with an MIC value of 1.56 x $10^{-1}$ mg/mL.

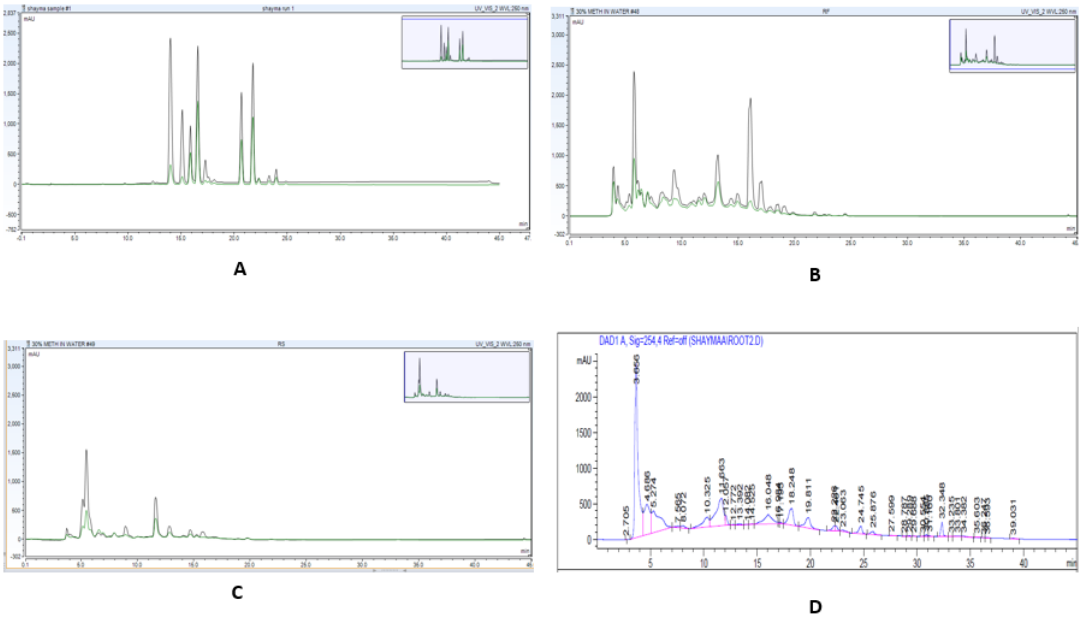


***Figure 3.2**: Analytical HPLC results for R. chalepensis*

*A: RLM; B: RFM; C: RSM; D: RRM*

**Table 3.2**: The MIC values for antibiotics (positive controls)

| **Microbes** | **Antibiotics** | **MIC mg/mL** | **Ciprofloxacin mg/mL** |
|---|---|---|---|
| *Escherichia coli* | Nalidixic acid | $1.55 \times 10^{-2}$ | $1.55 \times 10^{-2}$ |
| *Pseudomonas aeruginosa* | Gentamycin | $1.22 \times 10^{-4}$ | $1.95 \times 10^{-3}$ |
| *Micrococcus luteus* | Chloramphenicol | $9.76 \times 10^{-4}$ | $3.90 \times 10^{-3}$ |
| *Staphylococcus aureus* | Chloramphenicol | $9.76 \times 10^{-4}$ | $3.90 \times 10^{-3}$ |
| *Candida albicans* | Nystatin | $9.76 \times 10^{-4}$ | N/A |

The most potent antimicrobial activity was observed with the MeOH extract of the stem (RSM) with an MIC value of 7.81 x $10^{-2}$ mg/mL against *M. luteus* and *C. albicans*, while the DCM extract of the stem (RSD) exhibited a moderate level of inhibition against all the tested microbes. The MIC value of the *n*-hexane stem extract (RSH) against all microbes as 6.25 x $10^{-1}$ mg/mL except against *C. albicans* with an MIC value of 1.95 x $10^{-1}$ mg/mL. Both the *n*-hexane (RRH) and DCM (RRD) extracts of the roots (RRH) were unable to show any inhibitory efficacy at test concentrations, while the MIC value of the MeOH extract (RRM) was 1.25 mg/mL against *M. luteus*. This result indicated that most of the extracts had certain levels of antimicrobial activity. Many previous studies on *R. chalepensis* documented its antimicrobial activity using different plant parts and methods (Alzoreky and Nakahara, 2003; Priya *et al.*, 2009; Babu-Kasimala *et al.*, 2014; Suliman, 2018). However, there is no report on the antimicrobial activity studies of *R. chalepensis* using the modified microtitre resazuurine assay. This current piece of work generated the first phytochemical report on the analysis of the fruits of Iraqi *R. chalepensis* species along with their antimicrobial activity using modified resazuurine microtitre assay.

After the antimicrobial screening of the crude extracts of *R. chalepensis*, the MIC 6.25 x $10^{-1}$ mg/mL was chosen as the minimum threshold of activity for any extract for further analysis leading to the isolation of compounds responsible for their antimicrobial activity.

### 3.1.5 Chromatographic fractionation of the extracts

#### 3.1.5.1 Vacuum liquid chromatography fractionation (VLC)

The active *n*-hexane and DCM extracts were fractionated by VLC over silica gel using the method **A** and the method **C**, respectively. Table 3.4 summarizes the yield of various fractions. The VLC fractions of the *n*-hexane extracts were analysed by TLC using the method **E** (Figure 3.3), while the VLC fractions of the DCM extracts were analysed by the TLC method **F** (Figure 3.4).

**Table 3.3**: The minimum inhibitory concentration (MIC) values for crude extracts of *R. chalepensis*

| **Bacteria and fungi** | | **Extract** | **Plant parts (mg/mL)** | | | |
|---|---|---|---|---|---|---|
| | | | Leaves | Stems | Fruits | Roots |
| Gram-negative | *E. coli* | *n*-Hexane | $6.25 \times 10^{-1}$ | $6.25 \times 10^{-1}$ | $3.12 \times 10^{-1}$ | N/A |
| | | DCM | $3.12 \times 10^{-1}$ | $6.25 \times 10^{-1}$ | $3.12 \times 10^{-1}$ | N/A |
| | | Methanol | $6.25 \times 10^{-1}$ | $3.12 \times 10^{-1}$ | $6.25 \times 10^{-1}$ | 5 |
| | *P. aeruginosa* | *n*-Hexane | $6.25 \times 10^{-1}$ | $6.25 \times 10^{-1}$ | $3.12 \times 10^{-1}$ | N/A |
| | | DCM | $3.12 \times 10^{-1}$ | $6.25 \times 10^{-1}$ | $6.25 \times 10^{-1}$ | N/A |
| | | Methanol | $6.25 \times 10^{-1}$ | $3.12 \times 10^{-1}$ | $1.56 \times 10^{-1}$ | 2.5 |
| Gram-positive | *M. lluteus* | *n*-Hexane | $1.56 \times 10^{-1}$ | $6.25 \times 10^{-1}$ | $3.12 \times 10^{-1}$ | N/A |
| | | DCM | $1.56 \times 10^{-1}$ | $6.25 \times 10^{-1}$ | $7.81 \times 10^{-2}$ | N/A |
| | | Methanol | $1.95 \times 10^{-2}$ | $7.81 \times 10^{-2}$ | $3.90 \times 10^{-2}$ | 1.25 |
| | *S. aureus* | *n*-Hexane | $6.25 \times 10^{-1}$ | $6.25 \times 10^{-1}$ | $6.25 \times 10^{-1}$ | N/A |
| | | DCM | $6.25 \times 10^{-1}$ | $6.25 \times 10^{-1}$ | $6.25 \times 10^{-1}$ | N/A |
| | | Methanol | $3.12 \times 10^{-1}$ | $3.12 \times 10^{-1}$ | $3.12 \times 10^{-1}$ | 5 |
| Pathogenic yeast | *C. albicans* | *n*-Hexane | $6.25 \times 10^{-1}$ | $1.95 \times 10^{-1}$ | $1.56 \times 10^{-2}$ | N/A |
| | | DCM | $3.12 \times 10^{-1}$ | $3.12 \times 10^{-1}$ | $3.90 \times 10^{-2}$ | N/A |
| | | Methanol | $1.95 \times 10^{-2}$ | $7.81 \times 10^{-2}$ | $3.90 \times 10^{-2}$ | 2.5 |

*N/A: No Activity

Various chromatographic fractionation techniques were performed for the active crude extracts using vacuum liquid chromatography fractionation (VLC) and solid phase extraction (SPE) as described in the experimental section.

### 3.1.5.2 Solid-phase extractions (SPE)

The active MeOH extracts were fractionated by SPE using the method **D** to collect four fractions from every extract. Table 3.4 summarizes the yield of fractions. All fractions were then subjected to analytical HPLC.

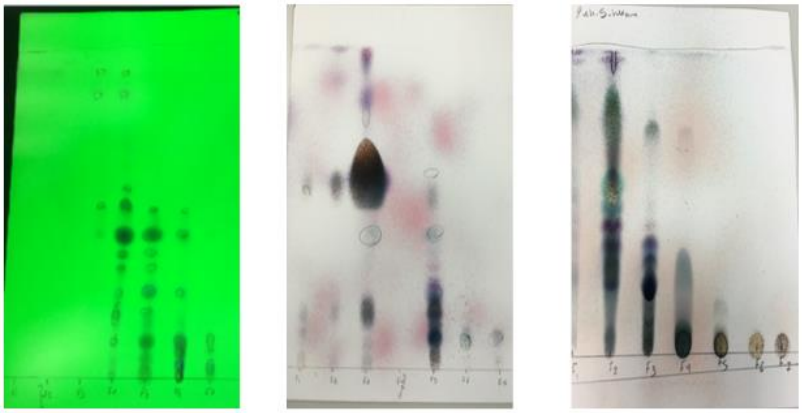


***Figure 3.3**: TLC analysis of n-hexane extracts of R. chalepensis*

*A: Fruit; B: Leaves; C: Stems*

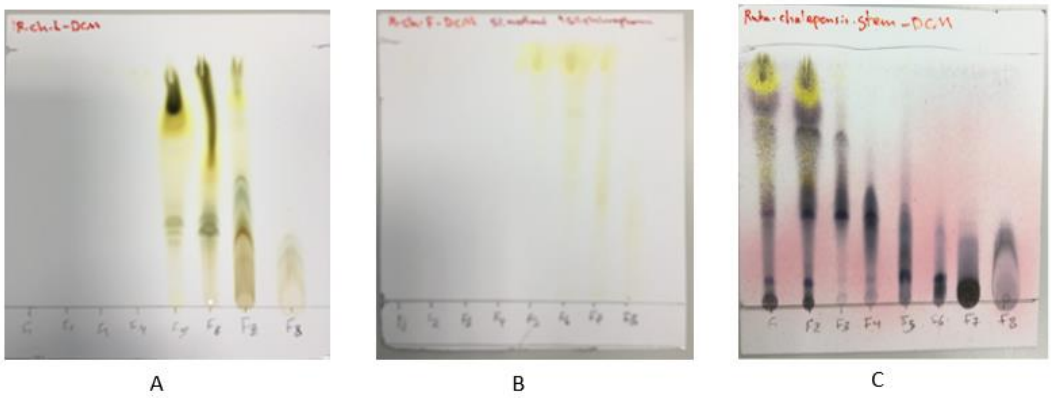


***Figure 3.4**: TLC analysis of the DCM extracts of R. chalepensis*

*A: Leaves; B: Fruits; C: Stem*

**Table 3.4**: The yields of fractions of the active extracts of various parts of *R. chalepensis*

| Plant parts | Type of extract | Weight of extract (g) | Fractions yield % | | | | | | | |
|---|---|---|---|---|---|---|---|---|---|---|
| | | | **F1** | **F2** | **F3** | **F4** | **F5** | **F6** | **F7** | **F8** |
| **Fruits** | *n*-Hexane | 3.080 | 0.46 | 0.60 | 46.70 | 23.93 | 14.44 | 16.33 | 3.61 | - |
| | DCM | 3.1244 | 0.40 | 0.30 | 3.00 | 4.26 | 30.88 | 39.77 | 6.55 | 8.80 |
| | Methanol | 1.7894 | 42.64 | 20.68 | 4.87 | 2.85 | - | - | - | - |
| **Leaves** | *n*-Hexane | 3.002 | 0.66 | 2.25 | 5.38 | 25.00 | 13.08 | 10.94 | 6.66 | - |
| | DCM | 2.7291 | 0.40 | 0.50 | 0.52 | 1.01 | 5.43 | 28.79 | 3.89 | 8.50 |
| | Methanol | 1.776 | 28.80 | 18.45 | 2.26 | 4.15 | - | - | - | - |
| **Stems** | *n*-Hexane | 2.9634 | 3.86 | 6.26 | 3.96 | 8.97 | 6.01 | 2.16 | 0.62 | - |
| | DCM | 2.1195 | 12.87 | 2.44 | 1.41 | 1.43 | 1.52 | 1.01 | 2.08 | 2.25 |
| | Methanol | 1.8021 | 31.93 | 9.12 | 3.98 | 1.83 | - | - | - | - |

### 3.1.6 Screening of *R. chalepensis* fractions for antimicrobial activity

All VLC and SPE fractions were screened for their antimicrobial activity against *Escherichia coli* (NCTC 12241), *Pseudomonas aeruginosa* (NCTC 12903), *Micrococcus luteus* (NCTC 7508), *Staphylococcus aureus* (NCTC 12981) and *Candida albicans* (ATCC 90028).

The VLC fraction 4 from the *n*-hexane extract of the fruits showed significant inhibitory activity against all the microbial strains used in this study, specifically against *M. lutues* with an MIC value of $7.81\times10^{-3}$ mg/mL. Moreover, the VLC fraction 7 from the DCM extract of the fruits presented strong inhibitory activity to inhibit all the microbes used in this test with different MIC values. Regarding the MeOH extract of the fruits, the SPE fractions 2 and 3 displayed remarkable reduction of growth of the tested microbial strains with different MIC values (Table 3.5). Table 3.5 outlines the MIC values of the fractions of various extracts of the fruits of *R. chalepensis*.

Most of the fractions of the *n*-hexane extract of the leaves did not show significant antimicrobial activity, while VLC fraction 7 (F7) of the DCM extract of the leaves displayed good inhibition of growth of all five microbial strains, particularly against *M. luteus* with an MIC value of $3.12\times10^{-2}$ mg/mL. Furthermore, both SPE fractions 2 and 3 from MeOH extract of the leaves exhibited significant antimicrobial activity (Table 3.6). Table 3.6 summarizes the MIC values of the fractions of the extracts of the leaves of *R. chalepensis* leaves. As for the stems, the VLC fractions originating from both *n*-hexane and DCM extracts had weak antimicrobial activity, but the SPE fractions 2 and 3 of the MeOH extract displayed notable inhibitory activity against all microbial strains used in this study, particularly, the SPE fraction 2 inhibited *C. albicans* with an MIC value of $3.12 \times 10^{-2}$ mg/mL. Table 3.7 outlines the MIC values of various fractions of extracts of stems of *R. chalepensis*.

**Table 3.5**: MIC values (in mg/mL) of *Ruta chalepensis* fruit fractions

| **Microbes** | **Type of extract** | **F1** | **F2** | **F3** | **F4** | **F5** | **F6** | **F7** | **F8** |
|---|---|---|---|---|---|---|---|---|---|
| *Escherichia coli* | *n*-Hexane | N/A | N/A | N/A | $6.25 \times 10^{-2}$ | N/A | N/A | N/A | - |
| | DCM | N/A | N/A | N/A | N/A | N/A | N/A | $3.12 \times 10^{-2}$ | N/A |
| | MeOH | N/A | $7.81 \times 10^{-3}$ | $1.56 \times 10^{-2}$ | N/A | - | - | - | - |
| *Pseudomonas aeruginosa* | *n*-Hexane | N/A | N/A | N/A | $1.25 \times 10^{-1}$ | N/A | N/A | N/A | |
| | DCM | N/A | N/A | N/A | N/A | N/A | N/A | $6.25 \times 10^{-2}$ | N/A |
| | MeOH | N/A | $6.25 \times 10^{-2}$ | $2.5 \times 10^{-1}$ | N/A | - | - | - | - |
| *Micrococcus luteus* | *n*-Hexane | N/A | 1 | 1 | $6.25 \times 10^{-2}$ | $5 \times 10^{-1}$ | $5 \times 10^{-1}$ | 1 | - |
| | DCM | N/A | N/A | 1 | 1 | 1 | 1 | $3.12 \times 10^{-2}$ | 1 |
| | MeOH | N/A | $6.25 \times 10^{-2}$ | $3.12 \times 10^{-2}$ | N/A | - | - | - | - |
| *Staphylococcus aureus* | *n*-Hexane | N/A | N/A | N/A | $7.81 \times 10^{-3}$ | N/A | N/A | N/A | |
| | DCM | N/A | N/A | N/A | N/A | N/A | N/A | $5 \times 10^{-1}$ | N/A |
| | MeOH | N/A | $5 \times 10^{-1}$ | $1.25 \times 10^{-1}$ | N/A | - | - | - | - |
| *Candida albicans* | *n*-Hexane | N/A | N/A | N/A | $3.12 \times 10^{-2}$ | $5 \times 10^{-1}$ | $5 \times 10^{-1}$ | 0.1 | |
| | DCM | 0.5 | 0.25 | N/A | N/A | $6.25 \times 10^{-2}$ | $3.12 \times 10^{-2}$ | 0.5 | N/A |
| | MeOH | N/A | $3.12 \times 10^{-2}$ | $1.56 \times 10^{-2}$ | N/A | - | - | - | - |

*N/A: No Activity

**Table 3.6**: MIC values (in mg/mL) of *Ruta chalepensis* leaves fractions

| **Microbes** | **Type of extract** | **F1** | **F2** | **F3** | **F4** | **F5** | **F6** | **F7** | **F8** |
|---|---|---|---|---|---|---|---|---|---|
| *Escherichia coli* | *n*-Hexane | N/A | N/A | N/A | N/A | N/A | N/A | N/A | - |
| | DCM | N/A | N/A | N/A | N/A | N/A | N/A | N/A | N/A |
| | MeOH | N/A | $5 \times 10^{-1}$ | $2.5 \times 10^{-1}$ | N/A | - | - | - | - |
| *Pseudomonas aeruginosa* | *n*-Hexane | N/A | N/A | N/A | N/A | N/A | N/A | N/A | |
| | DCM | N/A | N/A | N/A | N/A | N/A | N/A | | N/A |
| | MeOH | N/A | $1.25 \times 10^{-1}$ | $2.5 \times 10^{-1}$ | N/A | - | - | - | - |
| *Micrococcus luteus* | *n*-Hexane | N/A | 1 | N/A | N/A | 1 | $5 \times 10^{-1}$ | $5 \times 10^{-1}$ | |
| | DCM | $5 \times 10^{-1}$ | $5 \times 10^{-1}$ | 1 | N/A | N/A | N/A | N/A | N/A |
| | MeOH | N/A | $5 \times 10^{-1}$ | $5 \times 10^{-1}$ | N/A | - | - | - | - |
| *Staphylococcus aureus* | *n*-Hexane | N/A | N/A | N/A | N/A | N/A | N/A | N/A | |
| | DCM | $5 \times 10^{-1}$ | $5 \times 10^{-1}$ | N/A | N/A | N/A | N/A | | N/A |
| | MeOH | N/A | $5 \times 10^{-1}$ | $2.5 \times 10^{-1}$ | N/A | - | - | - | - |
| *Candida albicans* | *n*-Hexane | N/A | N/A | N/A | N/A | N/A | 1 | $5 \times 10^{-1}$ | |
| | DCM | $5 \times 10^{-1}$ | $5 \times 10^{-1}$ | N/A | N/A | N/A | N/A | N/A | $5 \times 10^{-1}$ |
| | MeOH | N/A | $3.12 \times 10^{-2}$ | $1.25 \times 10^{-1}$ | N/A | - | - | - | - |

*N/A: No Activity

**Table 3.7**: MIC values (in mg/mL) of *Ruta chalepensis* stems fractions

| **Microbes** | **Type of extract** | **F1** | **F2** | **F3** | **F4** | **F5** | **F6** | **F7** | **F8** |
|---|---|---|---|---|---|---|---|---|---|
| *Escherichia coli* | *n*-Hexane | N/A | N/A | N/A | N/A | N/A | N/A | N/A | - |
| | DCM | N/A | N/A | N/A | N/A | N/A | N/A | $5 \times 10^{-1}$ | N/A |
| | MeOH | N/A | $5 \times 10^{-1}$ | $2.5 \times 10^{-1}$ | N/A | - | - | - | - |
| *Pseudomonas aeruginosa* | *n*-Hexane | N/A | N/A | N/A | N/A | N/A | N/A | N/A | - |
| | DCM | N/A | N/A | N/A | N/A | N/A | N/A | $5 \times 10^{-1}$ | N/A |
| | MeOH | N/A | $1.25 \times 10^{-1}$ | $5 \times 10^{-1}$ | N/A | - | - | - | - |
| *Micrococcus luteus* | *n*-Hexane | N/A | N/A | N/A | N/A | N/A | 1 | $5 \times 10^{-1}$ | |
| | DCM | N/A | N/A | 1 | 1 | $5 \times 10^{-1}$ | $5 \times 10^{-1}$ | $3.12 \times 10^{-2}$ | $5 \times 10^{-1}$ |
| | MeOH | N/A | $1.56 \times 10^{-2}$ | $6.25 \times 10^{-2}$ | N/A | - | - | - | - |
| *Staphylococcus aureus* | *n*-Hexane | N/A | N/A | N/A | N/A | N/A | N/A | N/A | |
| | DCM | N/A | N/A | N/A | N/A | N/A | N/A | $2.5 \times 10^{-1}$ | $5 \times 10^{-1}$ |
| | MeOH | N/A | $1.25 \times 10^{-1}$ | $2.5 \times 10^{-1}$ | N/A | - | - | - | - |
| *Candida albicans* | *n*-Hexane | N/A | N/A | N/A | $5 \times 10^{-1}$ | N/A | 1 | N/A | - |
| | DCM | N/A | N/A | 1 | 1 | 1 | $1.56 \times 10^{-2}$ | $1.25 \times 10^{-1}$ | N/A |
| | MeOH | N/A | $1.25 \times 10^{-1}$ | $3.12 \times 10^{-2}$ | 1 | - | - | - | - |

*N/A: No Activity

### 3.1.7 Phytochemistry of *Ruta chalepensis*

Chromatographic separation of the active fractions of the *n*-hexane, DCM and MeOH extracts of different parts of *R. chalepensis* afforded nineteen compounds (Figure 3.5): bergapten (**43**), kokusaginine (**99**), isokokusaginine (**100**), skimmianine (**41**), rutin (**48**), rutin 3'-methyl ether (**101**), rutin 7,4'-dimethyl ether (**102**), 6-hydroxy-rutin-3'-7-dimethyl ether (**103**), chalepin (**45**), chalepensin (**46**), rutamarin (**47**), isopimpinellin (**44**), γ-fagarine (**42**), imperatorin (**104**), graveoline (**105**), ribalinium (**106**), arborinine (**107**), 3`,6-disinapoylsucrose (**108**) and hexadecane (**109**) (Figure 3.5). All the isolated compounds were identified by spectroscopic means (NMR and HRESIMS) and the spectral data of known compounds were compared with the respective published data. Of the isolated compounds, except 6-hydroxy-rutin-3'-7-dimethyl ether (**103**), all isolated compounds are known natural products. To the best of our knowledge, this is the first report on the phytochemical studies on the fruits of the Iraqi species of *R. chalepensis*. Compounds **100-102** and **108** are reported here for the first time from *R. chalepensis*.

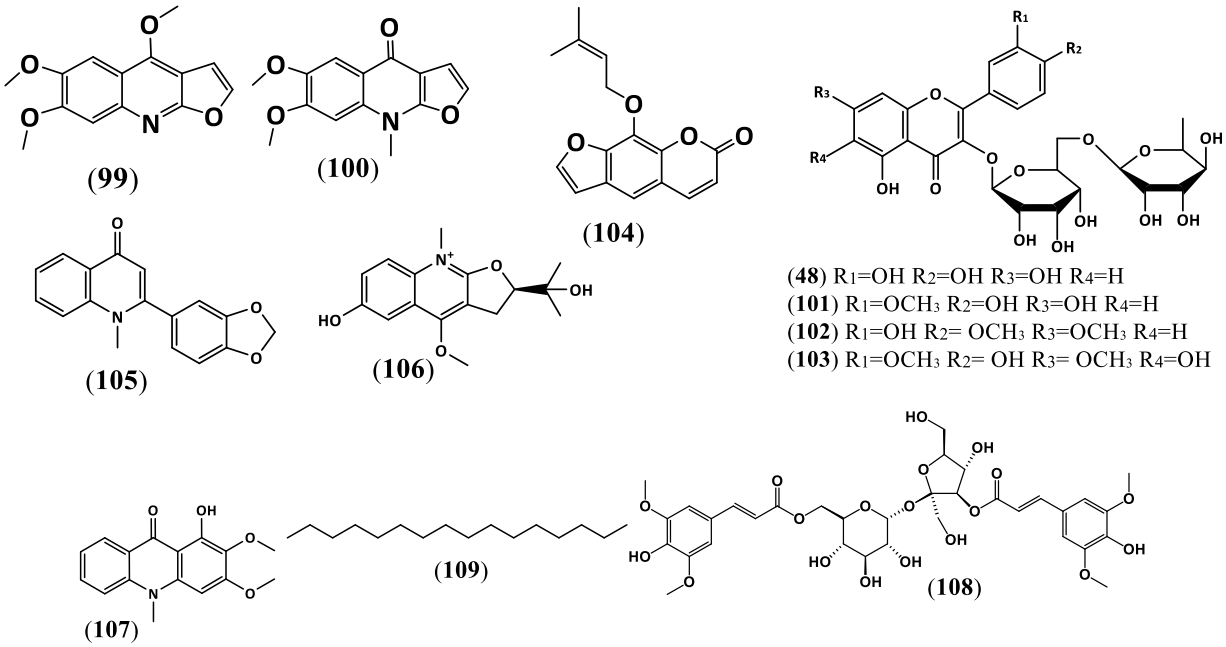


***Figure 3.5***: Isolated compounds from *R. chalepensin*

Kokusaginine (**99**), isokokusaginine (**100**), rutin 3'-methyl ether (**101**), rutin 7,4'-dimethyl ether (**102**), 6-hydroxy-rutin-3'-7-dimethyl ether (**103**), imperatorin (**104**), graveoline (**105**), ribalinium (**106**), arborinine (**107**), 3`,6-disinapoylsucrose (**108**) and hexadecane (**109**)

### 3.1.8 Isolation compounds from active fractions of *Ruta chalepensis*

All the active fractions were subjected to different chromatographic methods, *e.g.*, PTLC and/or prep-HPLC to isolate the active compounds.

#### 3.1.8.1 *R. chalepensis* fruit *n*-hexane fraction 4

The VLC fraction 4 obtained from the *n*-hexane extract of fruits was subjected to analytical TLC using the method **E** (Figure 3.6) because of its significant antimicrobial activity against all the five strains used in this study.

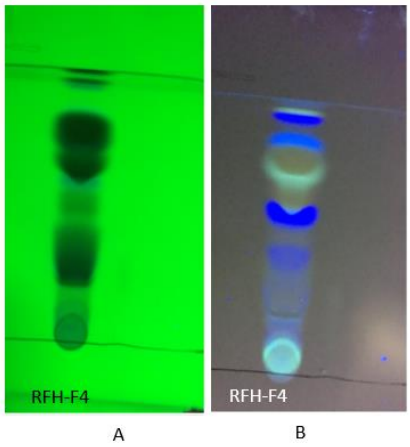


***Figure 3.6****: Analytical TLC (using method **E**) of the VLC fraction 4 of the n-hexane extract of R. chalepensis fruits*

The method **B** was selected for further fractionation based on the analysis of the TLC chromatography that had been developed using method **E**. The application of the method **B** gave 11 fractions from fraction 4 (Figure 3.7) and then these fractions were subjected to tests for their antimicrobial activities. Out of these 11 fractions, only the fractions RFH4-3, RFH4-4, RFH4-5 and RFH4-11 was showed a significant antimicrobial activity (Table 3.8). To determine the responsible active compound, method **I** was used to develop PTLC, in RFH4-3, RFH4-4 and RFH4-5, while RFH4-11 subjected to method **K**. (Figure 3.8). The final compounds (**42**), (**43)**, (**46)**, (**47)** and (**99)** were obtained from these chromatographic techniques suggesting the possible antimicrobial activity of these fractions.

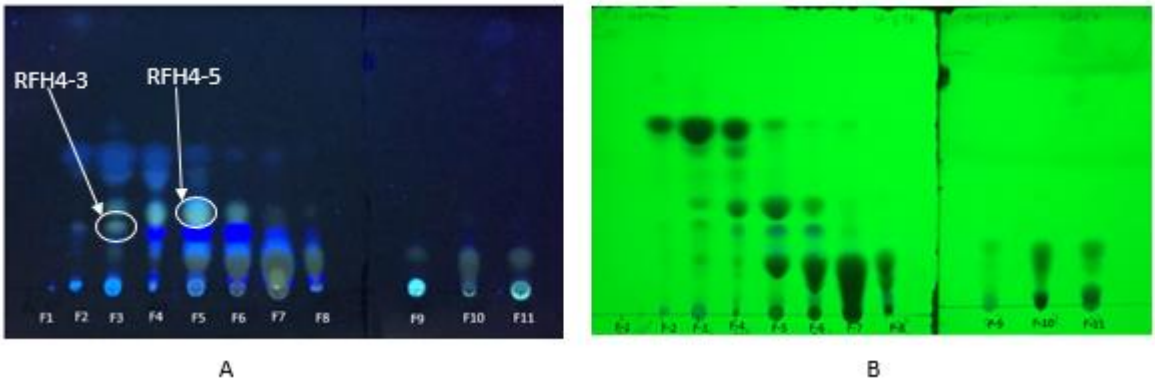


***Figure 3.7**: Analytical TLC (using method I) of the VLC fractions of R. chalepensis fruit fraction 4*

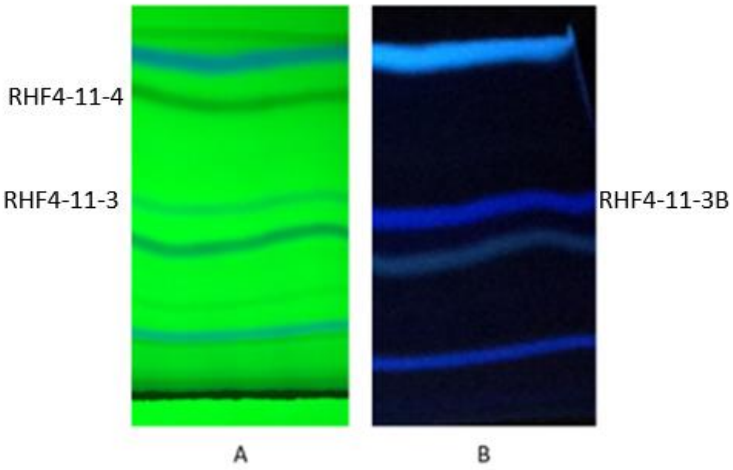


***Figure 3.8**: Preparative TLC (using method K) of R. chalepensis fruit fraction 11 derived from fraction 4*

**Table 3.8**: The MIC values of the VLC fractions of *R. chalepensis* fruit fraction 4, and compounds isolated from the active fractions

| **Fractions** | Microbes (MIC in mg/mL) | | | | | Methods | | Extracts name | Isolated compounds | |
|---|---|---|---|---|---|---|---|---|---|---|
| | *E. coli* | *P. aeruginosa* | *M. luteus* | *S. aureus* | *C.albicans* | Type | Name | | Name | Number |
| F1 | N/A | N/A | N/A | N/A | N/A | - | - | - | - | - |
| F2 | N/A | N/A | N/A | N/A | N/A | - | - | - | - | - |
| F3 | N/A | $5\times10^{-1}$ | $1.25\times10^{-1}$ | $5\times10^{-1}$ | $2.5\times10^{-1}$ | PTLC | I | RFH4-3 | Chalepensin | **46** |
| F4 | N/A | N/A | $5\times10^{-1}$ | N/A | $2.5\times10^{-1}$ | - | I | RFH4-4 | Chalepensin | **46** |
| F5 | N/A | N/A | $5\times10^{-1}$ | N/A | $5\times10^{-1}$ | - | I | RFH4-5 | Rutamarin | **47** |
| F6 | N/A | N/A | N/A | N/A | N/A | - | - | - | - | - |
| F7 | N/A | N/A | N/A | N/A | N/A | - | - | - | - | - |
| F8 | N/A | N/A | N/A | N/A | N/A | - | - | - | - | - |
| F9 | N/A | N/A | N/A | N/A | N/A | - | - | - | - | - |
| F10 | N/A | N/A | N/A | N/A | N/A | - | - | - | - | - |
| F11 | $5\times10^{-1}$ | $2.5\times10^{-1}$ | $1.56\times10^{-2}$ | $1.25\times10^{-1}$ | $3.12\times10^{-2}$ | PTLC | K | RFH4-11-4 | Bergapten | **43** |
| | | | | | | | | RFH4-11-3 | γ-Fagarine | **42** |
| | | | | | | | | RFH4-11-3B | Kokusaginine | **99** |

*N/A: No Activity

### 3.1.8.2 *R. chalepensis* fruit DCM fraction 7

The antimicrobial screening of *R. chalepensis* fruit DCM fractions revealed that the most active fraction was fraction 7, which was subjected to the prep-HPLC (Agilent) using method **M** for 35 min. The injection volume was 300 µL and the flowrate was 10 mL/min (Figure 3.9). This separation method was gave six compounds, arborinine (**107**), (0.3 mg) (Knölker, 2017; Kumar, 2018), graveoline (**105**, 0.2 mg) (Ulubelen *et al*., 1986), kokusaginine (**99**, 0.3 mg) (Adamska-Szewczyk *et al*., 2016), γ-fagarine (**42**, 0.5 mg) (Ulubelen *et al*., 1986), skimmianine (**41**, 1.2 mg) (Ulubelen *et al.,* 1986) and chalepensin (**46**, 0.4 mg) (Adamska-Szewczyk *et al*., 2016).

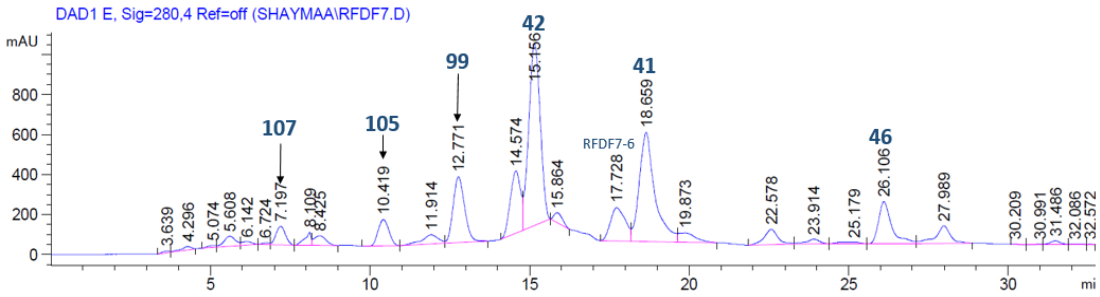


***Figure 3.9****: Preparative- HPLC chromatogram of isolated compounds from R. chalepensis fruit DCM extract fraction 7, using method* ***M***

### 3.1.8.3 *R. chalepensis* fruit MeOH fraction 2

The method **L** in prep-HPLC was used to isolate the active compounds from fraction 2 of the fruit MeOH extract (Figure 3.10). The injection volume was 200 µL and the flow rate was 10 mL/min. The separation process obtained gave mixed peak (RFF2-11) and seven compounds, ribalinium (**106**, 0.5 mg), rutin (**48**, 1.2 mg) (Hamad, 2012), rutin 3'-methyl ether (**101**, 1.0 mg), 6-hydroxy-rutin-3'-7-dimethyl ether (**103**, 0.3 mg), graveoline (**105**, 1.2 mg) (Ulubelen et al., 1986), isopimpinellin (**44**, 1.0 mg) (Richardson *et al*., 2016) and γ-fagarine (**42**, 0.4 mg) (Adamska-Szewczyk *et al*., 2016).

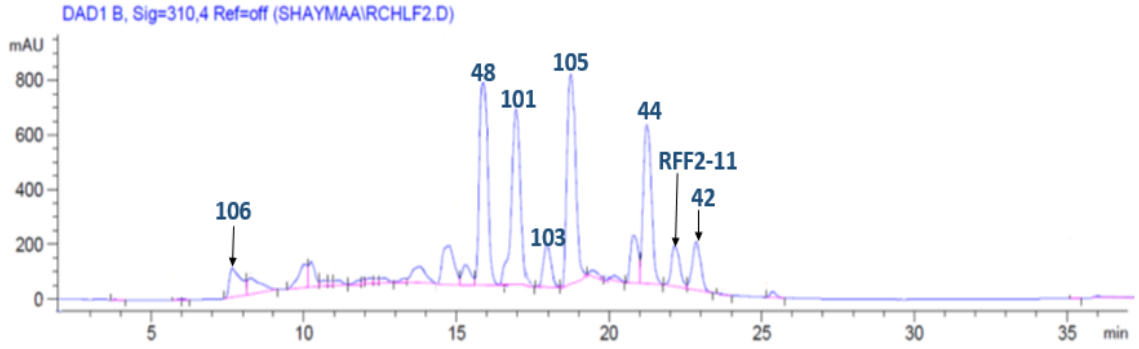


***Figure 3.10**: Preparative-HPLC chromatogram of isolated compounds from R. chalepensis fruit MeOH extract fractions 2 using method **L***

***Purification of RFF2-11***

The peak RFF2-11 was isolated as a mixture of compounds. This mixture was subjected to PTLC using the method **J** to isolate two pure compounds **43** (3 mg; $R_f$ = 0.19) and **99** (2 mg; $R_f$ = 0.47), which were analysed by MS and NMR spectroscopic techniques.

### 3.1.8.4 *R. chalepensis* fruit MeOH fraction 3

This active fraction was subjected to prep-HPLC using method **L** for 35 min. The injection volume was 300 µL and the flowrate was 10 mL/min (Figure 3.11). The separation process was obtained six compounds rutin (**48**, 0.6 mg) (Hamad, 2012), skimmianine (**41**, 0.5 mg) (Ulubelen *et al*., 1986), imperatorin (**104,** 1.8 mg)**,** chalepensin (**46**, 0.2 mg), chalepin (**45**, 1.2 mg) (Richardson *et al*., 2016) and rutamarin (**47**, 1.5 mg) (Adamska-Szewczyk *et al.*, 2016).

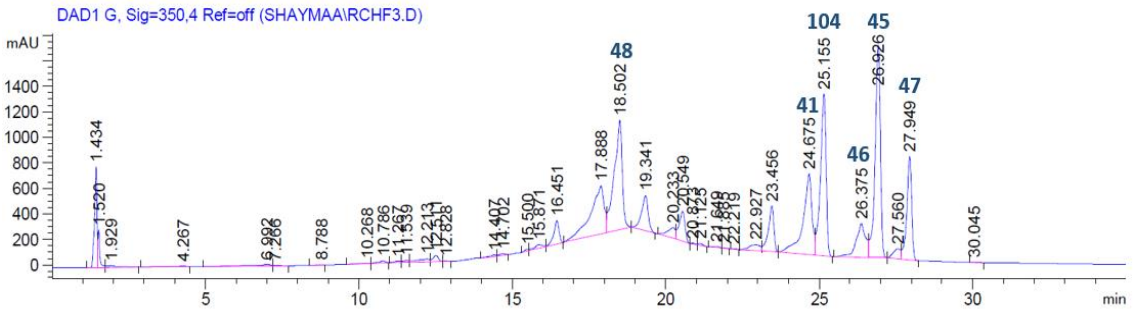


***Figure 3.11**: Preparative- HPLC chromatogram of isolated compounds from R. chalepensis fruit MeOH extract fraction 3, using method **L***

### 3.1.8.5 *R. chalepensis* leaves DCM fraction 7

The method **O** in prep-HPLC was used to seperate the target compounds from fraction 7 of leaves DCM extract (Figure 3.12). The injection value was 350µL and the flowrate was 10 mL/min. The isolation techniques were obtained four pure compounds, graveoline (**105**, 1.0 mg) (Ulubelen *et al*., 1986), kokusaginine (**99**, 0.6 mg) (Adamska-Szewczyk *et al.*, 2016), arborinine (**107**, 0.4 mg) (Knölker, 2017; Kumar, 2018) and chalepin (**45**, 0.9 mg) (Richardson *et al*., 2016). The injection value was 350 µL and the flowrate was 10 mL/min.

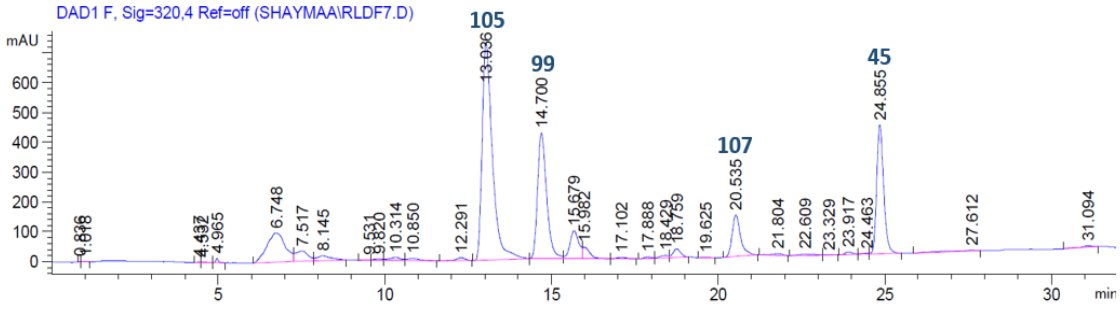


***Figure 3.12**: Preparative- HPLC chromatogram of isolated compounds from R. chalepensis leaves DCM extract fraction 7, using method **O***

### 3.1.8.6 *R. chalepensis* leaves MeOH fraction 2

This *R. chalepensis* leaves fraction 2 of MeOH extract was analysed by prep-HPLC using method **L**. The injection value was 250 µL and the flowrate was 10 mL/min for 33min. The separation process were obtained two fractions RLF2-5, RLF2-7 and four compounds bergapten (**43**, 1.3 mg) (Gonzalez *et al.*, 1977), rutin (**48**, 0.3 mg) (Hamad, 2012), γ-fagarine (**42**, 0.3 mg) (Adamska-Szewczyk *et al.*, 2016) and kokusaginine (**99**, 1.0 mg) (Adamska-Szewczyk *et al.*, 2016).

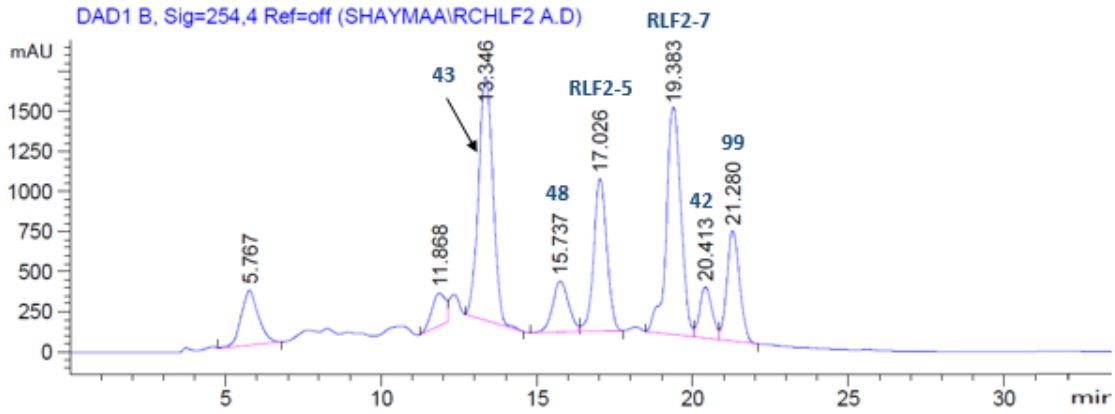


***Figure 3.13**: Preparative- HPLC chromatogram of isolated compounds from R.chalepensis leaves MeOH extract fraction 2, using method **L***

***Purification of RLF2-5***

The peak RLF2-5 was isolated as a mixture of compounds. This mixture was subjected to semi-prep-HPLC using method **U** to isolate two pure compounds rutin 3'-methyl ether (**101**, 0.5 mg) and rutin 7,4′- dimethyl ether (**102**, 0.3 mg). The injection volume was 100 µL and the flow rate was 2 mL/min for 20 min (Figure 3.14).

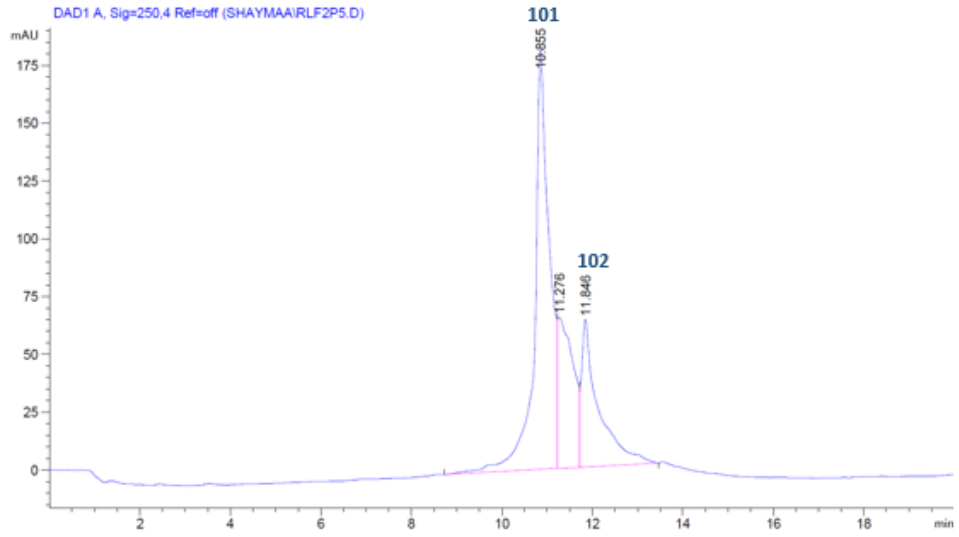


***Figure 3.14**: Semi-preparative-HPLC chromatogram of purification compounds from RLF2-5, using method **U***

***Purification of RLF2-7***

This peak RLF2-7 was separated as a mixture of compounds. This mixture was purified by semi-prep-HPLC using method **P** for 21 min**.** The injection value was 100 µL and the flowrate was 2 mL/min (Figure 3.15). The separation process gave three compounds rutin (**48**, 0.2 mg) (Hamad, 2012), isokokusaginine (**100**, 1.5 mg) (Openshaw, 1967) and graveoline (**105**, 1.2 mg) (Ulubelen *et al*., 1986).

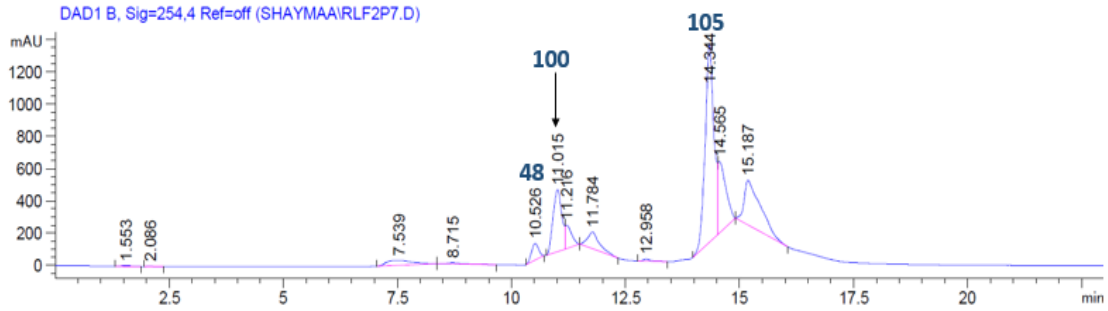


***Figure 3.15****: Semi-preparative- HPLC chromatogram of purification compounds from RLF2-7, using method* ***P***

### 3.1.8.7 *R. chalepensis* leaves MeOH fraction 3

The *R. chalepensis* leaves fraction 3 of the MeOH extract was subjected to prep-HPLC using method **L** for 37min. (Figure 3.16). The injection volume was 250 µL, while the flow rate was 10 mL/min. The separation process produced eight compounds, rutin (**48**, 0.2 mg), graveoline (**105**, 1.3 mg) (Ulubelen *et al*., 1986), bergapten (**43**, 0.2 mg) (Gonzalez *et al.*, 1977), kokusaginine (**99**, 1.5 mg) (Adamska-Szewczyk *et al.*, 2016), γ-fagarine (**42**, 0.5 mg) (Adamska-Szewczyk *et al.*, 2016), arborinine (**107**, 0.3 mg) (Knölker, 2017; Kumar, 2018), chalepin (**45**, 1.2 mg) (Richardson *et al*., 2016) and chalepensin (**46**, 0.2 mg) (Adamska-Szewczyk *et al.*, 2016).

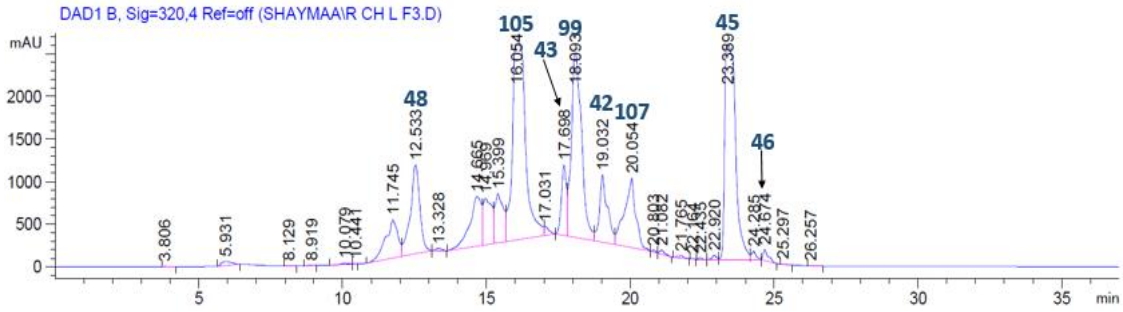


***Figure 3.16**: Preparative-HPLC chromatogram of isolated compounds of R. chalepensis leaves MeOH extract fraction 3, using method **L***

### 3.1.8.8 *R. chalepensis* stem MeOH fraction 2

The method **L** in semi-prep-HPLC was used to isolate the active compounds from fraction 2 of stem MeOH extract (Figure 3.17). The injection value was 100 µL and the flow rate was 2 mL/min. The separation process gave three compounds 3',6-disinapoylsucrose (**108**, 1.0 mg), rutin (**48**, 0.8 mg) (Hamad, 2012) and rutin 7,4'- dimethyl ether (**102**, 0.2 mg).

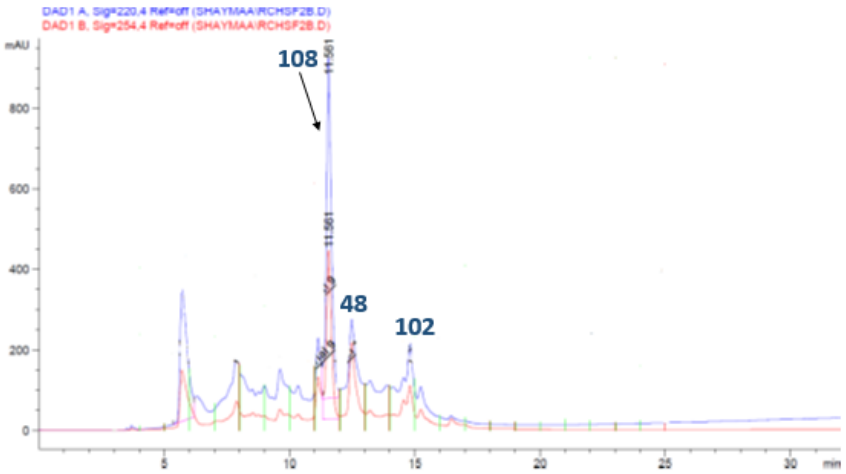


***Figure 3. 17**: Semi -preparative- HPLC Chromatogram of isolated compounds of R. chalepensis stem MeOH extract fraction 2, using method **L***

### 3.1.8.9 *R. chalepensis* stem MeOH fraction 3

The *R. chalepensis* stem fraction 3 of the MeOH extract was subjected to semi-prep-HPLC using method **L** for 40 min (Figure 3.18). The injection value was 200 µL and flow rate was 2 mL/min. The separation process afforded six compounds, kokusaginine (**99**, 0.9 mg) (Adamska-Szewczyk *et al.*, 2016), γ-fagarine (**42**, 0.4 mg ) (Adamska-Szewczyk *et al.*,

2016), bergapten (**43**, 1.6 mg) (Gonzalez *et al.*, 1977), arborinine (**107**, 0.7 mg) (Knölker, 2017; Kumar, 2018), chalepin (**45**, 0.2 mg) and chalepensin (**46**, 0.4 mg) (Adamska-Szewczyk *et al.*, 2016).

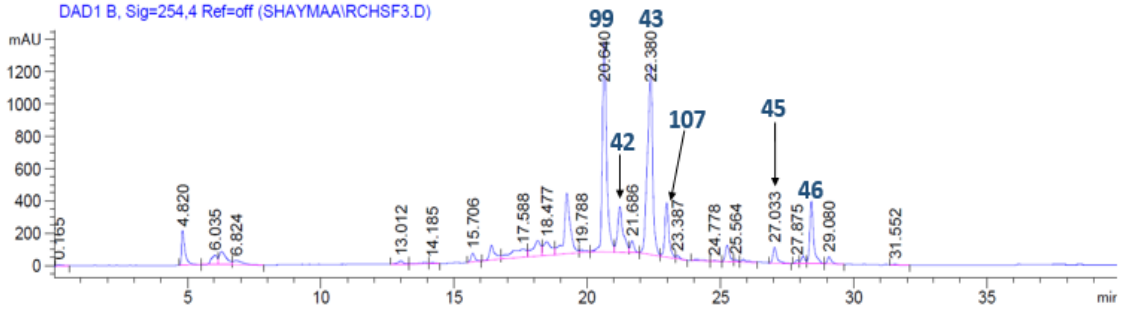


***Figure 3.18**: Preparative-HPLC chromatogram of isolated compounds from R. chalepensis stem MeOH extract fraction 3, using method **L***

### 3.1.9 Characterisation and structure elucidation of isolated compounds

#### 3.1.9.1 Structure elucidation of kokusaginine (99)

The compound **99** was isolated as a colourless powder. The HRESIMS (Figure 3.19) suggested the empirical formula as $C_{14}H_{14}NO_4$ and in the positive ion mode it showed $[M+H]^+$ peak at *m/z* 260.0917 (calculated 260.0922). The $^1$H NMR spectrum (Figure 3.20, Table 3.9) exhibited signals for three methoxy groups at $\delta_H$ 4.44 (3H, s, 4-OMe), 4.03 (3H, s, 7-OMe), 4.02 (3H, s,6-OMe) and two olefinic protons at $\delta_H$ 7.57 (1H, d, *J* = 2.80 Hz, H-2) and 7.04 (1H, d, *J* = 2.80 Hz, H-3′). Moreover, two aromatic protons resonated at $\delta_H$ 7.48 (1H, s, H-5) and 7.34 (1H, s, H-8). The $^{13}$C-NMR (Figure 3.21, Table 3.9) presented seven quaternary carbons at $\delta_C$ 163.4 (C-2), 102.5 (C-3), 155.9 (C-4), 148.1 (C-6), 152.9 (C-7), 142.7 (C-9), 113.2 (C-10); three methyl groups at $\delta_C$ 59.1 (4-OMe), 56.3 (7-OMe), 56.3 (6-OMe) and two olefinic carbons at $\delta_C$ 142.74 (C-2′) and 104.9 (C-3′). In addition, there were two aromatic methine carbon signals at $\delta_C$ 100.5 (C-5) and 107.0 (C-8). The $^1$H-$^1$H COSY spectrum showed the connection between H-2′/H-3′. The HMBC (Figure 3.22) displayed the correlation from H-3′ to C-2, 3, 2′ and H-2′ showed $^2J$ correlation to C-2 and C-3. Moreover, the long-rang correlation was observed from H-8 to C-6, C-7, C-9, C-10 and from H-5 to C-

4, C-6, C-7, C-9, C-10. The HMBC confirmed the positions of methoxy groups by revealing the correlation of OMe/C-4, OMe/C-6 and OMe/C-7. Thus, compound **99** was identified as 4,6,7-trimethoxyfuro[2,3-b]quinolone or kokusaginine. The spectroscopic data of compound **99** were in a good agreement with respective published data of kokusaginine (Wu *et al.*, 2003; Elaine Monteiro *et al.*, 2010). Kokusaginine (**99**) was previously isolated from other species of the Rutaceae including *Ruta* species. Kokusaginine (**99**) was reported to possess antioxidant, anti-leishmanic and anticholinesterase activities (Ulubelen *et al.*, 1986; El Sayed *et al.*, 2000; Wu *et al.*, 2003; Adamska-Szewczyk *et al.*, 2016).

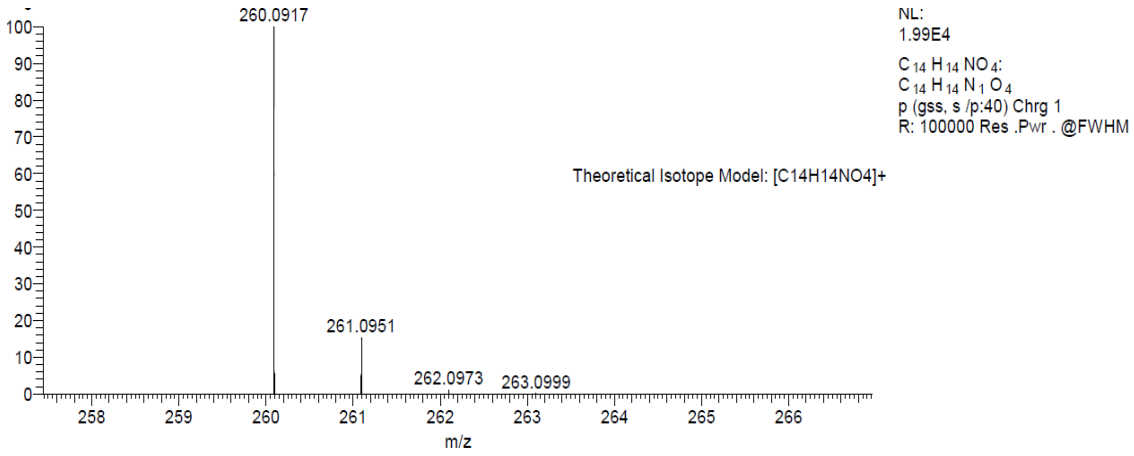


***Figure 3.19**: The HRESIMS spectrum of compound **99***

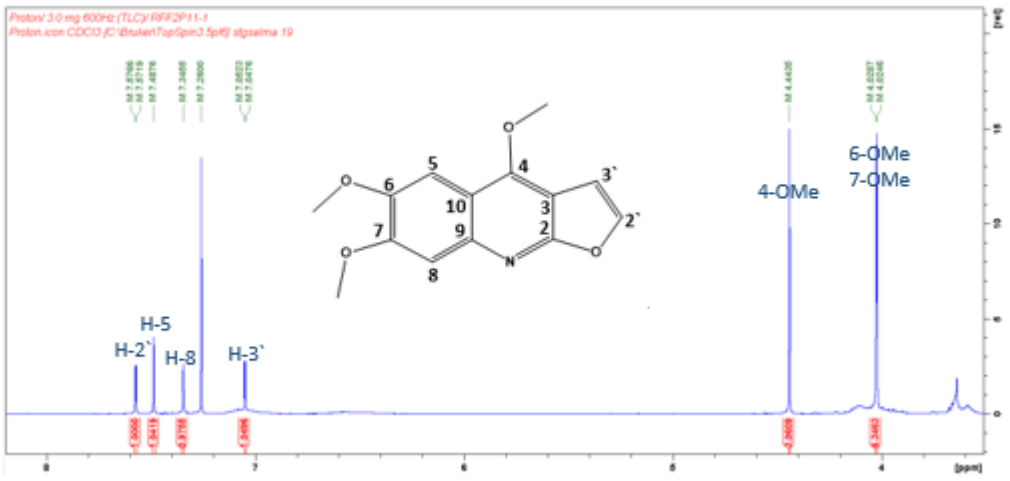


***Figure 3.20**:* The $^{1}$H NMR (600 MHz, $CDCl_3$) spectrum of compound **99**

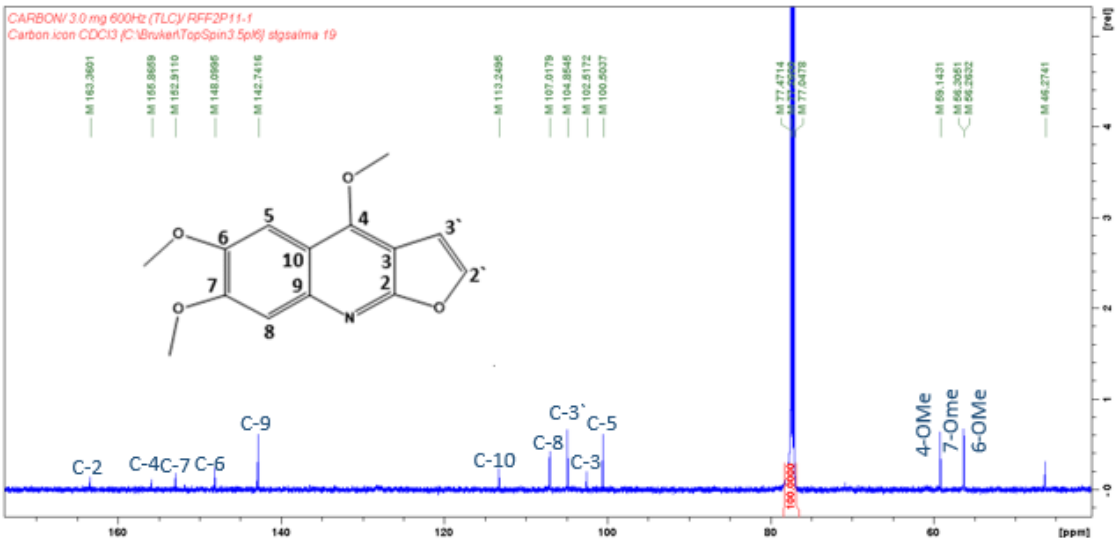


***Figure 3.21**: The $^{13}C$ NMR (150 MHz, $CDCl_3$) spectrum of compound **99***

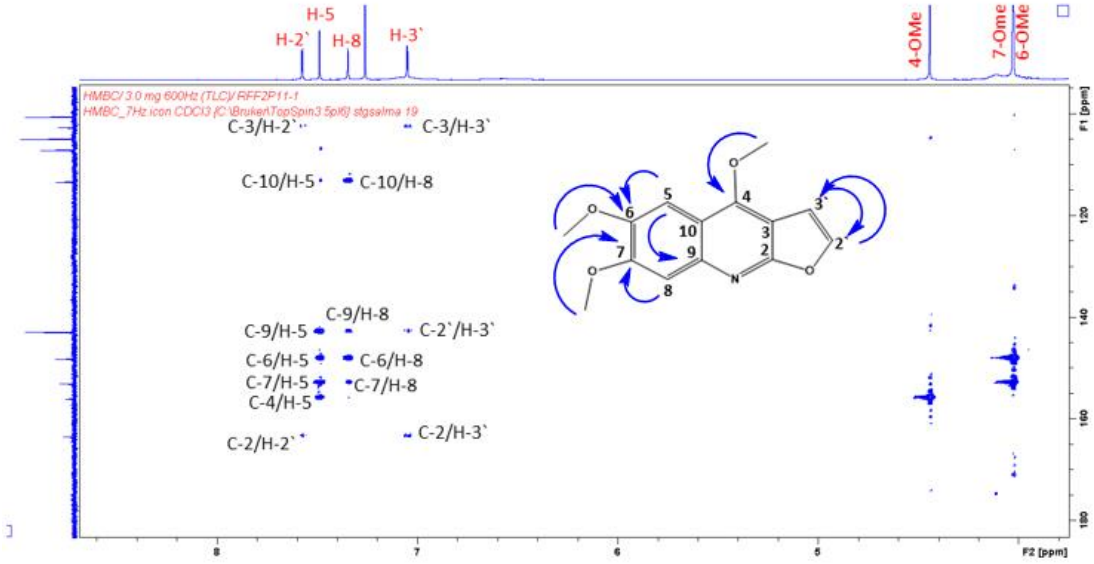


***Figure 3.22**: The HMBC correlations of compound **99***

### 3.1.9.2 Structure elucidation of isokokusaginine (100)

The compound **100** was isolated as pale yellow powder. The HRESIMS (Figure 3.23) suggested the empirical formula as $C_{14}H_{13}NO_4$ and in the positive ion mode it showed $[M+H]^+$ peak at *m/z* 260.0919 (calculated 260.0922). The $^1H$ NMR spectrum (Figure 3.24, Table 3.9) displayed two sets of methyl signals at $\delta_H$ 3.98 (3H) and 4.07 (2X 3H). The deshielded methyl signals at $\delta_H$ 4.07 must be assigned as OMe groups whereas other methyl could be accounted for NMe. The $^1H$ NMR spectrum also two aromatic protons resonated at

$\delta_H$ 7.87, 7.21 and also olefinic protons at $\delta_H$ 7.60 and 7.09. The DEPTQ spectrum (Figure 3.25, Table 3.9) exhibited presence of a total of fourteen carbons which could be assigned based on the correlation observed in the HSQC and HMBC spectra. In the HSQC experiment, the three protons signals at $\delta_H$ 3.98 showed direct correlation to the carbon at $\delta_C$ 32.6 whilst other methyl signals at $\delta_H$ 4.07 revealed direct connection to the carbons at $\delta_C$ 56.7 and 57.0. The HMBC experiment (Figure 3.26) played a key role in the confirmation of the structure of the compound. In the HMBC experiment, the methoxyl group protons at $\delta_H$ 4.07 (2 x OMe) showed $^3J$ connectivity to the oxygenated quaternary carbons at $\delta_C$ 135.6 (C-6) and 154.5 (C-7) while the quaternary carbons at *N*-methyl protons at $\delta_H$ 3.98 was connected to two quaternary carbons at $\delta_c$ 156.1 (C-2) and 146. 2 (C-9) by $^3J$. The protons at $\delta_H$ 7.09 (H-3′) and 7.87 (H-5) revealed a common $^3J$ HMBC correlation to the carbonyl at $\delta_C$ 172.8 (C-4). Thus, compound **100** was identified as 6,7-dimethoxy-9-methylfuro[2,3-b]quinolin-4(9H)-one or isokokusaginine. The spectroscopic data of compound **100** were in a good agreement with respective published data of isokokusaginine. Isokokusaginine (**100**) was previously isolated from *Ruta graveolines* and other plants (Openshaw, 1967). Isokokusaginine (**100**) is here reported for the first time isolated from *R. chalepensis*.

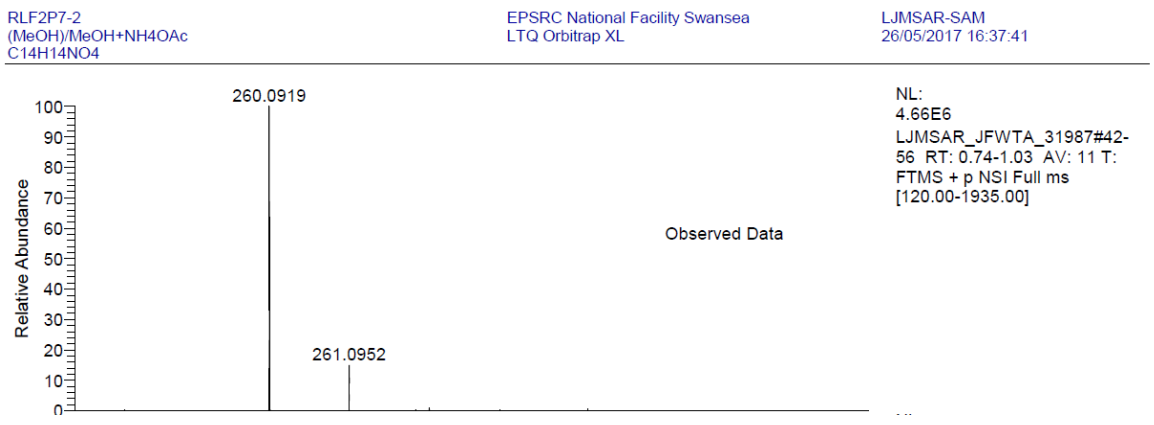


***Figure 3.23**: The HRESIMS spectrum of compound **100***

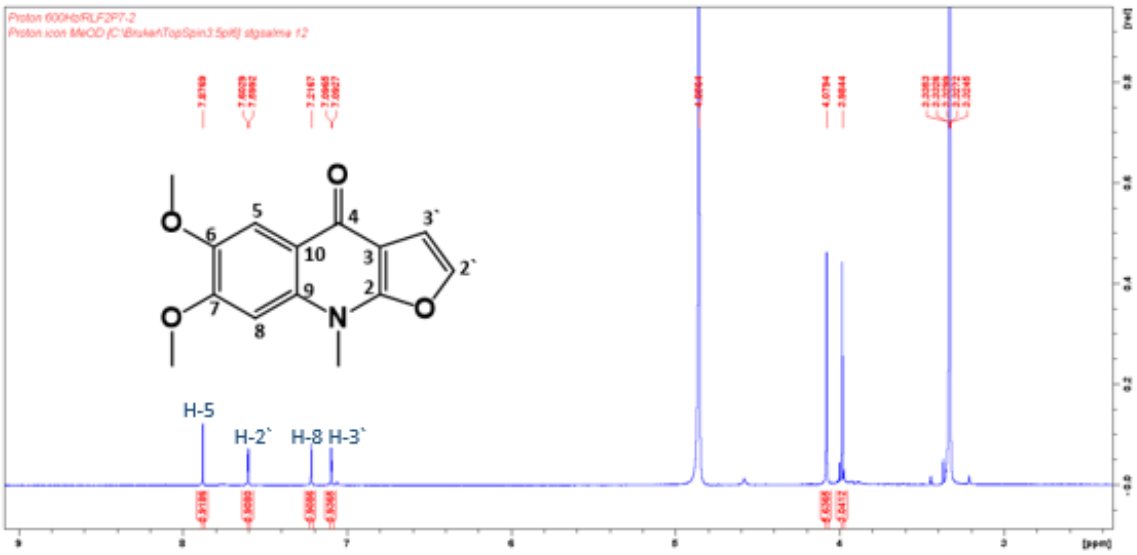


***Figure 3.24**:* The $^{1}$H NMR (600 MHz, $CD_3OD$) spectrum of compound **100**

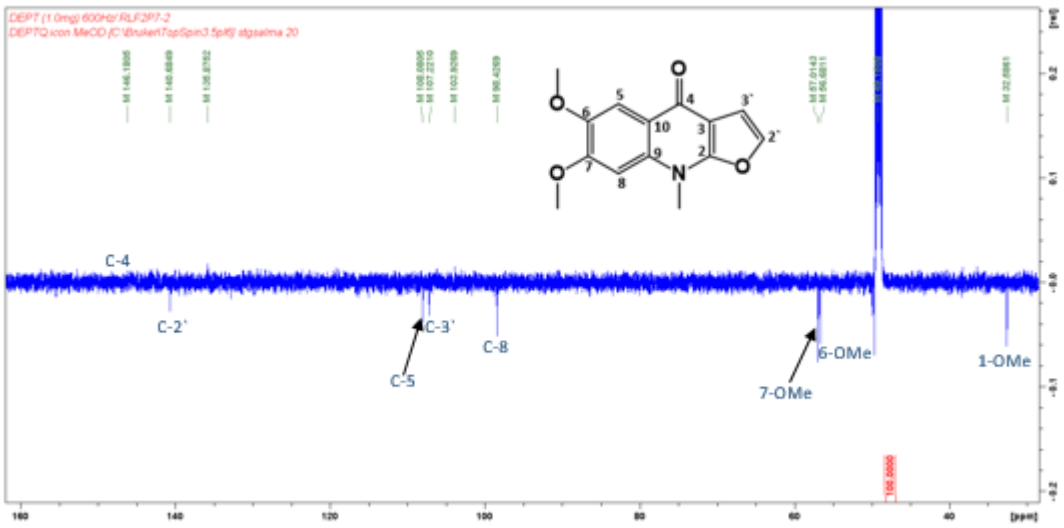


***Figure 3.25**: The DEPT NMR (150 MHz, $CD_3OD$) spectrum of compound **100***

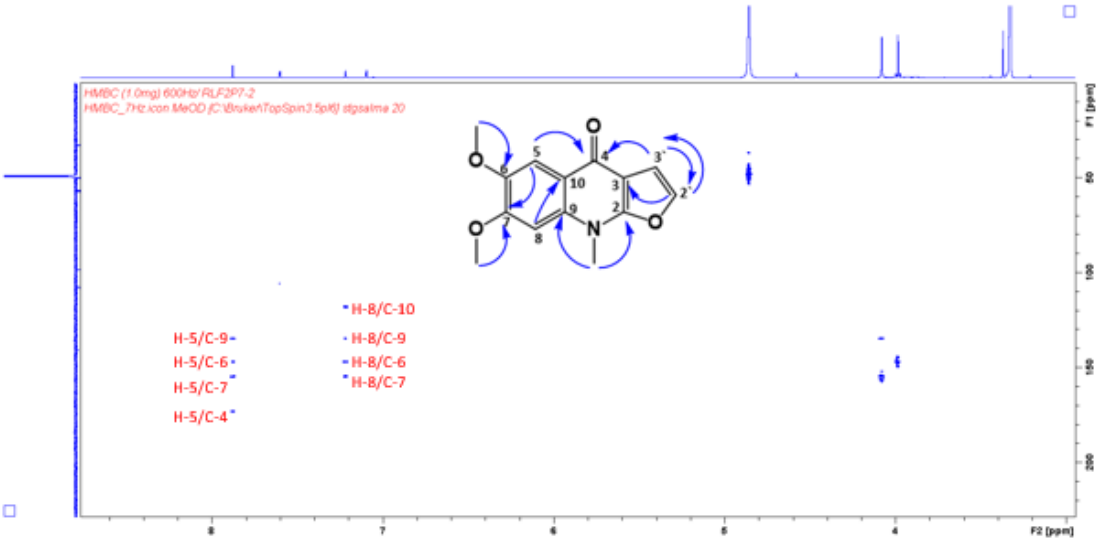


***Figure 3.26**:* The HMBC correlations of compound **100**

### 3.1.9.3 Structure elucidation of γ-fagarine (42)

The compound **42** was isolated as a pale brown crystal from different part extracts of *R. chalepensis*. The HRESIMS (Figure 3.27) suggested the empirical formula as $C_{13}H_{11}NO_3$ and in the positive ion mode it showed $[M+H]^+$ peak at *m/z* 230.0814 (calculated 230.0817). The $^1$H NMR spectrum (Figure 3.28, Table 3.9) showed two sets of methoxy signals at $\delta_H$ 4.45 (3H) and 4.08 (3H), four aromatic protons resonated at $\delta_H$ 7.85, 7.36, 7.36 and 7.06 and two olefinic protons at $\delta_H$ 7.65 and 7.08 as a part of furan ring. The DEPTQ spectrum (Figure 3.29, Table 3.9) exhibited a total of thirteen carbons, two methoxyl, six quaternary carbons and five olefinic carbons. The protons at $\delta_H$ 4.08 and 4.45 revealed direct correction to the corresponding carbons at δc 56.4 and 59.3 in the HSQC spectrum. In the $^1$H-$^1$H COSY spectrum (Figure 3.30), proton at $\delta_H$ 7.36 (H-6) showed interaction with protons at $\delta_H$ 7.85 (H-5) and 7.06 (H-7). $^1$H-$^1$H COSY interaction was also revealed between protons at $\delta_H$ 7.65 (H-2′) and 7.08 (H-3′). In the HMBC experiment (Figure 3.31), H-5, H-3′ and methoxyl protons at $\delta_H$ 4.45 (MeO-4) displayed $^3J$ connectivity to the oxygenated quaternary carbon at $\delta_C$157.4 (C-4) whilst H-6 and methoxyl protons at $\delta_H$ 4.05 were collated to another oxygen bearing quaternary carbon at $\delta_C$ 157.4 (C-4). Thus, compound **42** was

identified as 8-methoxydictamnine or γ-fagarine. The spectroscopic data of compound **42** were in a good agreement with respective published data of γ-fagarine (Boyd *et al.*, 2013). γ-fagarine (**42**) was previously isolated from *Rutaceae* family *Ruta* genus and *Ruta chalepensis*. γ-fagarine (**42**) was reported as antimicrobial, antiplasmodial and anti-HCV effect on 20 µg/ml concentration (Tavares *et al.*, 2014; Adamska-Szewczyk *et al.*, 2016).

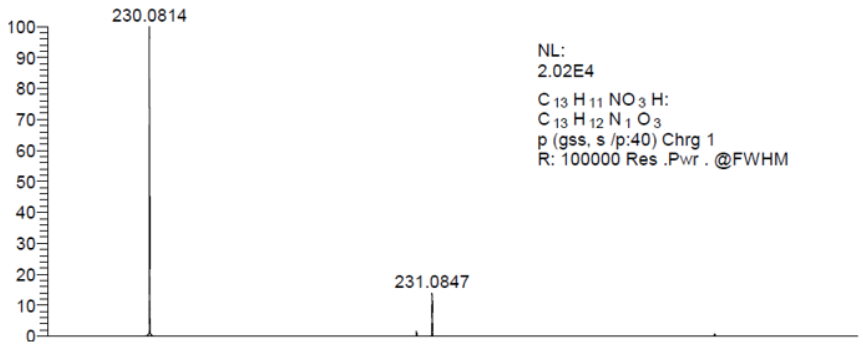


***Figure 3.27**: The HRESIMS spectrum of compound **42***

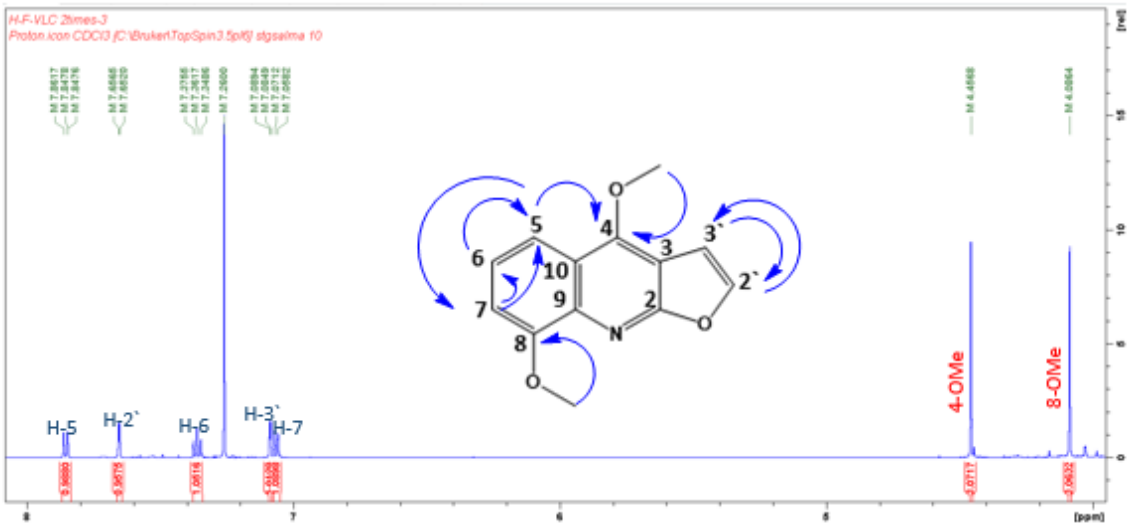


***Figure 3.28**: $^{1}H$ NMR (600 MHz, $CDCl_3$) spectrum of compound **42***

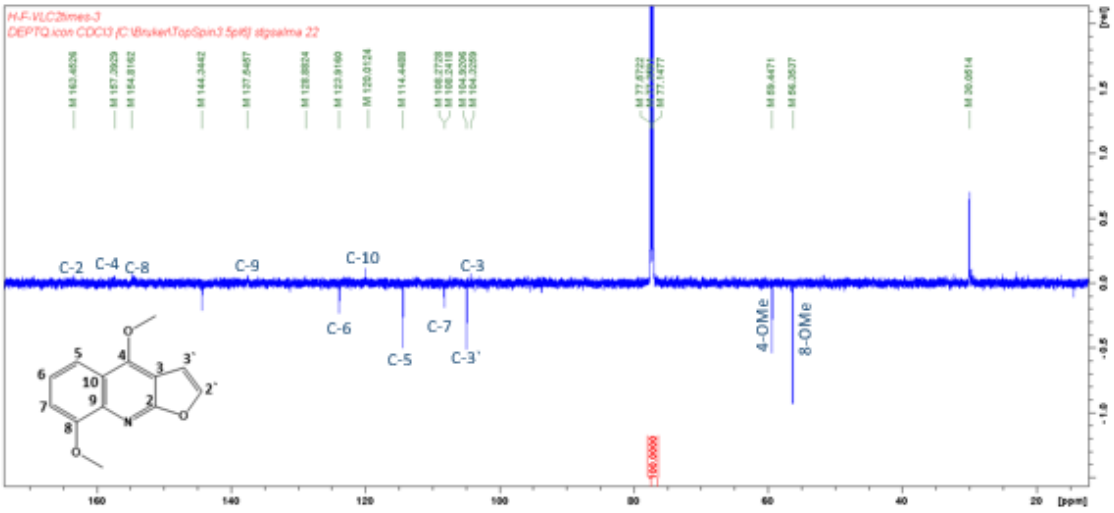


***Figure 3.29**: DEPT NMR (150 MHz, $CDCl_3$) spectrum of compound **42***

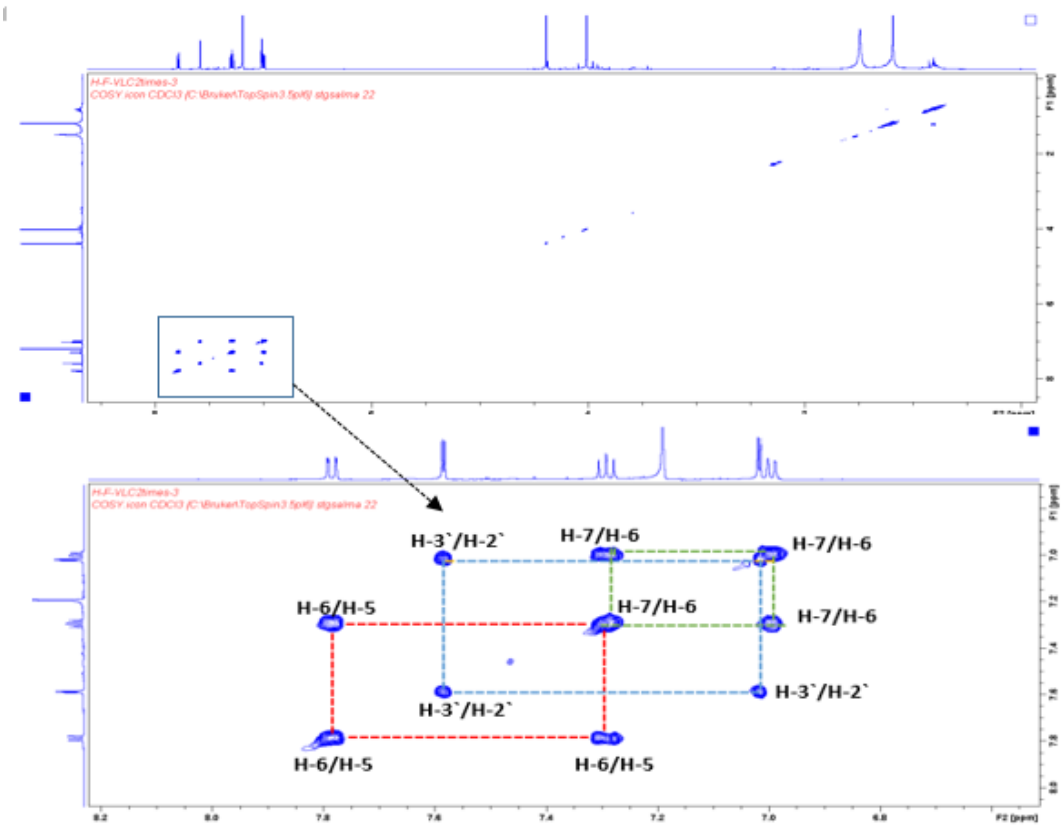


***Figure 3.30**: COSY NMR spectrum of compound **42***

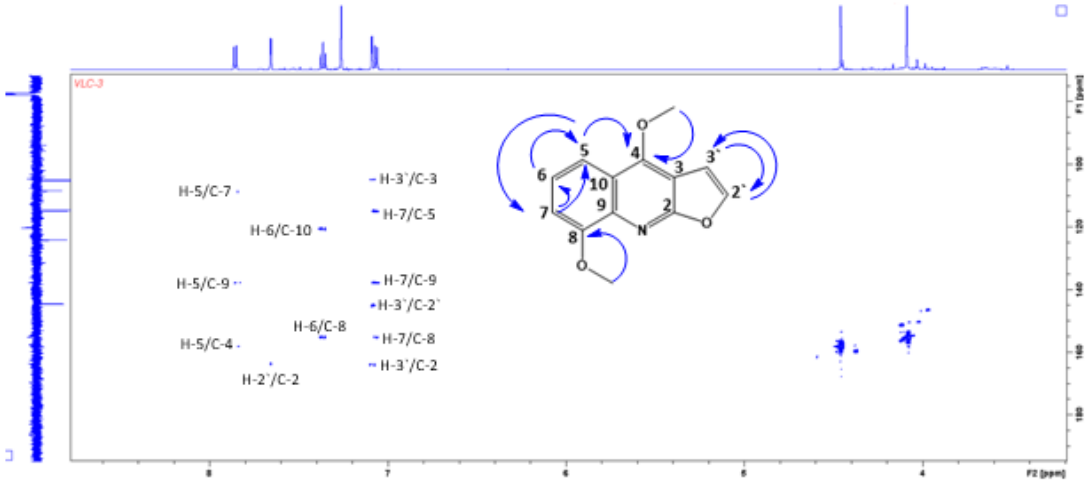


***Figure 3.31**: The HMBC correlations of compound **42***

### 3.1.9.4 Structure elucidation of skimmianine (41)

The compound **41** was isolated as a colourless powder. The HRESIMS (Figure 3.32) suggested the empirical formula as $C_{14}H_{13}NO_4$ and in the positive ion mode it showed $[M+H]^+$ peak at *m/z* 260.0919 (calculated 260.0923). The $^1$H NMR spectra (Figure 3.33, Table 3.9) showed three sets of methoxyl signals at $\delta_H$ 3.99 (3H), 4.04 (3H) and 4.51 (3H) and *ortho*-coupled (*J*= 9.2 Hz) protons at $\delta_H$ 7.40 (H-6) and 8.08 (H-5) also, two olefinic signals at $\delta_H$ 7.35 (H-3′) and $\delta_H$ 7.78 (H-2′) confirming the formation of furan ring. The $^{13}$C-NMR (Figure 3.34, Table 3.9) spectra showed a total of fourteen carbons including three methoxyl (OMe) and seven quaternary carbons. In the HSQC, H-2′, H-2′, H-5 and H-6 exhibited direct connectivity to the corresponding methine carbons $\delta_C$ 106.5, 144.6, $\delta_C$ 119.8 and 113.6 whilst the methoxyl group protons at $\delta_H$ 3.99, 4.04 and 4.51 revealed direct connection to the carbons at $\delta_C$ 61.9, 57.4 and 60.0. In the HMBC experiment, H-5, H-3′ and methoxyl protons at $\delta_H$ 4.51 revealed $^3J$ correlation to the oxygenated quaternary carbon at $\delta_c$ 159.4 while the methoxyl protons at $\delta_H$ 4.04 and H-5 showed $^3J$ correlation to another oxygen bearing quaternary carbon at $\delta_C$ 154.0. Based on these spectral data and their correlation in the HSQC and HMBC, the compound **41**, quinoline alkaloid, was identified as 5,4,7,8-trimethoxyfuro[2,3-b]quinolone, commonly known as skimmianine. The

spectroscopic data of compound **41** were in a good agreement with respective published data of skimmianine, which is considered one of the common compounds in the Rutaceae family (Ulubelen *et al.*, 1986). Skimmianine (**41**) was isolated from different species of the genus *Ruta*. Previous studies confirmed the anti-inflammatory effect and antimicrobial activity of skimmianine (**41**) (El Sayed *et al.*, 2000; Ratheesh *et al.*, 2013).

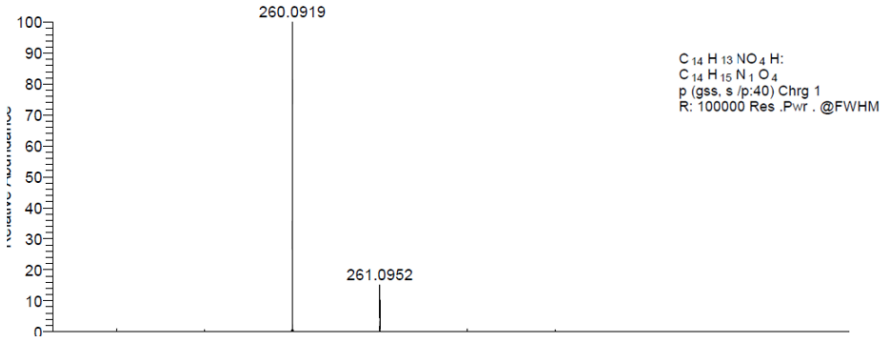


***Figure 3.32**: The HRESIMS spectrum of compound **41***

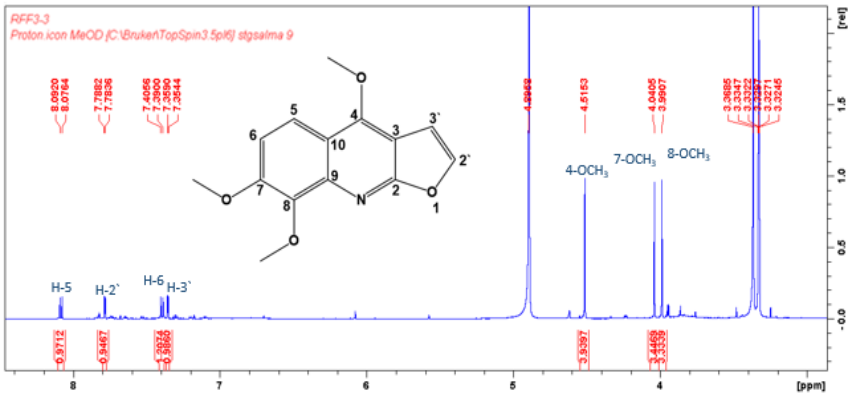


***Figure 3.33**: $^{1}H$ NMR (600 MHz, $CD_3OD$) spectrum of compound **41***

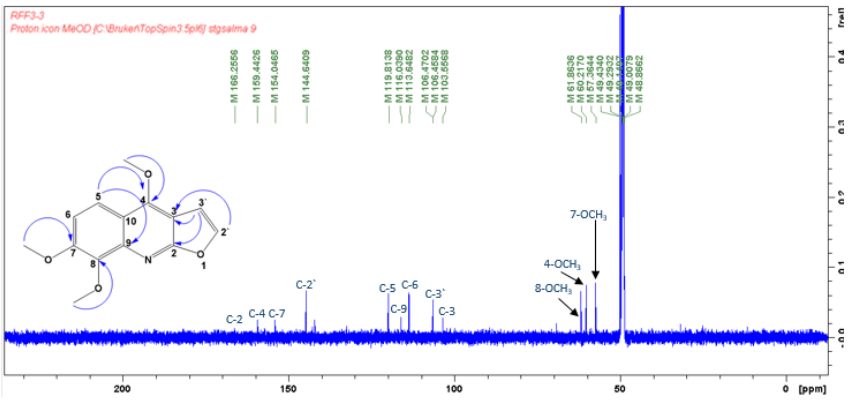


***Figure 3.34**: The $^{13}C$ NMR (150 MHz, $CD_3OD$) spectrum of compound **41***

**Table 3.9**: $^{1}$H NMR (600 MHz) and $^{13}$C NMR data of compounds **41, 42, 99,100**

| **Position** | **$\delta_H$ m (*J* in Hz)** | | | | **$\delta_C$** | | | |
|---|---|---|---|---|---|---|---|---|
| | **99** | **100** | **42** | **41** | **99** | **100** | **42** | **41** |
| 2 | - | - | - | - | 163.3 | 156.1 | 163.5 | 166.2 |
| 3 | - | - | - | - | 102.5 | 106.2 | 104.3 | 103.5 |
| 4 | - | - | - | - | 155.8 | 172.8 | 157.4 | 159.4 |
| 5 | 7.48 s | 7.87 s | 7.85 *d* (8.34) | 8.08 *d* (9.2) | 100.5 | 107.2 | 114.3 | 119.8 |
| 6 | - | - | 7.36 *dd* (8.34,7.8) | 7.40 *d* (9.2) | 148.0 | 135.9 | 123.9 | 113.6 |
| 7 | - | - | 7.06 *d* (7.8) | - | 152.9 | 154.5 | 108.3 | 154.0 |
| 8 | 7.34 s | 7.21 s | - | - | 107.0 | 98.4 | 154.8 | 144.7 |
| 9 | - | - | - | - | 142.7 | 146.2 | 137.5 | 116.0 |
| 10 | - | - | - | - | 113.2 | 117.6 | 120.0 | 106.4 |
| 2′ | 7.57 *d* (2.80) | 7.60 *d* (2.22) | 7.65 *d* (2.7) | 7.78 *d* (2.2) | 142.7 | 140.7 | 144.3 | 144.6 |
| 3′ | 7.04 *d* (2.80) | 7.09 *d* (2.22) | 7.08 *d* (2.7) | 7.35 *d* (2.2) | 104.8 | 108.1 | 105.0 | 106.5 |
| N- $CH_3$ | - | 4.07 s | - | - | - | 32.6 | - | - |
| 4- $OCH_3$ | 59.14 s | - | 4.45 s | 4.51 s | 59.1 | - | 59.4 | 60.2 |
| 6- $OCH_3$ | 4.02 s | 3.98 s | - | - | 56.2 | 56.7 | - | - |
| 7- $OCH_3$ | 56.30 s | 4.07 s | - | 4.04 s | 56.3 | 57.0 | - | 57.4 |
| 8- $OCH_3$ | - | - | 4.08 s | 3.99 s | - | - | 56.3 | 61.9 |

### 3.1.9.5 Structure elucidation of bergapten (43)

The compound **43** was isolated as pale yellow crystals. The HRESIMS (Figure 3.36) suggested the empirical formula as $C_{12}H_8O_4$ and in the positive ion mode it showed $[M+H]^+$ peak at *m/z* 217.0495 (calculated 217.0501). The UV spectrum showed absorption maxima ($\lambda_{max}$) at 210 nm, typical of a coumarin. The $^1$H NMR spectrum (Figure 3.37, Table 3.10) exhibited one aromatic proton as singlet at $\delta_H$ 7.14, two *ortho*-coupled (*J*=9.7 Hz) protons at $\delta_H$ 8.15 (H-4) and 6.27 (H-3) and one methoxyl signal at $\delta_H$ 4.26 (3H). Moreover, the presence of two aromatic protons displayed at $\delta_H$ 7.59 (1H, d, *J* = 2.4 Hz, H-2′) and 7.02 (1H, d, *J* = 2.4 Hz, H-3′) in the $^1$H NMR spectrum constituted a furan ring. The $^{13}$C NMR spectrum (Figure 3.38, Table 3.10) presented a total of twelve carbons including a carbonyl at $\delta_c$ 161.6 (C-2), a methoxyl at $\delta_C$ 60.5, five methane carbons at $\delta_C$ 113.0 (C-3), 139.6 (C-4), 94.3 (C-8), 145.1 (C-2′),105.3 (C-3′) and five quaternary carbons at $\delta_C$ 113.1 (C-6), 158.7 (C-7), 153.0 (C-9), 149.9 (C-5), 106.8 (C-10). In the HMBC experiment (Figure 3.39), long rang correlations were observed from H-2′ to C-6, C-7 and from H-3 to C-5, C-6 C-7. In the HMBC experiment (Figure 3.44), a common $^3J$ correlation from protons at $\delta_H$ 8.15 (H-4), 7.02 (H-3′) and 4.26 (OMe) to an oxygen bearing quaternary carbon at $\delta_C$ 149.9 confirmed the presence of methoxyl group at C-5. The H-4 also showed $^3J$ correlation to the carbonyl $\delta_C$ 161.6 (C-2) and another oxygenated quaternary at $\delta_C$ 153.0 (C-9) while the H-3 revealed $^3J$ correlation to a quaternary at $\delta_C$ 106.8 (C-10). In addition, H-8 displayed HMBC connectivity to C-9 (by $^2J$), C-7 ($\delta_C$ 158.7; $^2J$), C-6 ($\delta_C$ 113.1; $^3J$) and C-10 ($\delta_C$ 106.8; $^3J$). Thus, compound **43** was identified as bergapten, a common furocoumarin present in the plant family, Rutaceae. The spectroscopic data of compound **43** were in a good agreement with respective published data of bergapten (Um *et al.*, 2010; O′Neill *et al.*, 2013; Dehghan *et al.*, 2017). Bergapten (**43**) was previously isolated from *Ruta* and *Citrus* species (Dreyer, 1966; Gonzalez *et al.*, 1977). The researchers also reported the cytotoxic activity of

bergapten against different cancer cell line including ovarian, prostate, lung and breast (De Amicis, 2015). The antimicrobial activity of bergapten (**43**) against *E. coli*, *S. aureus* and *H. pylori* was confirmed (Santoro *et al.*, 2016).

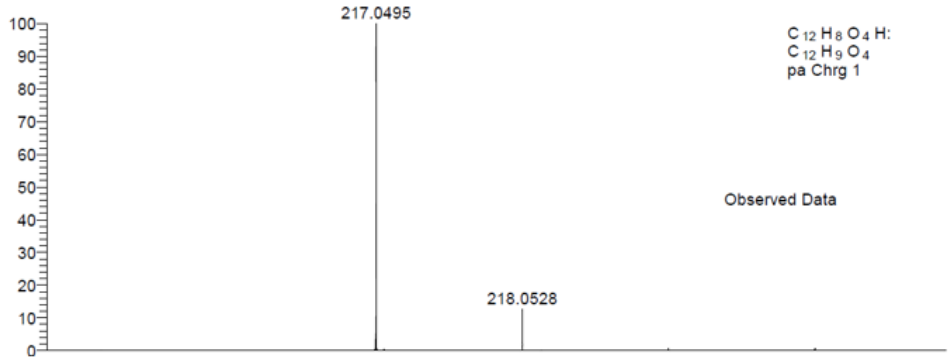


***Figure 3.35**: The HRESIMS spectrum of compound **43***

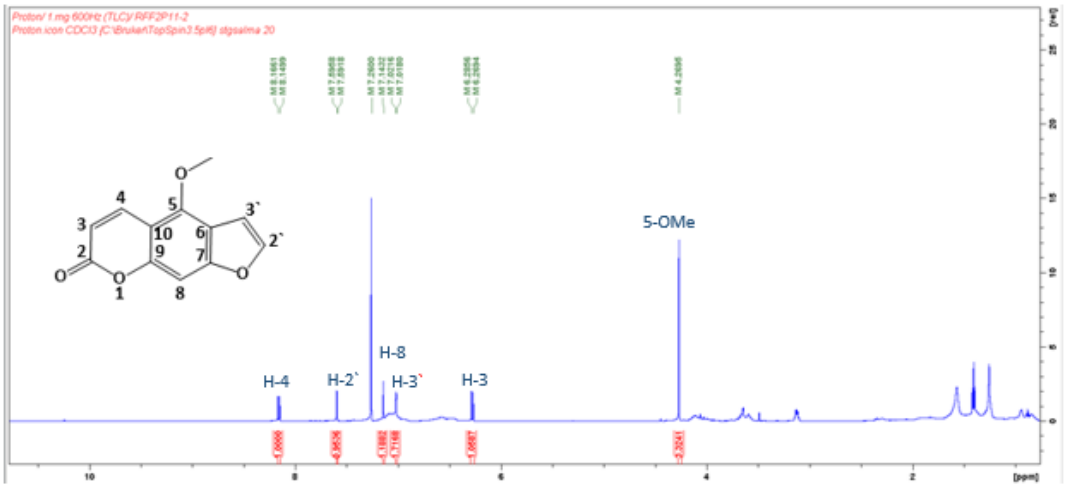


***Figure 3.36**: $^{1}H$ NMR (600 MHz, $CDCl_3$) spectrum of compound **43***

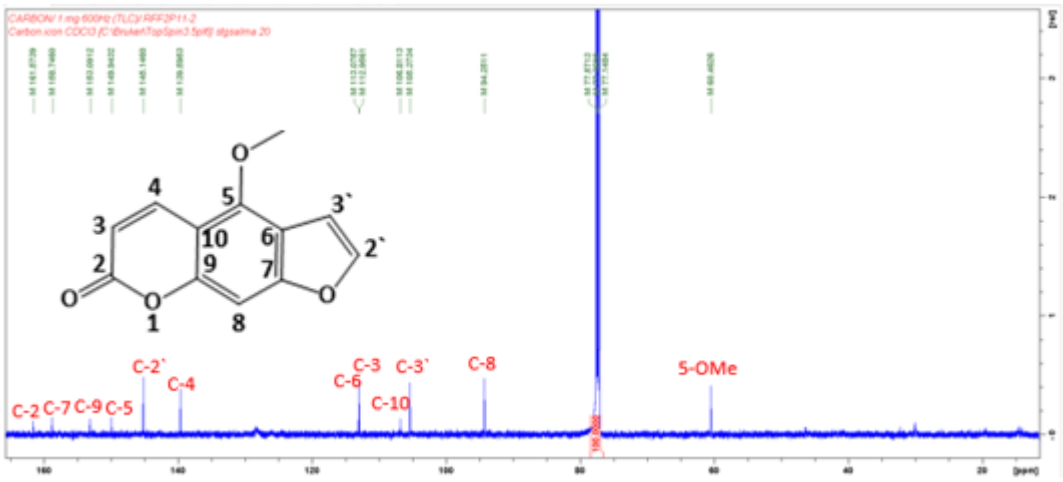


***Figure 3.37**: The $^{13}C$ NMR (150 MHz, $CDCl_3$) spectrum of compound **43***

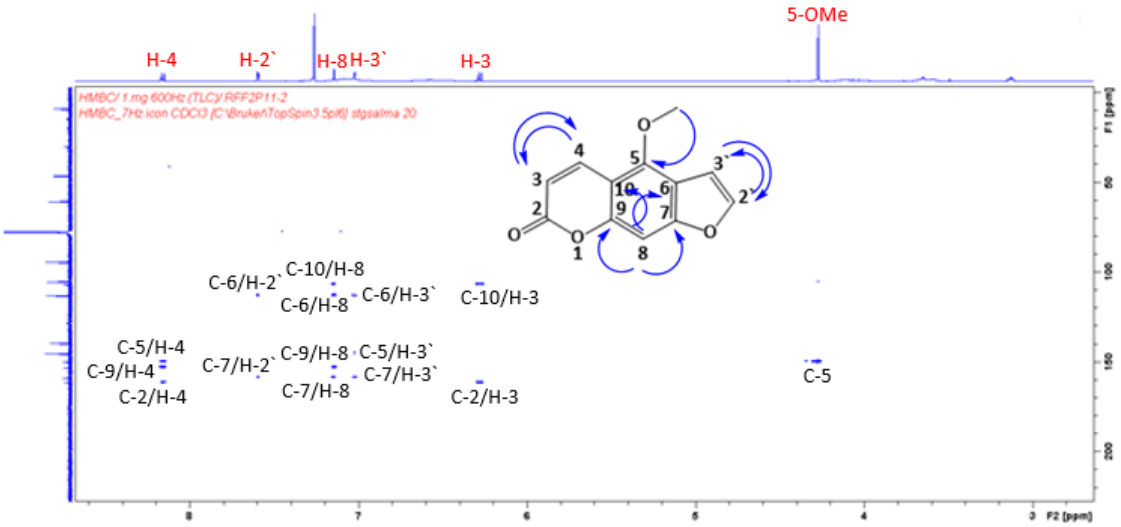


***Figure 3.38**: The HMBC correlations of compound **43***

### 3.1.9.6 Structure elucidation of isopimpinellin (44)

The compound **44** was isolated as colourless needles. The HRESIMS (Figure 3.40) suggested the empirical formula as $C_{13}H_{10}O_5$ and in the positive ion mode it showed $[M+H]^+$ peak at *m/z* 247.0604 (calculated 247.0606). The $^1$H NMR and $^{13}$C NMR spectra of compound **44** are very similar to those of **43**. The $^1$H NMR spectrum (Figure 3.41, Table 3.10) displayed two sets of methoxy signals at $\delta_H$ 4.13 (3H) and 4.23 (3H) and four aromatic methines at $\delta_H$ 6.32 (1H, d, *J*= 9.78 Hz), 8.28 (1H, d, *J*= 9.78 Hz), 7.85 (1H, d, *J*=2.34 Hz) and 7.25 (1H, d, *J*=2.34 Hz). The DEPTQ spectrum (Figure 3.42, Table 3.10) revealed a total of thirteen carbons comprising one carbonyl at $\delta_C$ 162.8, six quaternary carbons, four aromatic methines at $\delta_C$ 113.3, 141.6, 147.2, 106.5 and two methoxy carbons at $\delta_C$ 61.6 and 62.2. In the HMBC experiment, the methoxyl signals at $\delta_H$ 4.22 and 4.13 revealed $^3J$ correlation to the oxygen bearing quaternary carbons at $\delta_C$ 145.6 (C-5) and 192.6 (C-8), respectively and thereby confirmed their positions in the molecule. The H-3 exhibited $^3J$ correlation to a quaternary carbon at $\delta_C$ 108.8 (C-10) while H-4 presented $^3J$ correlation to C-5 and also the carbonyl group at $\delta_C$ 162.8 (C-2) and oxygenated quaternary carbon at $\delta_C$ 145.0 (C-9). Moreover, H-2′ showed HMBC connectivity to C-3′ (106.5 by $^2J$) and C-6 (116.5 by $^3J$) whilst H-3′ exhibited HMBC correlation to C-5 ($^3J$) and C-7

(151.8; by $^{3}J$). Thus, compound **44** identified as 5,8-dimethoxy-6,7-furanocoumarin or isopimpinellin. The spectroscopic data of compound **44** were in a good agreement with respective published data of isopimpinellin (Wu *et al.*, 2003; Shu Shan *et al.*, 2013). The antimicrobial activity of isopimpinellin (**44**) was reported to prevent the growth of *Cryptococcus neoformans* with $IC_{50}$ 40 mg/mL (Ngunde Ngwendson *et al.*, 2003) and successively inhibited *Staphylococcus aureus, Escherichia coli, Pseudomonas aeruginosa* and *Candida albicans* with MIC 3.75, >7.5, >7.5 and 0.93, respectively (Golfakhrabadi *et al.*, 2016).

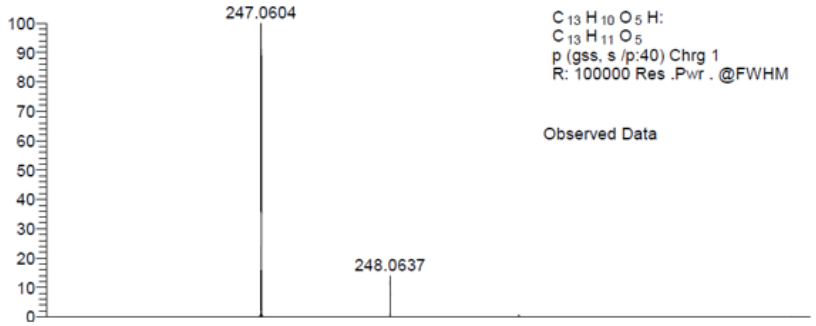


***Figure 3.39**: The HRESIMS spectrum of compound **44***

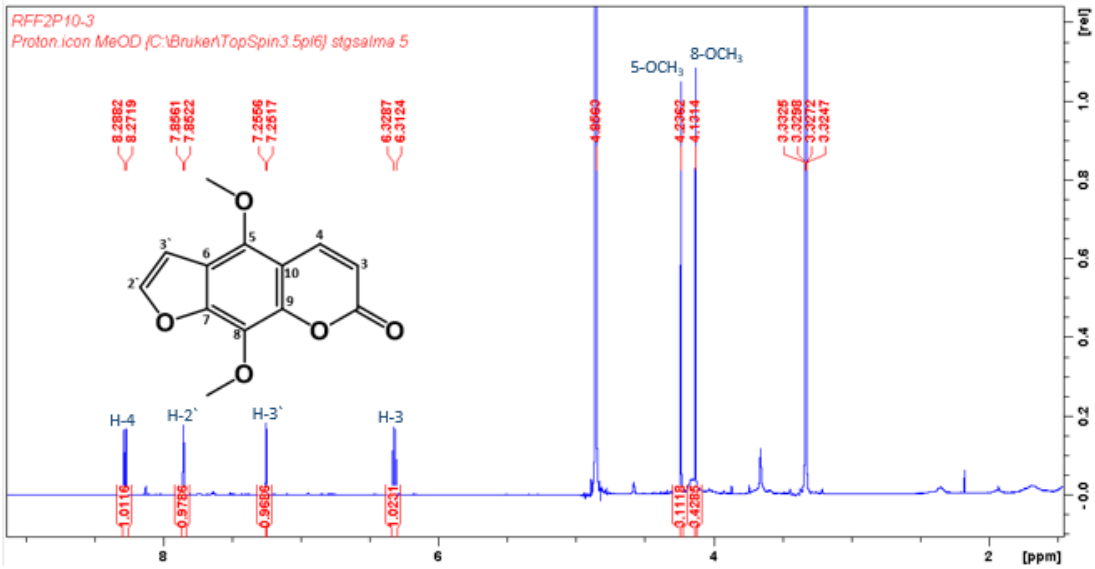


***Figure 3.40**: $^{1}H$ NMR (600 MHz, $CD_3OD$) spectrum of compound **44***

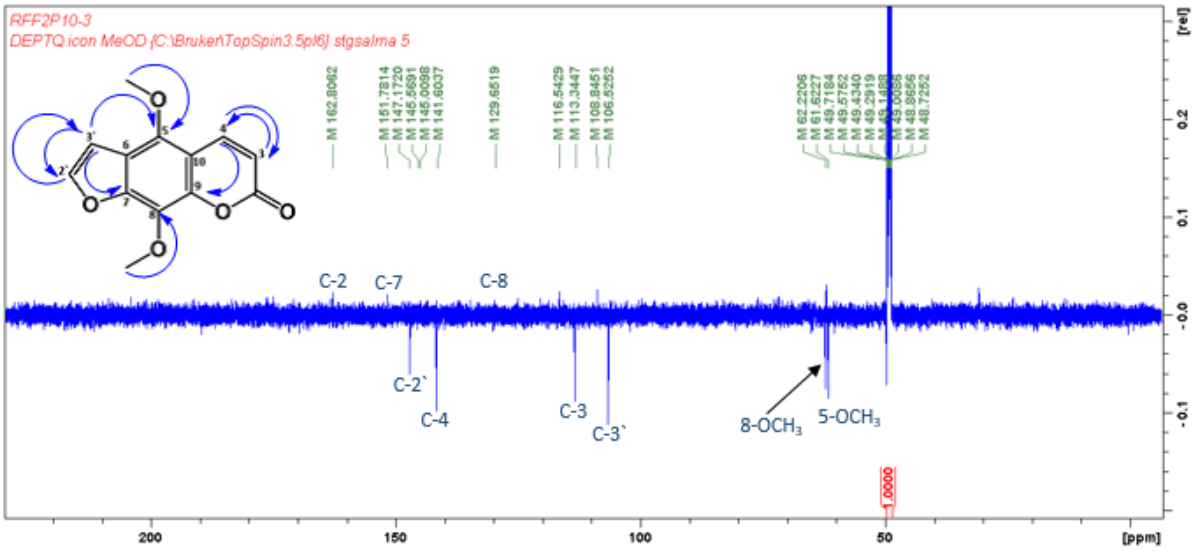


***Figure 3.41**: DEPT NMR (150 MHz, $CD_3OD$) spectrum of compound **44***

### 3.1.9.7 Structure elucidation of chalepin (45)

The compound **45** was isolated as white crystals. The HRESIMS (Figure 3.43) suggested the empirical formula as $C_{19}H_{22}O_4$ and in the positive ion mode it showed $[M+H]^+$ peak at *m/z* 315.1596 (calculated 315.1596). The $^1$H NMR spectra (Figure 3.44, Table 3.10) exhibited three sets of methyl signals at $\delta_H$ 1.22 (3H), 1.36 (3H) and 1.46 (2X 3H) and three aromatic methine signals at $\delta_H$ 7.47 (H-5), 7.19 (H-4) and 6.70 (H-9). Moreover, the $^1$H NMR presented three olefinic protons at $\delta_H$ 6.15 (1H, dd, *J*= 17.4, 10.7 Hz, H-4′), 4.71 (1H, dd, *J*= 17.4, 6.00 Hz, H-2), 5.08 (2H, dd, *J*=3.5, 10.6 Hz, H-4′, H-5′) and two protons multiplet at $\delta_H$ 3.20 (H-3). The $^{13}$C NMR spectrum (Table 3.10) showed a total of nineteen carbons including carbonyl at $\delta_C$ 160.53 (C-7), four methyls, one methylene, seven quaternary and the remaining carbons methines. In the HMBC experiment, the methyl protons at $\delta_H$ 1.46 (H2′, 3′) showed $^3J$ correlation to quaternary carbon at $\delta_C$ 131.2 (C-6) and methine carbon at $\delta_C$ 145.9 (C-4′) while the methyl groups at $\delta_H$ 1.22 (H-2′′) and 1.26 (H-3′′) revealed $^3J$ correlation to an oxymethine carbon at $\delta_C$ 91.2 (C-2). Based on these spectral data and their correlations in the HSQC and HMBC, the compound **45** was assigned as chalepin, a furanocoumarin. The spectroscopic data of compound **45** were in a good

agreement with respective published data of chalepin (Richardson *et al.*, 2016) which is widespread compound on *Ruta* species (Richardson *et al.*, 2016). Chalepin (**45**) was documented to exhibit excellent cytotoxicity against lung cancer cells with an $IC_{50}$ value 8.69 µg/ml and worked as an antimicrobial agent (Richardson *et al.*, 2016; Tamene and Endale, 2019).

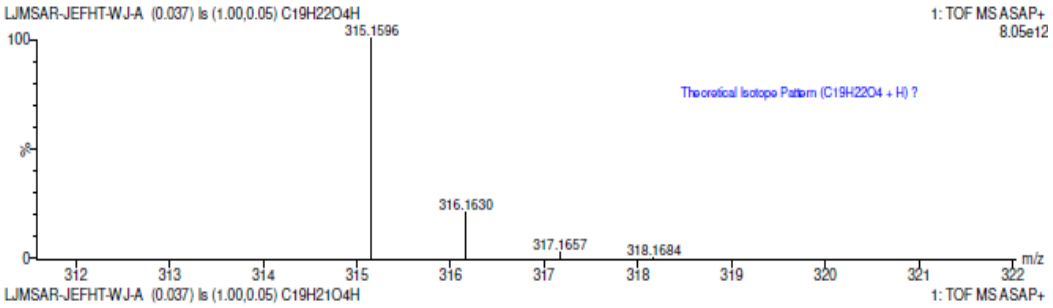


***Figure 3.42**: The HRESIMS spectrum of compound **45***

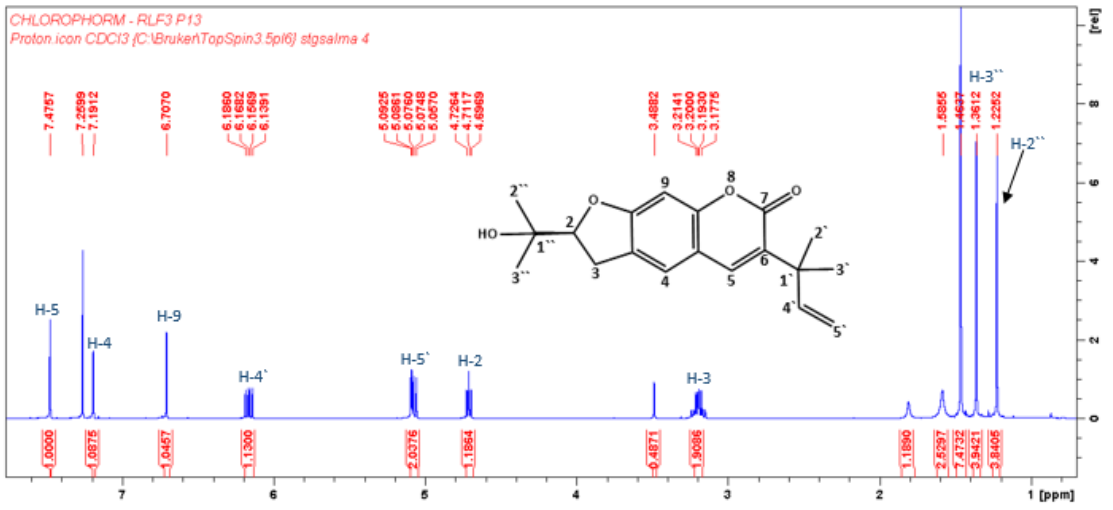


***Figure 3.43**:* $^{1}$H NMR (600 MHz, $CDCl_3$) spectrum of compound **45**

### 3.1.9.8 Structure elucidation of rutamarin (47)

The compound **47** was isolated as a colourless prism. The HRESIMS (Figure 3.45) suggested the empirical formula as $C_{21}H_{24}O_5$ and in the positive ion mode it showed $[M+H]^+$ peak at *m/z* 357.1702 (calculated 357.1702). The 1D and 2D NMR spectra of compound **47** were similar to chalepin (**45**). The only difference was the presence of an additional signal at $\delta_H$ 1.98 (3H, H-5″) in the $^{1}$H NMR spectrum of compound **47** (Figure 3.47, Table 3.10)

and extra peaks for the presence of an acetyl group ($\delta_C$ 21.4 for methyl and $\delta_C$170.6 carbonyl group in the $^{13}C$ NMR spectrum (Table 3.10). The observation of the cross peak in the HSQC spectrum approved the direct connectivity of proton at $\delta_H$ 1.98 (H-5′′) to carbon at $\delta_C$ 21.4 (C-5′′). In the HMBC experiment the methyl groups at $\delta_H$ 1.50 (H-2′′) and 1.55 (H-3′′) exposed $^3J$ correlation to $\delta_C$ 170.6 (C-4′′). The NMR and mass spectroscopic data as well as the correlation revealed in the HSQC and HMBC confirmed the identification of compound **47** as chalepin acetate or rutamarin (Wu *et al.*, 2003). The spectroscopic data of compound **47** were in a good agreement with respective published data of rutamarin (Wu *et al.*, 2003). The isolation of rutamarin (**47**) was confirmed from the Rutaceae (Adamska-Szewczyk *et al.*, 2016). Rutamarin was shown to inhibit HT29 cells (Colon Adenocarcinoma cell line) with $IC_{50}$ 5.6 µM (Suhaimi *et al.*, 2017) and the antiviral activity of rutamarin was reported (Xu *et al.*, 2014). Rutamarin (**47**) improved glucose homeostasis in mice (Mancuso *et al.*, 2015).

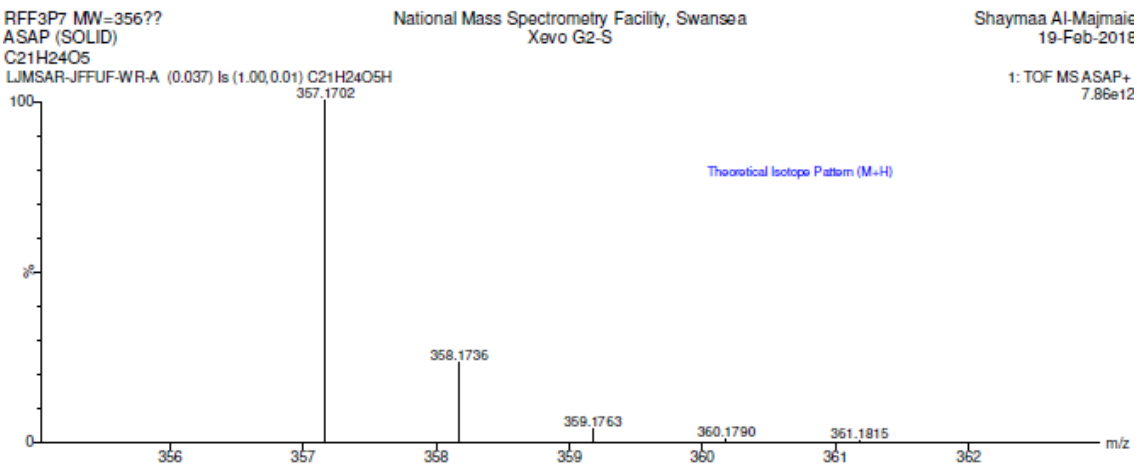


***Figure 3.44**: The HRESIMS spectrum of compound **47***

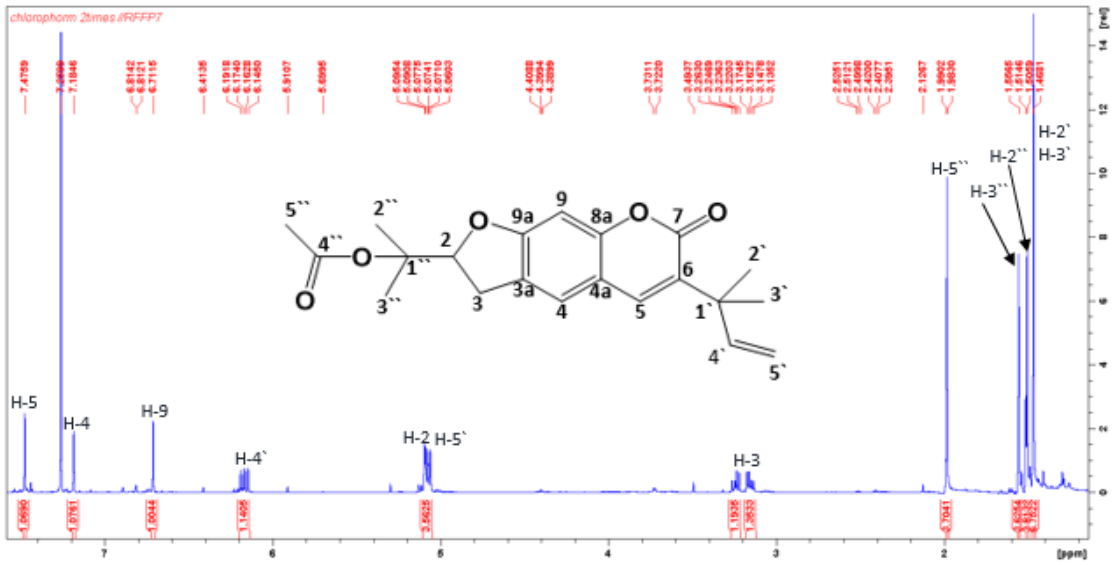


***Figure 3.45**: [1]H NMR (600 MHz, $CDCl_3$) spectrum of compound **47***

### 3.1.9.9 Structure elucidation of chalepensin (**46**)

The compound **46** was isolated as white crystals. The HRESIMS (Figure 3.47) suggested the empirical formula as $C_{16}H_{14}O_3$ and in the positive ion mode it showed $[M+H]^+$ peak at *m/z* 255.1021 (calculated 255.1021). The 1D and 2D NMR spectra of compound **46** were very similar to those of compounds **45** and **47** except for the absence of one side chain. The $^1$H NMR spectra for compound **46** (Figure 3.48, Table 3.10) showed *ortho*-coupling of olefinic protons at $\delta_H$ 7.66 and 6.81 which confirmed the presence of a furan ring in the molecule. The $^{13}$C NMR spectra revealed a total of fourteen carbons including two sets of methyl signals at $\delta_C$ 26.5, five methine carbons at $\delta_C$ 106.7 (H-2), 146.9 (H-3), 119.8 (H-4), 138.6 (H-5) and 99.4 (H-9) and one carbonyl at $\delta_C$ 160.2 (C-7). The HSQC experiment revealed the direct connectivity from protons at $\delta_H$ 7.66 (H-2) and 6.81 (H-3) to carbons at $\delta_c$ 146.9 (C-2) and 106.7 (C-3), respectively. In the HMBC experiment, H-2 revealed $^3J$ correlation to the quaternary carbons at $\delta_C$ 124.9 (C-4a) and 151.7 (C-9a) while H-3 showed $^3J$ to olefinic carbon at $\delta_C$ 119.8 (C-4) and quaternary carbons at $\delta_c$ 151.7 (C-9a). Based on these spectral data and their correlation in the HSQC and HMBC experiments, the structure of compound **46** was confirmed as chalepensin. The spectroscopic data of compound **46** were in good agreement with respective published data of chalepensin (Wu *et al.*, 2003).

Chalepensin (**46**) was previously isolated from other *Ruta* species (San Miguel, 2003; Adamska-Szewczyk *et al.*, 2016). Chalepensin (**46**) was reported to reduce the activity of the primary enzyme responsible about the oxidation of nicotine and cotinine, which is cytochrome P450 (CYP) 2A69 (Ueng *et al.*, 2011). Chalepensin (**46**) showed significant cytotoxic activity against lung and blood cancer cells (Khlifi *et al.*, 2013; Wannes *et al.*, 2017). One of the traditional uses of *R. chalepensis* was curing tooth pain and the studies revealed that *Streptococcus mutans*, which is found in the cavity of the human mouth and is a major contributor to tooth decay is inhibited by chalepensin with MIC 7.8 µg/mL (Gomez-Flores *et al.*, 2016).

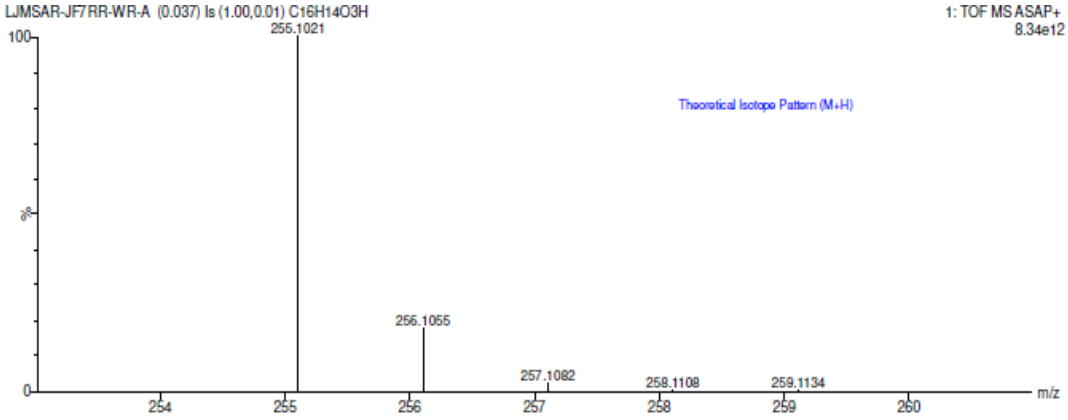


***Figure 3.46**: The HRESIMS spectrum of compound **46***

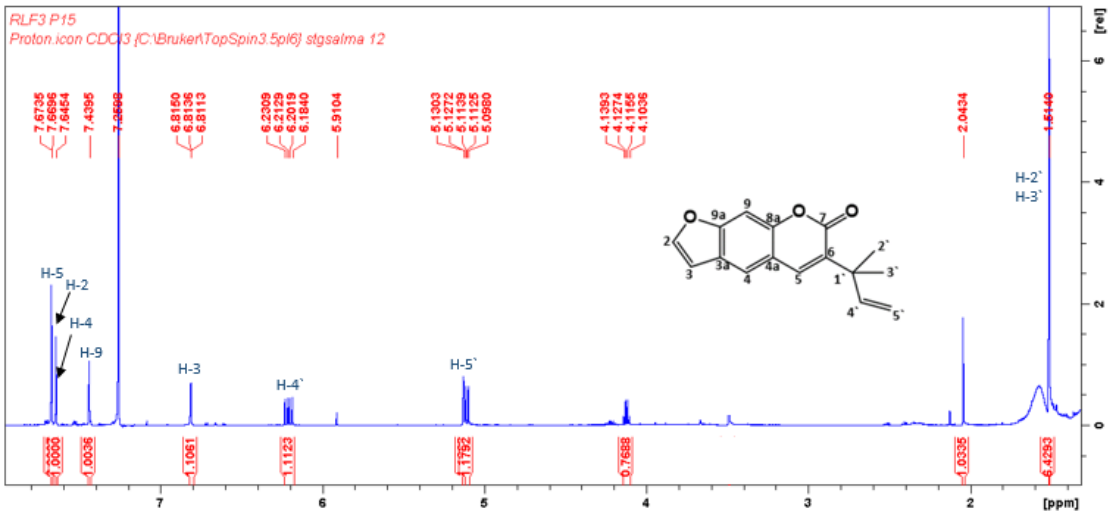


***Figure 3.47**: $^{1}H$ NMR (600 MHz, $CDCl_3$) spectrum of compound **46***

**Table 3.10**: $^{1}$H NMR (600 MHz) and $^{13}$C NMR data of compounds **43-47**

| | $\delta_H$ (*J* in Hz) | | | | | $\delta_C$ | | | | |
|---|---|---|---|---|---|---|---|---|---|---|
| **Position** | **45** | **46** | **47** | **43** | **44** | **45** | **46** | **47** | **43** | **44** |
| 2 | 4.71 *dd* (17.4) | 7.65 *d* (2.22) | 5.07 t | - | - | 91.2 | 146.9 | 88.3 | 161.6 | 162.8 |
| 3 | 3.20 m | 6.81 *d* (2.22) | 3.15 m, 3.24 m | 6.27 *d* (9.7) | 6.32 *d* (9.78) | 29.9 | 106.7 | 29.7 | 113.0 | 113.3 |
| 3a | - | - | - | - | - | 124.9 | 124.9 | 124.2 | - | - |
| 4 | 7.19 s | - | 7.18 s | 8.15 *d* (9.7) | 8.28 *d* (9.78) | 123.6 | 119.8 | 123.4 | 139.6 | 141.6 |
| 4a | - | - | - | - | - | 113.5 | 116.3 | 112.4 | - | - |
| 5 | 7.47 s | 7.64 s | 7.47 s | - | - | 138.4 | 138.6 | 138.3 | 150.0 | 145.6 |
| 6 | - | - | - | - | - | 131.2 | 133.5 | 131.3 | 113.1 | 116.5 |
| 7 | 160.53 | - | - | - | - | 160.5 | 160.2 | 160.5 | 158.7 | 151.8 |
| 8 | - | - | - | 7.14 s | - | - | - | - | 94.2 | 129.6 |
| 8a | - | - | - | - | - | 155.0 | 151.7 | 155.1 | - | - |
| 9 | 6.70 s | 7.43 s | 6.71 s | - | - | 97.5 | 99.3 | 97.5 | 153.0 | 145.0 |
| 9a | - | - | - | - | - | 162.6 | 156.2 | 162.8 | - | - |
| 10 | - | - | - | - | - | - | - | - | 106.8 | 108.8 |
| 1` | - | - | - | - | - | 40.6 | 40.9 | 40.8 | - | - |
| 2` | 1.46 s | 1.51 s | 6.17 m | 7.59 *d* (2.4) | 7.85 d (2.34) | 26.4 | 26.5 | 26.1 | 145.1 | 174.1 |
| 3` | 1.46 s | 1.51 s | 5.08 m | 7.02 *d* (2.4) | 7.25 d (2.34) | 26.4 | 26.5 | 26.1 | 105.3 | 106.5 |
| 4` | 6.1 m | 6.20 m | 1.46 s | - | - | 145.9 | 145.8 | 146.0 | - | - |
| 5` | 5.08 m | 5.11 m | 1.46 s | - | - | 112.4 | 112.7 | 112.0 | - | - |
| 1`` | - | - | - | - | - | 72.0 | - | 82.2 | - | - |
| 2`` | 1.22 s | - | 1.50 s | - | - | 24.5 | - | 22.3 | - | - |
| 3`` | 1.36 s | - | 1.55 s | - | - | 24.5 | - | 22.6 | - | - |
| 4`` | - | - | | - | - | - | - | 170.6 | - | - |

| | | | | | | | | | | |
|---|---|---|---|---|---|---|---|---|---|---|
| 5`` | - | - | 1.98 s | - | - | - | - | 21.4 | - | - |
| 5- $CH_3$ | - | - | - | 4.26 | 24.5 | - | - | - | 60.5 | 61.6 |
| 8- $CH_3$ | - | - | - | - | 24.5 | - | - | - | - | 62.2 |

### 3.1.9.10 Structure elucidation of imperatorin (104)

The compound **104** was isolated as a colourless powder. The HRESIMS (Figure 3.49) suggested the empirical formula as $C_{16}H_{14}O_4$ and in the positive ion mode it showed $[M+H]^+$ peak at *m/z* 271.0966 (calculated 271.0927). The $^1$H NMR spectrum (Figure 3.50, Table 3.11) exhibited one aromatic proton at $\delta_H$ 7.57 and *ortho*-coupling (*J* = 9.5 Hz ) protons at $\delta_H$ 8.03 and 6.38; and two olefinic protons at $\delta_H$ 7.89 (1H, *d*, *J* = 2.0 Hz), 6.96 (1H, d, *J* = 2.0 Hz) as a part of furan ring. The presence of an oxymethylene at $\delta_H$ 4.99, an olefinic triplet at $\delta_H$ 5.56 and two sets of methyl groups at $\delta_H$ 1.68 and 1.72 in the $^1$H NMR spectrum confirmed the presence of prenyloxy group in the molecule. The DEPTQ spectrum (Figure 3.51, Table 3.11) displayed a total of sixteen carbons including a carbonyl at $\delta_C$ 162.9, two methyl signals at $\delta_C$ 26.1, 18.8, one methylene ($\delta_C$ 71.0), seven methane and six quaternary carbons. The HMBC experiment played a key role in the confirmation of the structure of compound **104** to be a furanocoumarin. In the HMBC experiment (Figure 3.52), H-5 ($\delta_H$ 8.03) showed $^3J$ correlation to a methane carbon at $\delta_C$ 115.3 (C-4) and the carbonyl at $\delta_C$ 162.9 (C-7) while H-3 ($\delta_H$ 7.57) exposed $^3J$ correlation to quaternary carbon at $\delta_C$150.2 (9a) and to a methine carbon at $\delta_C$ 115.3 (C-4). The H-1′ ($\delta_H$ 4.98) revealed $^3J$ correlation to carbons $\delta_C$ 132.5 (C-9) and 141.1 (C-3′) and thereby confirmed the connectivity of the prenyloxy group to the molecule through C-9. Thus, compound **104** identified as 9-[(3-methyl-2-buten-1-yl)oxy]-7H-furo[3,2-g]chromen-7-one or imperatorin. The spectroscopic data of compound **104** were in a good agreement with respective published data of imperatorin (Shu Shan *et al.*, 2013). Compound **104** inhibited colon cancer cell growth (HT-29) with $IC_{50}$ value of 78 μM (Zheng *et al.*, 2016). Imperatorin (**104**) was reported to possess antimicrobial properties against *Escherichi a coli*, *Asperigillus niger* and *Cladosporiuma cladosporioides* with MIC 1000 (μg/mL) and inhibited *Bacillus subtilis* with MIC 500 (μg/mL) (Kwon *et al.*, 2002).

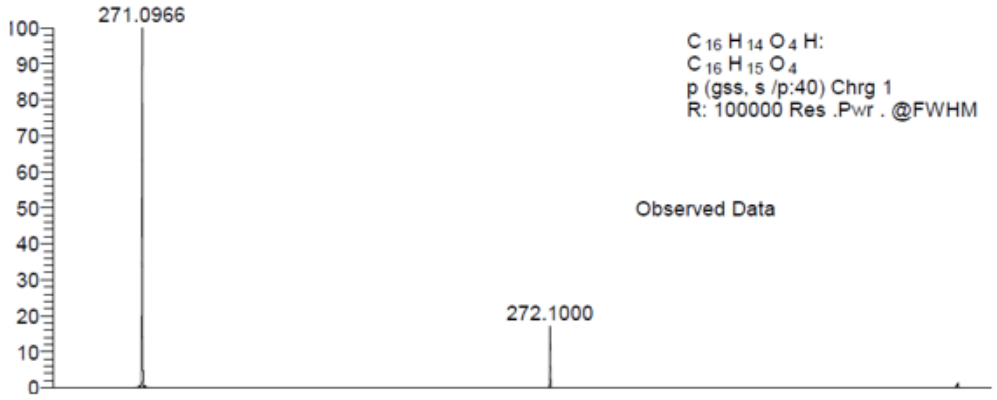


***Figure 3.48**: The HRESIMS spectrum of compound **104***

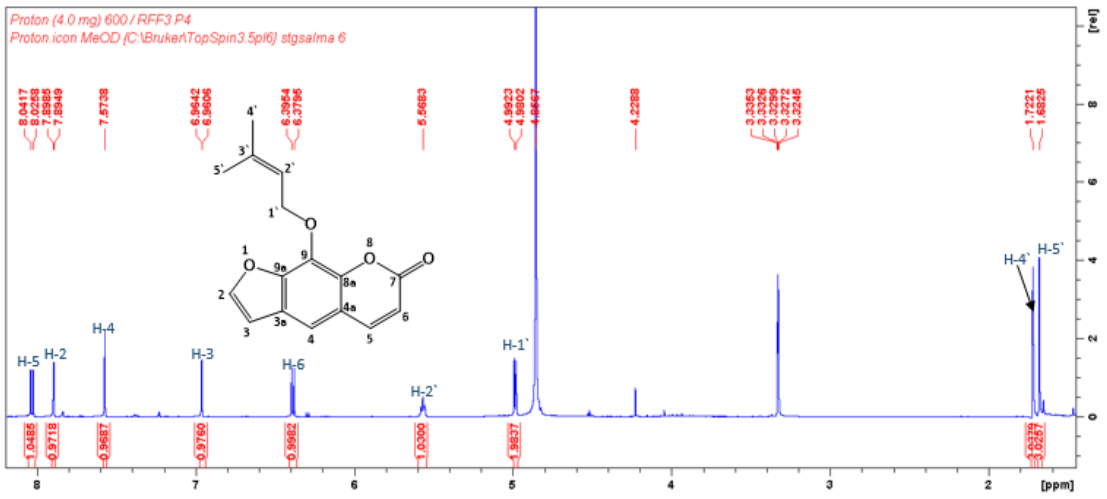


***Figure 3.49**: $^{1}H$ NMR (600 MHz, $CD_3OD$) spectrum of compound **104***

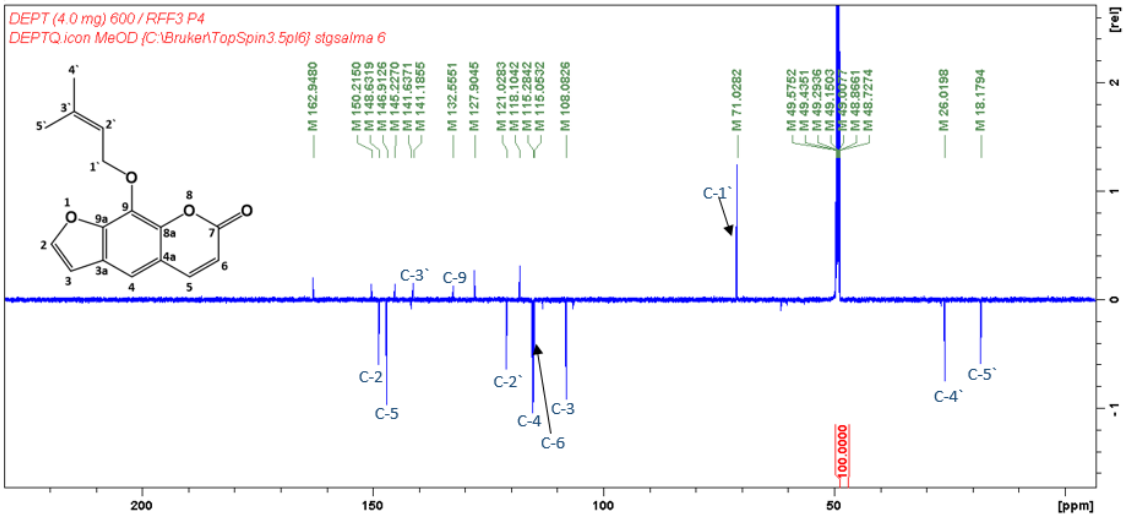


***Figure 3.50**: DEPT NMR (150 MHz, $CD_3OD$) spectrum of compound **104***

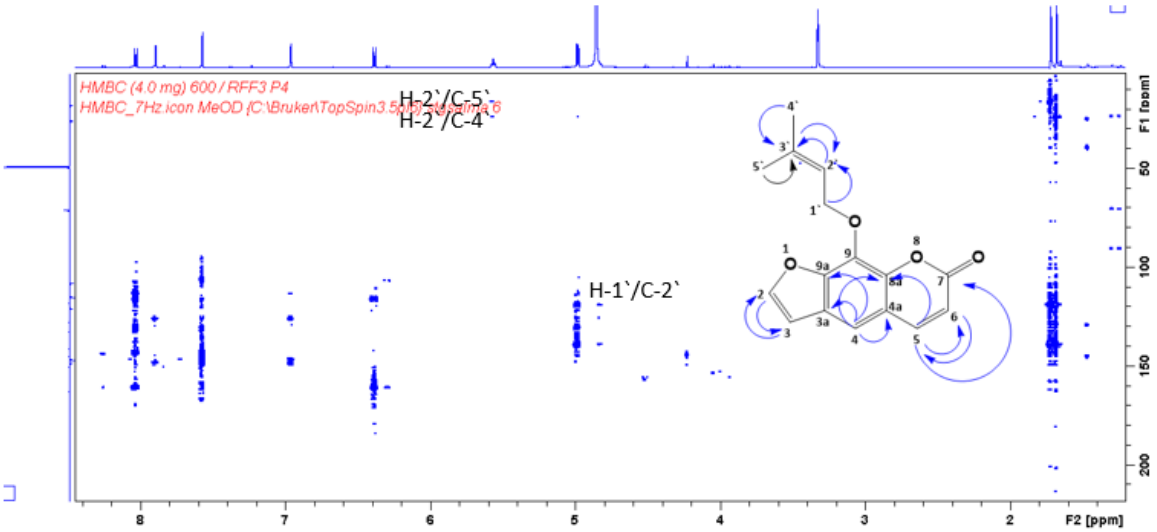


***Figure 3.51**: The HMBC correlations of compound **104***

**Table 3.11**: $^{1}$H NMR (600 MHz) and $^{13}$C NMR data of compound **104**

| **Position** | **(104) Chemical Shift δ (ppm), *J* in Hz** | | **Position** | **(104) Chemical Shift δ (ppm), *J* in Hz** | |
|---|---|---|---|---|---|
| | **$^{1}$H** | **$^{13}$C** | | **$^{1}$H** | **$^{13}$C** |
| 2 | 7.89 *d* (2.0) | 148.6 | 8a | - | 145.2 |
| 3 | 6.96 *d* (2.0) | 108.1 | 9 | - | 132.5 |
| 3a | - | 127.9 | 9a | - | 150.2 |
| 4 | 7.57, s | 115.3 | 1′ | 4.98 t | 71.0 |
| 4a | - | 118.1 | 2′ | 5.56 t | 121.0 |
| 5 | 8.03 *d* (9.5) | 146.9 | 3′ | - | 141.1 |
| 6 | 6.38 *d* (9.5) | 115.0 | 4′ | 1.68 s | 26.0 |
| 7 | - | 162.9 | 5′ | 1.72 s | 18.8 |

### 3.1.9.11 Structure elucidation of arborinine (107)

The compound **107** was isolated as yellow needles. The HRESIMS (Figure 3.53) suggested the empirical formula as $C_{16}H_{15}NO_4$ and in the positive ion mode it showed $[M+H]^+$ peak at *m/z* 286.1074 (calculated 286.1079). The $^{1}$HNMR spectrum (Figure 3.54, Table 3.12) exhibited a hydrogen bonded hydroxyl at $\delta_H$ 14.74, four aromatic protons as

ABCD patern at $\delta_H$ 7.51 (d, *J*= 8.7 Hz), 7.72 (dd, *J*= 8.7, 7.4 Hz), 7.30 (dd, *J*= 8.7, 7.4 Hz), 8.45 (d, *J*= 8.1 Hz), another aromatic proton as singlet at $\delta_H$ 6.28, three sets of three protons singlets at $\delta_H$ 3.84 (NMe), 3.93 (OMe), 4.04 (OMe). The $^{13}$C NMR spectrum (Figure 3.55, Table 3.12) displayed a total of sixteen carbons including a carbonyl at $\delta_C$ 181.21, five methine carbons, three sets of methyl carbon signals at $\delta_C$ 60.15, 56.36 and 34.47 and seven quaternary carbons. In the HMBC experiment (Figure 3.56) the methoxyl group at $\delta_H$ 3.93 and 4.04 revealed $^3J$ correlations to quaternary carbons at $\delta_C$ 130.6 (C-2) and 168.1 (C-3), respectively. Theses correlations confirmed the position of OMe groups through C-2 and C-3 in the molecule. Moreover, $^3J$ correlations from the methyl at $\delta_H$ 3.84 to quaternary carbons at $\delta_c$ 140.91 (C-11) and 142.39 (C-14) confirmed it to be the nitrogen bearing methyl group (NMe). Thus, compound **107** was identified as an acridone alkaloid, arborinine. The spectroscopic data of compound **107** were in a good agreement with respective published data of arborinine (Pal *et al.*, 2011). Compound **107** was previously isolated from *Ruta* species (Knölker, 2017; Kumar, 2018). Arborinine (**107)** was reported as an anticancer agent against HeLa (cervical cancer cells), MCF7 (breast cancer cell) and A431 cells (skin cancer) (Réthy *et al.*, 2007). The antimicrobial activity of arborinine (**107**) was confirmed against *Escherichia coli* and *Shigella dysenteriae* with zones of inhibition of 7 mm and 9 mm respectively. Moreover, arborinine (**107**) inhibited *Klebsiella aerogenes* and *Providencia stuartii* with MIC 256 µg/mL and 512 µg/mL, respectively (Sohrab *et al.*, 2004; Fouotsa *et al.*, 2013).

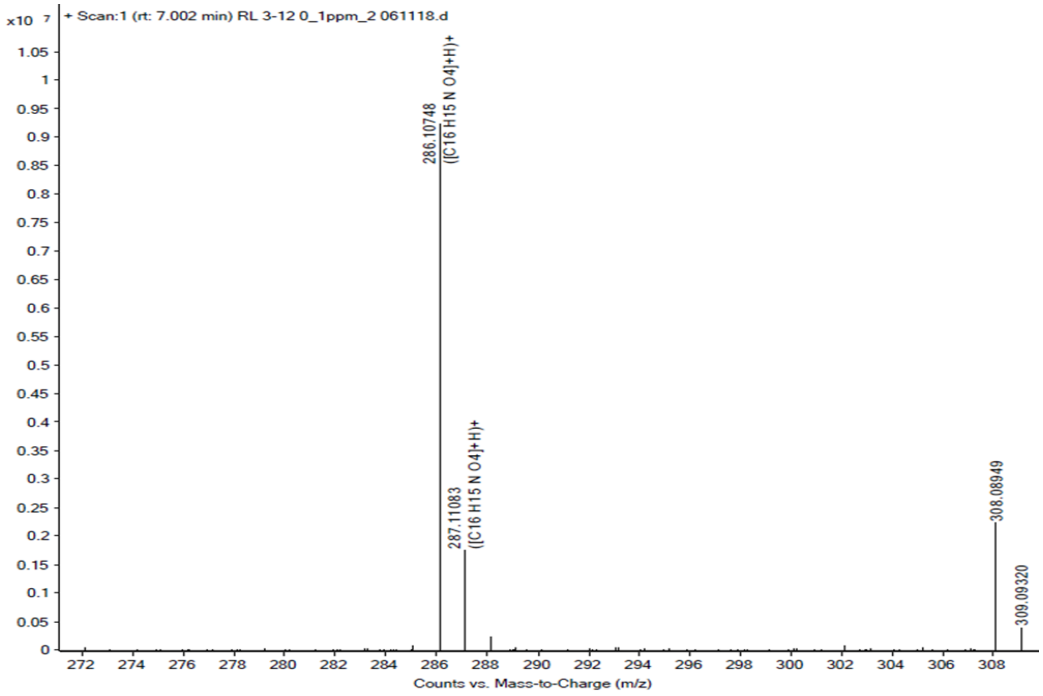


***Figure 3.52**: The HRESIMS spectrum of compound **107***

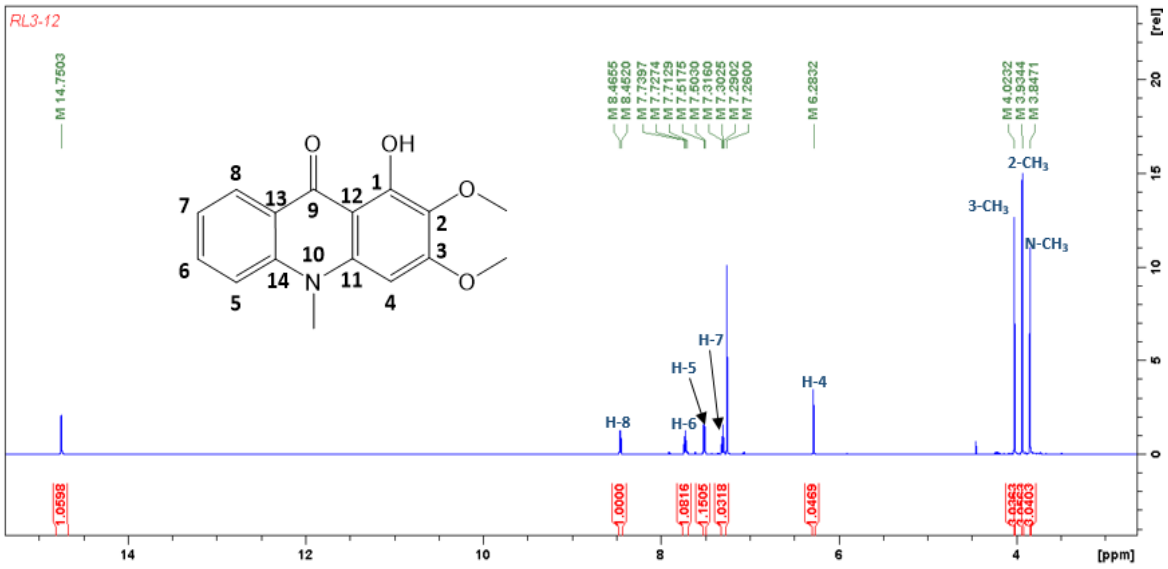


***Figure 3.53**: $^{1}H$ NMR (600 MHz, $CHCl_3$) spectrum of compound **107***

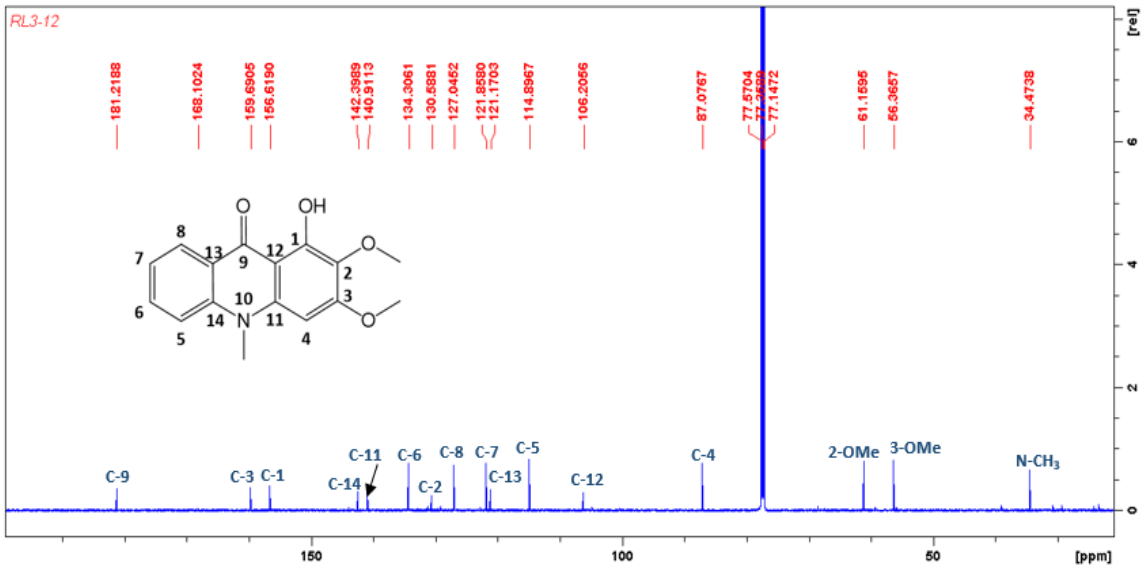


***Figure 3.54***: *$^{13}C$ NMR (150 MHz, $CHCl_3$) spectrum of compound* ***107***

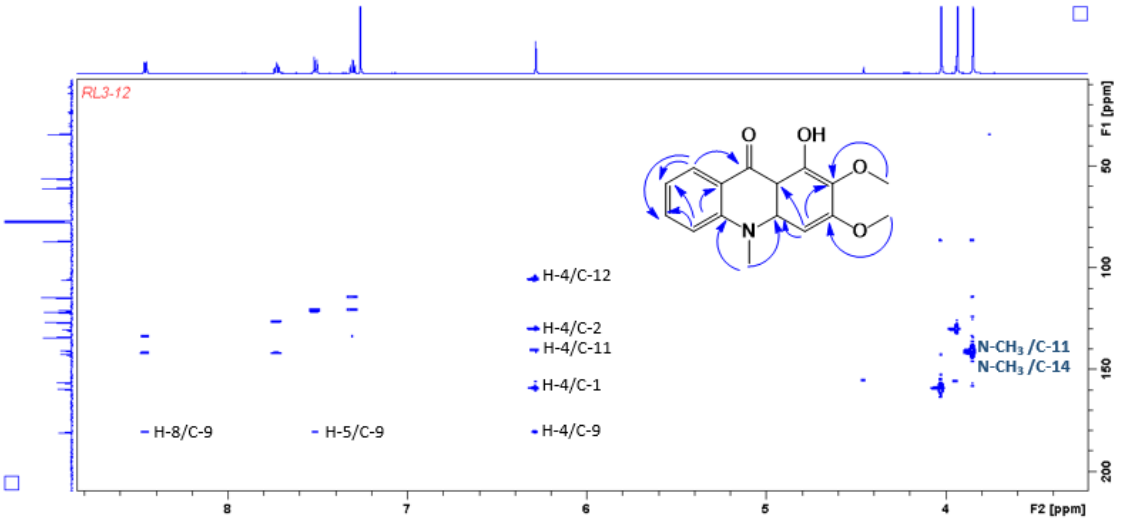


***Figure 3.55***: *The HMBC correlations of compound* ***107***

**Table 3.12**: $^{1}H$ NMR (600 MHz) and $^{13}C$ NMR data of compound **107**

| **Position** | **(107) Chemical Shift δ (ppm), *J* in Hz** | | **Position** | **(107) Chemical Shift δ (ppm), *J* in Hz** | |
|---|---|---|---|---|---|
| | **$^{1}H$** | **$^{13}C$** | | **$^{1}H$** | **$^{13}C$** |
| 1 | - | 159.7 | 9 | - | 181.2 |
| 2 | - | 130.6 | 11 | - | 140.9 |
| 3 | - | 168.1 | 12 | - | 106.2 |
| 4 | 6.28 s | 87.1 | 13 | - | 121.2 |
| 5 | 7.51 *d* (8.7) | 114.9 | 14 | - | 142.4 |
| 6 | 7.72 *dd* (8.7, 7.38) | 134.3 | 3-$OCH_3$ | 4.02, s | 56.4 |
| 7 | 7.30 *dd* (8.7, 7.38) | 121.8 | 2-$OCH_3$ | 3.93, s | 61.1 |
| 8 | 8.45 *d* (8.1) | 127.0 | *N*-$CH_3$ | 3.84, s | 34.5 |

### 3.1.9.12 Structure elucidation of ribalinium (106)

The compound **106** was isolated as a dark brown amorphous powder. The HRESIMS suggested the empirical formula as $C_{16}H_{20}NO_4$ and in positive ion mode it showed $[M+H]^+$ peak at *m/z* 291.1401 (calculated 291.1470). The $^1$H NMR spectrum (Figure 3.57, Table 3.13) exhibited four sets of methyl signals including deshielded methyls at $\delta_H$ 4.07 and 4.51, three aromatic protons as ABX pattern $\delta_H$ 7.89 (d, *J* = 8.9 Hz), 7.47 (dd, *J* = 8.9, 2.0 Hz) and 7.57 (d, *J* = 2.0 Hz) and signals for a methylene ($\delta_H$ 3.90) and oxymethine ($\delta_H$ 5.22). The $^{13}$C NMR spectrum (Figure 3.58) exhibited a total of sixteen carbons including seven quaternary carbons, three aromatic methines at $\delta_C$ 108.6 (C-5), 119.4 (C-8), 124.7 (C-7), one methylene at $\delta_C$ 30.2 (C-3′), one oxymethine at $\delta_C$ 95.4 (C-2′) and four methyls which were characterized as a *N*-methyl at $\delta_C$ 34.9 ($\delta_H$ 4.1 from HSQC), two methyl at $\delta_C$ 25.0 (C-2″), 26.1 (C-3″) and a methoxy at $\delta_C$ 60.4 (4-OMe). In the HMBC experiment, the two sets of methyl protons at $\delta_H$ 1.32 ($\delta_C$ 25.0) and 1.47 ($\delta_C$ 26.1) which existed in *geminal* position were connected to an oxymethine carbon at $\delta_C$ 95.41 (C-2′) and oxygen bearing quaternary carbon at $\delta_C$ 72.07 (C-1‴). The $^3J$ correlations from methyl group at $\delta_H$ 4.77 to carbons at $\delta_C$ 166.5 (C-2) and 131.85 (C-9) confirmed this as N-methyl (NMe) Thus, compound **106** was identified as rabalinium quinoline alkaloids. The spectroscopic data of compound **106** were in a good agreement with published data of rabalinium (Gaston *et al.*, 1980; Pal *et al.*, 2011). Compound **106** was previously isolated from *Ruta graveolens* and reported here for the first time from *R. chalepensis.*

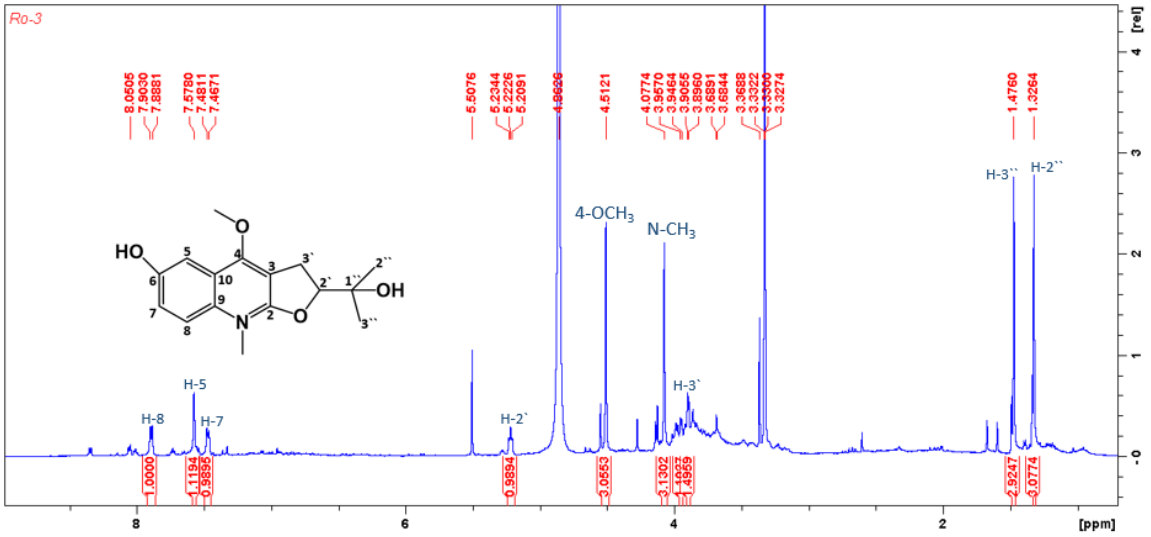


***Figure 3.56**: [1]H NMR (600 MHz, $CDCl_3$) spectrum of compound **106***

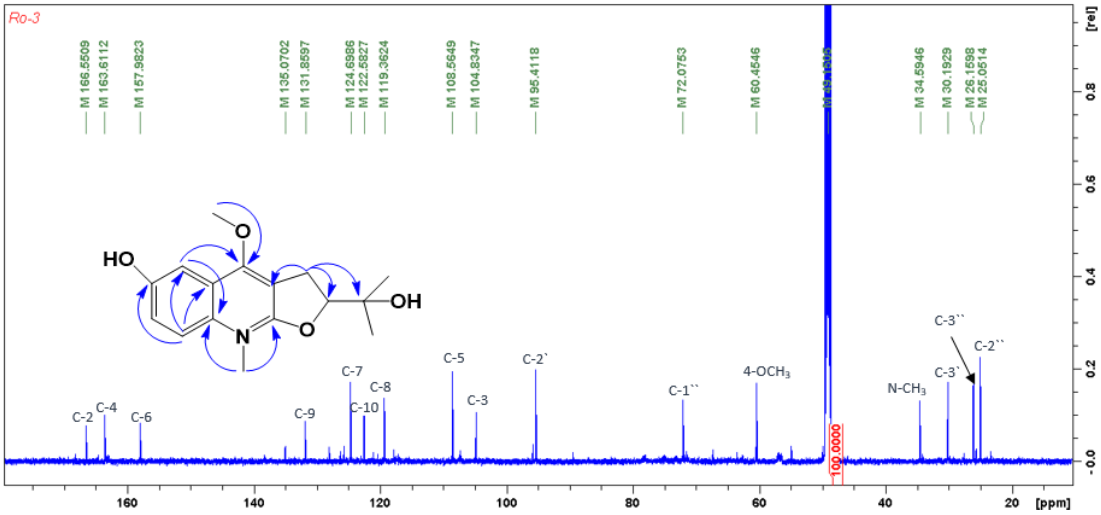


***Figure 3.57**: [13]C NMR (150 MHz, $CHCl_3$) spectrum of compound **106***

**Table 3.13:** [1]H NMR (600 MHz) and [13]C NMR data of compound **106**

| **Position** | **(106) Chemical Shift δ (ppm), *J* in Hz** | | **Position** | **(106) Chemical Shift δ (ppm), *J* in Hz** | |
|---|---|---|---|---|---|
| | **$^{1}$H** | **$^{13}$C** | | **$^{1}$H** | **$^{13}$C** |
| 2 | - | 166.5 | 10 | - | 122.6 |
| 3 | - | 104.8 | 2′ | 5.22 m | 95.4 |
| 4 | - | 163.6 | 3′ | 3.90 m | 30.2 |
| 5 | 7.57 *d* (2.00) | 108.6 | 1″ | - | 72.1 |
| 6 | - | 158.0 | 2″ | 1.32 s | 25.0 |
| 7 | 7.45 *dd* (8.94, 2.00) | 124.7 | 3″ | 1.47 s | 26.1 |
| 8 | 7.89 *d* (8.94) | 119.4 | 4-$OCH_3$ | 4.51 s | 60.4 |
| 9 | - | 131.8 | N-CH3 | 4.07 s | 34.9 |

### 3.1.9.13 Structure elucidation of compound 3′,6-disinapoylsucrose (108)

The compound **108** (Figure 3.58) was isolated as a white amorphous powder. The HRESIMS suggested the empirical formula as $C_{34}H_{42}O_{19}$ and in the negative ion mode it showed $[M+H]^+$ peak at *m/z* 753.2300 (calculated 753.2242). The $^1H$ NMR spectrum (Figure 3.59) exhibited four methoxy groups presented by two signals at $\delta_H$ 3.71 (6H) and 3.88 (6H), four olefinic protons at $\delta_H$ 7.68 (lH, d, *J* = 15.7 Hz, H-7), 7.60 (lH, d, *J* = 16.3 Hz, H-7), 6.48 (lH, d, *J* = 16 Hz, H-8) and 6.46 (lH, d, *J* = 16.6 Hz, H-8), two aromatic methines at $\delta_H$ 6.94 (H-2) and 6.88 (H-6). The presence of an anomeric proton at $\delta_H$ 5.53 (1H, d, *J* = 4.8 Hz, H-1′) suggested the existence of a sugar as part of the molecule. The $^{13}C$ NMR spectrum (Figure 3.60) revealed a total of thirty four carbons, twelve for sugars, two carbonyls at $\delta_C$169.2 and 168.4 (C-9) and four carbons of methoxyl groups. The HMBC showed $^3J$ correlation from H-6′ to C-9. Also, the key correlation observed from H-3′′ to carbons C-8 ($^3J$), C-9 ($^4J$). Moreover, H-1′ showed long range correlation to carbon at $\delta_C$ 115.8 (C-2′′). Thus, compound **108** was identified as a sinapoyl glycoside. The data of compound **108** were in a good agreement with respective data for 3′,6-disinapoylsucrose (Chen *et al.*, 2001; Wu *et al.*, 2014; Jin *et al.*, 2016). Sinapoyl glycosides (**108**) was isolated from *Ruta graveolens* and the research suggested it has bioavailability effect (Chen *et al.*, 2001; Dhale *et al.*, 2010; Chen *et al.*, 2013). Depending on available data, compound (**108**) isolated for the first time from *R. chalepensis.*

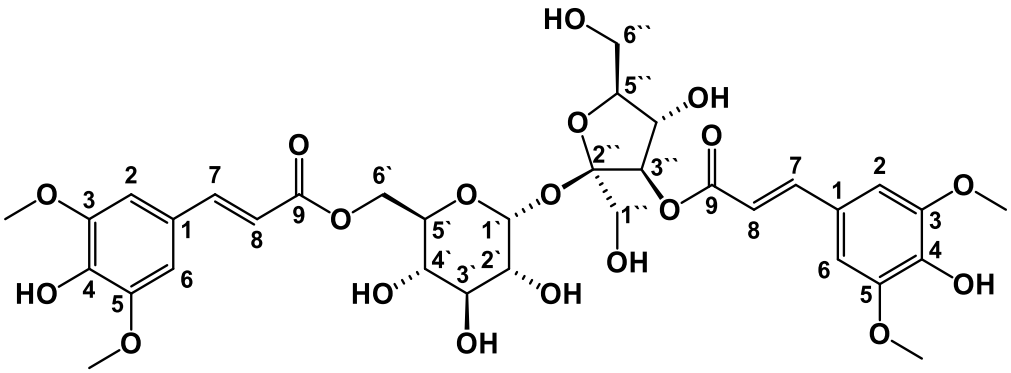


***Figure 3.58**: Compound 3′,6-disinapoylsucrose (**108**) with numbering atoms*

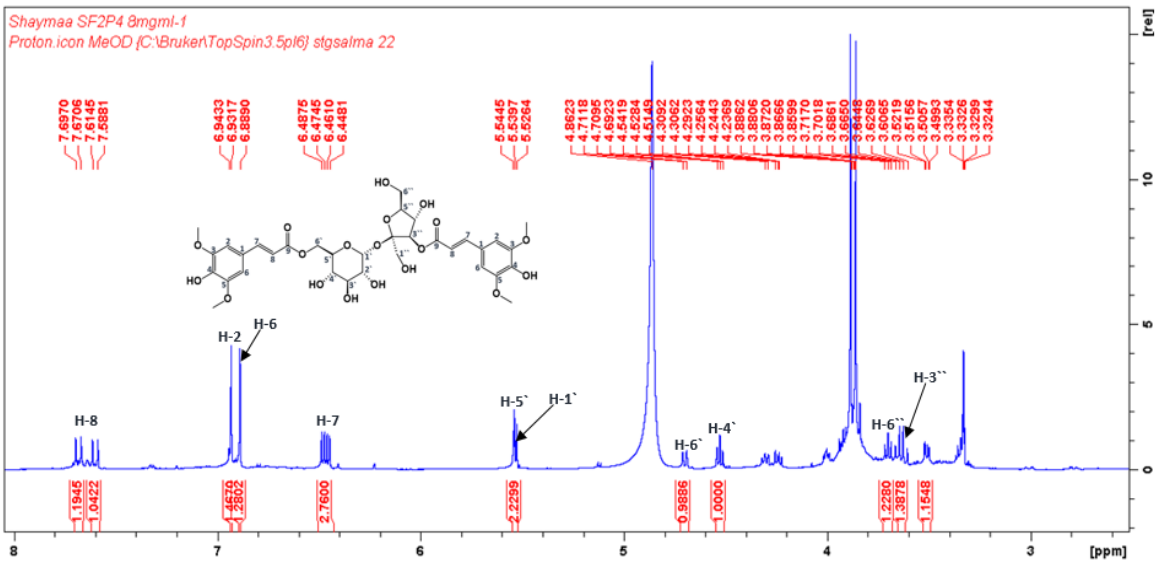


***Figure 3.59**: [1]H NMR (600 MHz, $CDCl_3$) spectrum of compound **108***

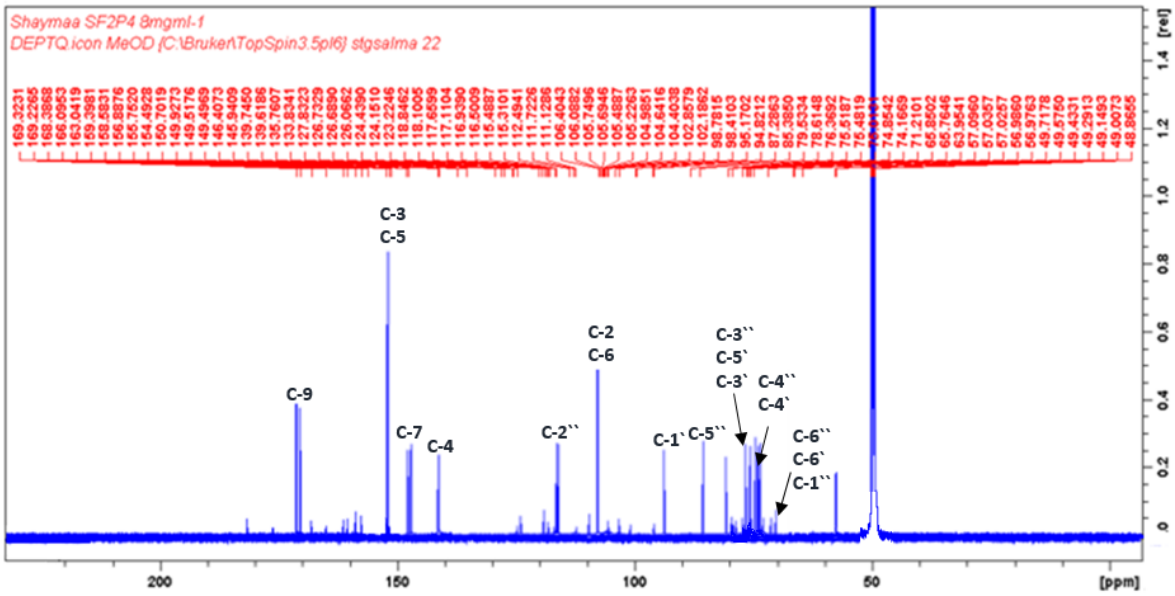


***Figure 3.60**: [13]C NMR (150 MHz, $CDCl_3$) spectrum of compound **108***

### 3.1.9.14 Structure elucidation of graveoline (105)

The compound **105** was isolated as a yellow powder. The HRESIMS (Figure 3.62) suggested the empirical formula as $C_{17}H_{13}NO_3$ and in the positive ion mode, it showed $[M+H]^+$ peak at *m/z* 280.0868 (calculated 280.097369). The $^1$H NMR spectrum (Figure 3.63, Table 3.14) exhibited a methyl signal at $\delta_H$ 3.60 (3H), a symmetrical ether at $\delta_H$ 6.01 and three aromatic protons as ABX pattern resonating at $\delta_H$ 6.82 (d, *J*=1.6 Hz), 6.84 (d, *J*= 8.0 Hz), 6.85 (dd, *J*=8.0, 2.1 Hz). Moreover, four olefinic protons as ABCD pattern indicating

at $\delta_H$ 7.52 (*d*, *J*=8.94 Hz), 7.36 (*dd*, *J*=8.60, 7.84 Hz), 7.89 (*dd*, *J*=7.84, 8.94 Hz) and 8.42 (*d*, *J* =8.60 Hz) and singlet proton at $\delta_H$ 6.26. The $^{13}$C NMR spectrum (Figure 3.64, Table 3.14) revealed a total of seventeen carbons including a carbonyl at $\delta_C$ 207.8, one methylenedioxy ($\delta_C$ 101.7), one methyl ($\delta_C$ 37.4), eight aromatic methines and five quaternary carbons. In the HMBC experiment, H-7′ revealed $^3J$ correlations to carbons at $\delta_C$ 108.9 (C-3′) and 148.8 (C-4′) while, H-2′ and H-6 exhibited a long range correlation to carbon resonating at $\delta_c$ 154.6 (C-2). Moreover, a $^3J$ correlation from methyl protons to the quaternary carbons at $\delta_H$ 154.6 (C-2) and 141.9 (C-8a) in the HMBC experiment confirmed the presence of a nitrogen atom with this methyl (NMe). Thus, compound **105** was identified to be graveoline alkaloid. The data of compound **105** were in a good agreement with respective published data of graveoline (**105**) (Bandatmakuru and Arava, 2018; Kamal *et al.*, 2018; Sampaio *et al.*, 2018). The antimicrobial activity of graveoline (**105**) has confirmed against *Staphylococcus aureus, Enterococcus faecalis* and *Escherichia coli* with MIC 1000, 500, 1000 µg/mL, respectively (Kamal *et al.*, 2018). Graveoline (**105**) promoted the apoptotic and autophagic cell death for skin melanoma cells, which indicted the anticancer activity (Ghosh *et al.*, 2014).

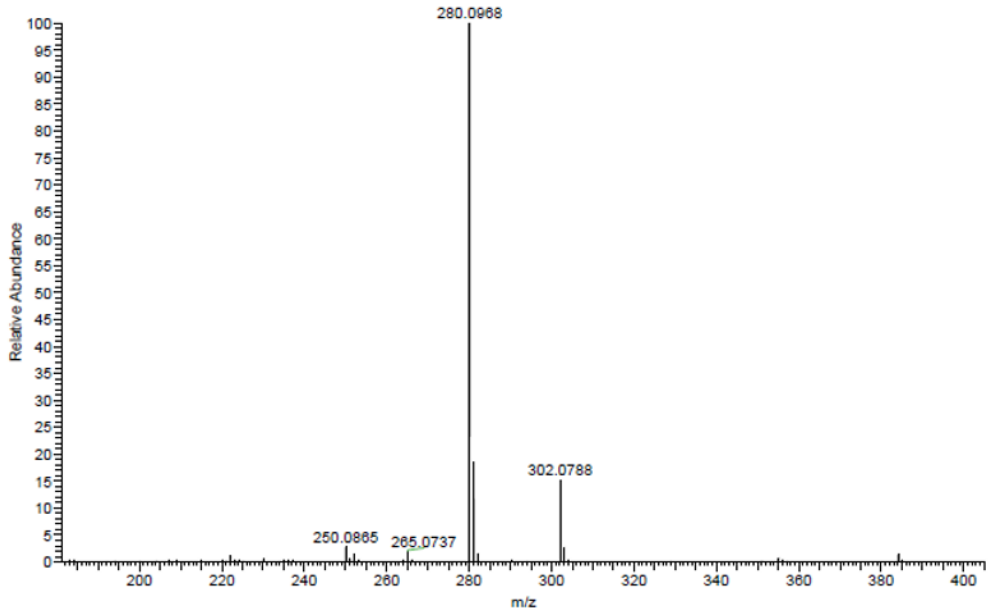


***Figure 3.61**: The HRESIMS spectrum of compound **105***

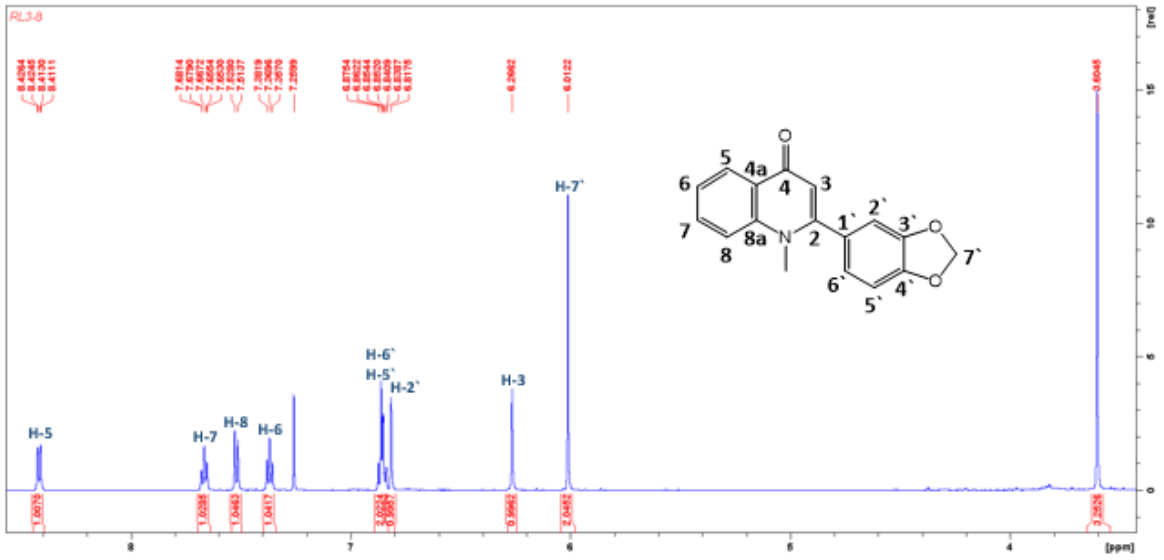


***Figure 3.62**: [1]H NMR (300 MHz, $CDCl_3$) spectrum of compound **105***

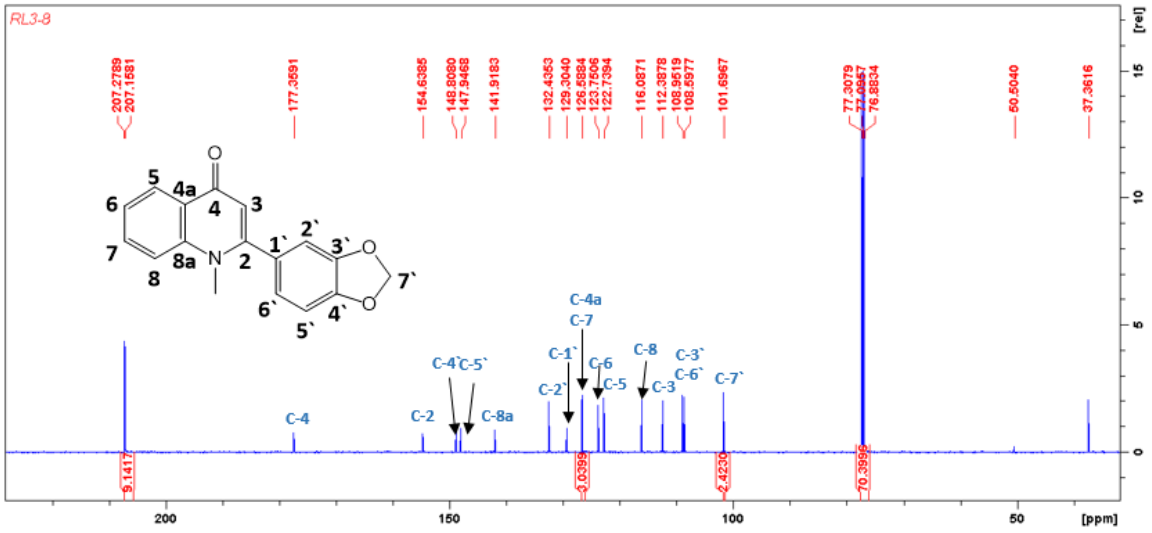


***Figure 3.63**: [13]CNMR (75 MHz, $CDCl_3$) spectrum of compound **105***

### 3.1.9.15 Structure elucidation of rutin (48)

The compound **48** was isolated as a yellow amorphous solid. The HRESIMS (Figure 3.65) suggested the empirical formula as $C_{27}H_{30}O_{16}$ and in the negative ion mode it showed $[M-H]^-$ peak at *m/z* 609.1461 (calculated 609.1455). The $^1$H NMR spectrum (Figure 3.66, Table 3.15) exhibited three aromatic protons as ABX pattern resonating at $\delta_H$ 7.69 (*d*, *J* = 2.0 Hz), 6.89 (*d*, *J* = 8.4 Hz) and 7.65 (*dd*, *J* = 2.0, 8.4 Hz) and two meta-coupled protons at $\delta_H$ 6.23 (*d*, *J* = 2.1 Hz), 6.42 (*d*, *J* = 2.1Hz). Moreover, the rutinosyl moiety was revealed by the presence of a glucose anomeric proton at $\delta_H$ 5.12 (*d*, *J* = 7.7 Hz), while rhamnose

anomeric proton resonated at $\delta_H$ 4.54 (*d*, *J*=1.5 Hz) and methyl protons of rhamnose at $\delta_H$ 1.14 (*d*, *J* = 6.2). The primary elucidation of the $^1$H NMR spectrum of compound **48** expected this compound to be flavanone glycoside. The $^{13}$C NMR spectrum showed a total of twenty seven carbon signals including carbonyl at δc 179.5, methoxyl and twelve carbons constituted the rutinosyl moiety. Moreover, five carbons of olefinic protons were recognised from HSQC resonated at δc 163.2 (C-5), 166.2 (C-7), 146.0 (C-3′) and 150.4 (C-4′) and the remaining are quaternary carbons. The HMBC experiment showed the long correlation from H-1‴ ($\delta_H$ 4.54) carbons at $\delta_C$ 68.7 (C-6″) which confirmed the connectivity of glucose and rhamnose. Another $^3J$ correlation from proton at $\delta_H$ 5.12 (H-1″) to oxygenated quaternary carbon at $\delta_C$135.7 (C-3) confirmed the linkage of sugar through C-3. Thus, compound **48** was identified as rutin. The spectroscopic data of compound **48** was in a good agreement with respective published data of rutin (R. Markham *et al.*, 1987; Li *et al.*, 2014a; Souravh Bais and Abrol, 2016). Rutin (**48**) was documented as an antioxidant agent (Terashima *et al.*, 2012) and showed activity against human lung and colon cancer cell lines by adjusting cells behaviour (Ben Sghaier *et al.*, 2016). The combination of rutin and sunscreens gave strong and safe protective activity on skin (Graziola *et al.*, 2016), which indicated compound **48** may be important in the cosmetic industry.

**Table 3.14**: $^1$H NMR (300 MHz) and $^{13}$C NMR data of compound **105**

| **Position** | **(105) Chemical Shift δ (ppm), *J* in Hz** | | **Position** | **(105) Chemical Shift δ (ppm), *J* in Hz** | |
|---|---|---|---|---|---|
| | **$^1$H** | **$^{13}$C** | | **$^1$H** | **$^{13}$C** |
| 2 | - | 154.6 | 1′ | - | 129.3 |
| 3 | 6.26 s | 112.4 | 2′ | 6.82 *d* (1.6) | 132.4 |
| 4 | - | 177.3 | 3′ | - | 108.9 |
| 4a | - | 126.6 | 4′ | - | 148.8 |
| 5 | 8.42 *d* (8.60) | 122.7 | 5′ | 6.84 *d* (8.0) | 147.9 |
| 6 | 7.36 *dd* (8.60, 7.84) | 123.75 | 6′ | 6.85 *dd* (1.6, 8.0) | 108.6 |
| 7 | 7.89 *dd* (7.84,8.94) | 126.6 | 7′ | 6.01 s | 101.7 |
| 8 | 7.52 *d* (8.94) | 116.1 | *N*-CH3 | 3.60 s | 37.4 |
| 8a | - | 141.9 | - | - | - |

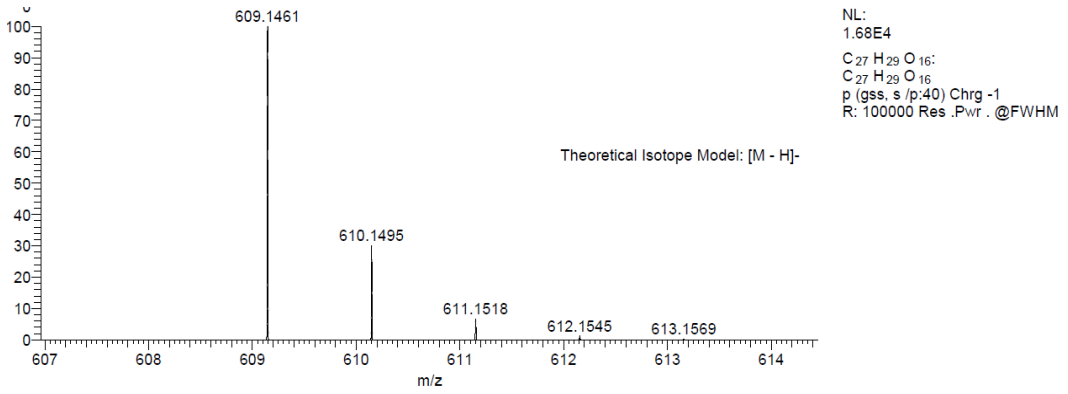


***Figure 3.64***: The *HRSEIMS spectrum of compound* ***48***

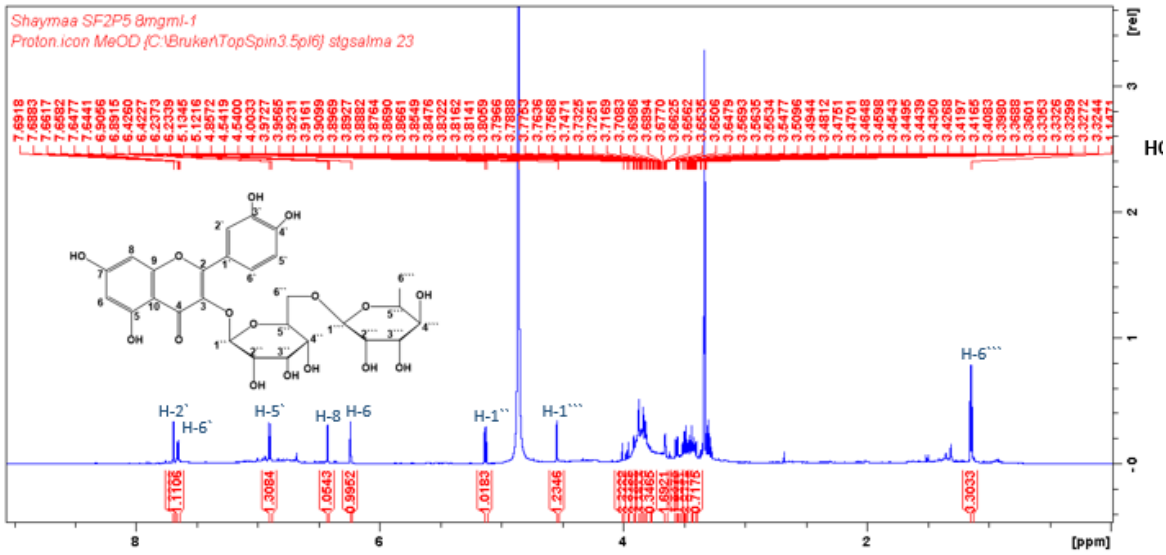


***Figure 3.65***: *$^{1}$H NMR (600 MHz, $CD_3OD$) spectrum of compound* ***48***

### 3.1.9.16 Structure elucidation of rutin-3′-methyl ether (101)

The compound **101** was isolated as a brown amorphous solid. The HRESIMS (Figure 3.67) suggested the empirical formula as $C_{28}H_{32}O_{16}$ and in the positive ion mode it showed $[M+H]^+$ peak at *m/z* 625.1763 (calculated 625.176865). The 1D and 2D spectra of compound **101** (Figure 3.68, Table 3.15) were very similar to rutin (**48**) except, there is an extra signal of an oxygenated methyl at $\delta_H$ 3.97 (3H), in HSQC this OMe group connected to the carbon at δc 56.9. The HMBC confirmed the position of methoxy group to be in C-3′ by finding long-range correlation from OMe to C-3′ (148.5). Thus, compound **101** was identified as methoxy rutin**.** The spectroscopic data of compound **101** were in a good agreement with

respective published data of rutin 3′-methyl ether (R. Markham *et al.*, 1987; Li *et al.*, 2014a; Souravh Bais and Abrol, 2016). Based on available data, this is the first report for isolation of compound **101**from *Ruta chalepensis*.

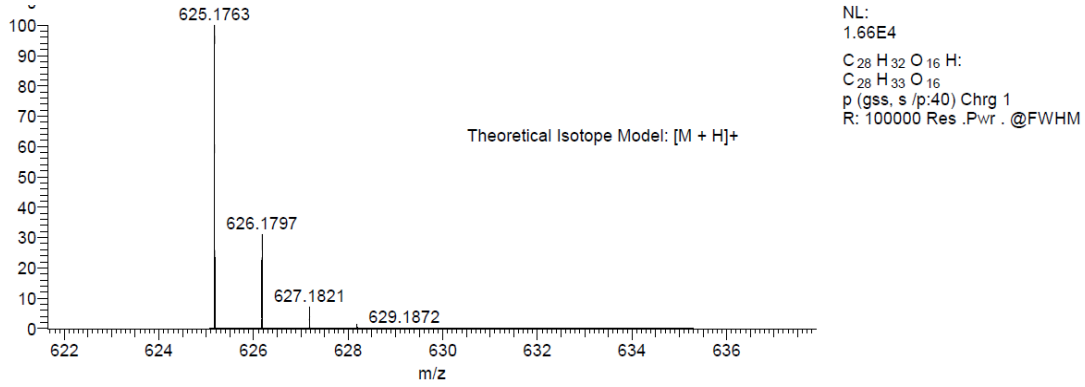


***Figure 3.66**: The HRESIMS of spectrum compound **101***

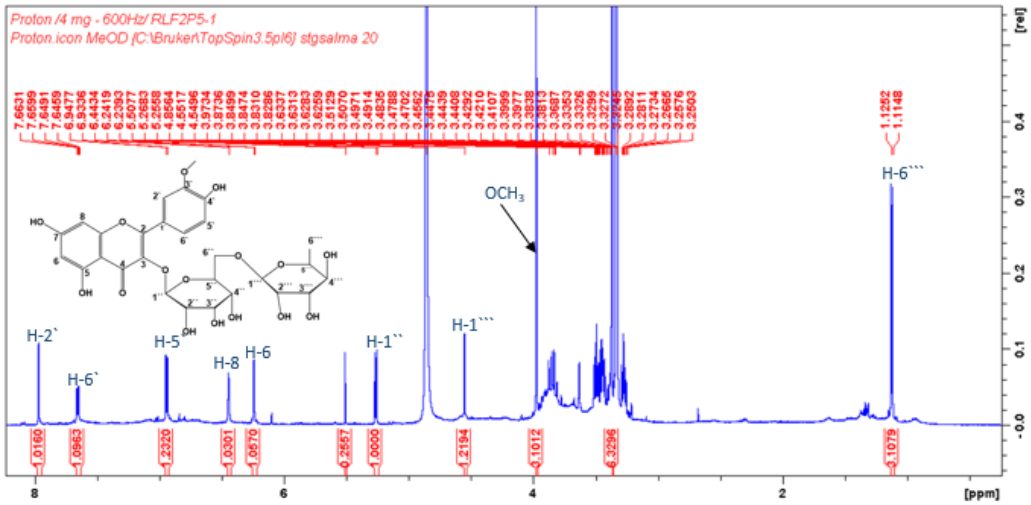


***Figure 3.67**: $^{1}H$ NMR (150 MHz, $CD_3OD$) spectrum of compound **101***

### 3.1.9.17 Structure elucidation of rutin-7,4′-dimethyl ether (102)

The compound **102** was isolated as a brown amorphous solid. The HRESIMS suggested the empirical formula as $C_{29}H_{34}O_{16}$ and in the positive ion mode it showed $[M+H]^+$ peak at *m/z* 639.1950 (calculated 639.1925). The 1D and 2D spectra of compound **102** were similar to compound **101.** The only difference was the presence two methoxy groups at $\delta_H$ 3.96 (3H) and 3.97 (3H) in the $^{1}H$ NMR spectrum of compound **102** (Figure 3.69, Table 3.15) instead of one methoxy in compound **101**. The $^{13}$CNMR and HSQC (Table 3.16)

showed a cross link from oxygenated an methyl at $\delta_H$ 3.96, 3.97 to carbons at δc 57.4 and 56.1, respectively. The HMBC experiment showed $^3J$ correlation from methoxyl groups at $\delta_H$ 3.96, 3.97 to carbons at δc 167.3 (C-7) and 151.0 (C-4′) respectively, to confirm their position in the moleule. Thus, compound **102** was identified as dimethoxy rutin**.** The spectroscopic data of compound **102** were in a good agreement with respective published data of rutin 7, 4′-methyl ether (Matsuda *et al.*, 2002). Based on available data, this is the first report of the isolation of rutin-7,4′-dimethyl ether from *R. chalepensis*.

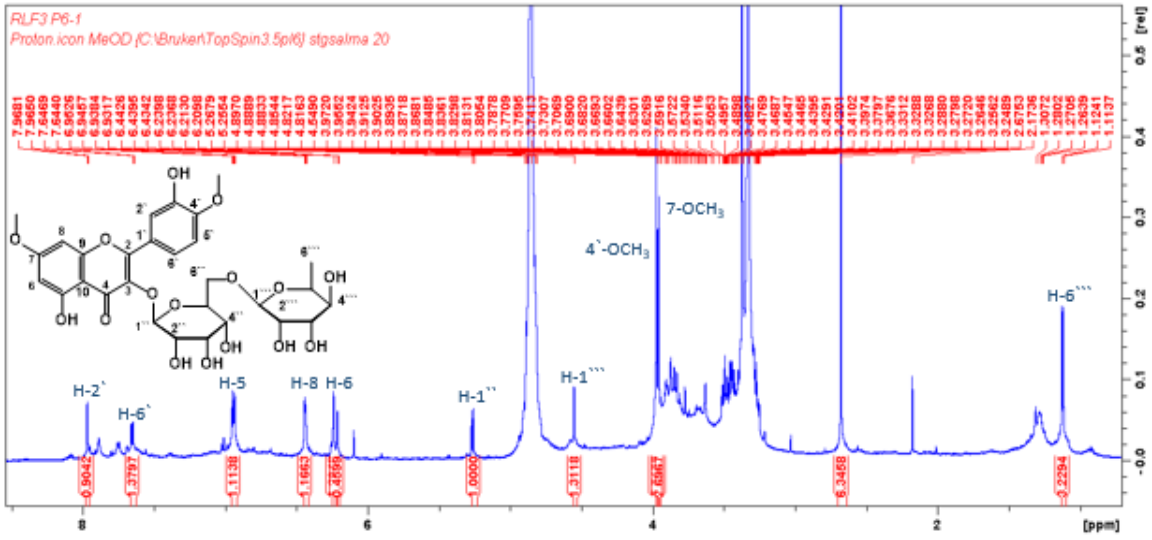


***Figure 3.68**: $^1H$ NMR (300 MHz, $CDCl_3$) of compound **102***

### 3.1.9.18 Structure elucidation of 6-hydroxy-rutin 3′-7-dimethyl ether (103)

The compound **103** was isolated as a brown amorphous solid. The HRESIMS (Figure 3.70) suggested the empirical formula as $C_{29}H_{35}O_{17}$ and in the positive ion mode it showed $[M+H]^+$ peak at *m/z* 655.1870 (calculated 655.1874). The 1D and 2D spectrum were identical with data of compound **48**, **101** and **102** to confirm the main skeleton of compound **103** to be a flavonoid glucoside. In the $^1H$ NMR spectrum (Figure 3.71, Table 3.15) of compound **103** there was a downfield 6H singlet at $\delta_H$ 3.97, and instead of the usual shielded aromatic *meta*-coupled proton signals for H-6 and H-8 in the flavonol skeleton, there was only a $^1H$ singlet at $\delta_H$ 6.53 suggesting that one of those protons was substituted by an extra functional group, most likely a hydroxyl group based on the HRESIMS data. The DEPTQ spectrum of

compound **103** (Figure 3.72, Table 3.16) showed the presence of an additional oxygenated aromatic quaternary signal at δc 145.3, which could be assigned to C-6 or C-8. Whilst a COSY experiment of compound **103** established all major $^{1}$H-$^{1}$H scalar couplings, $^{1}$H-$^{13}$C direct ($^{1}J$) couplings were obtained from an HSQC experiment confirming the assignment of all protonated carbon signals to their respective $^{1}$H signals. An HMBC experiment displayed all major $^{1}$H-$^{13}$C long-range ($^{2}J$ and $^{3}J$) correlations (Figure 3.73). The rhamnose anomeric proton (H-1‴) showed a $^{3}J$ correlation to C-6‴ of the glucose unit, and the glucose anomeric proton (H-1″) displayed a $^{3}J$ correlation to C-3 of the flavonol aglycones, confirming the formation of the disaccharide, rutinose, and its connection to C-3 (as in compounds **48**, **101** and **102**). Similarly, $^{3}J$ correlations from the methoxyl signal at $\delta_H$ 3.97 (6H) to C-7 and C-3′ established methyl ether formation at C-7 and C-3′. The $^{13}$C NMR (Table 3.16) signal at δc 96.4 confirmed that the hydroxylation was indeed on C-6 in compound **103**, and this fact was further corroborated from the $^{1}$H- $^{13}$C HMBC long-range correlations from H-8 signal to C-6 and C-10. Thus, the compound **103** was identified as 6-hydroxy-rutin 3′,7-dimethyl ether (**103**), which to the best of our knowledge, is a new natural product.

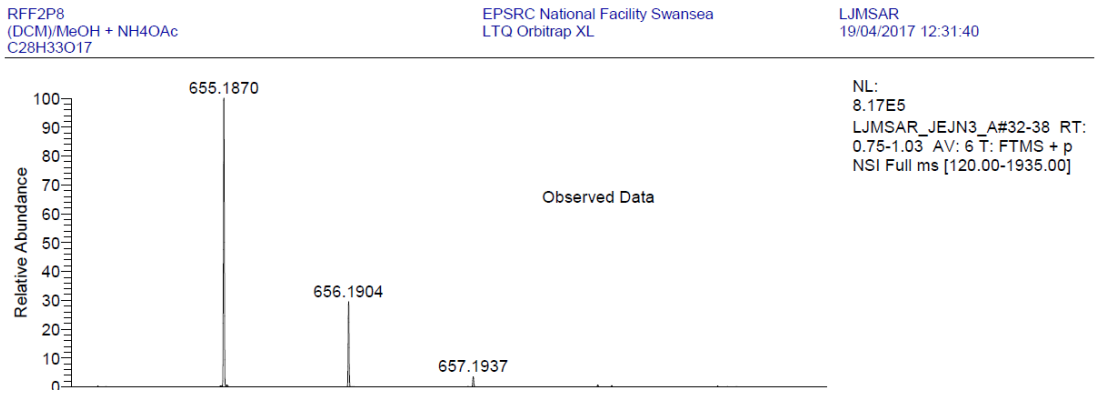


***Figure 3.69**: The HRESIMS of compound **103***

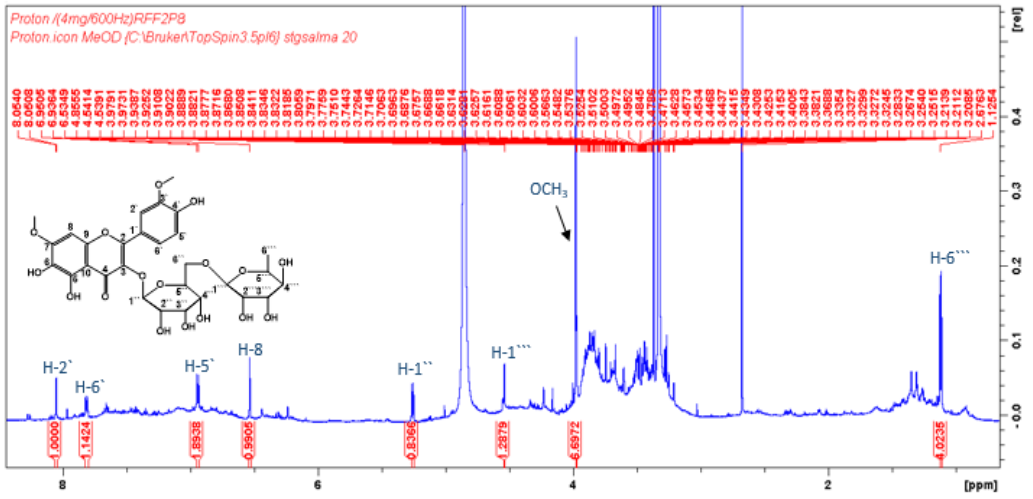


***Figure 3.70**: [1]H NMR (600 MHz, $CD_3OD$) of compound **103***

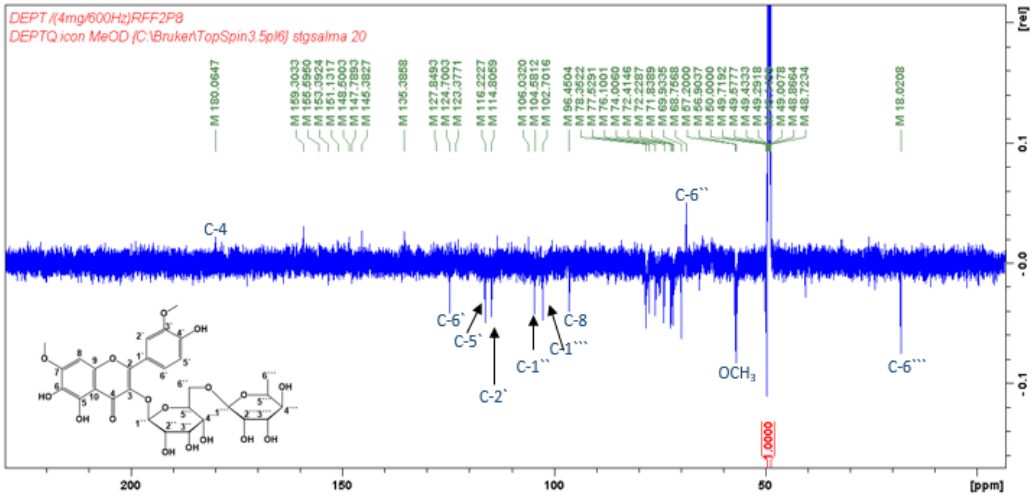


***Figure 3.71**: [13]C NMR (150 MHz, $CD_3OD$) of compound **103***

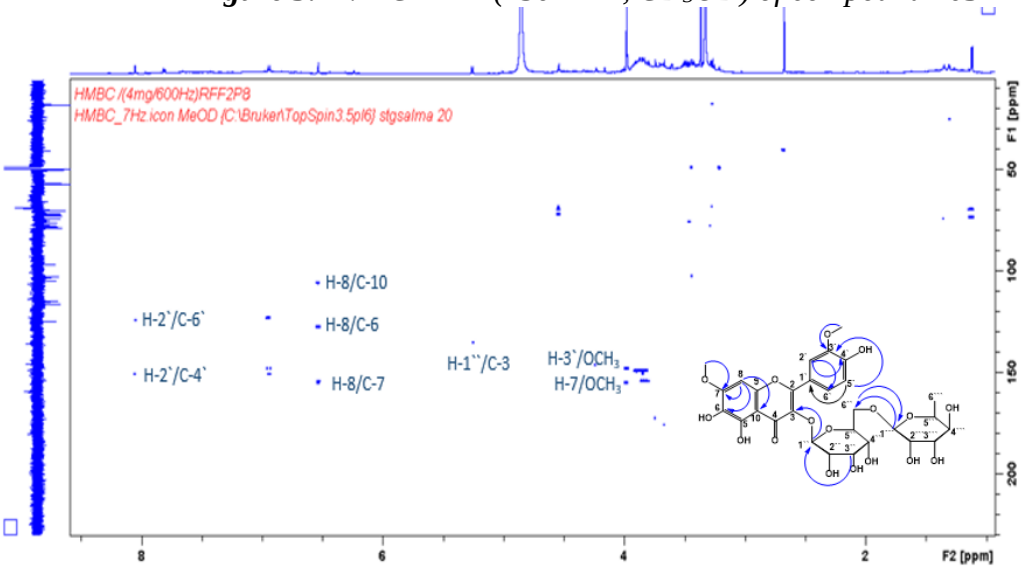


***Figure 3.72**: The HMBC correlations of compound **103***

**Table 3.15**: $^{1}$H NMR data for compounds **48,101-103 (**at 600 MHz in $CD_3OD$, $\delta$ in ppm, *J* in Hz)

| **Position** | **48** | **101** | **102** | **103** |
|---|---|---|---|---|
| 6 | 6.23 *d* (2.1) | 6.23 *d* (2.0) | 6.23 *d* (2.0) | - |
| 8 | 6.42 *d* (2.1) | 6.44 *d* (2.0) | 6.43 *d* (2.0) | 6.53 s |
| 2' | 7.69 *d* (2.0) | 7.96 *d* (2.0) | 7.66 *d* (2.0) | 8.00 *d* (2.0) |
| 5' | 6.89 *d* (8.4) | 6.94 *d* (8.4) | 6.93 *d* (8.4) | 6.94 *d* (8.4) |
| 6' | 7.65 *dd* (2.0, 8.4) | 7.65 *dd* (2.0, 8.4) | 7.64 *d* (8.4) | 7.80 *dd* (2.0, 8.4) |
| 7-OMe | - | - | 3.96 s | 3.97 s |
| 3'-OMe | - | 3.97 s | - | 3.97 s |
| 4'-OMe | - | - | 3.97 s | - |
| 1'' | 5.12 *d* (7.7) | 5.25 *d* (7.6) | 5.25 *d* (7.5) | 5.25 *d*, (7.4) |
| 2'' | 3.49* | 3.49* | 3.49* | 3.49* |
| 3'' | 3.31* | 3.32* | 3.32* | 3.31* |
| 4'' | 3.29* | 3.30* | 3.28* | 3.29* |
| 5'' | 3.43* | 3.46* | 3.43* | 3.43* |
| 6'' | 3.41*<br>3.81 m | 3.44*<br>3.84 m | 3.44*<br>3.84 m | 3.44*<br>3.84 m |
| 1''' | 4.54 *d* (1.5) | 4.55 *d* (1.5) | 4.54 *d* (1.4) | 4.54 *d* (1.4) |
| 2''' | 3.65* | 3.63* | 3.63* | 3.60* |
| 3''' | 3.55* | 3.56* | 3.53* | 3.54* |
| 4''' | 3.30* | 3.28* | 3.28* | 3.28* |
| 5''' | 3.46* | 3.43* | 3.43* | 3.43* |
| 6''' | 1.14 *d* (6.2) | 1.11 *d* (6.2) | 1.12 *d* (6.2) | 1.11 *d* (6.3) |

* Overlapped peaks – confirmed from COSY, HSQC and HMBC experiments

### 3.1.9.19 Structure elucidation of hexadecane (109)

The compound **109** was isolated as white glittering bright paticles solid. . The HRESIMS (Figure 3.74) suggested the empirical formula as $C_{16}H_{34}$ from the $[M+Na]^+$ peak at *m/z* 249.1562 (calculated 249.255820). The $^{1}$H NMR spectrum (Figure 3.75) exhibited one huge peak at $\delta_H$ 1.10, typical of a number of methylenes of a long chain alkane. The DEPTQ spectrum (Figure 3.76) showed the presence of two-methyl groups at $\delta_c$ 14.10 and a number of methylene groups. The analysis of HMBC correlation along with 1D data observation suggested compound **109** to be a long chain alkane. Based on mass spectrometric and NMR spectroscopic data, compound **109** was identified as hexadecane, which was previously reported from *R. graveolens* (De Feo *et al.*, 2002; Diwan and Malpathak, 2011).

**Table 3.16**: $^{13}C$ NMR data for compounds **48, 101-103 (**at 150 MHz in $CD_3OD$)

| **Position** | **Chemical shift δ in ppm** | | | |
|---|---|---|---|---|
| | **48** | **101** | **102** | **103** |
| 2 | 159.5 | 159.0 | 159.4 | 159.3 |
| 3 | 135.7 | 135.6 | 135.2 | 135.3 |
| 4 | 179.5 | 179.5 | 180.0 | 180.0 |
| 5 | 163.2 | 163.2 | 161.4 | 153.2 |
| 6 | 100.0 | 100.1 | 98.0 | 127.8 |
| 7 | 166.2 | 166.2 | 167.3 | 155.5 |
| 8 | 95.0 | 95.0 | 92.8 | 96.4 |
| 9 | 158.5 | 158.7 | 158.4 | 145.3 |
| 10 | 105.7 | 105.9 | 104.2 | 106.0 |
| 1' | 123.2 | 123.2 | 123.2 | 123.3 |
| 2' | 117.8 | 114.7 | 114.7 | 114.8 |
| 3' | 146.0 | 148.5 | 148.2 | 148.5 |
| 4' | 150.4 | 151.0 | 151.0 | 151.0 |
| 5' | 116.2 | 116.3 | 116.3 | 116.2 |
| 6' | 123.7 | 124.2 | 124.7 | 124.7 |
| 7-OMe | - | - | 57.4 | 57.2 |
| 3'-OMe | - | 56.9 | - | 56.9 |
| 4'-OMe | - | - | 56.1 | - |
| 1'' | 104.8 | 104.5 | 104.5 | 104.5 |
| 2'' | 75.9 | 76.1 | 76.3 | 76.1 |
| 3'' | 77.4 | 72.4 | 72.4 | 72.4 |
| 4'' | 71.5 | 77.5 | 77.5 | 77.5 |
| 5'' | 78.3 | 78.3 | 78.3 | 78.3 |
| 6'' | 68.7 | 68.1 | 68.1 | 68.7 |
| 1''' | 102.5 | 102.7 | 102.6 | 102.7 |
| 2''' | 72.2 | 72.2 | 72.2 | 72.2 |
| 3''' | 72.4 | 71.8 | 71.8 | 71.8 |
| 4''' | 74.1 | 74.0 | 74.0 | 74.0 |
| 5''' | 69.8 | 69.9 | 69.98 | 69.9 |
| 6''' | 18.0 | 18.0 | 18.0 | 18.0 |

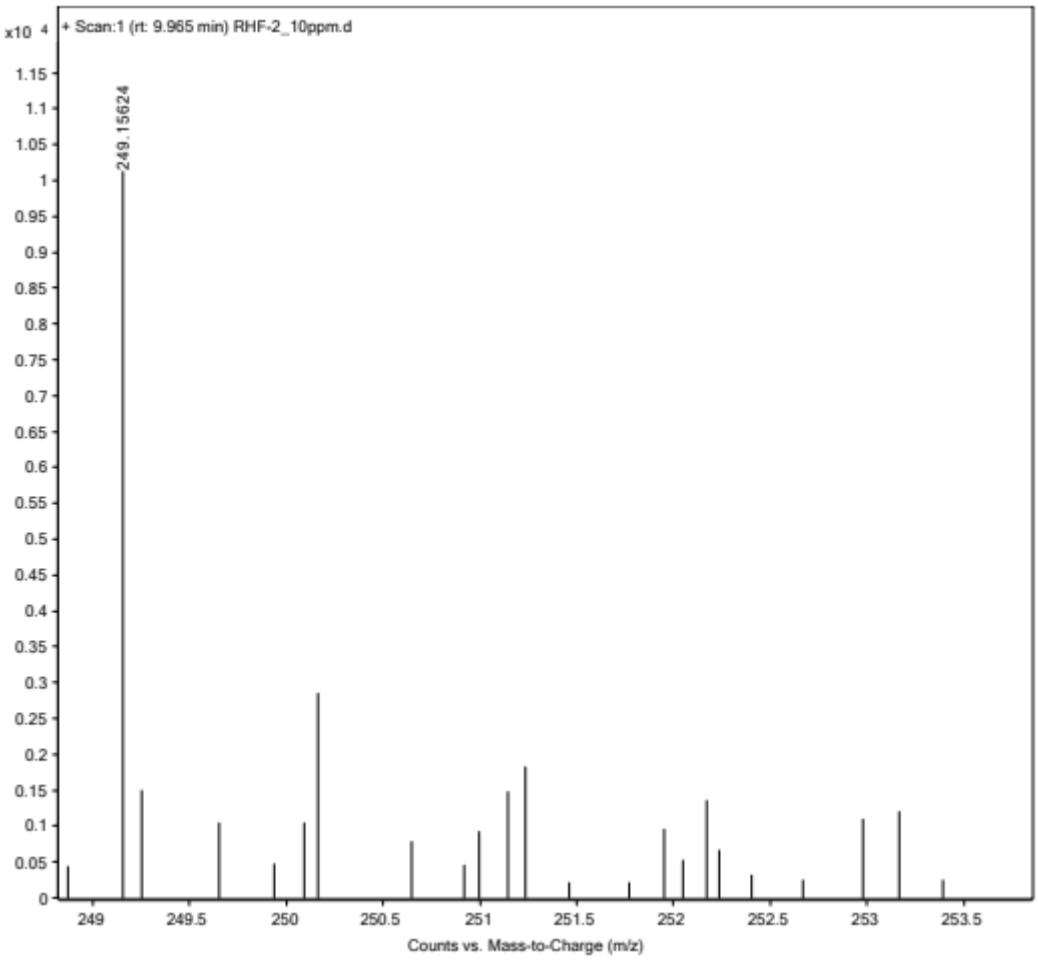


***Figure 3.73**: The HRESIMS of compound **109***

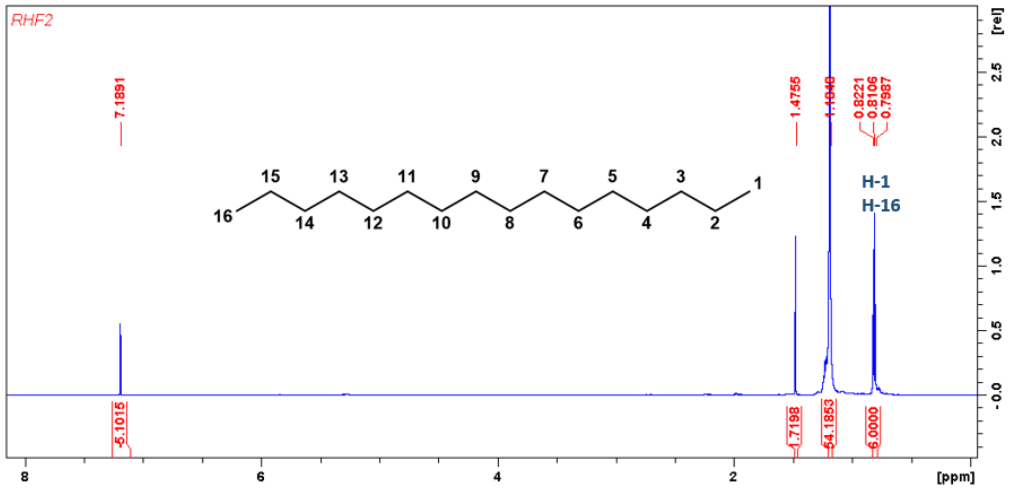


***Figure 3.74**: $^{1}H$ NMR (300 MHz, $CDCl_3$) spectrum of compound **109***

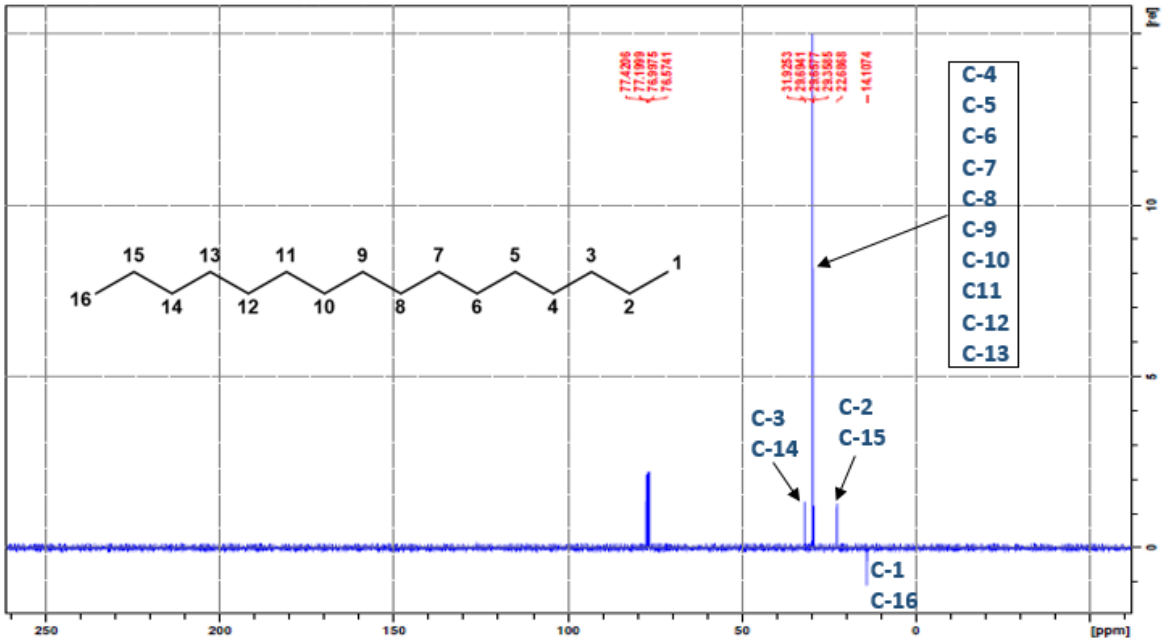


***Figure 3.75**: $^{13}C$ NMR (75 MHz, $CD_3OD$) spectrum of compound **109***

### 3.1.10 Antimicrobial activity of the isolated compounds from *R. chalepensis*

The isolated compounds from *R. chalepensis* were screened to evaluate their antimicrobial activities and determine their minimum inhibition concentration (MIC) by serial dilution using microtitre assay. The antimicrobial method was performed on four bacteria species *S. aureus* (NCTC 12981), *E. coli* (NCTC 12241), *P. aeruginosa* (NCTC 12903), *M. luteus* (NCTC 7508) and one fungal strain *C. albicans* (ATCC 90028). The highest test concentration of compounds were 1mg/mL. The observed MIC values are outlined in Table 3.17.

The analyses of biological evaluation for the pure compounds revealed that all the tested compounds except compound **109** succeeded to constrain the growth of *C. albicans* and *M. luteus* with different concentrations. Out of fourteen compounds, only compounds **42** and **109** failed to prevent *S. aureus* growth, while five compounds inhibited the growth of *E. coli*. Moreover, five compounds (**46**, **47**, **48**, **101** and **107**) presented significant inhibitory activities against *P. aeruginosa* with different MIC values. Four distinct compounds (**46**, **101**, **103** and **107**) inhibited all the tested strains, while there was no biological activity for compound **109** within the concentration range tested.

Different antibiotics, summarized in Table 3.3, were used as positive controls in the microtitre assay, these antibiotics have a wide inhibit any range for different bacterial strain such as: nalidixic acid, gentamycin, chloramphenicol and ciprofloxacin while, nystatin was used as apositive control to inhibit *C. albicans*. The nutrient broth, water and normal saline were used as negative controls in the antimicrobial tests.

**Table 3.17**: The MIC for isolated compounds from *R. chalepensis*

| **Compounds** | **All concentrations in (mg/mL)** | | | | |
|---|---|---|---|---|---|
| | *Staphylococcus aureus* (NCTC 12981) | *Escherichia coli* (NCTC 12241) | *Pseudomonas aeruginosa* (NCTC 12903) | *Micrococcus luteus* (NCTC 7508) | *Candida albicans* (ATCC 90028) |
| **42** | N/A | N/A | N/A | $5x10^{-1}$ | $5x10^{-1}$ |
| **43** | N/A | N/A | N/A | $5x10^{-1}$ | $5x10^{-1}$ |
| **44** | $5x10^{-1}$ | N/A | N/A | 6.25×10-2 | $5x10^{-1}$ |
| **45** | $1.25\times10^{-1}$ | $5x10^{-1}$ | N/A | $1.25\times10^{-1}$ | $1.25\times10^{-1}$ |
| **46** | $1.25\times10^{-1}$ | $1.25\times10^{-1}$ | $5x10^{-1}$ | $2.5\times10^{-1}$ | $6.25\times10^{-2}$ |
| **47** | $1.25\times10^{-1}$ | N/A | $5x10^{-1}$ | $2.5\times10^{-1}$ | $2.5\times10^{-1}$ |
| **48** | $2.5\times10^{-1}$ | N/A | $5x10^{-1}$ | $2.5\times10^{-1}$ | $2.5\times10^{-1}$ |
| **99** | $5x10^{-1}$ | N/A | N/A | $5x10^{-1}$ | $5x10^{-1}$ |
| **101** | $2.5\times10^{-1}$ | $2.5\times10^{-1}$ | $2.5\times10^{-1}$ | $2.5\times10^{-1}$ | $2.5\times10^{-1}$ |
| **103** | $2.5\times10^{-1}$ | $2.5\times10^{-1}$ | $2.5\times10^{-1}$ | $6.25\times10^{-2}$ | $6.25\times10^{-2}$ |
| **104** | $5x10^{-1}$ | N/A | N/A | $2.5x10^{-1}$ | $2.5x10^{-1}$ |
| **105** | $5x10^{-1}$ | N/A | N/A | $5x10^{-1}$ | $5x10^{-1}$ |
| **107** | $2.5x10^{-1}$ | $5x10^{-1}$ | $5x10^{-1}$ | $1.25x10^{-1}$ | $6.25\times10^{-2}$ |
| **109** | N/A | N/A | N/A | N/A | N/A |

*N/A: No Activity

### 3.1.11 Discussion

The Rutaceae is one of the largest botanical families distributed worldwide, which including plants, herbs, shrubs and trees. In traditional medicine, the Rutaceae family is considered as an exhaustive pharmacy due to the successful indications for curing skin lesions, inflammatory diseases, intestines disorder, peptic ulcers, ear problems, respiratory infections, asthma and rheumatism and being a cardio tonic. In addition, the strong fragrance of the Rutaceae members led to the discovery of essential oils and led to use as a perfume and insect repellent. All these features attracted the researchers to discover and isolated

hundreds of compounds from this family (San Miguel, 2003a; Orwa *et al.*, 2008; Arbab *et al.*, 2012).

The phytochemical studies on the Rutaceae family were rich with many secondary metabolites such as alkaloids, coumarins, flavonoids, glycosides and tannins. The biological research confirmed the antimicrobial activity, antimalarial activity, anti-inflammatory effect and there is a positive significant result on treating cancer cell. The scientific reviews discovered the antioxidant effect of the Rutaceae members that led to using these materials as antioxidant agents in the cosmetics industry (Gunatilaka *et al.*, 1994; Viljoen *et al.*, 2006; Supabphol and Tangjitjareonkun, 2014)

The present study included one of the important members of the Rutaceae family, *Ruta chalepensis.* The current research screened the antimicrobial activity of different parts (fruit, stem, leaves and roots) of the Iraqi genus *R. chalepensis*. Microtitre assay was the biological assay used in this study and performed on two Gram-positive bacteria *Micrococcus luteus* (NCTC 7508), *Staphylococcus aureus* (NCTC 12981); two Gram-negative *Escherichia coli* (NCTC 12241); *Pseudomonas aeruginosa* (NCTC 12903) and *Candida albicans* (ATCC 90028), which is considered one of the most common pathogenic fungi. The primarily screening of three extracts (*n*-hexane, DCM, MeOH) for every part (fruit, stem, leaves and roots) of *R. chalepensis* revealed that all extract successively inhibited the microbial strain with different MIC values and the most active extract was *n*-hexane fruits against C. *albicans* with MIC 1.56 $x10^{-2}$ mg/mL. The root extracts showed a weak effect with the maximum concentration tested which was 10 mg/mL.

Nineteen compounds were isolated from different plant parts and active fractions including eight alkaloids γ-fagarine (**42**), arborinine (**107**), graveoline (**105**), imperatorin (**104**), isokokusaginine (**100**), kokusaginine (**99**), ribalinium (**106**) and skimmianine (**41**). Five coumarins bergapten (**43**), chalepin (**45**), chalepensin (**46**), isopimpinellin (**44**) and rutamarin (**47**); one sinapoyl glycoside, 3', 6-disinapoylsucrose (**108**) and one alkane hexadecane **(109).** Four glycosylated flavonoids rutin (**48**), rutin 3' -methyl ether (**101**), rutin

7,4' - dimethyl ether (**102**) and 6-Hydroxy-rutin 3' -7-dimethyl ether (**103**) which to the best of our knowledge, is a new natural product.

Fourteen of the isolated compounds were tested against the microbes used in this work. In general, all alkaloids showed significant antimicrobial activity. Previous studies have reported finding and isolating alkaloids from *Ruta* spp. Compound **107** successively inhibited all strains tested with high MIC value 1.25 x $10^{-1}$, 6.25 × $10^{-2}$ mg/mL against *M. lutues* and *C. albicanus*, respectively. Compound **107** is an acridone alkaloid with a wide spectrum of activity, which has a hydroxyl on position 1; methyl on position 10 and two oxygenated methyl groups on position 2 and 3. The high activity of compound **107** maybe belonging to the variety of substitution attached to this compound in addition for the presence of a nitrogen atom.

The coumarin compounds showed considerable antimicrobial activity and particularly compound **46** against *C. albicans* with MIC 6.25 × $10^{-2}$ mg/mL. The analysis of data of microbiological test led to realise that there was a structure-activity relationship, the coumarins with substituted 3,3-dimethylbut-1-ene (chalepin **45**, chalepensin **46**, rutamarin **47**) showed a remarkable inhibitory activity greater than other coumarins (bergapten **43**, isopimpinellin **44**). Among the most active three coumarins **45**, **46**, **47**, compound chalepensin **46** was the most active one.

The furanocoumarin chalepensin (**46**) occurs in many medicinal plants of the Rutaceae family, which have a wide range of pharmacological activities such as anti-inflammatory, antifertility, antiplatelet aggregation and anticancer activities (Lo *et al.*, 2012; Quintanilla-Licea *et al.*, 2014; Nakano *et al.*, 2017).

The hexadecane **(109)** was obtained after, the vacuum liquid chromatography (VLC) of the *n*-hexane leafe extracts. The biological experiment showed compound **109** did not have any inhibitory activity within the tested concentration range (1mg/ mL).

Flavonoids, one of the biggest class of natural products, play vital roles for plants and have many potential pharmaceutical proprieties. Flavonoids are associated with a number of claimed health benefits because of their free radical-scavenging properties. Research has shown the antimicrobial activity, anti-inflammatory activity, antioxidant effect, antimutagenic and anticarcinogenic activity for flavonoids (Rice-Evans *et al.*, 1996; Pietta, 2000; Cushnie and Lamb, 2005; Mabry *et al.*, 2012). Four glycosylated flavonoids **48**, **101**, **102, 103** were isolated from different parts of *R. chalepensis*. Rutin (**48**), one of the most well known compounds, which has different biological activities, was the first flavonoid isolated on this work. Rutin consists of three benzene rings A, B, C connecting to a rutinosyl moiety. All the examined glycosylated flavonoid revealed significant inhibited activity against microbe tested practically compound **103** with MIC $6.25\times10^{-2}$ mg/mL against *M. luteus* and *C. albicans*. The 1D and 2D spectra of compound **103** were similar to rutin (**48**) with additional two oxygenated methyl and extra hydroxyl on position 6 which identified it as new compound discovered for the first time. The primary testing to determine the mechanism of action for the tested compounds revealed all the tested compounds were bacteriostatic.

### 3.2 The *Citrus*

*Citrus* fruits are a major commodity in the world. *Citrus* species are used as traditional medicinal herbs in several countries. *Citrus* fruits are good sources of nutrition, mineral elements, and secondary metabolites (Davenport, 1990; Spiegel-Roy and Goldschmidt, 1996; Ladanyia and Ladaniya, 2010). This work includes a study of the phytochemicals and antimicrobial activity of *Citrus sinensis* (leaves and peels) and *Citrus grandis* (leaves) against *Escherichia coli* (NCTC 12241), *Pseudomonas aeruginosa* (NCTC 12903), *Micrococcus luteus* (NCTC 7508), *Staphylococcus aureus* (NCTC 12981) and *Candida albicans* (ATCC 90028).

### 3.2.1 Extraction

The Soxhlet apparatus was utilized for extraction of leaves and peels of *Citrus sinensis* and leaves of *Citrus grandis* using three solvents consecutively, *n*-hexane, dichloromethane (DCM) and methanol (MeOH). The highest percentage yield of extraction for *Citrus* was 7.63% for methanolic leaves extract of *C. sinensis* (SLM) and the lowest extraction percentage was 0.42% for the peels methanolic extract of *C. sinensis* (PLM). The percentage yield of extracts summarized in Table 3.18

**Table 3.18**: Percentage yield of *Citrus*

| ***Citrus* species** | ***Citrus* parts** | **Weights (gm)** | **Extract type** | **% Yield** |
|---|---|---|---|---|
| *Citrus sinensis* | Leaves | 64.86 | *n*-hexane (SLH) | 0.60 |
| | | | DCM (SLD) | 0.75 |
| | | | MeOH (SLM) | 7.63 |
| | Peels | 131.13 | *n*-hexane (PLH) | 2.13 |
| | | | DCM (PLD) | 3.77 |
| | | | MeOH (PLM) | 0.42 |
| *Citrus grandis* | Leaves | 117.00 | *n*-hexane (GLH) | 1.69 |
| | | | DCM(GLD) | 1.15 |
| | | | MeOH (GLM) | 4.41 |

### 3.2.2 Preliminary analytical TLC screening

The first analysis for the development TLC plates of the *n*-hexane and DCM extracts of *Citrus* were performed following method **H** (Figure 3.75). The developed TLC plates were viewed under short (254 nm) and long (366 nm) were UV light followed by spraying with anisaldehyde reagent and then heating at 100ºC for 5 min to reveal different coloured spots.

### 3.2.3 Analytical HPLC screening of the MeOH extracts

The three MeOH *Citrus* extracts (10 mg/mL) were subjected to analytical -HPLC. The leaf MeOH extract (Figure 3.76) of *C. sinensis* were successively analysed using method **Q** while, the method **L** was followed to analyze the MeOH extract of *C. sinensis* peel (Figure 3.77). The MeOH extract of *C. grandis* leaves were (Figure 3.78) loaded on to analytical HPLC using method **R**.

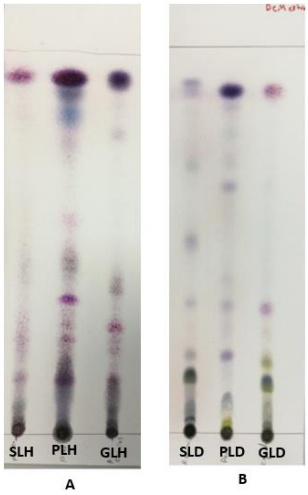


***Figure 3.76**: The TLC plates for Citrus extracts*

*A: n-hexane extracts B: DCM extracts*

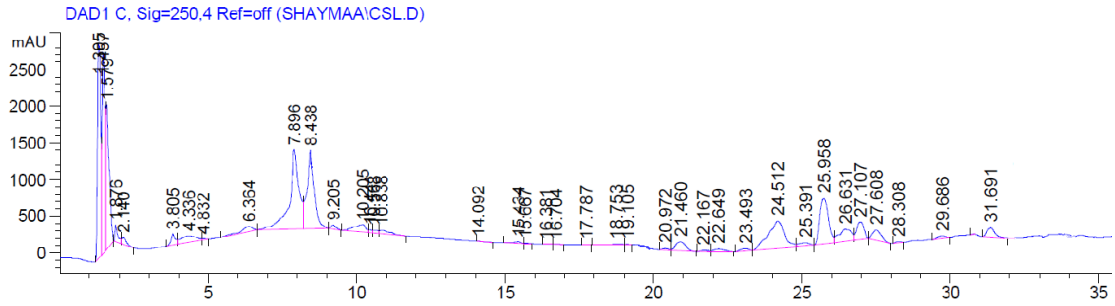


***Figure 3.77**: Analytical HPLC chromatogram of MeOH extract of C. sinensis leaves*

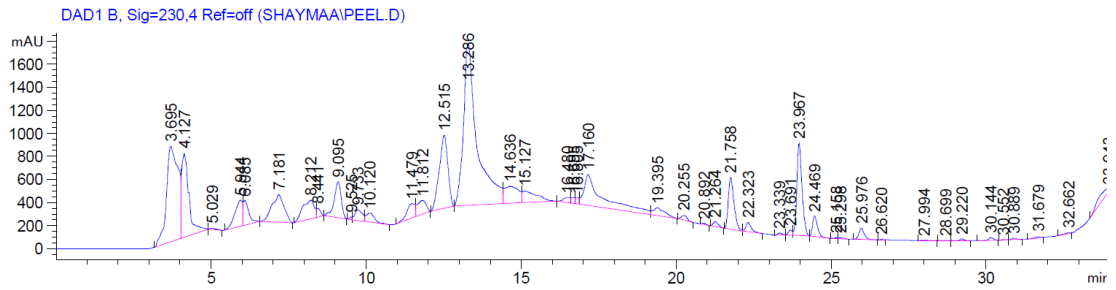


***Figure 3.78**: Analytical HPLC chromatogram of MeOH extract of C. sinensis peel*

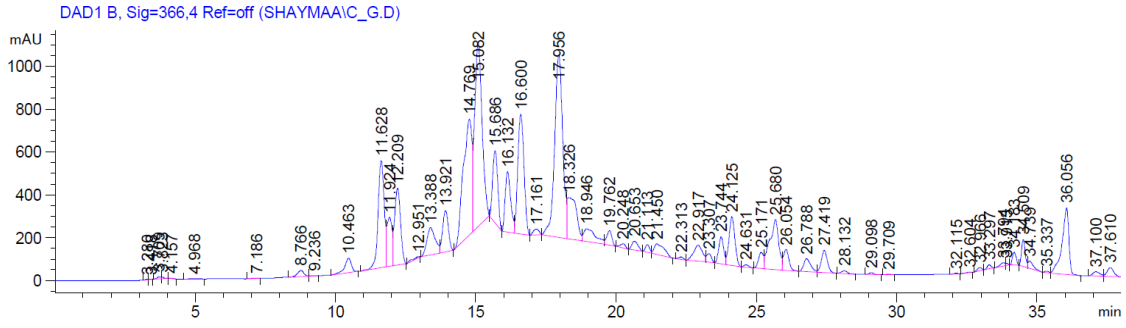


***Figure 3.79**: Analytical HPLC chromatogram of MeOH extract of C. grandis*

### 3.2.4 The antimicrobial screening for *Citrus sinensis* and *Citrus grandis*

All the six extracts of *C. sinensis* and three extracts of *C. grandis* with maximum concentrate 10 mg/mL were investigated for their antimicrobial proprieties against *Escherichia coli* (NCTC 12241), *Pseudomonas aeruginosa* (NCTC 12903), *Micrococcus luteus* (NCTC 7508), *Staphylococcus aureus* (NCTC 12981) and *Candida albicans* (ATCC 90028) using the modified microtitre plate assay (Sarker *et al.*, 2007). The findings (Table 3.19) suggested that the peel DCM extract had potent antimicrobial activity against *M. luteus* with a MIC value $4.88\times10^{-3}$ mg/mL. In general, the three DCM extract inhibited all the microbes used in this study with MIC $6.25\times10^{-1}$ mg/mL and less. The *n-hexane* extracts failed to present any antimicrobial effect within the maximum concentration (10 mg/mL) used in this study. Whereas, the peel MeOH extract showed moderate antimicrobial activity against *M. luteus* and *C. albicans* and the MIC values was $3.12\times10^{-1}$, $6.25\times10^{-1}$ mg/mL, respectively.

**Table 3.19**: MIC values (mg/mL) of *Citrus* extracts

| **Bacteria and fungi** | **Extract** | ***Citrus sinensis*** | | ***Citrus grandis*** |
|---|---|---|---|---|
| Gram-negative | | Leaves | Peels | Leaves |
| *Escherichia coli* | *n*-Hexane | 2.5 | 5 | 5 |
| | DCM | $6.25\times\times10^{-1}$ | $3.12\times10^{-1}$ | $3.12\times\times10^{-1}$ |
| | MeOH | 2.5 | 1.25 | 1.25 |
| *Pseudomonas aeruginosa* | *n*-Hexane | N/A | 5 | - |
| | DCM | 5 | $6.25 \times 10^{-1}$ | $3.12 \times 10^{-1}$ |
| | MeOH | 5 | 1.25 | 5 |
| Gram-positive | | | | |
| *Micrococcus luteus* | *n*-Hexane | 5 | $1.56 \times 10^{-1}$ | $6.25 \times 10^{-1}$ |
| | DCM | $3.12 \times 10^{-1}$ | $4.88 \times 10^{-3}$ | $3.125 \times 10^{-1}$ |
| | MeOH | 1.25 | $3.12 \times 10^{-1}$ | $6.25 \times 10^{-1}$ |
| *Staphylococcus aureus* | *n*-Hexane | 5 | - | - |
| | DCM | $6.25 \times 10^{-1}$ | $6.25 \times 10^{-1}$ | $6.25 \times 10^{-1}$ |
| | MeOH | 2.5 | 5 | 5 |
| Pathogenic fungi | | | | |
| *Candida albicans* | *n*-Hexane | N/A | 2.5 | 5 |
| | DCM | $3.12 \times 10^{-1}$ | $1.56 \times 10^{-1}$ | $6.25 \times 10^{-1}$ |
| | MeOH | 5 | $6.25 \times 10^{-1}$ | 2.5 |

*N/A: No Activity

### 3.2.5 Chromatographic fractionation of the extracts

Based on the result of the primary screening of *Citrus* crude extracts and following bioassay guided the MIC value 6.25 x $10^{-1}$ mg/mL was selected as the minimum threshold concentration for the future work. Further fractionation for the most active crude extract involved using vacuum liquid chromatography fractionation (VLC) and solid phase extraction (SPE) as described in the experimental section.

#### 3.2.5.1 Vacuum liquid chromatography fractionation (VLC)

The DCM extracts *Citrus* were subjected to VLC over silica gel using the method **C** and fractionated to eight fractions. Table 3.20 summarizes the yields of all fractions. The DCM fractions obtained were analysed by the TLC using method **F** (Figure 3.80).

#### 3.2.5.2 Solid-phase extraction (SPE)

The MeOH extract of *C. sinensis* peels was fractionated by SPE using method **D** to obtain four fractions and their yield is summarized in Table 3.20.

### 3.2.6 Screening of *Citrus* fractions for antimicrobial activity

All the obtained fractions were screened for their antimicrobial activity against *Escherichia coli* (NCTC 12241), *Pseudomonas aeruginosa* (NCTC 12903), *Micrococcus luteus* (NCTC 7508), *Staphylococcus aureus* (NCTC 12981) and *Candida albicans* (ATCC 90028). The results are summarized in Table 3.21 and Table 3.22.

The highest activity of the DCM fractions in leaves of *C. sinensis* and *C. grandis* were shown by fraction 7 (F7). The DCM fractions of the *C. sinensis* peel showed a significant antimicrobial activity and specifically fraction 6 (F6) and fraction 7 (F7) against *M. luteus* and *C. albicans* with MIC $1.56\times10^{-2}$. In addition, fraction 3 (F3) of the methanolic extract of *C. sinensis* peel gave considerable activity against all microbial strains used in this study. Fraction 2 (F2) showed strong activity against *M. luteus* with MIC $6.25\times10^{-1}$. The phytochemical and antimicrobial work was continued with fractions which were found to be active.

**Table 3.20**: The yield of *Citrus* fractions

| Plant extracts | Type of extract | Weight of extract (gm) | Fractions yield % | | | | | | | |
|---|---|---|---|---|---|---|---|---|---|---|
| | | | **F1** | **F2** | **F3** | **F4** | **F5** | **F6** | **F7** | **F8** |
| *C. sinensis* leaves | DCM | 2.5142 | 22.63 | 3.28 | 38.41 | 23.30 | 7.07 | 3.97 | 4.86 | 9.19 |
| *C. sinensis* peels | DCM | 2.1655 | 4.42 | 2.31 | 8.08 | 15.09 | 6.30 | 6.86 | 19.71 | 15.64 |
| | MeOH | 1.8210 | 48.68 | 6.74 | 3.14 | 2.67 | - | - | - | - |
| *C. grandis* Leaves | DCM | 2.2044 | 7.34 | 6.35 | 45.86 | 10.24 | 4.94 | 2.54 | 4.81 | 5.34 |

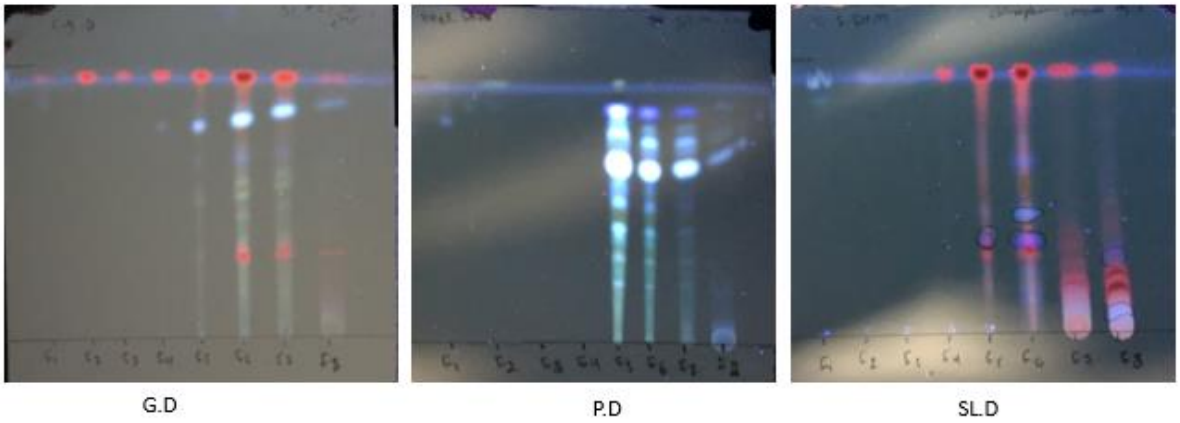


***Figure 3.80**: The analysis TLC for Citrus DCM fractions*

**G.D**: *C. grandis* leaves; **P.D**: *C. sinensis* Peel; **SL.D**: *C. sinensis* leaves

**Table 3.21**: The MIC values (mg/mL) of DCM fractions for *Citrus*

| **Plant name and part** | **Extract type** | **Microbes** | **Fractions** | | | | | | | |
|---|---|---|---|---|---|---|---|---|---|---|
| | | | **F1** | **F2** | **F3** | **F4** | **F5** | **F6** | **F7** | **F8** |
| *C. sinensis* leaves | DCM | *E. coli* | N/A | N/A | N/A | N/A | N/A | N/A | N/A | N/A |
| | | *P. aeruginosa* | N/A | N/A | N/A | N/A | N/A | 1 | 1 | N/A |
| | | *M. luteus* | N/A | N/A | N/A | N/A | N/A | N/A | $6.25\times10^{-2}$ | N/A |
| | | *S. aureus* | N/A | N/A | N/A | N/A | N/A | 1 | N/A | N/A |
| | | *C. albicans* | N/A | N/A | N/A | N/A | N/A | N/A | $6.25\times10^{-2}$ | 1 |
| *C. sinensis* peels | DCM | *E. coli* | N/A | N/A | N/A | N/A | N/A | $5\times10^{-1}$ | N/A | N/A |
| | | *P. aeruginosa* | N/A | N/A | N/A | N/A | 1 | $5\times10^{-1}$ | 1 | N/A |
| | | *M. luteus* | N/A | N/A | N/A | $5\times10^{-1}$ | $5\times10^{-1}$ | $7.81\times10^{-3}$ | $1.56\times10^{-2}$ | N/A |
| | | *S. aureus* | N/A | N/A | N/A | N/A | N/A | 1 | $5\times10^{-1}$ | N/A |
| | | *C. albicans* | N/A | N/A | N/A | $5\times10^{-1}$ | $5\times10^{-1}$ | $7.81\times10^{-3}$ | $1.56\times10^{-2}$ | N/A |
| *C. grandis* leaves | DCM | *E. coli* | N/A | N/A | N/A | N/A | N/A | **1** | $6.25\times10^{-2}$ | N/A |
| | | *P. aeruginosa* | N/A | N/A | N/A | N/A | N/A | $5\times10^{-1}$ | $1.25\times10^{-1}$ | N/A |
| | | *M. luteus* | N/A | N/A | N/A | N/A | N/A | $5\times10^{-1}$ | $1.56\times10^{-2}$ | N/A |
| | | *S. aureus* | N/A | N/A | N/A | N/A | N/A | 1 | $2.5\times10^{-1}$ | N/A |
| | | *C. albicans* | N/A | N/A | N/A | N/A | N/A | $5\times10^{-1}$ | $3.12\times10^{-2}$ | N/A |

*N/A: No Activity

**Table 3.22:** The MIC (mg/mL) of MeOH extract of *C. sinensis* peels

| **Microbial name** | **Fractions** | | | |
|---|---|---|---|---|
| | F1 | F2 | F3 | F4 |
| *E. coli* | N/A | 1 | $2.5\times10^{-1}$ | N/A |
| *P. aeruginosa* | N/A | N/A | $5\times10^{-1}$ | N/A |
| *M. luteus* | $5\times10^{-1}$ | $6.25\times10^{-1}$ | $3.12\times10^{-2}$ | $5\times10^{-1}$ |
| *S. aureus* | N/A | 1 | $1.25\times10^{-1}$ | N/A |
| *C. albicans* | $5\times10^{-1}$ | $5\times10^{-1}$ | $1.56\times10^{-2}$ | $5\times10^{-1}$ |

*N/A: No Activity

### 3.2.7 Phytochemistry of *Citrus* species

The active fractions of DCM and methanolic extracts of *Citrus*, which exhibited a significant antimicrobial activity, were subjected to preparative-HPLC to separate the phytochemical constituents. The chromatographic separation and spectroscopic technique (NMR and HRESIMS) afforded isolation and characterization of fifteen compounds (Figure 3.81). The spectral data of known compounds were compared with the documented data. They were classified as hesperidin (**50**), rutin (**48**), narirutin (**51**), rutin 3`-methyl ether (**101**), 3-methoxynobiletin (**110**), nobiletin (**57**), sinensetin (**111**), 6,7,8,3',4'-pentamethoxyl-flavone (**112**), demethylnobiletin (**113**), 5-desmethylsinensetin (**114**), cirsilineol (**115**), tangeritin (**116**), tetramethylscutellarein (**117**), salvigenin (**118**) and Marcitrus (**119**) .

All fourteen compounds isolated from the *Citrus* were identified as flavonoids. The literature depicts the flavonoids as one of the important medical natural product treatment material distributed in most the plant species, especially in the Rutaceae family (Havsteen, 2002). To the best of our knowledge, this is the first report on the phytochemical studies on leaves of the Iraqi genus *C. grandis* and compound **119** is reported here for the first time as a natural product.

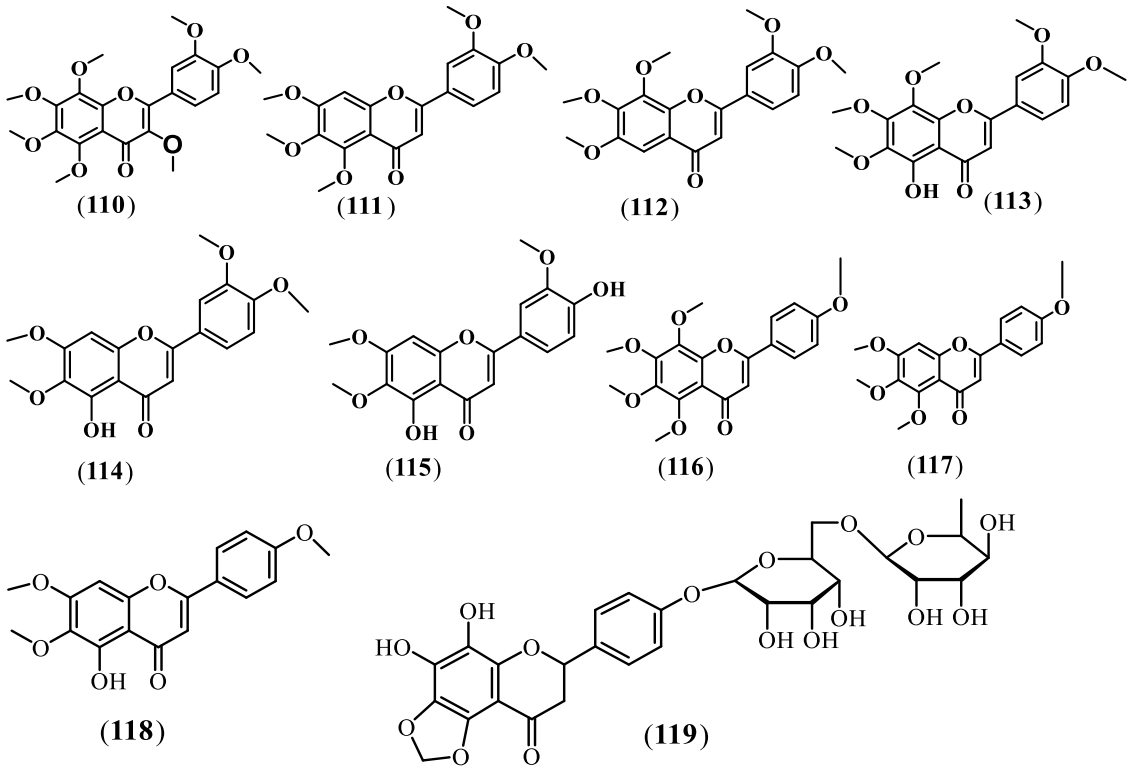


***Figure 3.81**: Isolated compounds from Citrus*

3-methoxynobiletin (**110**), sinensetin (**111**), 6,7,8,3',4'-pentamethoxyl-flavone (**112**), demethylnobiletin (**113**), 5-desmethylsinensetin (**114**), cirsilineol (**115**), tangeritin (**116**), tetramethylscutellarein (**117**), salvigenin (**118**) and marcitrus (**119**)

### 3.2.8 Isolation compounds from active fractions of *Citrus*

Based on the results of screening for the antimicrobial activity of the fractions, all the most active fractions were subjected to different chromatographic methods to isolate the active compounds.

#### 3.2.8.1 *Citrus grandis* leaves DCM extract fraction 7

The fraction 7 of *C. grandis* leaves DCM extract was subjected to prep-HPLC (Agilent) using method **T** for 35 min. The volume of injection was 350 µL and the flow rate was 10 mL/min (Figure 3.82). The separation process obtained six compounds, 6,7,8,3',4'-pentamethoxyl-flavone (**112**, 0.5 mg) (Harborne, 2013), sinensetin (**111**, 1.5 mg) (Han *et al.*, 2010), cirsilineol (**115**, 0.9 mg) (Hammoud *et al.*, 2012), nobiletin (**57**, 2.3 mg) (Li *et al.*, 2018), 5-desmethylsinensetin (**114**, 0.7 mg) (Alarif *et al.*, 2013) and hesperidin (**50**, 1.0 mg) (Chiba *et al.*, 2003).

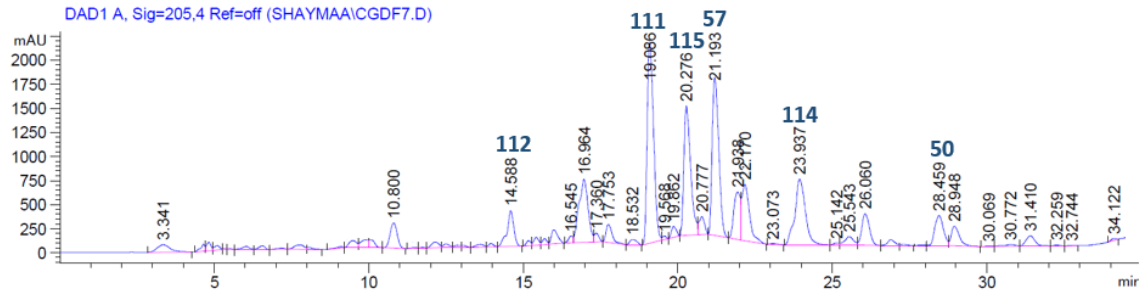


***Figure 3.82**: Preparative-HPLC chromatogram of isolated compounds from Citrus grandis leaves DCM extract fraction 7, using method **T***

### 3.2.8.2 *Citrus sinensis* leaves DCM extract fraction 7

The method **N** in prep-HPLC for 35 min was used to isolate the active compounds from fraction 7 of *C. sinensis* leaves (Figure 3.83). The injection volume was 250 µL and the flow rate was 10 ml/min. The separation process afforded five compounds. They were identified as nobiletin (**57**, 1.0 mg) (Li *et al.*, 2018), 5-desmethylsinensetin (**114**, 0.3 mg) (Alarif *et al.*, 2013), 6,7,8,3',4'-pentamethoxyl-flavone (**112**, 0.4 mg) (Harborne, 2013), cirsilineol (**115**, 0.3 mg) (Hammoud *et al.*, 2012) and hesperidin (**50**, 0.7 mg) (Chiba *et al.*, 2003).

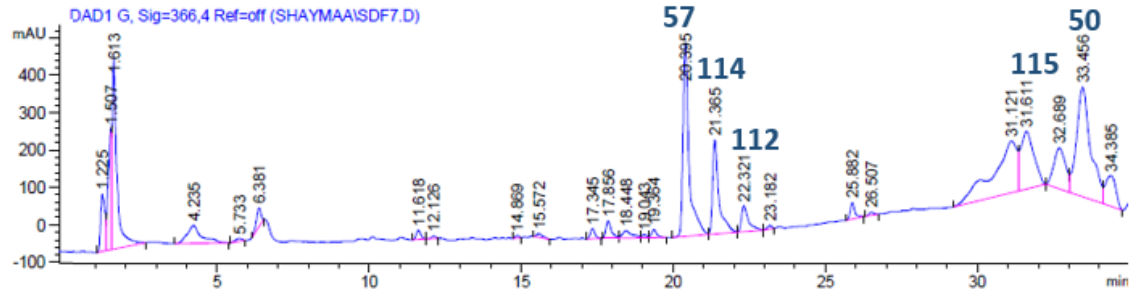


***Figure 3.83**: Preparative-HPLC chromatogram of isolated compounds from Citrus sinensis leaves DCM extract fraction 7, using method **N***

### 3.2.8.3 *Citrus sinensis* peels DCM extract fraction 6

The fraction 6 of the *C. sinensis* peels DCM extract was subjected to prep-HPLC (Agilent) following method **S** for 40 min. The volume of injection was 200 µL and the flow rate was 8 mL/min (Figure 3.84). The isolation procedure produced six compounds,

sinensetin (**111**, 1.3 mg) (Han *et al.*, 2010), nobiletin (**57**, 1.9 mg) (Li *et al.*, 2018), tetramethylscutellarein (**117**, 1.0 mg) (Li *et al.*, 2018), 3-methoxynobiletin (**110**, 0.7 mg) (Li *et al.*, 2006), tangeritin (**116**, 0.7 mg) (Hamdan *et al.*, 2011) and demethylnobiletin (**113**, 0.4 mg) (Wang *et al.*, 2005).

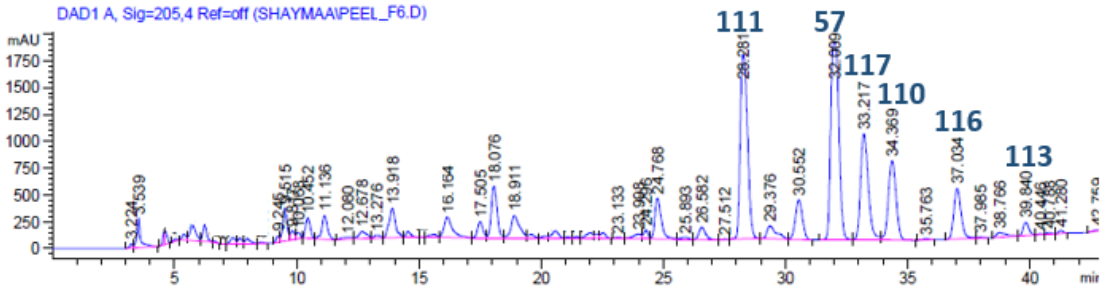


***Figure 3.84**: Preparative-HPLC chromatogram of isolated compounds from Citrus sinensis peel DCM extract fraction 6, using method **S***

### 3.2.8.4 *Citrus sinensis* peels DCM extract fraction 7

The VLC fraction 7 of the DCM extract of *C. sinensis* peels was separated by prep-HPLC (Agilent) using method **T** (Figure 3.85). The injection volume was 100 µL and the flow rate was 8 mL/min. The separation process gave seven compounds, rutin (**48**, 0.3 mg) (Kamel *et al*., 2014), narirutin (**51**, 0.4 mg) (Abu-Gharbieh and Shehab, 2017), sinensetin (**111**, 1.3 mg) (Han *et al.*, 2010), nobiletin (**57**, 1.8 mg) (Li *et al.*, 2018), tetramethylscutellarein (**117**, 1.1 mg) (Li *et al.*, 2018), 3-Methoxynobiletin (**110**, 0.8 mg) (Li *et al.*, 2006) and tangeritin (**116**, 0.4 mg) (Hamdan *et al.*, 2011).

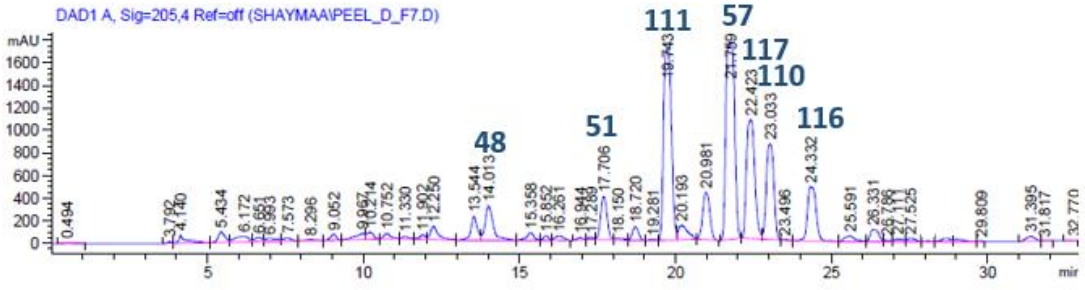


***Figure 3.85**: Preparative-HPLC chromatogram of isolated compounds from Citrus sinensis peel DCM extract fraction 7, using method **T***

### 3.2.8.5 *Citrus sinensis* peel MeOH extract fraction 2

The method **R** for 35 min on prep-HPLC was used to isolate the active compounds from fraction 2 of the *C. sinensis* peelMeOH extracts (Figure 3.86). The injection volume was 100 µL and the flow rate was 10 mL/min. The separation process afforded five compounds identified as rutin (**48**, 0.3 mg) (Kamel *et al*., 2014), Marcitrus (**119**) (0.5 mg), rutin 3`-methyl ether (**101**, 0.3 mg), narirutin (**51**, 1.2 mg) (Abu-Gharbieh and Shehab, 2017) and hesperidin (**50**, 2.3 mg) (Chiba *et al*., 2003).

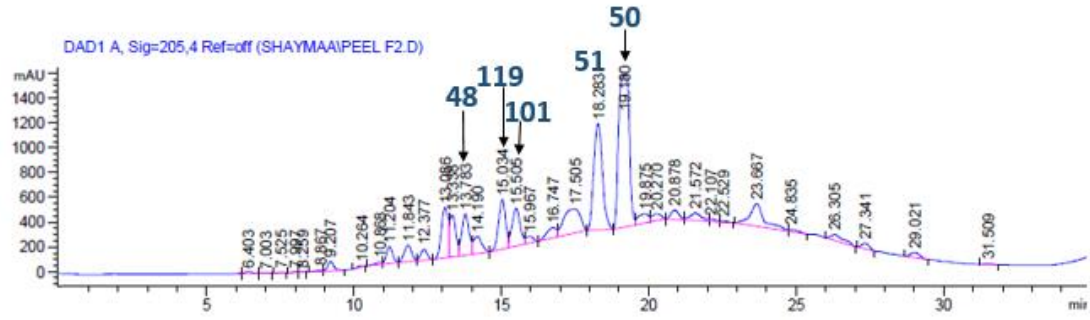


***Figure 3.86****: Preparative-HPLC chromatogram of isolated compounds from Citrus sinensis peel MeOH extract fraction 2, using method* ***R***

### 3.2.8.6 *Citrus sinensis* peels MeOH extract fraction 3

The method **R** for 35 min on prep-HPLC was used to isolate the active compounds from fraction 3 of the methanolic extract of *C. sinensis* peel (Figure 3.87). The injection volume was 200 µL and the flow rate was 10 mL/min. The separation process revealed four compounds, characterized as rutin (**48**, 1.2 mg) (Kamel *et al*., 2014), tangeritin (**116**, 0.9 mg) (Hamdan *et al.*, 2011), 3-methoxynobiletin (**110**, 2.1 mg), (Li *et al.*, 2006) and nobiletin (**57**, 0.5 mg) (Li *et al.*, 2018).

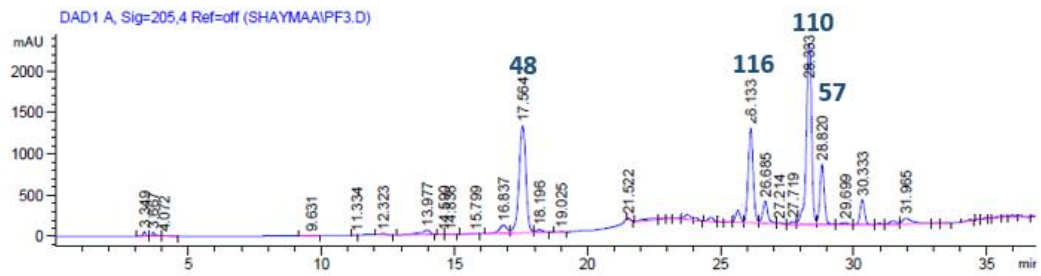


***Figure 3.87****: Preparative-HPLC chromatogram of isolated compounds from Citrus sinensis peel MeOH extract fraction 3, using method* ***R***

### 3.2.9 Characterisation and structure elucidation of isolated compounds.

#### 3.2.9.1 Structure elucidation of 3-methoxynobiletin (110)

The compound **110** was isolated as dark yellow needles. The HRESIMS (Figure 3.88) suggested the empirical formula as $C_{22}H_{24}O_9$ and in the positive ion mode it showed peak $[M+H]^+$ at *m/z* 433.1577 (calculated 432.142035). The $^1$H NMR spectrum (Figure 3.89, Table 3.23) exhibited three aromatic protons as ABX pattern resonating at $\delta_H$ 7.01 (d, *J*=8.52 Hz), 7.84 (dd, *J*= 8.7, 2.1 Hz), 7.80 (d, *J*= 2.1 Hz) and seven methoxy groups at $\delta_H$ 3.88 (3H), 3.94 (3H), 3.96 (3H), 4.00 (3H) and 4.09 (3H). The $^{13}$C NMR spectrum (Figure 3.90, Table 3.23) showed a total of twenty two carbons including a carbonyl at $\delta_c$ 174.3 (C-4), seven methoxyl carbons, three aromatic methines and the remaining as quaternary carbons. In the HMBC experiment (Figure 3.91), $^3J$ correlations were observed from methoxyl at $\delta_H$ 3.88, 3.94 , 3.96 , 4.00 and 4.09 to the oxygenated quaternary carbons at 141.1 (C-3), 144.2 (C-6), 151.4 (C-4′), 138.6 (C-8) and 151.7 (C-7) respectively, while the methoxyl at $\delta_H$ 3.97 (2X 3H) revealed $^3J$ correlation to oxygen bearing quaternary carbons at $\delta_C$ 148.6 (C-5) and 149.1 (C-3′). Moreover, H-6′ showed long range correlation to $\delta_C$ 111.3 (C-2′) and 151.4 (C-4′) and the H-5 exhibited $^3J$ correlation to $\delta_C$149.1 (C-3′) and 123.8 (C-1`). The NMR spectroscopic and mass spectrometric data as well as the correlation revealed in the HSQC and HMBC confirmed the identification of compound **110** as 3,5,6,7,8,3′,4′-heptamethoxyflavone, a poly methoxy flavonoid. The spectroscopic data of compound **110** were in a good agreement with respective published data of 3,5,6,7,8,3′,4′-heptamethoxyflavone (Li *et al.*, 2014b; Owis, 2019) isolated from *C. sinensis* peel (Li *et al.*, 2006).

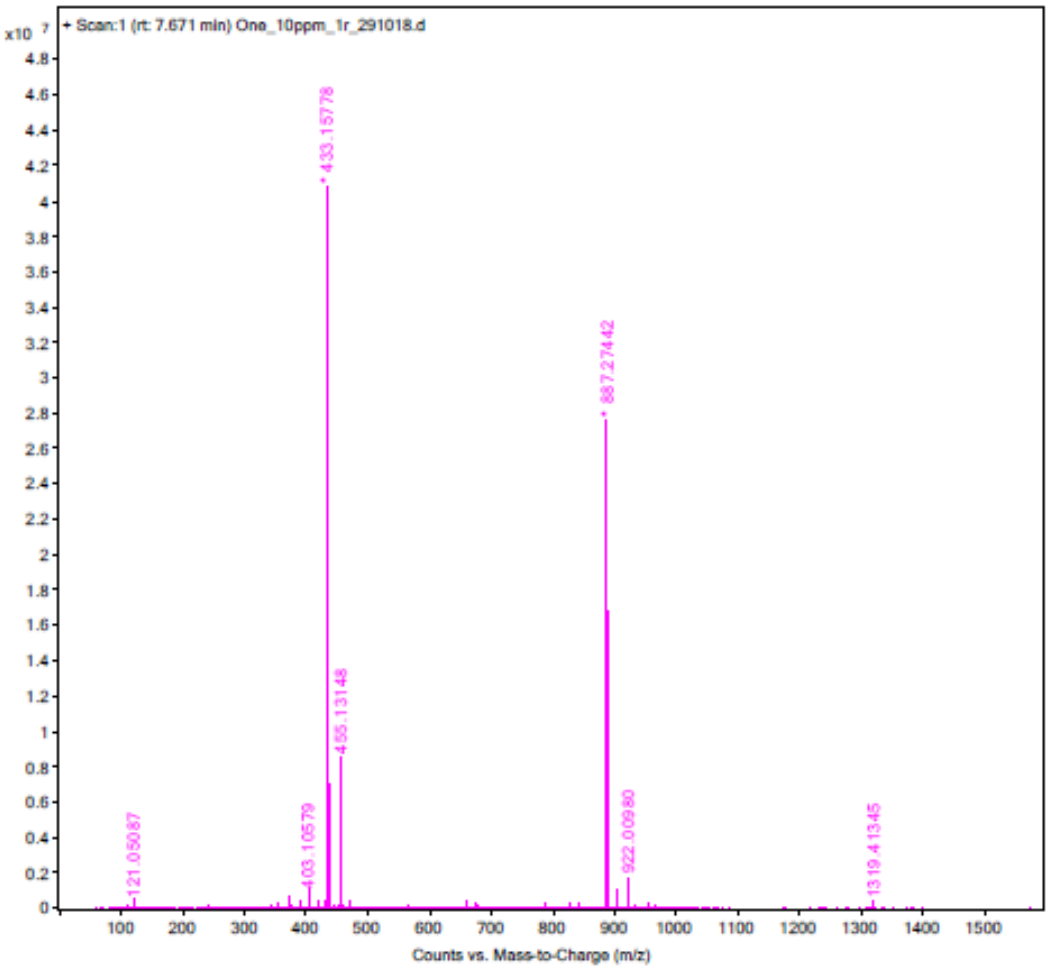


***Figure 3.88**: The HRESIMS spectrum of compound **110***

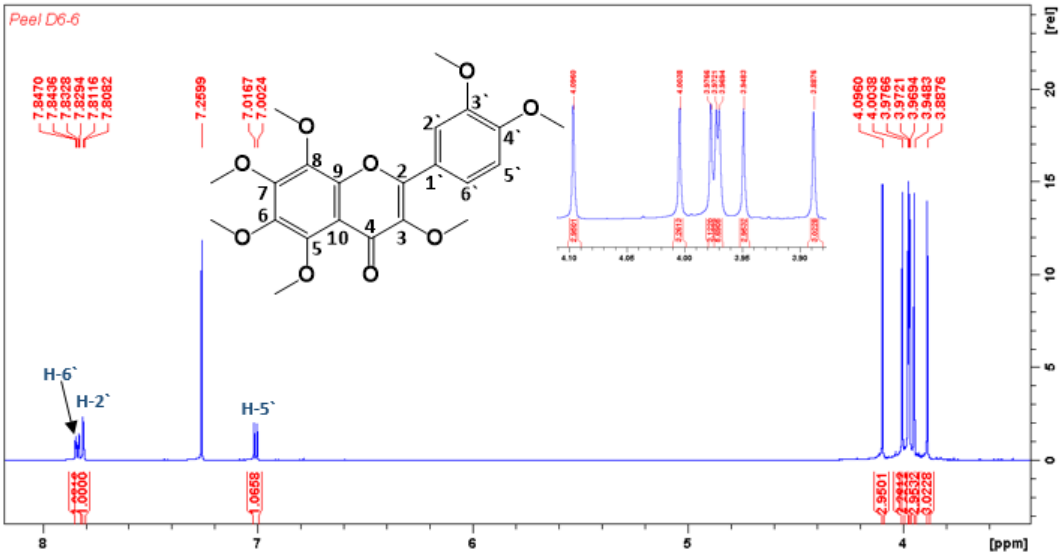


***Figure 3.89**: $^{1}H$ NMR (600 MHz, $CDCl_3$) spectrum of compound **110***

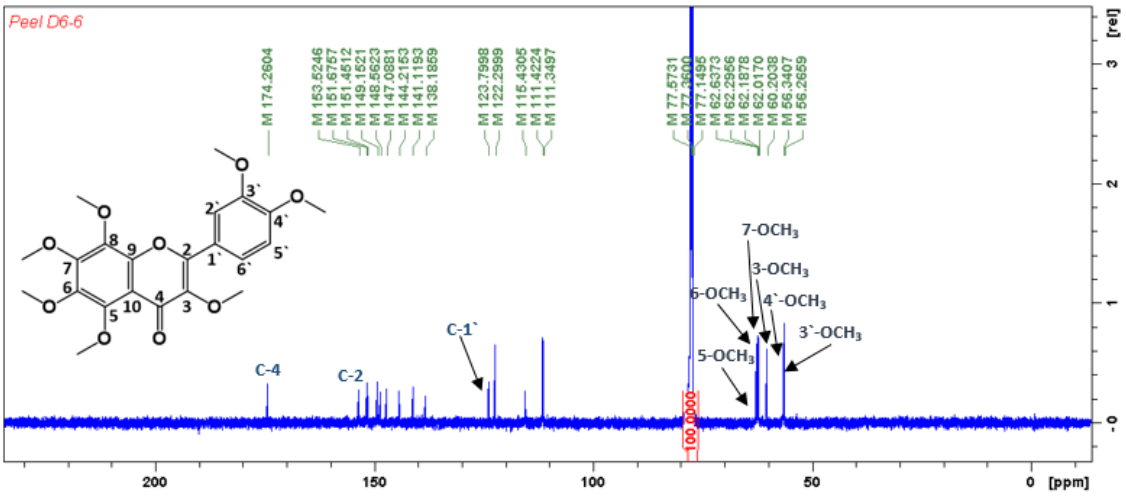


***Figure 3.90**: $^{13}C$ NMR (150 MHz, $CDCl_3$) spectrum of compound **110***

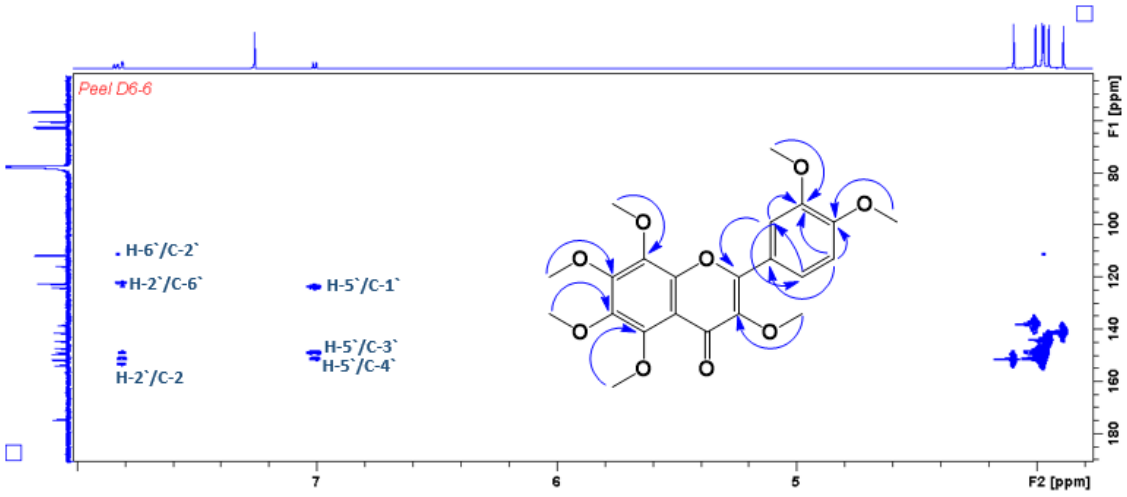


***Figure 3.91**: The HMBC correlation of compound **110***

### 3.2.9.2 Structure elucidation of nobiletin (57)

The compound **57** was isolated as a sharp white needle crystal. The HRESIMS (Figure 3.92) suggested the empirical formula as $C_{21}H_{22}O_8$ and in positive ion mode it showed $[M+H]^+$ peak at *m/z* 403.1388 (calculated 403.1392). The 1D and 2D NMR spectra of compound **57** were similar to compound **110**. The main differences were the presence of an additional olefinic proton at $\delta_H$ 6.64 (H-3) and six methoxyl signals instead of seven in the $^1H$ NMR spectrum (Figure 3.93, Table 3.23). The DEPTQ NMR spectrum (Figure 3.94, Table 3.23) exhibited a total of twenty-one carbons including one carbonyl group at $\delta_C$ 177.8, six methoxyls, four methines and eleven quaternary carbons. In the HMBC experiment (Figure 3.95), long rang correlations were observed from the olefinic proton at $\delta_H$ 6.64 (H-

3) to C-2 ($\delta_C$ 161.4, $^2J$), C-4 ($\delta_C$ 177.7, $^2J$), C-10 ($\delta_C$ 115.1, $^3J$) and C-1` ($\delta_C$ 124.2, $^3J$) which confirmed its position through C-3 in flavonoid molecule. Moreover, the methoxyl signals at $\delta_H$ 4.10 (3H), 4.02 (3H), 3.96 (H) and 3.97 (3H) obtained $^3J$ correlation to carbons $\delta_C$ 152.2 (C-7), 138.1 (C-8), 149.1 (C-3′) and 151.4 (C-4′) while the methoxyl at $\delta_H$ 3.95 (2X 3H) revealed long-range correlation to carbons $\delta_C$ 149.6 (C-5) and 144.4 (C-6). Thus, compound **57** identified as 5,6,7,8,3′,4′-hexamethoxyflavone or nobiletin. The spectroscopic data of compound **57** were in a good agreement with respective published data of nobiletin (Li *et al.*, 2018). Compound **57** has been reported to reduce skin and urinary inflammation (Murakami *et al.*, 2000; Li *et al.*, 2007) and it has an antidepressant effect (Wu *et al.*, 2015).

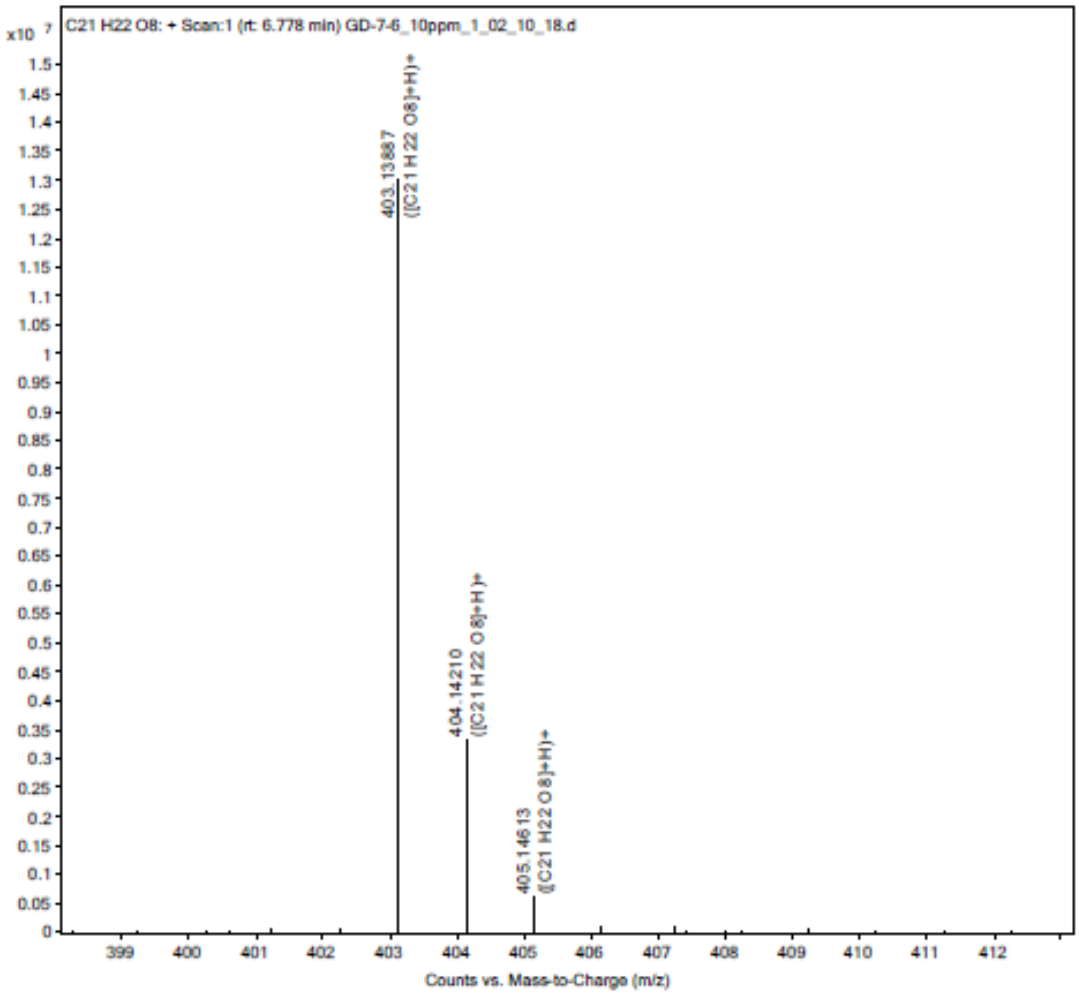


***Figure 3.92**: The HRESIMS spectrum of compound **57***

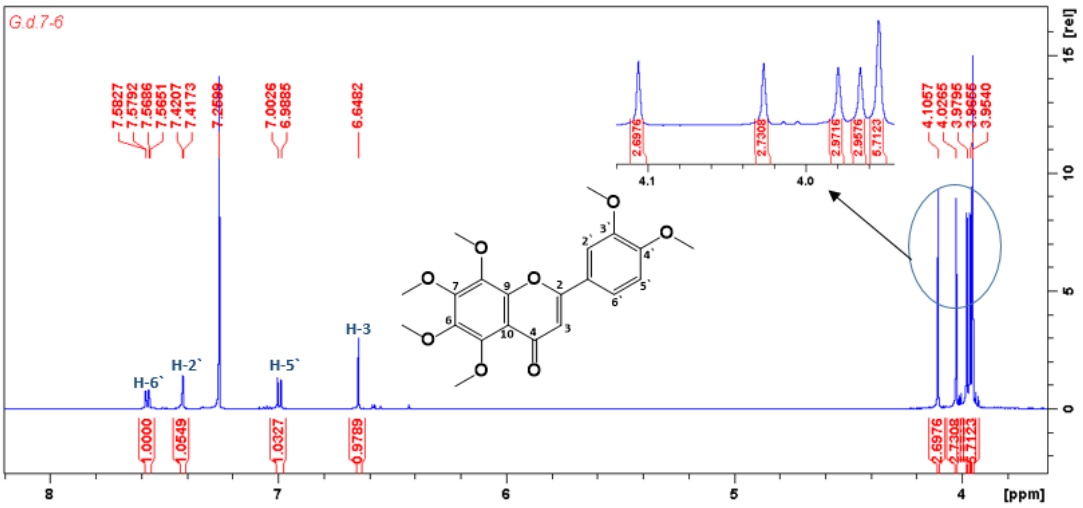


***Figure 3.93***: *$^{1}$H NMR (600 MHz, $CDCl_3$) spectrum of compound **57***

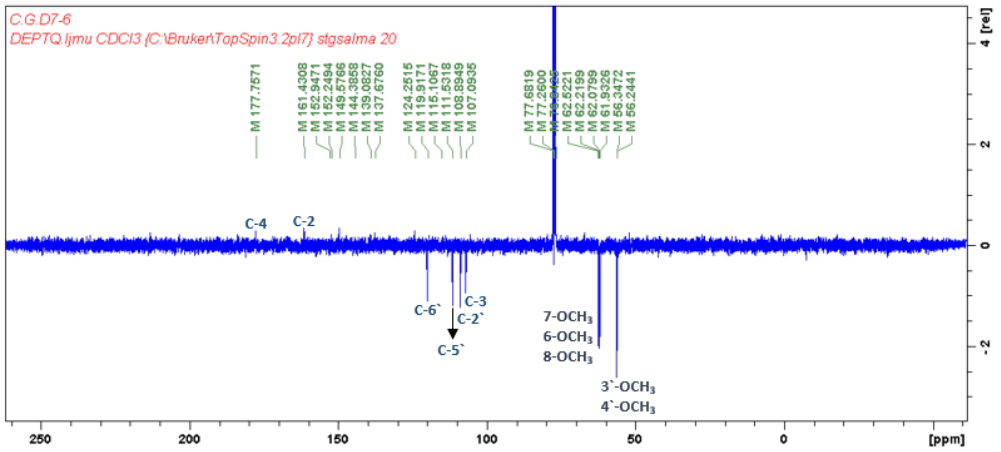


***Figure 3.94***: *$^{13}$C NMR (150 MHz, $CDCl_3$) spectrum of compound **57***

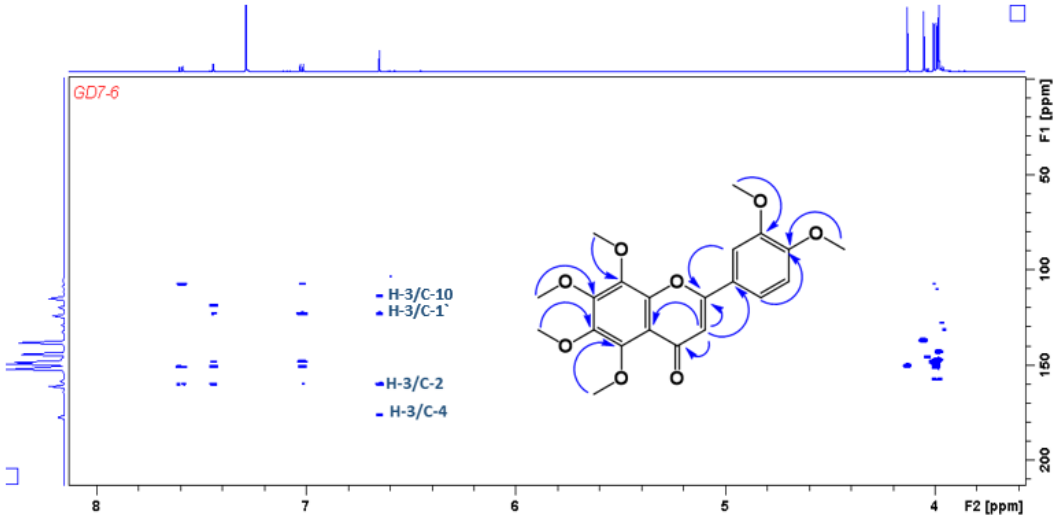


***Figure 3.95***: *The HMBC correlation compound **57***

### 3.2.9.3 Structure elucidation of sinensetin (111)

The compound **111** was isolated as a yellow powder. The HRESIMS (Figure 3.96) suggested the empirical formula as $C_{20}H_{20}O_7$ and in the positive ion mode it showed $[M+H]^+$ peak at *m/z* 373.1284 (calculated 373.1287). The 1D and 2D NMR spectra of compound **111** were very similar to compound **57**. The main differences were the presence of one extra aromatic methane proton at $\delta_H$ 6.60 and 6.79 and the presence of five methoxyl signals instead of six in the $^1$H NMR spectrum (Figure 3.97, Table 3.23). The $^{13}$C NMR spectrum (Figure 3.98, Table 3.23) revealed a total of twenty carbons five methoxyl groups, five methine carbons and ten quaternary carbons including a deshielded carbonyl at $\delta_C$ 177.70 (C-4). In the HMBC experiment (Figure 3.99), H-3 showed long range correlations to carbons at 161.7 (C-2, $^2J$), 177.7 (C-4, $^2J$), 115.1 (C-10, $^3J$), 124.2 (C-1′, $^3J$) while the aromatic methine proton at 6.79 (H-8) revealed $^3J$ correlations 115.1 (C-10), 140.79 (C-6) and 161.7 (C-2). These correlations confirmed the positions of two olefinic protons in the flavonoid molecule. Moreover, the methoxyl signals at $\delta_H$ 3.92 (3H), 3.96 (3H) and $\delta_C$ 3.98 (3H) obtained $^3J$ correlation to carbons 152.3 (C-5), 158.1 (C-7) and 149.7 (C-3′) while the methoxyl at 3.99 (2 x 3H) revealed long range correlations to carbons 140.8 (C-6) and 152.9 (C-4′). Thus, compound **111** identified as 5,6,7,3′,4′-pentamethoxyflavone. The data of compound **111** were in a good agreement with respective published data of sinensetin (Han *et al.*, 2010). Compound **111** has been reported to possess antioxidant (Akowuah *et al.*, 2004), antidepressant activities (Wu *et al.*, 2015) and worked as an angiogenesis agent (Lam *et al*., 2012).

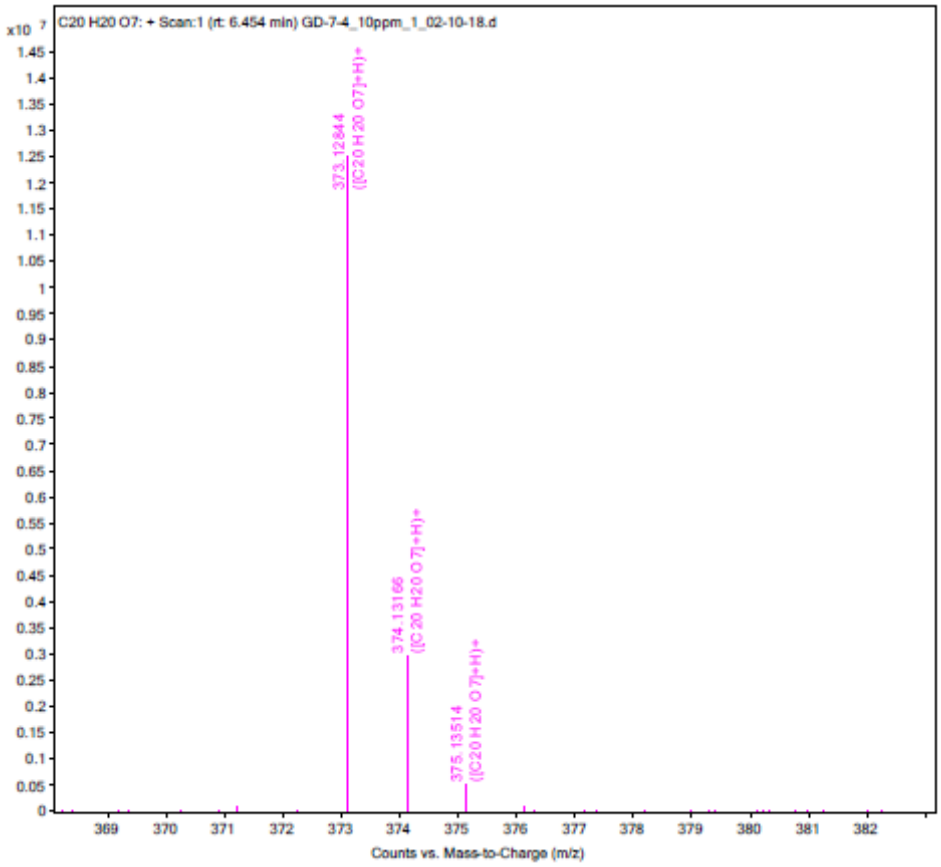


***Figure 3.96**: The HRESIMS of compound **111***

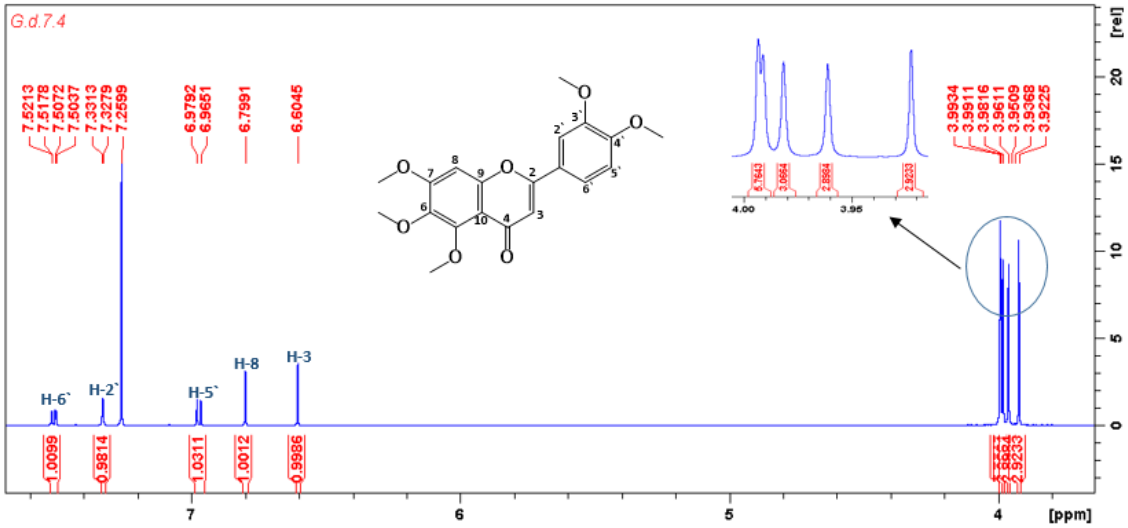


***Figure 3.97**: $^{1}H$ NMR (600 MHz, $CDCl_3$) of compound **111***

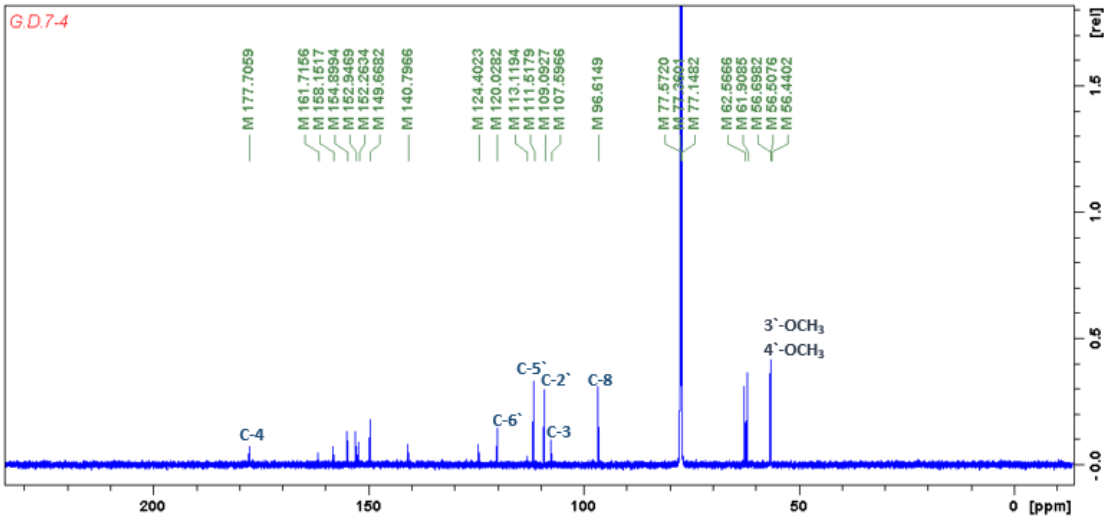


***Figure 3.98**: $^{13}C$ NMR (150 MHz, $CDCl_3$) of compound **111***

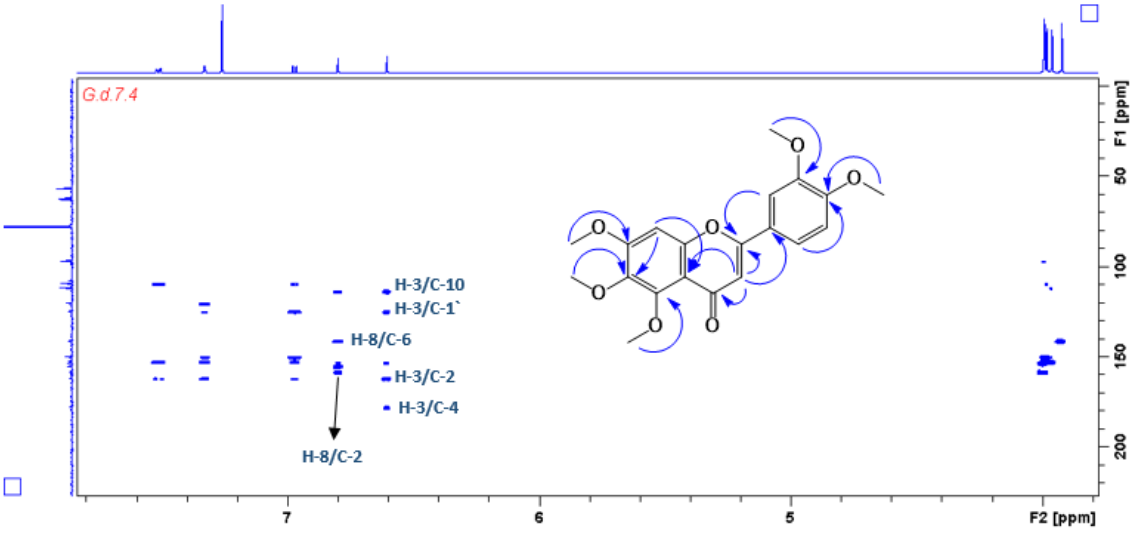


***Figure 3.99**: The HMBC correlation compound **111***

### 3.2.9.4 Structure elucidation of 6, 7, 8, 3′,4′-pentamethoxyflavone (112)

The compound **112** was isolated as deep yellow crystals. The HRESIMS (Figure 3.100) suggested the empirical formula as $C_{20}H_{20}O_7$ and in the positive ion mode it showed $[M+H]^+$ peak at *m/z* 373.1317 (calculated 373.1287). The $^1H$ NMR spectrum (Figure 3.101, Table 3.23), $^{13}C$ NMR spectrum (Figure 3.102, Table 3.23) and 2D experiments of compound **112** were identical to compound **111**. The only difference was the position of an aromatic methine at $\delta_H$ 6.80 in the $^1H$ NMR spectrum. In the HMBC experiment (Figure 3.103), the methoxyl signals at $\delta_H$ 3.92 (3H), 3.96 (3H) and 3.98 (3H) obtained $^3J$ correlation to carbons $\delta_C$ 140.7 (C-8), 153.0 (C-3′) and 149.7 (C-4′) while the methoxyl at $\delta_H$ 3.99 (2X

3H) revealed long range correlations to carbons at $\delta_C$ 125.2 (C-6) and 158.0 (C-7). Moreover, the aromatic proton at $\delta_H$ 6.80 showed long range correlations to $\delta_C$ 177.6 (C-4, $^3J$), 158.0 (C-7, $^3J$), 143.0 (C-9, $^3J$) and 113.2 (C-10, $^2J$) and confirmed its identity as H-5 in a flavonoid molecule. Thus, compound **112** was identified as pentamethoxy flavone. The data of compound **112** were in good agreement with respective published data for 6,7,8,3′,4′-pentamethoxyflavone (Han *et al.*, 2010).

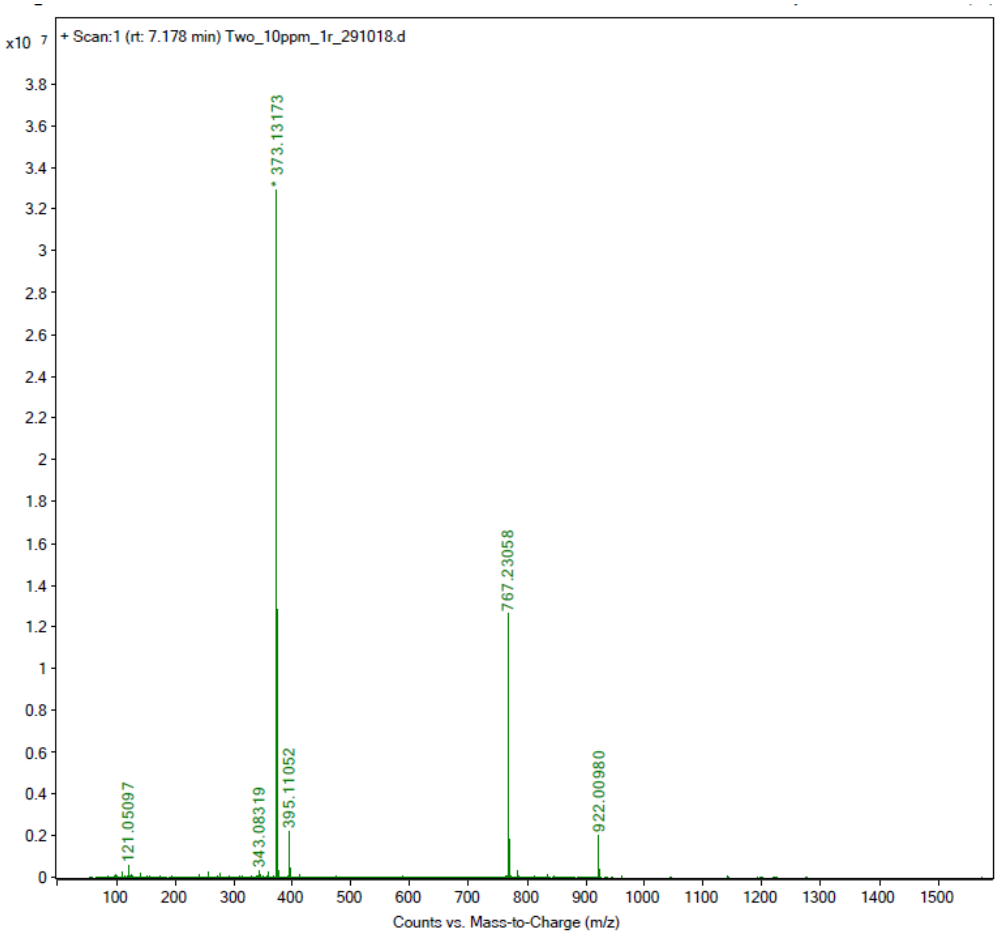


***Figure 3.100**: The HRESIMS spectrum of compound **112***

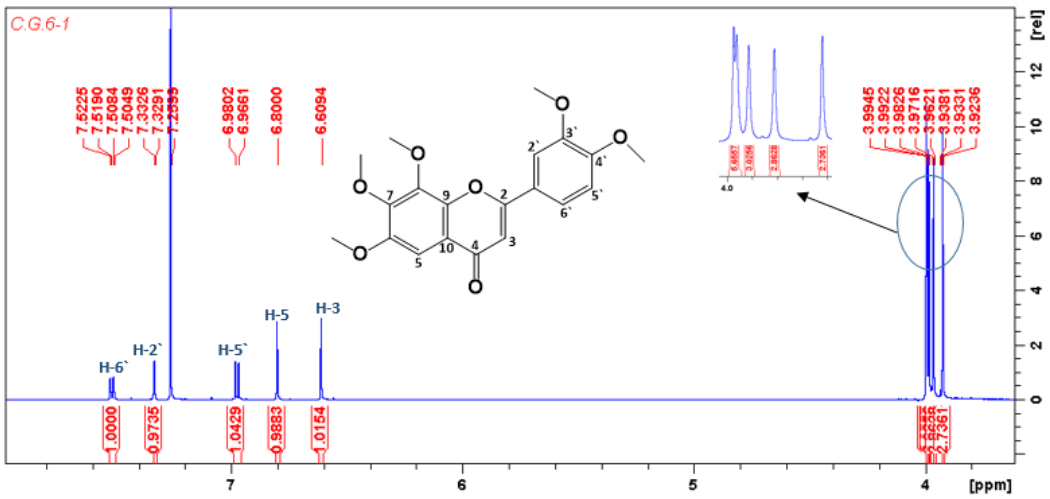


***Figure 3.101***: *$^{1}$H NMR (600 MHz, $CDCl_3$) spectrum of compound* ***112***

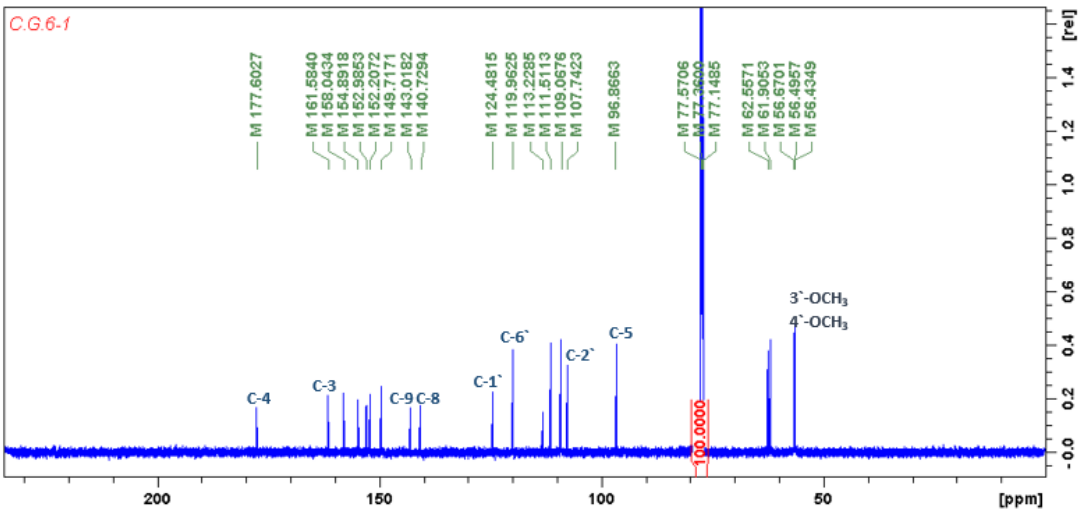


***Figure 3.102***: *$^{13}$C NMR (150 MHz, $CDCl_3$) spectrum of compound* ***112***

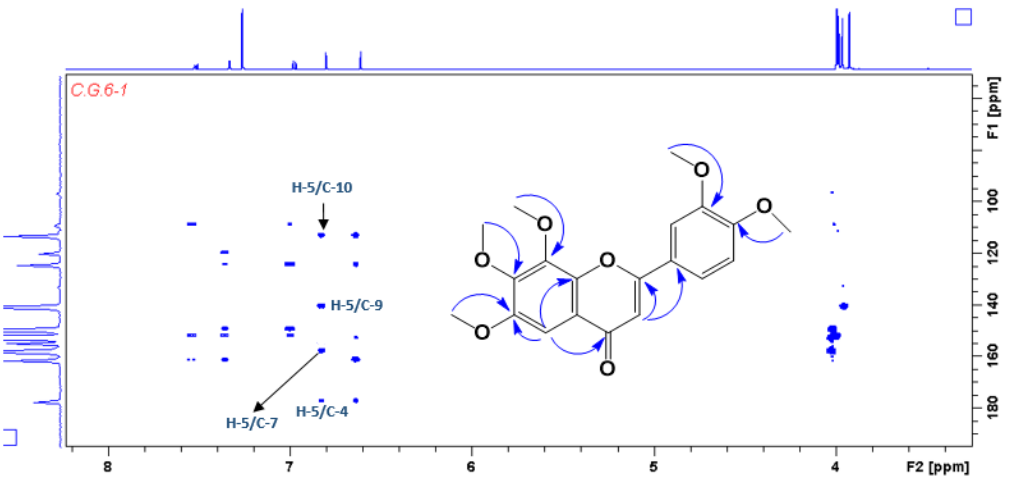


***Figure 3.103***: *The HMBC correlation of compound* ***112***

**Table 3.23**: $^{1}$H NMR (600 MHz) and $^{13}$C NMR data of compounds **57, 110, 111** and **112**

| Position | Chemical Shift $\delta_H$ (ppm), *J* in Hz | | | | Chemical Shift δc (ppm), *J* in Hz | | | |
|---|---|---|---|---|---|---|---|---|
| | **110** | **57** | **111** | **112** | **110** | **57** | **111** | **112** |
| 2 | - | - | - | - | 153.5 | 161.4 | 161.7 | 161.6 |
| 3 | - | 6.64 s | 6.60 s | 6.60 s | 141.1 | 107.1 | 107.6 | 107.7 |
| 4 | - | - | - | - | 174.3 | 177.7 | 177.7 | 177.6 |
| 5 | - | - | - | 6.97 s | 148.6 | 149.6 | 152.3 | 96.9 |
| 6 | - | - | - | - | 144.2 | 144.4 | 140.8 | 125.2 |
| 7 | - | - | - | - | 151.7 | 152.2 | 158.1 | 158.0 |
| 8 | - | - | 6.97,s | - | 138,6 | 138.1 | 96.6 | 140.7 |
| 9 | - | - | - | - | 147.1 | 148.7 | 154.9 | 143.0 |
| 10 | - | - | - | - | 115.4 | 115.1 | 113.1 | 113.2 |
| 1′ | - | - | - | - | 123.8 | 124.2 | 124.4 | 124.5 |
| 2′ | 7.81 *d* (2.04) | 7.41 *d* (2.1) | 7.33 *d* (2.1) | 7.33 *d* (2.1) | 111.3 | 108.9 | 109.1 | 109.1 |
| 3′ | - | - | - | - | 149.1 | 149.6 | 149.7 | 153.0 |
| 4′ | - | - | - | - | 151.4 | 152.9 | 152.9 | 149.7 |
| 5′ | 7.01 *d* (8.52) | 7.00 *d* (8.52) | 6.96 *d* (8.4) | 6.96 *d* (8.4) | 111.4 | 111.5 | 111.5 | 111.5 |
| 6′ | 7.83 *dd* (2.04, 8.52) | 7.57 *dd* (8.52, 2.1) | 7.51 *dd* (8.4, 2.1) | 7.51*dd* (8.4, 2.1) | 122.3 | 119.9 | 120.0 | 120.0 |
| 3-$OCH_3$ | 3.88 s | - | - | - | 60.2 | - | - | - |
| 5-$OCH_3$ | 3.97 s | 3.95 s | 3.92 s | - | 62.6 | 62.5 | 61.9 | - |
| 6-$OCH_3$ | 3.94 s | 3.95 s | 3.99 s | 3.99 s | 62.2 | 62.2 | 62.6 | 62.5 |
| 7- $OCH_3$ | 4.09 s | 4.10 s | 3.96 s | 3.99 s | 62.0 | 61.9 | 56.5 | 61.9 |
| 8-$OCH_3$ | 4.00 s | 4.02 s | - | 3.92 s | 62.3 | 62.1 | - | 56.7 |
| 3′-$OCH_3$ | 3.97 s | 3.96 s | 3.98 s | 3.96 s | 56.34 | 56.3 | 56.4 | 56.5 |
| 4′- 3 | 3.96 s | 3.97 s | 3.99 s | 3.98 s | 56.26 | 56.2 | 56.7 | 56.4 |

### 3.2.9.5 Structure elucidation of demethylnobiletin (113)

The compound **113** was isolated as a dark yellow amorphous solid. The HRESIMS (Figure 3.104) suggested the empirical formula as $C_{20}H_{20}O_8$ and in the positive ion mode it showed $[M+H]^+$ peak at *m/z* 389.1230 (calculate 389.1236). The $^1$H NMR spectrum (Figure 3.105, Table 3.24) exhibited three aromatic protons as ABX pattern resonating at $\delta_H$ 7.00 (d, *J*=8.46 Hz) , 7.59 (dd, *J*=2.1, 8.46 Hz) and 7.43 (d, *J*=2.1 Hz), aromatic methine at $\delta_H$ 6.60, hydrogen bonded hydroxyl signal at $\delta_H$ 12.75 and five methoxy groups at $\delta_H$ 4.11 (3H), 3.95 (3H), 3.98 (3H), 3.97 (3H) and 3.98 (3H). The $^{13}$C NMR spectrum (Figure 3.106, Table 3.24) showed a total of twenty carbons including a carbonyl at $\delta_C$ 183.3 (C-4), five methoxyl carbons, four aromatic methines and the remaining as quaternary carbons. In the HMBC experiment, $^3J$ correlations were observed from methoxyl at $\delta_H$ 4.11, 3.95, 3.98, 3.97 and 3.98 to the oxygenated quaternary carbons at $\delta_C$ 137.2 (C-6), 153.0 (C-7), 131.2 (C-8), 149.7 (C-3′) and 152.1 (C-4′) respectively, while H-3 showed long range correlations to $\delta_C$ 164.7 (C-2, $^2J$), 183.3 (C-4, $^2J$ ), 108.2 (C-10, $^3J$) and 124.1 (C-1′). Moreover, the OH group at $\delta_H$ 12.75 exhibited along range correlations to carbons at $\delta_C$ 153.6 (C-5; by $^2J$), 137.2 (C-6; by $^3J$) and 108.2 (C-10; by $^3J$) and these correlations confirmed the position of the hydroxyl group through C-5. Thus, compound **113** identified as 5-hydroxy-3′,4′,6,7,8-pentamethoxyflavone. The spectroscopic data of compound **113** were in good agreement with respective published data of demethylnobiletin (Wang *et al.,* 2005). According to Bas *et al.* (2007), compound **113** might have an effect on cell infiltration and induce e of the anti-inflammatory cytokine, interleukin-10. Moreover, demethylnobiletin (**113**) was reported to reduce the apoptosis of T cells, which is a type of lymphocyte (a subtype of white blood cell).

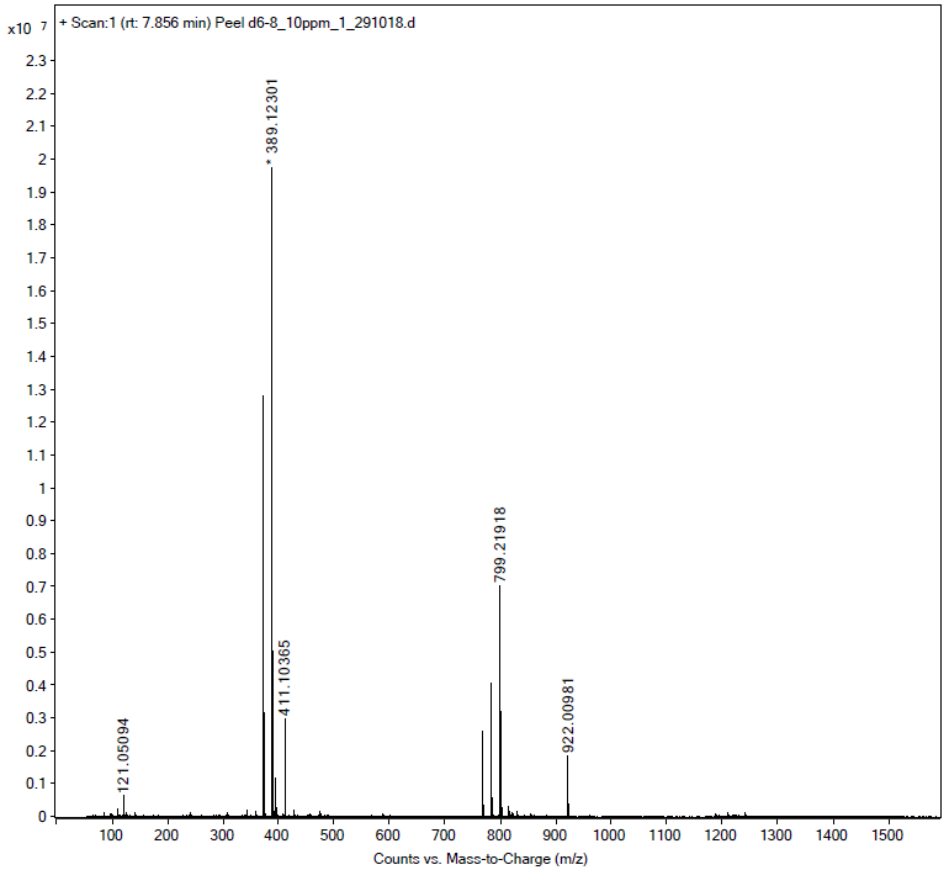


***Figure 3.104**: The HRESIMS spectrum of compound **113***

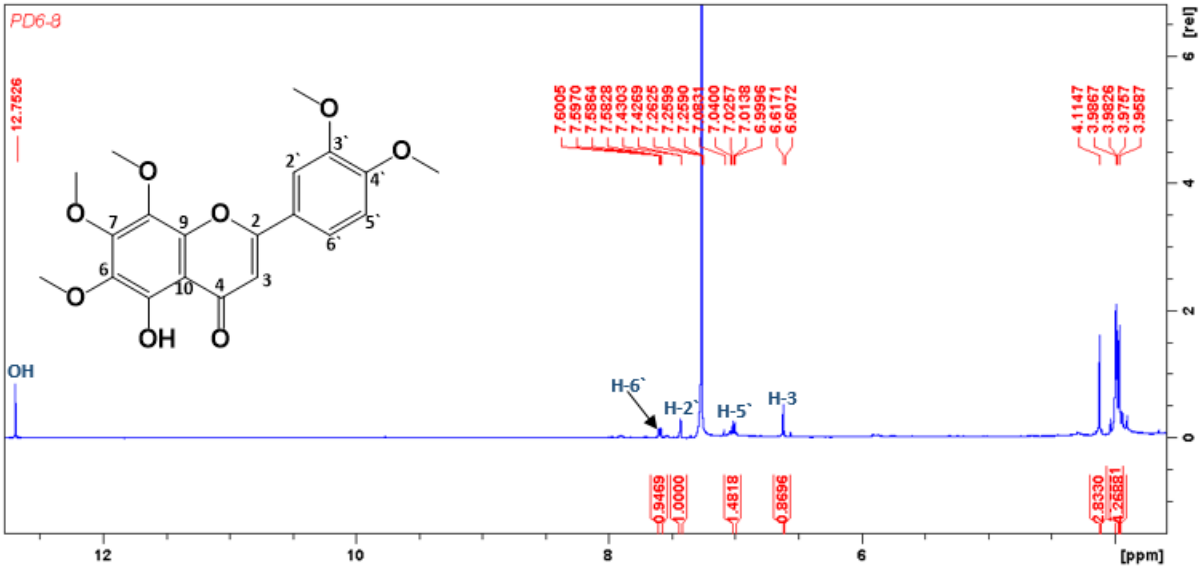


***Figure 3.105**: $^{1}H$ NMR (600 MHz, $CDCl_3$) spectrum of compound **113***

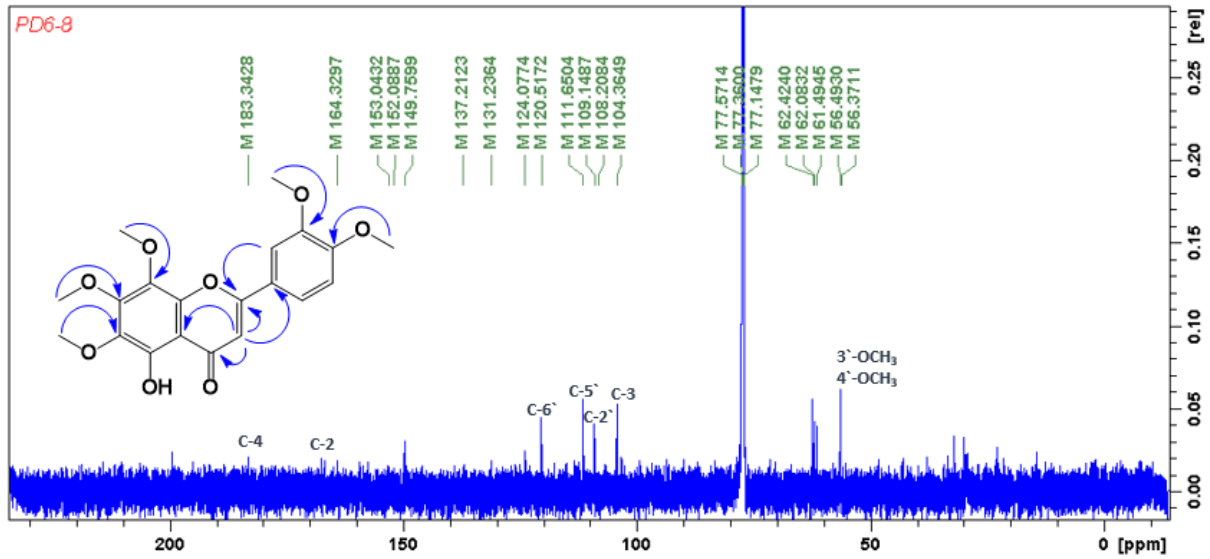


***Figure 3.106**: $^{13}C$ NMR (150 MHz, $CDCl_3$) spectrum of compound **113***

### 3.2.9.6 Structure elucidation of 5-desmethylsinensetin (114)

The compound **114** was isolated as a dark yellow amorphous solid. The HRESIMS (Figure 3.107) suggested the empirical formula as $C_{19}H_{18}O_7$ and in the positive ion mode it showed $[M+H]^+$ peak at *m/z* 359.1141 (calculated 359.1130). The 1D and 2D NMR spectra of compound **114** were very similar to compound **113**. The main differences were the presence of an additional olefinic proton at $\delta_H$ 6.55 (H-8) and four methoxyl signals instead of five in the $^1H$ NMR spectrum (Figure 3.108, Table 3.24). The $^{13}C$ NMR spectrum (Figure 3.109, Table 3.24) revealed a total of nineteen carbons including carbonyl at $\delta_C$183.0 (C-4), four methoxyl carbons, five aromatic methines and the remaining as quaternary carbons. The HMBC experiment (Figure 3.110) showed long range correlations from H-8 to quaternary carbons at $\delta_C$ 133.6 (C-6, $^3J$), 159.1 (C-7, $^2J$) and, 106.5 (C-10, $^3J$) and $^3J$ correlations were observed from the methoxyl at $\delta_H$ 3.98 (3H), 3.93 (3H), 3.97 (3H) , 3.99 and 3.98 to the oxygenated quaternary carbons at $\delta_C$ 159.1 (C-7), 91.0 (C-8), 152.7 (C-4′) and 149.7 (C-3′), respectively. Thus, compound **114** was identified as 5-hydroxy-3′,4′,6,7-tetramethoxyflavone. The data of compound **114** were in good agreement with respective published data of 5-desmethylsinensetin (Alarif *et al.*, 2013). Compound **114** is documented

as an antiphrastic agent because it inhibited *Trypanosoma cruzi* at 0.4 mg/mL concentration (Beer *et al.*, 2016) and revealed significant activity against (HL-60) leukaemia cell proliferation with induction of apoptosis (Owis, 2019).

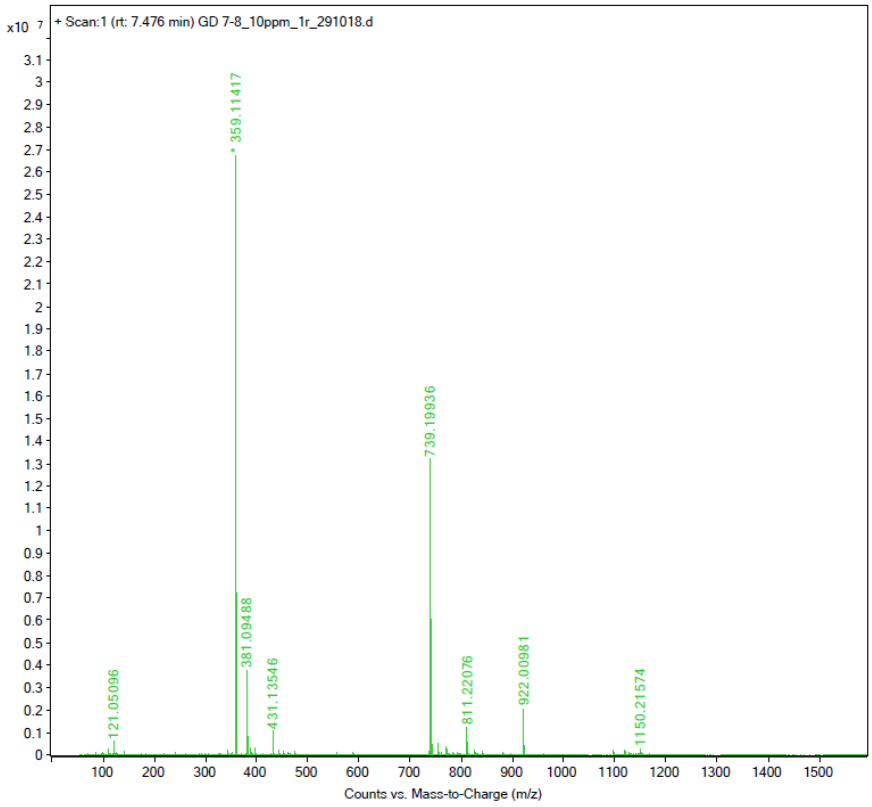


***Figure 3.107**: The HRESIMS spectrum of compound **114***

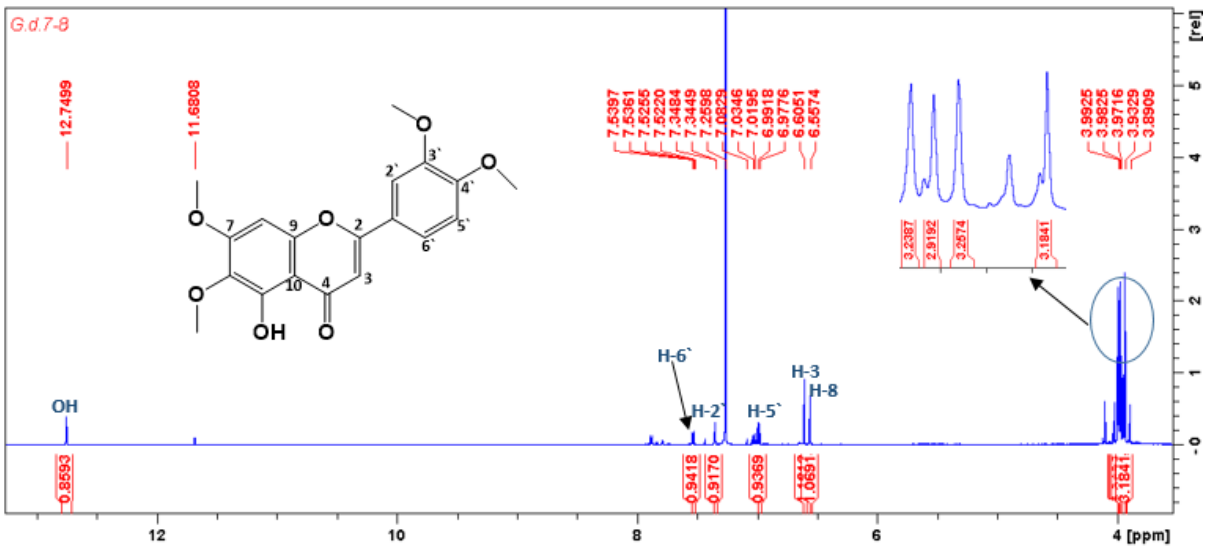


***Figure 3.108**: $^{1}H$ NMR (600 MHz, $CDCl_3$) spectrum of compound **114***

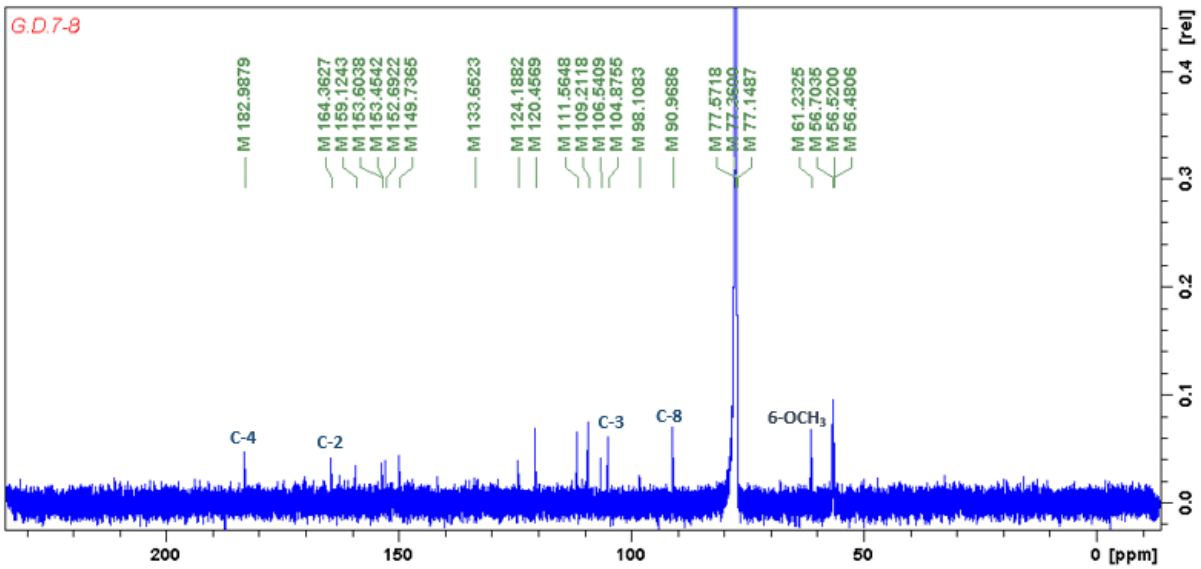


***Figure 3.109:*** *$^{13}C$ NMR (150 MHz, $CDCl_3$) spectrum of compound* ***114***

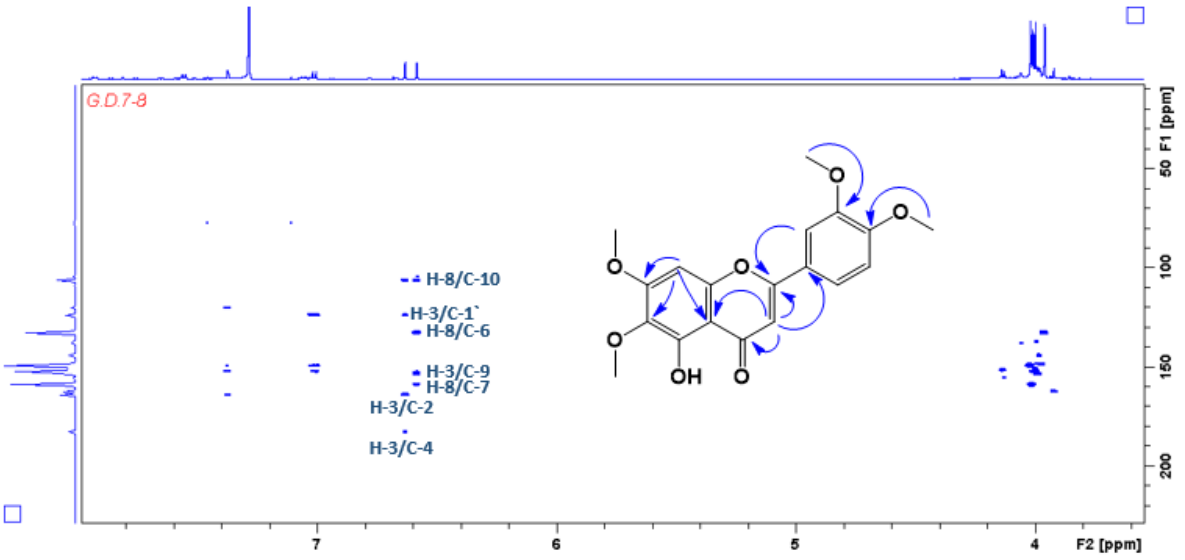


***Figure 3.110****: The HMBC correlation compound* ***114***

### 3.2.9.7 Structure elucidation of cirsilineol (115)

The compound **115** was isolated as a dark yellow amorphous solid. The HRESIMS (Figure 3.111) suggested the empirical formula as $C_{18}H_{16}O_7$ and in the positive ion mode it showed $[M+H]^+$ peak at *m/z* 345.0974 (calculated 345.0974). The 1D and 2D NMR spectra of compound **115** were very similar to compound **114**. The main differences were the presence of one extra hydroxyl group at $\delta_H$ 5.99 and the presence of three methoxyl signals instead of four in the $^1H$ NMR spectrum (Figure 3.112, Table 3.24). The $^{13}C$ NMR spectrum

(Figure 3.113, Table 3.24) revealed a total of eighteen carbons including deshelled carbonyl at $\delta_C$ 182.9 (C-4), three methoxyl groups, five methine carbons and the remains were quaternary carbons. The HMBC (Figure 3.114) showed the long range correlation from OH ($\delta_H$ 5.99) to carbons at $\delta_C$ 147.2 (C-3′, $^3J$), 149.6 (C-4′, $^2J$) and 115.4 (C-5`, $^3J$) while the OH group at $\delta_H$ 12.75 showed a correlation to carbons at $\delta_C$ 153.6 (C-5, $^2J$), 133.6 (C-6, $^3J$), 106.5 (C-10, $^3J$) these correlations confirmed the position of hydroxyl groups in the molecule. Moreover, $^3J$ correlations were observed from methoxyl at $\delta_H$ 3.93 (3H), 3.97 (3H) and 4.01 (3H) to the oxygenated quaternary carbons at $\delta_C$ 133.1 (C-6), 159.1 (C-7) and 147.2 (C-3′) respectively. Thus, compound **115** identified as 4′,5-dihydroxy-3′,6,7-trimethoxyflavone or cirsilineol. The spectroscopic data of compound **115** were in good agreement with respective published data for cirsilineol (Hammoud *et al.*, 2012). Compound **115** is reported to have anticancer activity against human ovarian cancer (Caov-3, Skov-3) and prostate cancer cell PC3 (Sheng *et al.*, 2008).

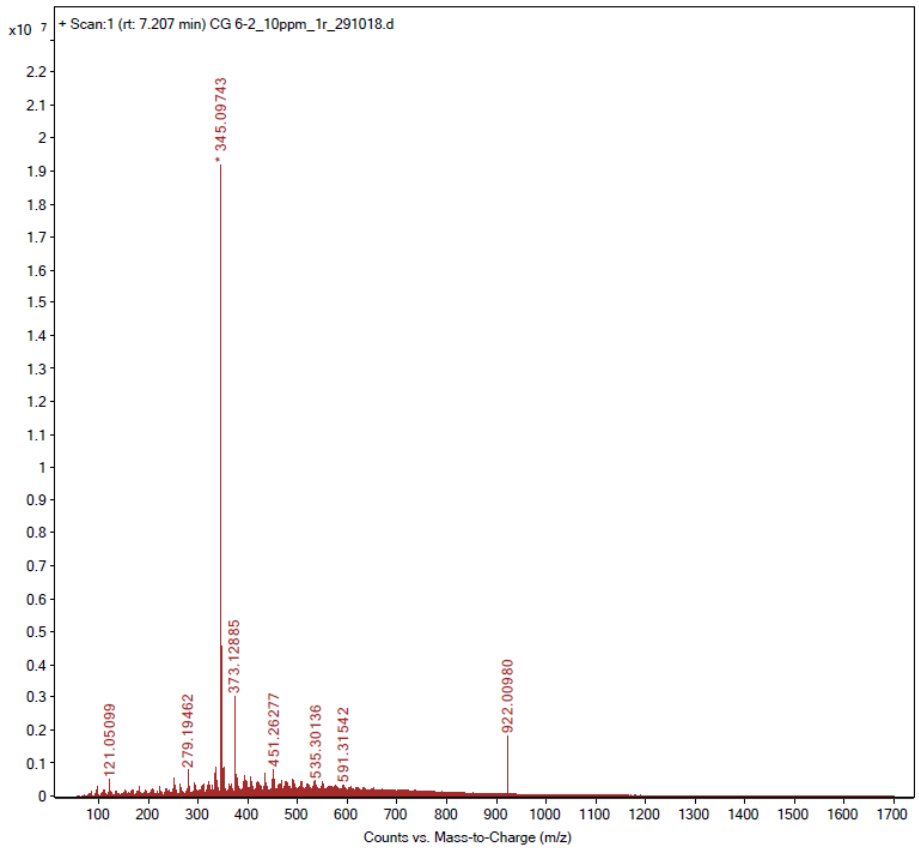


***Figure 3.111**: The HRESIMS spectrum of compound **115***

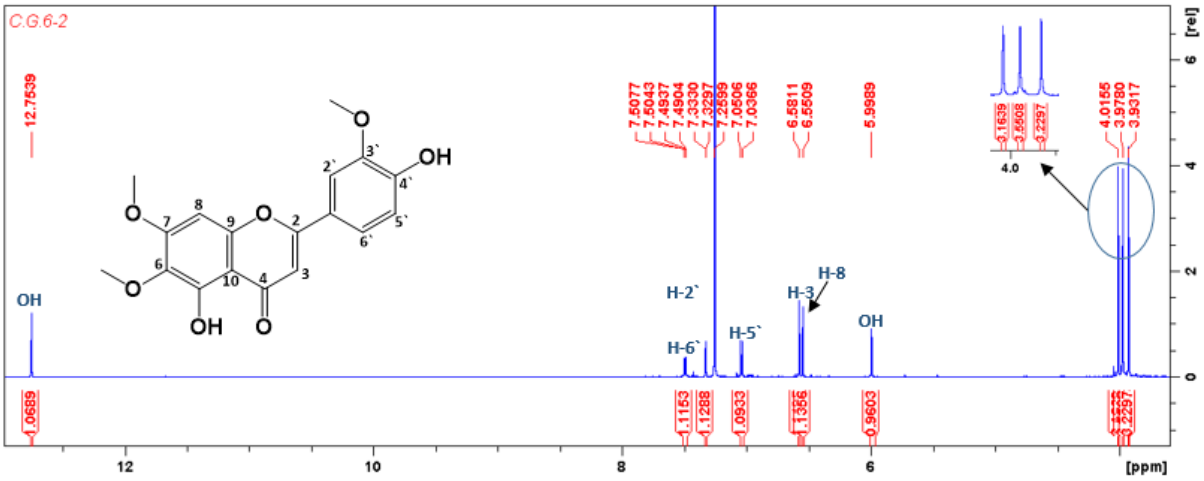


***Figure 3.112***: *$^{1}$H NMR (600 MHz, $CDCl_3$) spectrum of compound* ***115***

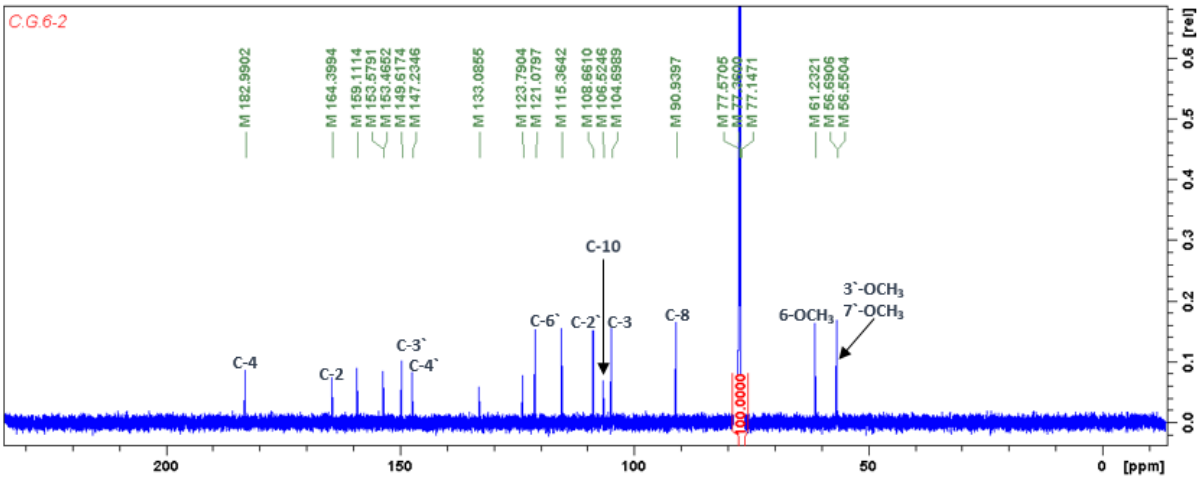


***Figure 3.113***: *$^{13}$C NMR (150 MHz, $CDCl_3$) spectrum of compound* ***115***

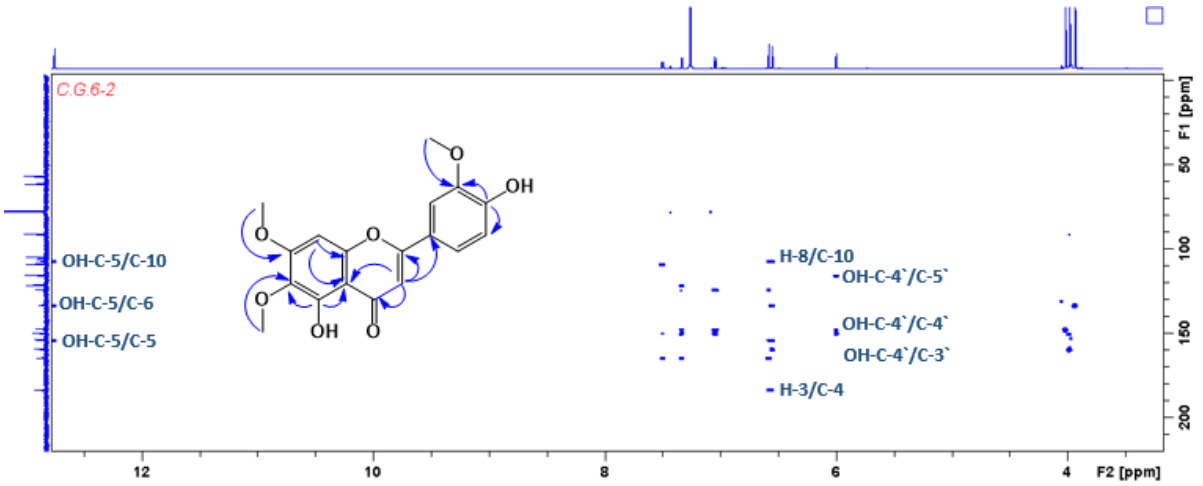


***Figure 3.114***: *The HMBC correlation compound* ***115***

**Table 3.24**: $^{1}$H NMR (600 MHz) and $^{13}$C NMR data of compounds **113-115**

| **position** | **Chemical Shift $\delta_H$ (ppm), *J* in Hz** | | | **Chemical Shift $\delta_C$ (ppm), *J* in Hz** | | |
|---|---|---|---|---|---|---|
| | **113** | **114** | **115** | **113** | **114** | **115** |
| 2 | - | - | - | 164.7 | 164.4 | 164.4 |
| 3 | 6.61 s | 6.60 s | 6.58 s | 104.4 | 104.9 | 104.7 |
| 4 | - | - | - | 183.3 | 183.0 | 183.0 |
| 5 | - | - | - | 149.9 | 153.6 | 153.6 |
| 6 | - | - | - | 137.2 | 133.6 | 133.1 |
| 7 | - | - | - | 153.0 | 159.1 | 159.1 |
| 8 | - | 6.55 s | 6.55 s | 131.2 | 91.0 | 91.0 |
| 9 | - | - | - | 146.3 | 153.4 | 153.5 |
| 10 | - | - | - | 108.2 | 106.5 | 106.5 |
| 1′ | - | - | - | 124.1 | 124.2 | 123.8 |
| 2′ | 7.43 *d* (2.1) | 7.34 *d* (2.04) | 7.33 *d* (2.1) | 109.14 | 109.2 | 108.7 |
| 3′ | - | - | - | 149.75 | 149.7 | 147.2 |
| 4′ | - | - | - | 152.08 | 152.7 | 149.6 |
| 5′ | 7.00 *d* (8.46) | 6.98 *d* (8.04) | 7.04 *d* (8.34) | 111.65 | 111.6 | 115.4 |
| 6′ | 7.59 *dd* (2.1, 8.46) | 7.53 *dd* (8.04, 2.04) | 7.50 *d* (8.34, 2.1) | 120.51 | 120.4 | 121.1 |
| 6-$OCH_3$ | 4.11 s | - | 3.93 s | 62.1 | - | 61.2 |
| 7-$OCH_3$ | 3.95 s | 3.98 s | 3.97 s | 61.4 | 56.7 | 56.7 |
| 8-$OCH_3$ | 3.98 s | 3.93 s | - | 62.4 | 61.2 | - |
| 3′-$OCH_3$ | 3.97 s | 3.99 s | - | 56.5 | 56.48 | 56.5 |
| 4′-$OCH_3$ | 3.98 s | 3.97 s | - | 56.4 | 56.5 | - |
| 5-OH | - | - | 12.77 s | - | - | - |
| 4'-OH | - | - | 5.99 s | - | - | - |

### 3.2.9.8 Structure elucidation of tangeritin (116)

The compound **116** was isolated as yellow amorphous powder. The HRESIMS (Figure 3.115) suggested the empirical formula as $C_{20}H_{20}O_7$ and in the positive ion mode it showed $[M+H]^+$ peak at *m/z* 373.1286 (calculated 373.1287). The $^{1}$H NMR spectrum (Figure 3.116, Table 3.25) exhibited three sets of aromatic protons at $\delta_H$ 7.88 (2H, d, *J*=8.82, H-2′, 6′), 7.03 (2H, d, *J*=8.82, H-3′, 5′), singlet at $\delta_H$ 6.60 (H-3) and methoxy groups at $\delta_H$ 3.89 (3H), 3.95 (2X 3H), 4.02 (3H) and 4.10 (3H). The $^{13}$C NMR spectrum (Figure 3.117, Table 3.25) showed a total of twenty carbons including a carbonyl group at $\delta_C$ 177.7, five

methoxyls groups, five methines and nine quaternary carbons. The HMBC experiment showed $^{3}J$ correlations from the methoxyl at $\delta_H$ 3.89 (3H), 4.02 (3H) and 4.10 (3H) to the oxygenated quaternary carbons at $\delta_C$ 162.6 (C-4′), 138.3 (C-8) and 151.7 (C-5) while the signal at $\delta_H$ 3.95 revealed correlations to carbons at $\delta_C$ 144.4 (C-6) and 148.8 (C-7). Moreover, a $^{3}J$ correlations were observed from H-2′ and H-6` to carbons at $\delta_C$ 161.5 (C-2) and 162.6 (C-4′) additionally, long range correlations detected from H-3′ and H-5′ to carbons at $\delta_C$ 124.2 (C-1′). Thus, compound **116** identified as 5,6,7,8,4′-pentamethoxyflavone or tangeritin. The data of compound **116** were in good agreement with respective published data for tangeritin (Hamdan *et al.*, 2011). Antioxidant and anti-inflammatory effect of compound **116** have been reported (Chen *et al.*, 2017). Tangeritin was showed a significant reduction in Parkinson's disease symptoms (Fatima *et al*., 2017).

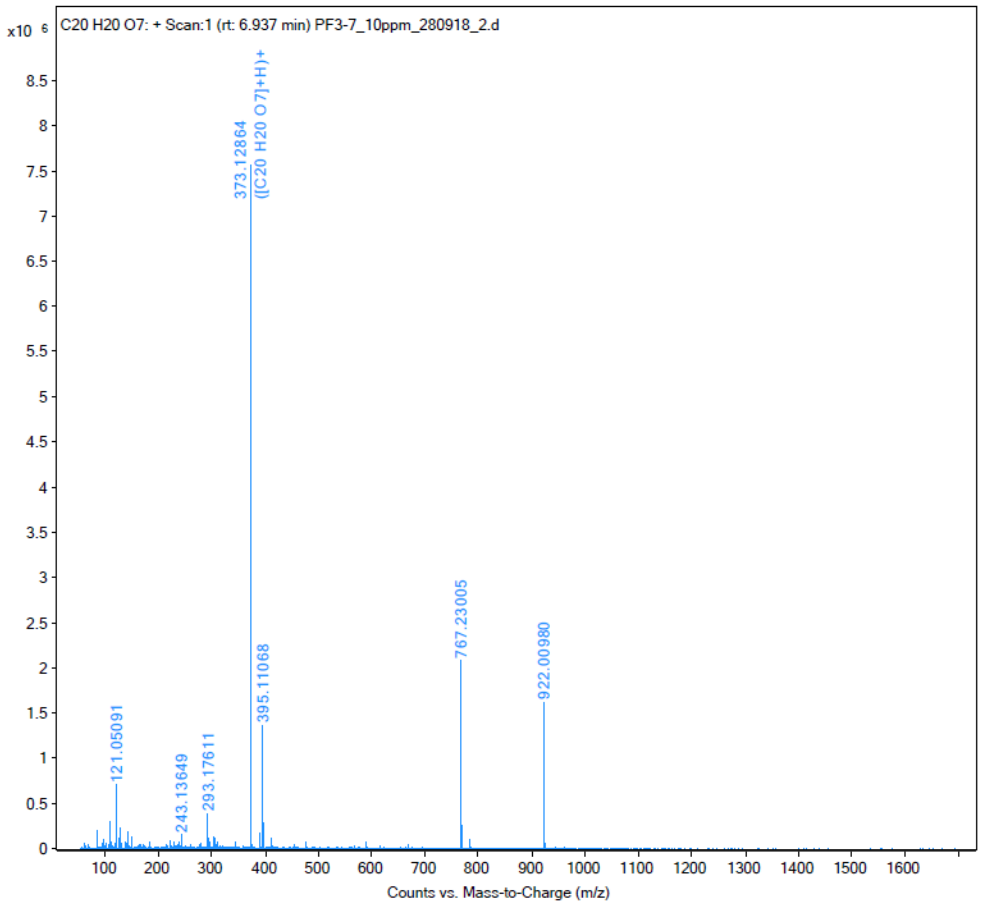


***Figure 3.115**: The HRESIMS spectrum of compound **116***

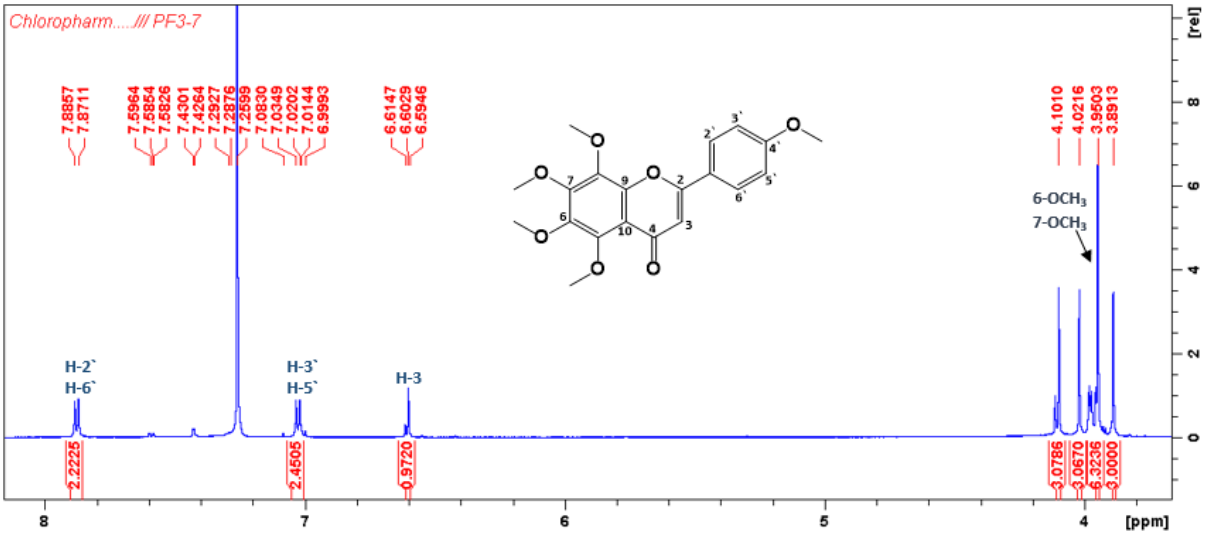


***Figure 3.116**: [1]H NMR (600 MHz, $CDCl_3$) spectrum of compound **116***

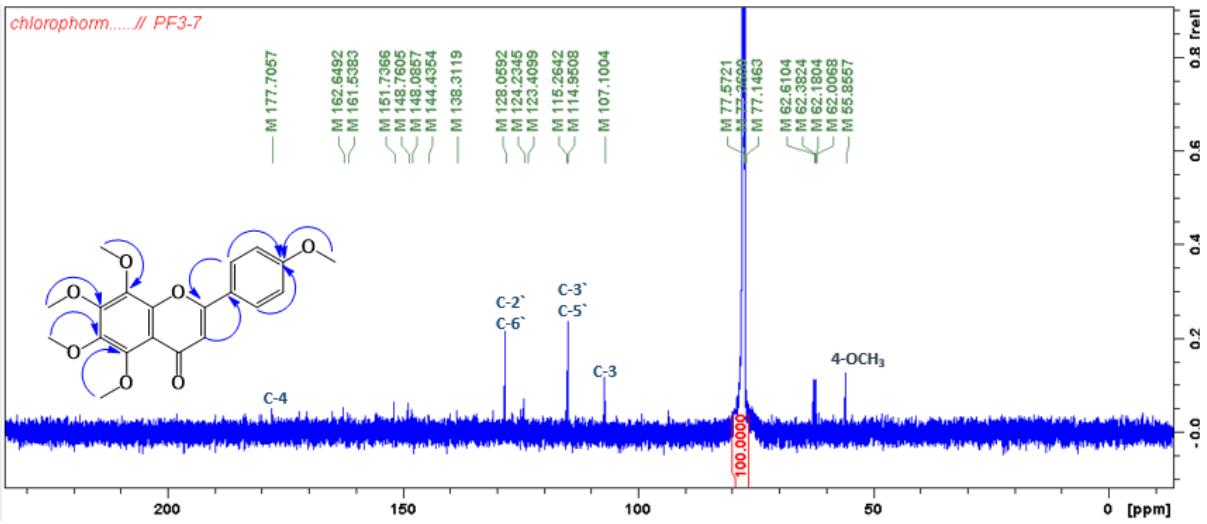


***Figure 3.117**: [13]C NMR (150 MHz, $CDCl_3$) spectrum of compound **116***

### 3.2.9.9 Structure elucidation of tetramethylscutellarein (117)

The compound **117** was isolated as a yellow powder. The HRESIMS (Figure 3.118) suggested the empirical formula as $C_{19}H_{18}O_6$ and in the positive ion mode it showed $[M+H]^+$ peak at *m/z* 343.1191 (calculated 343.1181). The 1D and 2D NMR spectra of compound **117** were very similar to compound **116.** The only differences were the presence of an additional olefinic proton at $\delta_H$ 6.79 (H-8) and four methoxyl signals instead of five in the $^1$H NMR spectrum (Figure 3.119, Table 3.25). The $^{13}$C NMR spectrum (Figure 3.120, Table 3.25) revealed a total of eighteen carbons including a carbonyl at $\delta_C$ 177.7, four methoxyl groups,

six methines and the others are quaternary carbons. In the HMBC experiment (Figure 3.121), long-range correlations from the singlet proton at $\delta_H$ 6.59 (H-8) were revealed to carbons resonating at $\delta_C$ 161.6 (C-2), 177.7 (C-4), 140.7 (C-6), 154.9 (C-9) and 113.1 (C-10). Moreover, $^3J$ correlations were observed from methoxyl at $\delta_H$ 3.98 (3H), 3.91 (3H), 3.97 (3H) and 3.88 (3H) to the oxygenated quaternary carbons at $\delta_C$ 152.9 (C-5), 140.7 (C-6), 158.0 (C-7) and 162.5 (C-4′) respectively. Thus, compound **117** was identified as 5,6,7,4′-tetramethoxyflavone. The data of compound **117** were in good agreement with respective published data of tetramethylscutellarein (Li *et al.*, 2018)**.** This compound **117** is repoted to have showed antidiabetic activity by inhibiting α-glucosidase enzyme with an $IC_{50}$ 0.75 mM (Damsud *et al.*, 2014).

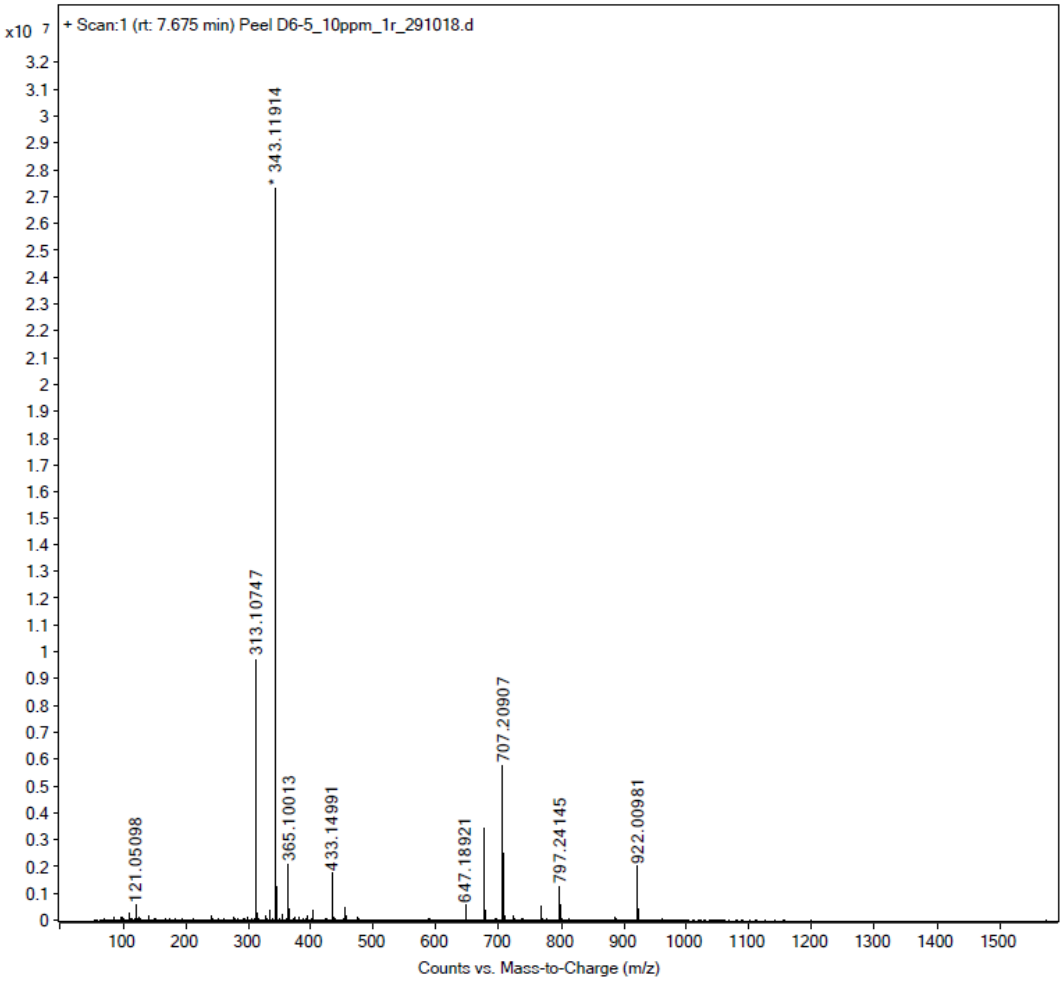


***Figure 3.118**: The HRESIMS spectrum of compound **117***

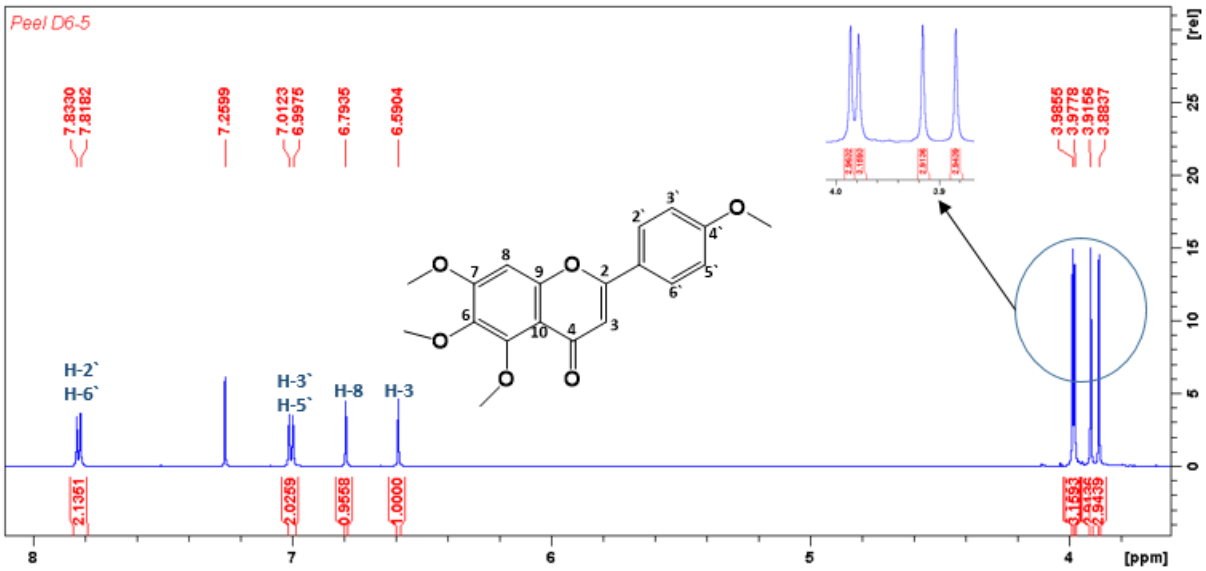


***Figure 3.119***: *$^{1}$H NMR (600 MHz, $CDCl_3$) spectrum of compound* ***117***

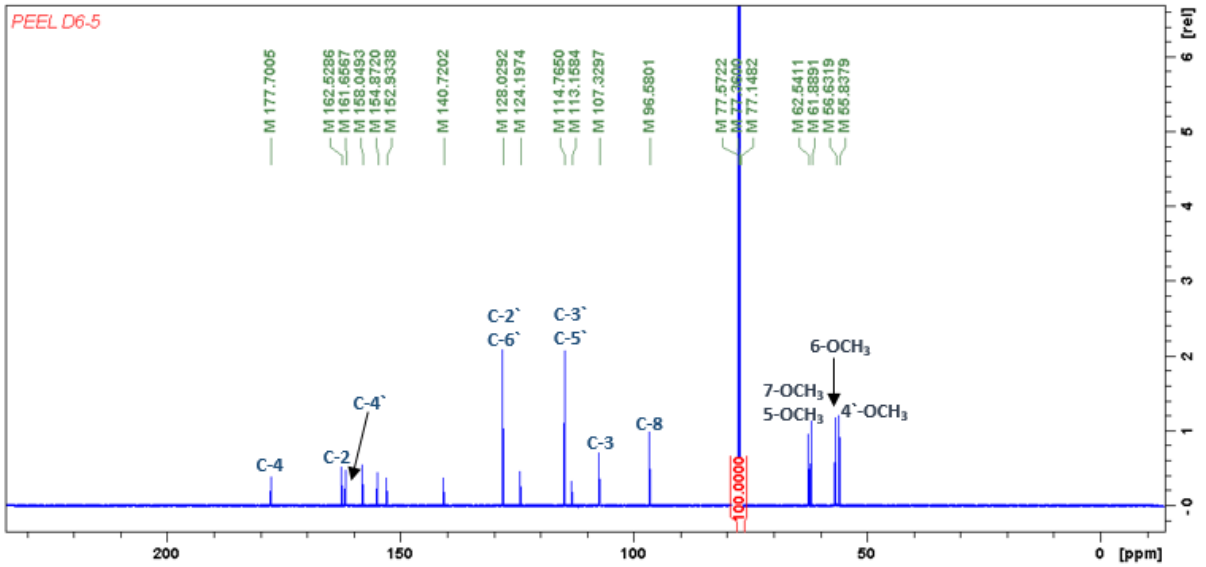


***Figure 3.120***: *$^{13}$C NMR (150 MHz, $CDCl_3$) spectrum of compound* ***117***

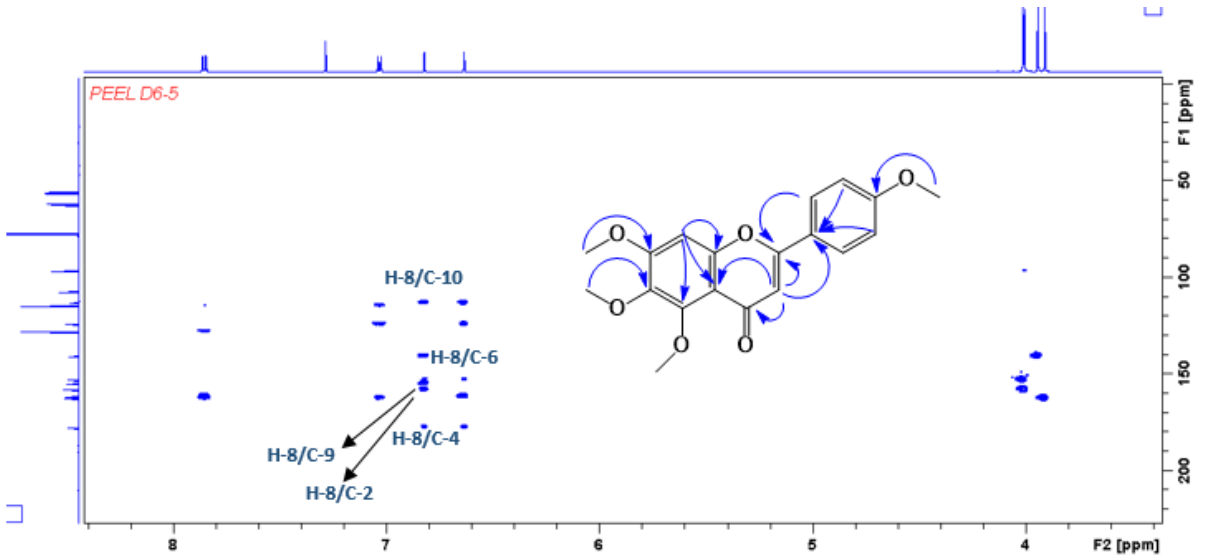


***Figure 3. 121***: *The HMBC correlation compound* ***117***

### 3.2.9.10 Structure elucidation of salvigenin (118)

The compound **118** was isolated as a yellow powder. The HRESIMS (Figure 3.122) suggested the empirical formula as $C_{18}H_{16}O_6$ and in the positive ion mode it showed $[M+H]^+$ peak at *m/z* 329.1259 (calculated 329.1025). The 1D and 2D NMR spectra of compound **118** were very similar to those of compound **117**. The main differences were the presence of a hydroxyl peak at $\delta_H$ 12.75 and the presence of three methoxyl signals instead of four in the $^1$H NMR spectrum (Figure 3.123, Table 3.25). The $^{13}$C NMR spectrum (Figure 3.124, Table 3.25) revealed a total of eighteen carbons including a carbonyl at $\delta_C$ 182.8, three methoxy groups, six methines and the remains are quaternary carbons. The HMBC experiment showed long correlation from the hydrogen bonded hydroxyl ($\delta_H$12.75) to the carbons at $\delta_C$ 154.88 (C-5), 131.94 (C-6) and 107.32 (C-10); these correlations confirmed the position of the hydroxyl group through C-5 in the molecule. Moreover, a $^3J$ correlations were observed from methoxyl at $\delta_H$ 3.88 (3H), 3.91 (3H) and 3.97 (3H) to the oxygenated quaternary carbons at $\delta_C$162.1 (C-4′), 131.9 (C-6) and 158.0 (C-7) respectively. Additionally, long range correlations were observed from H-2′ and H-6′ to carbons at $\delta_C$ 124.2 (C-1′) and 162.1 (C-4′). Thus, compound **118** identified as 5-hydroxy-6,7,4′-trimethoxyflavone. The spectroscopic data of compound **118** were in good agreement with respective published data of salvigenin (Morocho *et al.*, 2018). Compound **118** possesses anti-inflammation activity (Mansourabadi *et al.*, 2015) and cytotoxic activity agansit the breast cancer cell line (MCF-7) in a mouse model (Noori *et al.*, 2013).

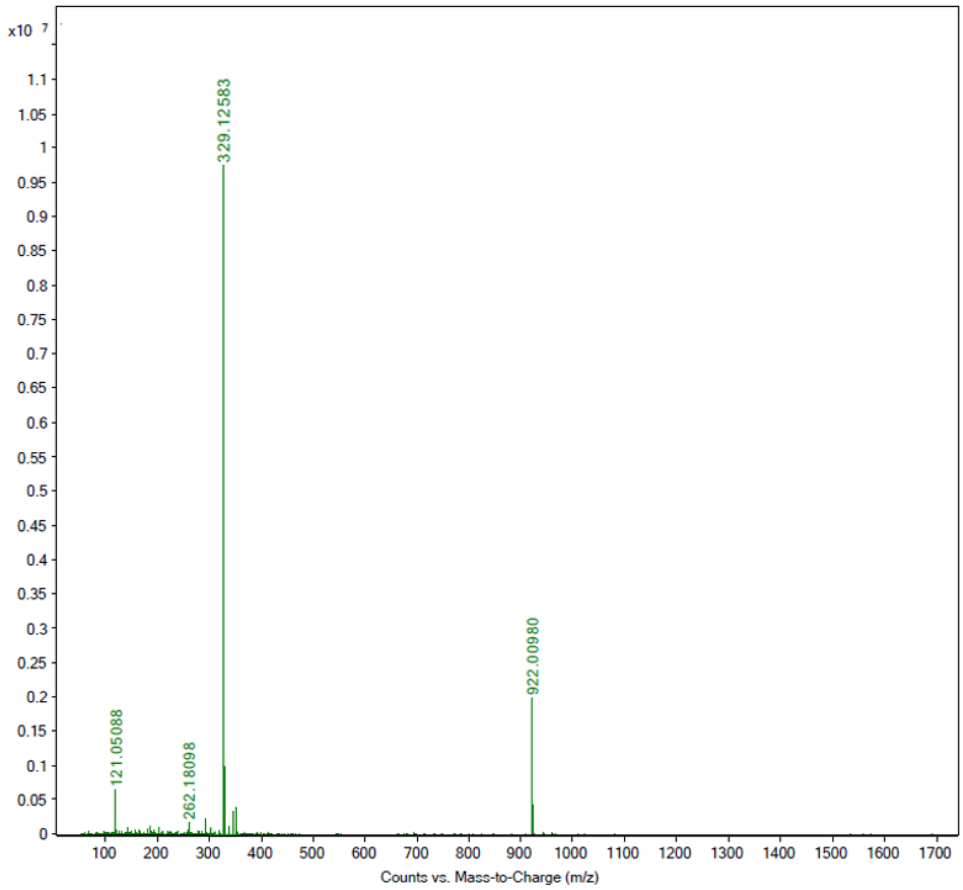


***Figure 3.122**: The HRESIMS spectrum of compound **118***

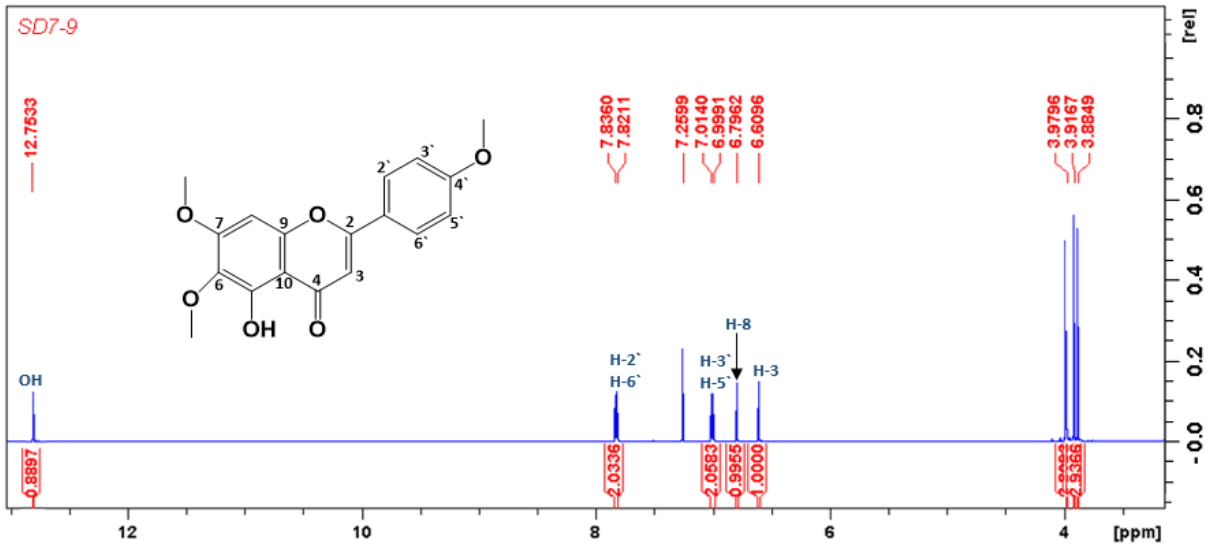


***Figure 3.123**: $^{1}H$ NMR (600 MHz, $CDCl_3$) spectrum of compound **118***

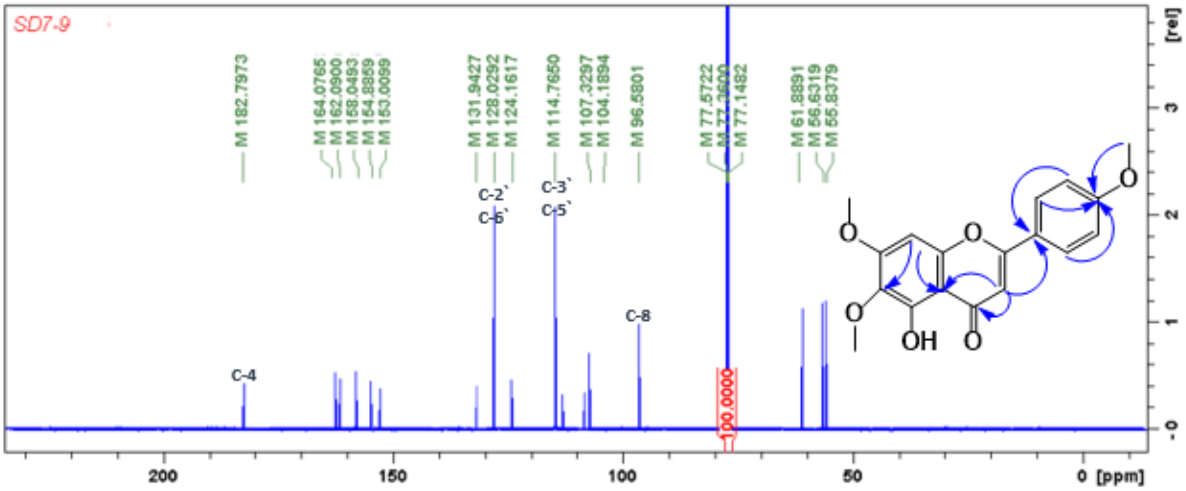


***Figure 3.124**: $^{13}C$ NMR (150 MHz, $CDCl_3$) spectrum of compound **118***

**Table 3.25**: $^{1}H$ NMR (600 MHz) and $^{13}C$ NMR data of compounds **116-118**

| position | Chemical Shift $\delta_H$ (ppm), *J* in Hz | | | Chemical Shift δc (ppm), *J* in Hz | | |
|---|---|---|---|---|---|---|
| | **116** | **117** | **118** | **116** | **117** | **118** |
| 2 | - | - | - | 161.5 | 161.6 | 164.1 |
| 3 | 6.60 s | 6.59 s | 6.60 s | 107.1 | 107.1 | 104.2 |
| 4 | - | - | - | 177.7 | 177.7 | 182.8 |
| 5 | - | - | - | 151.7 | 152.9 | 154.9 |
| 6 | - | - | - | 144.4 | 140.7 | 131.9 |
| 7 | - | - | - | 148.8 | 158.0 | 158.0 |
| 8 | - | 6.59 s | 6.79 s | 138.3 | 96.6 | 96.6 |
| 9 | - | - | - | 148.0 | 154.9 | 153.0 |
| 10 | - | - | - | 115.3 | 113.1 | 107.3 |
| 1′ | - | - | - | 124.2 | 124.2 | 124.2 |
| 2′ | 7.88 *d* (8.82) | 7.82 *d* (8.82) | 7.83 *d* (8.82) | 128.0 | 128.0 | 128.0 |
| 3′ | 7.03 *d* (8.82) | 7.00 *d* (8.82) | 7.00 *d* (8.82) | 115.0 | 114.8 | 114.8 |
| 4′ | - | - | - | 162.7 | 162.5 | 162.1 |
| 5′ | 7.03 *d* (8.82) | 7.00 *d* (8.82) | 7.00 *d* (8.82) | 115.0 | 114.8 | 114.8 |
| 6′ | 7.88 *d* (8.82) | 7.82 *d* (8.82) | 7.83 *d* (8.82) | 128.0 | 128.0 | 128.0 |
| 5-$OCH_3$ | 4.10 s | 3.98 s | - | 62.0 | 62.5 | - |
| 6-$OCH_3$ | 3.95 s | 3.91 s | 3.91 s | 62.4 | 61.9 | 61.9 |
| 7-$OCH_3$ | 3.95 s | 3.97 s | 3.97 s | 62.6 | 56.6 | 56.6 |
| 8-$OCH_3$ | 4.02 s | - | - | 62.2 | - | - |
| 4′-$OCH_3$ | 3.89 s | 3.88 s | 3.88 s | 55.8 | 55.8 | 55.8 |
| 5-OH | - | - | 12.7 | - | - | _ |

### 3.2.9.11 Structure elucidation of hesperidin (50)

The compound **50** was isolated as a white powder. The HRESIMS (Figure 3.125) suggested the empirical formula as $C_{28}H_{34}O_{15}$ and in the positive ion mode it showed peak $[M+H]^+$ at *m/z* 611.1953 (calculated 611.1976). The $^1$H NMR spectrum (Figure 3.126, Table 3.26) exhibited three aromatic protons as ABX pattern resonating at $\delta_H$ 6.91 (*dd, J*=8.34, 2.1 Hz), 6.93 (*d, J*=2.1 Hz), 6.95 (*d, J*=8.34 Hz) and two *meta*-coupled (*J*=2.5 Hz) protons at $\delta_H$ 6.14 (*d, J*=2.5 Hz, H-6) and 6.12 (*d, J*=2.5 Hz, H-8). Moreover, two hydroxyl peaks were observed at $\delta_H$ 12.96 and 9.08. Moreover, the rutinosyl moiety was revealed by the presence of a glucose anomeric proton at $\delta_H$ 4.98 (d, *J*=8.5 Hz), while the rhamnose anomeric proton resonated at $\delta_H$ 4.52 (d, *J*=1.92 Hz) and methyl protons of rhamnose at $\delta_H$ 1.09 (3H). The primary elucidation of the $^1$H NMR spectrum of compound **50** suggested this compound could be a flavanone glycoside. The $^{13}$C NMR spectrum (Figure 3.127, Table 3.26) showed a total of twenty eight signals including a carbonyl at $\delta_C$197.5, a methoxyl, seven quaternary carbons and two aliphatic methine carbons at $\delta_C$ 78.8 (C-2) and 42.5 (C-3). Among these, twelve carbons constituted the rutinosyl moiety. The HMBC experiment showed the long range correlation from H-1‴ ($\delta_H$ 4.52) to carbons at $\delta_C$ 66.78 (C-6″) which confirmed the connectivity of glucose and rhamnose. Another $^3J$ correlation from the proton at $\delta_H$ 4.98 (H-1″) to the oxygenated quaternary carbon at $\delta_C$165.60 (C-7) confirmed the linkage of sugar through C-7. The mehoxyl $\delta_H$ 3.78 revealed a correlation to oxygenated quaternary carbon at $\delta_C$146.9 (C-3′). Thus, compound **50** was identified as 7-rhamnoglucoside. The spectroscopic data of compound **50** were in good agreement with respective published data of hesperidin (Nieto and Gutierrez, 1986). Compound **50** is reported as a food supplement, decreasing the permeability of blood capillaries, is an antihypercholesterolaemia agent, antihyperlipidemic factor and an antioxidant (Garg *et al.*, 2001; Guardia *et al.*, 2001).

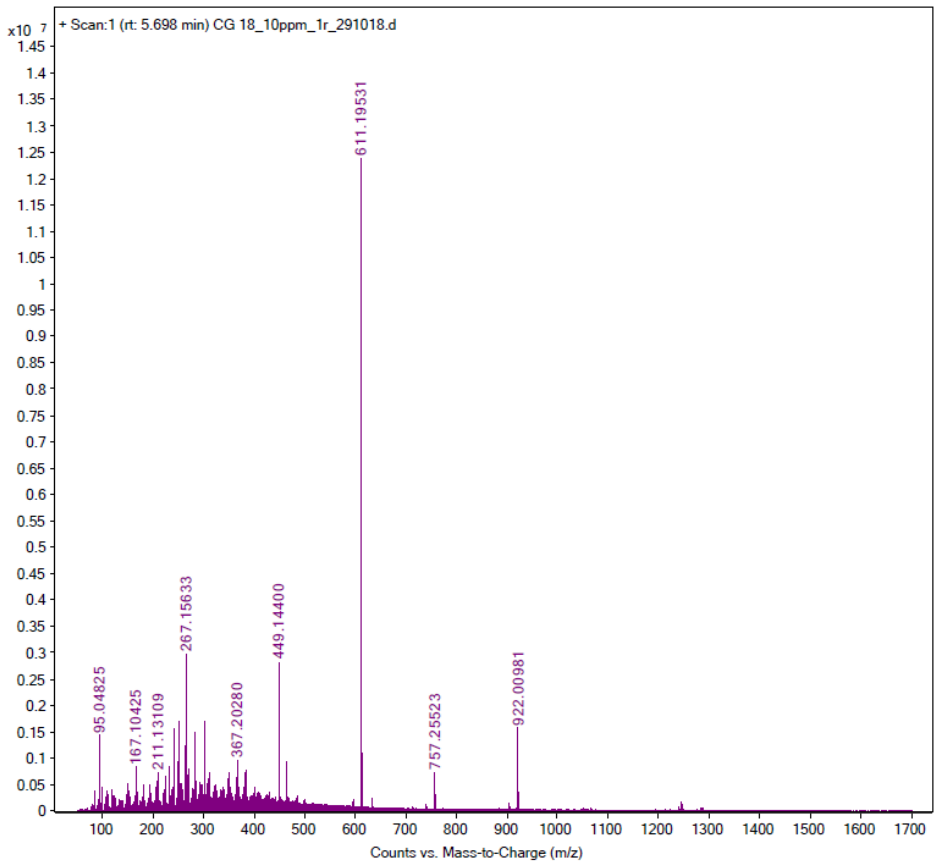


***Figure 3.125**: The HRESIMS spectrum of compound **50***

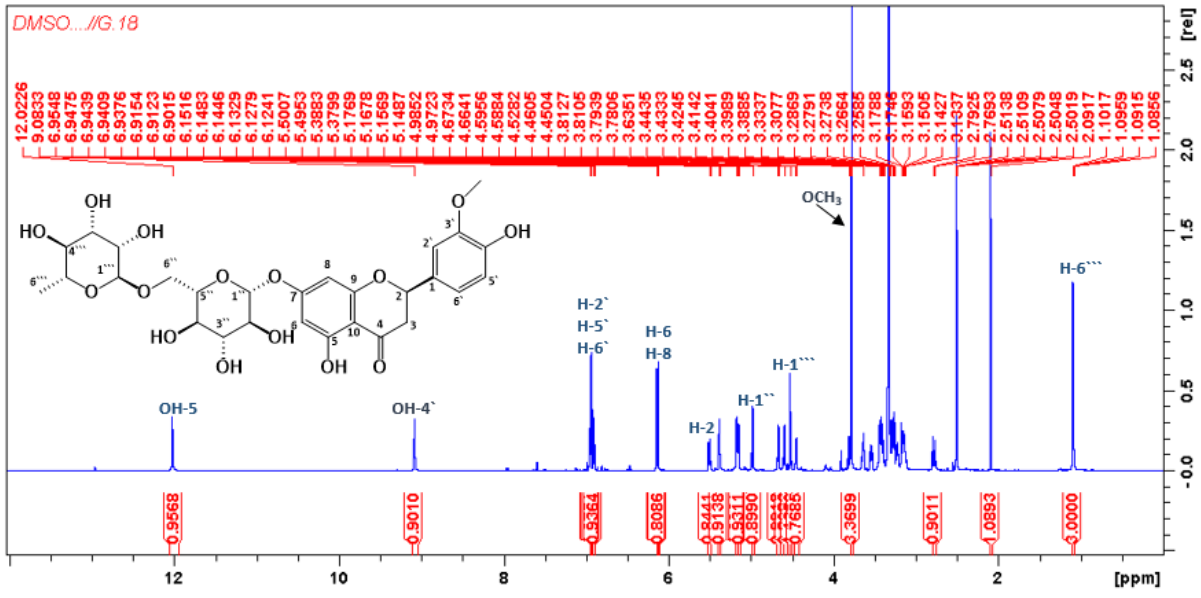


***Figure 3.126**: $^{1}H$ NMR (600 MHz, $CDCl_3$) spectrum of compound **50***

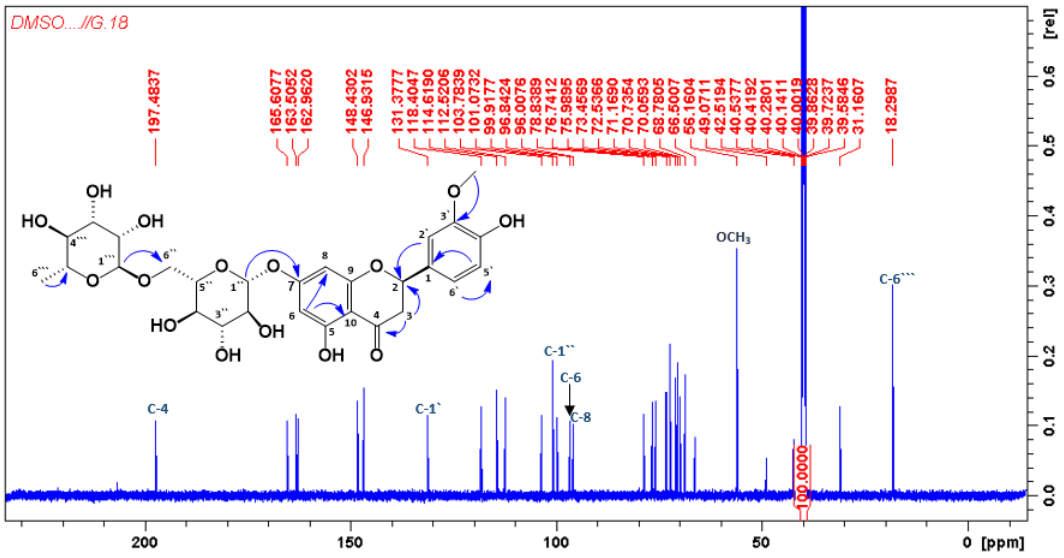


***Figure 3.127**: [13]C NMR (150 MHz, $CDCl_3$) of compound **50***

### 3.2.9.12 Structure elucidation of compound narirutin (51)

The compound **51** was isolated as a yellow powder. The HRESIMS suggested the empirical formula as $C_{27}H_{32}O_{14}$ and in the positive ion mode it showed $[M+H]^+$ peak at *m/z* 581.1895 (calculated 581.1870). The $^1$H NMR spectra (Figure 3.128, Table 3.26) exhibited a methyl signal at $\delta_H$ 1.21(3H) and two *meta*-coupled olefinic protons at $\delta_H$ 6.19 (H-6) and 6.22 (H-8) and *ortho* (*J*=8.52) coupled signals resonated at $\delta_H$ 7.36 (2H, H-2`, H-6`) and 6.85 (2H, H-3′, H-5′). The $^{13}$C NMR spectrum (Figure 3.129, Table 3.26) revealed a total of twenty-eight carbons including a carbonyl at $\delta_C$ 198.7, six quaternary carbons and two aliphatic methine carbons at $\delta_C$ 78.0 (C-2) and 42.3 (C-3) and twelve carbons forming the rutinosyl moiety. The HMBC experiment (Figure 3.130) showed $^3J$ correlation from H-2′ and H-6′ to carbon at carbons at $\delta_C$ 149.2 (C-4′) and 78.0 (C-2) while H-3′ and H-5′ revealed long range correlations to carbons $\delta_C$ 131.0 (C-1′, $^3J$) and 149.2 (C-4′, $^2J$). The cross peak correlation from the anomeric proton of rhamnose at $\delta_H$ 4.71 and carbon at $\delta_C$ 69.92 (C-6′′) confirmed the linking of rhamnose to glucose while the anomeric proton of glucose at $\delta_H$ 4.96 revealed a correlation to carbon at $\delta_C$166.95 (C-7) confirming the position of the rutinosyl moiety through C-7 in the molecule. Thus, compound **51** was identified as apigenin

7-*O*-β-D-glucopyranosyl (6 → 1)-α-L-rhamnopyranoside. The data of compound **51** were in good agreement with respective published data of narirutin (Abu-Gharbieh and Shehab, 2017). Compound **51** was reported to be useful for the treatment of bronchial asthma (Funaguchi *et al.*, 2007) and to reduce liver damage caused by drinking alcohol (Park *et al.*, 2013).

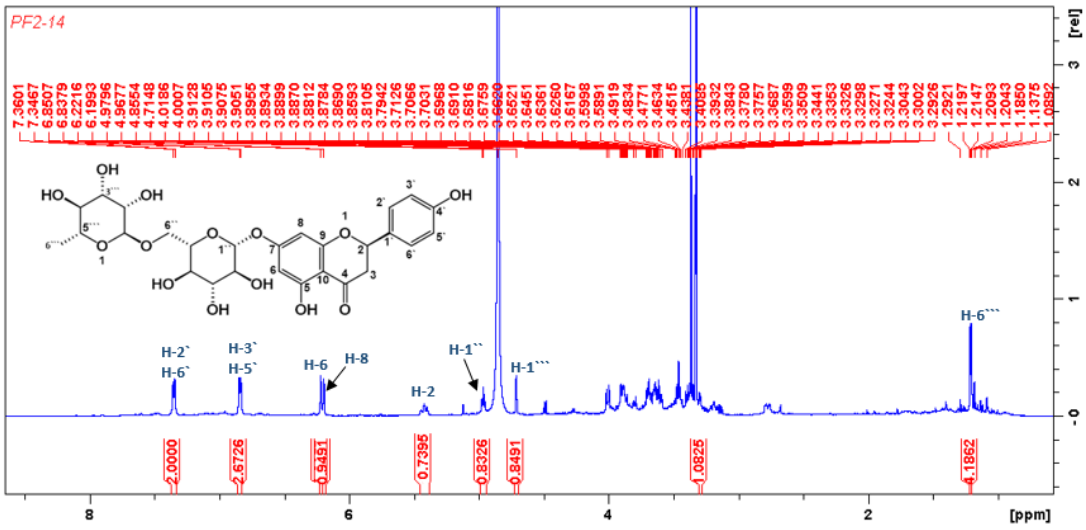


***Figure 3.128**: [1]H NMR (600 MHz, $CDCl_3$) spectrum of compound **51***

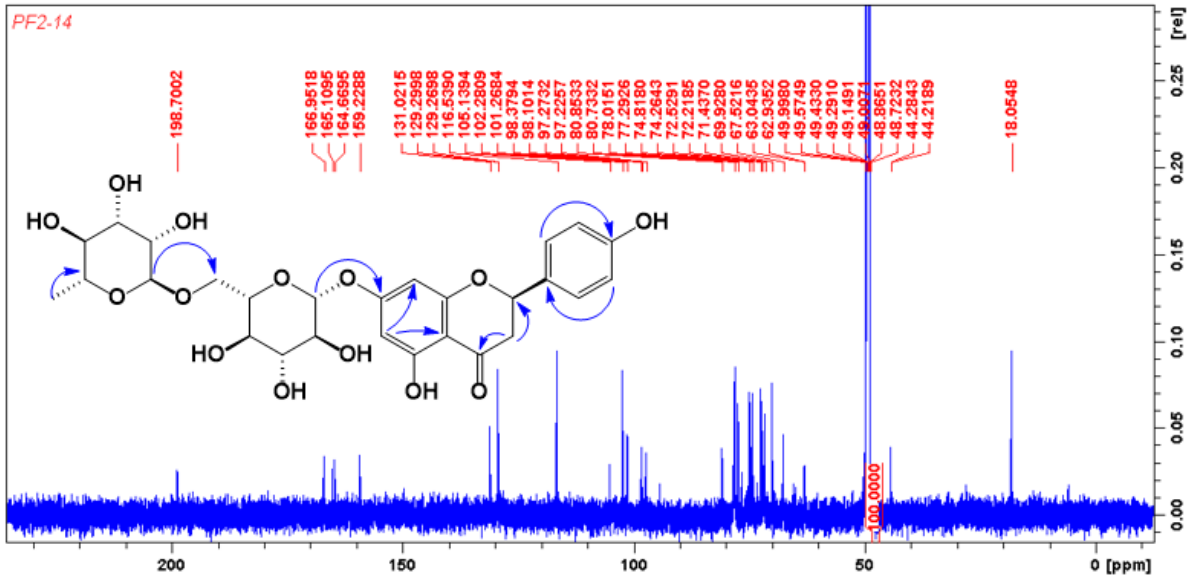


***Figure 3.129**: [13]C NMR (150 MHz, $CDCl_3$) spectrum of compound **51***

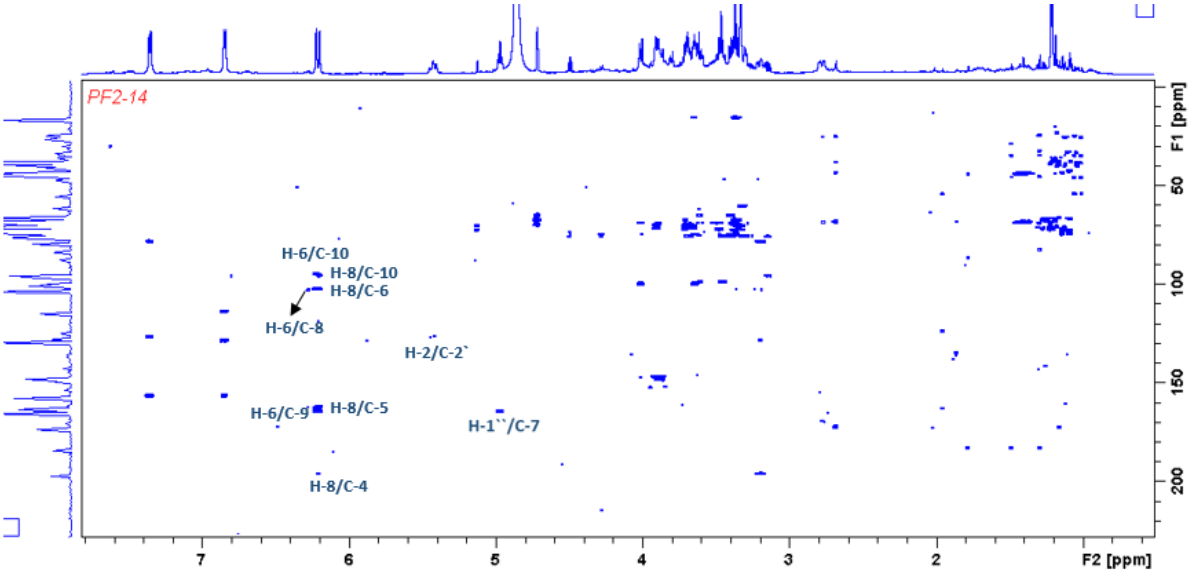


***Figure 3.130**: The HMBC correlation compound **51***

### 3.2.9.13 Structure elucidation of compound marcitrus (119)

This compound **119** was isolated as a yellow golden oil. The HRESIMS (Figure 3.131) suggested the empirical formula as $C_{28}H_{32}O_{16}$ and in the positive ion mode it showed $[M+H]^+$ peak at *m/z* 625.1761 (calculated 625.1768). The $^1$H NMR spectrum (Figure 3.132, Table 3.26) exhibited olefanic protons signals at $\delta_H$ 7.47 (2H, d, 8.76 Hz), 7.16 (2H, d, 8.76 Hz) and two anomeric protons at $\delta_H$ 4.96 (1H,d, *J*=7.00 Hz), 4.71 (1H,d, *J*=1.38 Hz) and singlet proton at $\delta_H$ 6.22 which integrated as 2H and so could be a dioxolane ring. The first suggestion of compound **119** was a glycosylated apigenin connected to a rutinosyl moiety with a dioxolane ring. The $^{13}$CNMR spectrum (Figure 3.133, Table 3.26) revealed a total of twenty eight carbons including a carbonyl at $\delta_C$ 203.6, twelve carbons for rutinosyl, seven olefinic carbons and the remains being quaternary carbons while the HSQC (Figure 3.134) showed the direct connections from protons to carbons. The COSY spectrum (Figure 3.135) showed the correlation from H-2′ and H-6′ to H-3′ and H-5′ while H-2 revealed a correlation to H-3. In the HMBC experiment (Figure 3.136) $^3J$ correlations were observed from the anomeric proton at $\delta_H$ (4.71, H-1‴) to carbon at $\delta_C$ 69.9 (C-6″) that confirmed the connection between the two sugar moieties. The protons at $\delta_H$ 4.96 (H-1″), 7.47 (H-2′, H-6′) and 7.16

(H-3′, H-5′) presented a long range HMBC correlation to the carbon at $\delta_C$160.39 (C-4′) confirming the connection of rutinosyl moiety to C-4′. Moreover, the analysis by HMBC showed the correlation from the proton at $\delta_H$ 6.22 to the carbon at $\delta_C$ 147.7 (C-5) and 135.4 (C-7) that confirmed the position of the dioxolane ring. All these observations confirmed the structure of the compound **119** to be 4,5-dihydroxy-7-(4-(((2*R*,4*S*,5*R*)-3,4,5-trihydroxy-6-((((2*R*,4*R*,5*S*,6*S*)-3,4,5-trihydroxy-6-methyltetrahydro-2H-pyran-2-yl)oxy)methyl)tetrahydro-2H-pyran-2-yl)oxy)phenyl)-7,8-dihydro-9H-[1,3]dioxolo[4,5-f]chromen-9-one. This is a new natural product, for which we propose the name marcitrus.

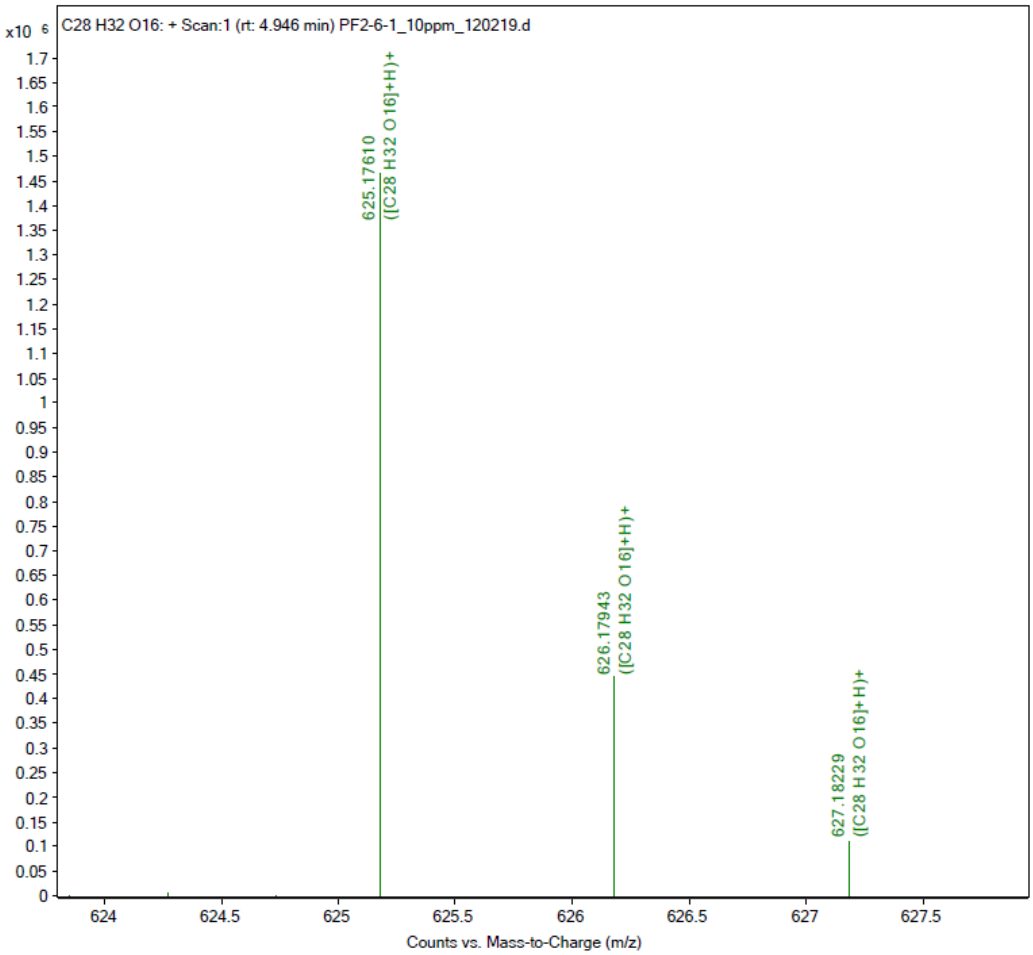


***Figure 3.131**: The HRESIMS spectrum of compound **119***

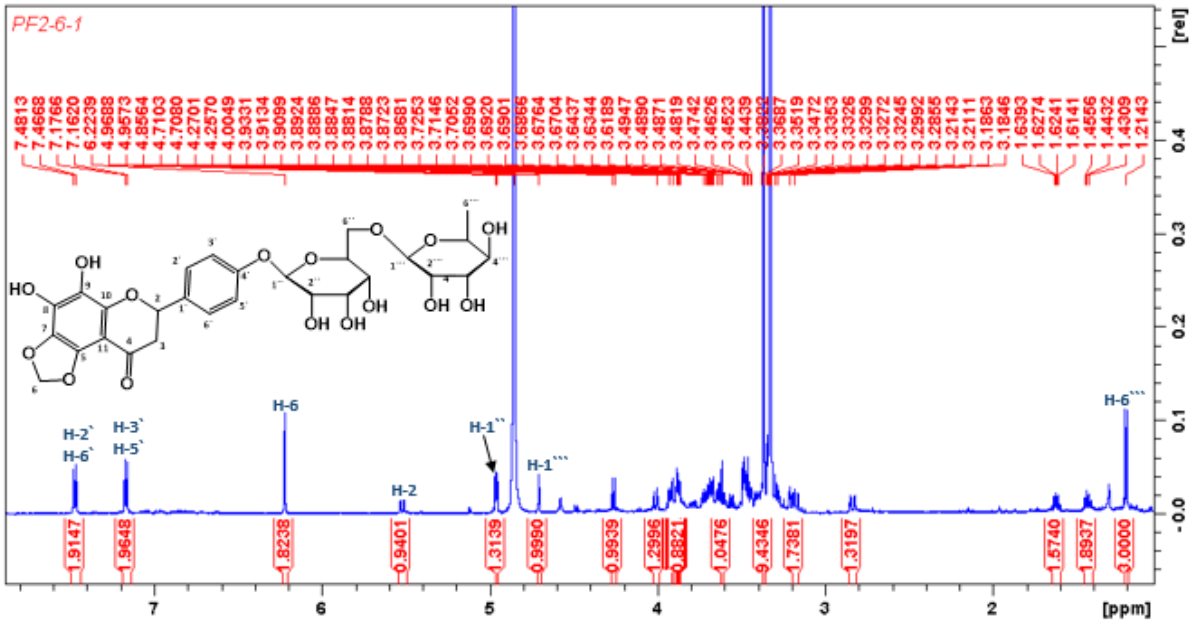


***Figure 3.132***: *$^{1}$H NMR (600 MHz, $CD_3OD$) spectrum of compound* ***119***

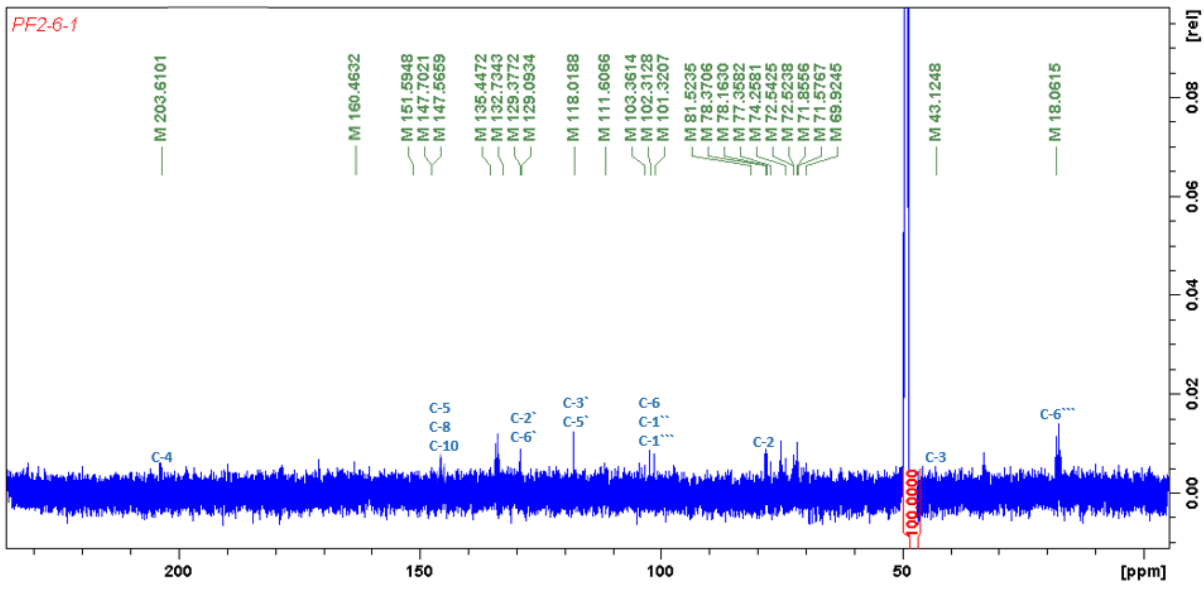


***Figure 3.133***: *$^{13}$C NMR (150 MHz, $CD_3OD$) spectrum of compound* ***119***

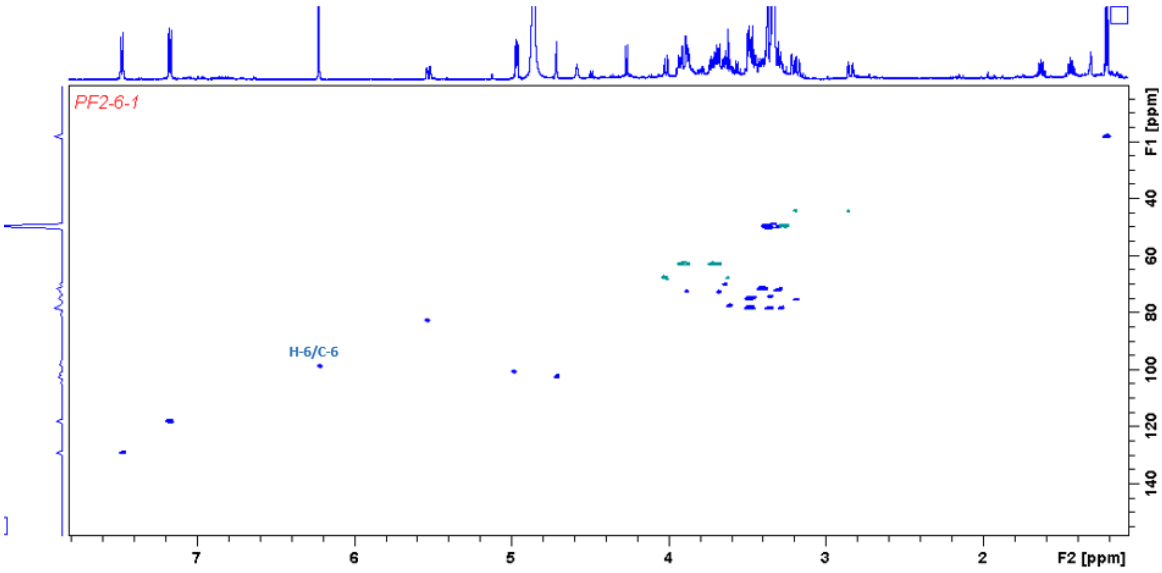


***Figure 3.134**: HSQC spectrum of compound **119***

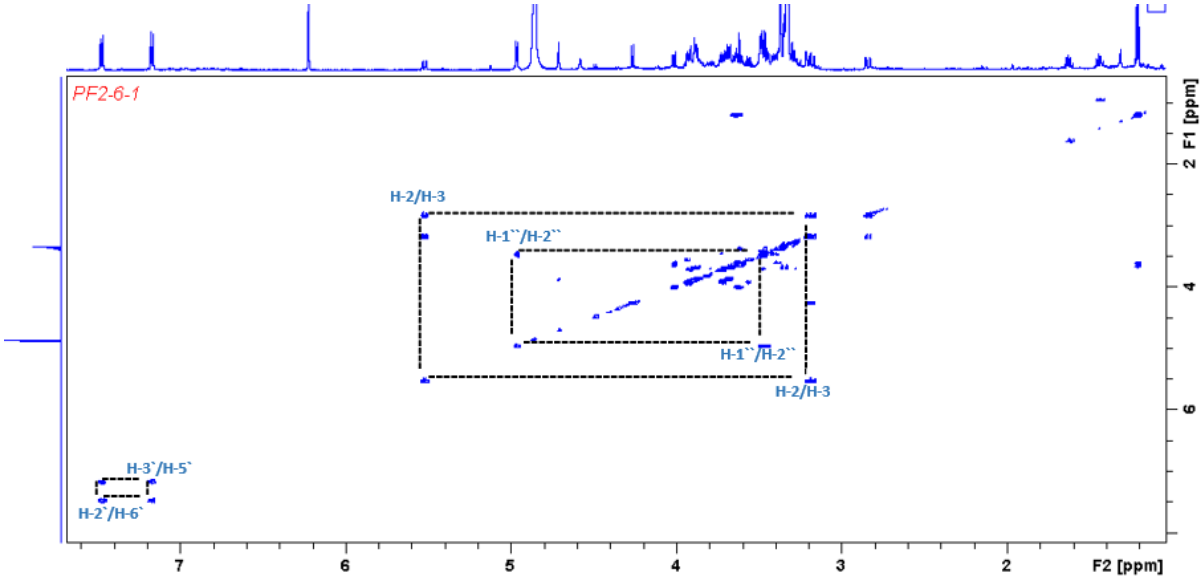


***Figure 3.135**: COSY spectrum of compound **119***

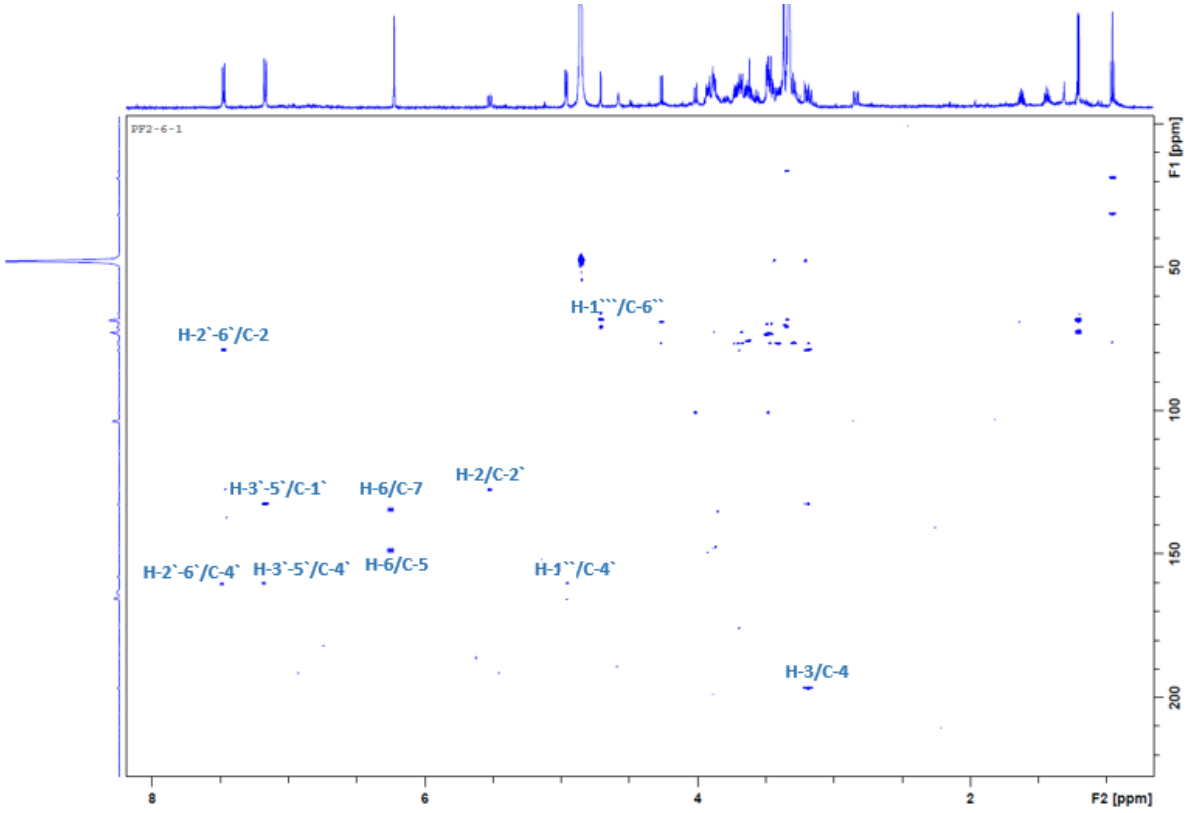


***Figure 3.136**: HMBC spectrum of compound **119***

### 3.2.10 Antimicrobial activity of the isolated compounds from *Citrus* species

To evaluate the antimicrobial activity of the compounds isolated from fractions and extracts of *C. grandis* and *C. sinensis*, which showed a notable antimicrobial effect, the isolated compounds were tested against *S. aureus* (NCTC 12981), *E. coli* (NCTC 12241), *P. aeruginosa* (NCTC 12903), *M. luteus* (NCTC 7508) and *C. albicans* (ATCC 90028) and the highest test concentration of compounds was 1 mg/mL using microtitre assay to determine their minimum inhibition concentration (MIC). The observed MIC values are summarized in Table 3.27. The results revealed all the tested compounds except compound **50** inhibited *M. luteus* with highest MIC of $1.25\times10^{-1}$ given by compounds **116** and **119**, while ten compounds efficiently hampering the growth of *C. albicans* and seven compounds exhibited a moderate inhibitory effect against *P. aeruginosa*.

**Table 3.26**: $^{1}$H NMR (600 MHz) and $^{13}$C NMR data of compounds **50, 51, 119**

| | **Chemical Shift $\delta_H$ (ppm), *J* in Hz** | | | **Chemical Shift $\delta_c$ (ppm), *J* in Hz** | | |
|---|---|---|---|---|---|---|
| **Position** | **50** | **51** | **119** | **50** | **51** | **119** |
| 2 | 5.50 *dd* (12.00,3.06) | 5.42 *dd* (12.36, 3.06) | 5.53 *dd* (3.12, 12.42) | 78.8 | 78.0 | 81.5 |
| 3 | 2.78 *dd* (3.06, 17.16) | 2.77 *dd* (3.06,17.16) 3.29 *dd* (17.16, 12.36) | 2.83 *dd* (3.12,17.1) 3.29 *dd* (17.1, 12.42) | 42.5 | 42.3 | 43.1 |
| 4 | - | - | - | 197.5 | 198.7 | 203.6 |
| 5 | - | - | - | 163.5 | 165.1 | 147.7 |
| 6 | 6.14 *d* (2.5) | 6.19 *d* (2.00) | 6.22 s | 96.8 | 98.1 | 101.3 |
| 7 | - | - | - | 165.6 | 167.0 | 135.4 |
| 8 | 6.12 *d* (2.5) | 6.22 *d* (2.00) | - | 96.00 | 97.3 | 147.6 |
| 9 | - | - | - | 163.0 | 164.7 | 129.4 |
| 10 | - | - | - | 103.8 | 105.1 | 151.6 |
| 11 | - | - | - | - | - | 111.6 |
| 1' | - | - | - | 131.37 | 131.0 | 132.7 |
| 2' | 6.93 *d* (2.1) | 7.36 *d* (8.52) | 7.47 *d* (8.76) | 114.6 | 129.3 | 129.1 |
| 3' | - | 6.85 *d* (8.52) | 7.16 *d* (8.76) | 146.9 | 116.5 | 118.0 |
| 4' | - | - | - | 148.4 | 149.2 | 160.4 |
| 5' | 6.95 *d* (8.34) | 6.85 *d* (8.52) | 7.16 *d* (8.76) | 112.5 | 116.5 | 118.0 |
| 6' | 6.91 *dd* (8.34, 2.1) | 7.36 d (8.52) | 7.47 *d* (8.76) | 118.4 | 129.3 | 129.1 |
| 1'' | 4.98 *d* (8.5) | 4.96 *d* (7.02) | 4.96 *d* (7.00) | 101.1 | 101.3 | 102.3 |
| 2'' | 3.63* | 3.36* | 3.88 | 76.0 | 72.5 | 75.5 |
| 3'' | 3.45* | 3.60* | 3.48 | 78.8 | 78.0 | 78.5 |
| 4'' | 3.40* | 3.90* | 3.39 | 70.7 | 71.4 | 71.6 |
| 5'' | 3.54* | 3.46* | 3.34 | 76.7 | 80.8 | 78.4 |
| 6'' | 3.42 m | 4.01* | 3.63 | 66.8 | 69.9 | 69.9 |
| 1''' | 4.52 *d* (1.92) | 4.71 *d* (2.1) | 4.71 *d* (1.38) | 103.8 | 102.3 | 103.4 |
| 2''' | 3.27* | 3.65* | 3.48 | 71.7 | 74.8 | 74.2 |
| 3''' | 3.28* | 3.33* | 3.29 | 72.5 | 72.2 | 71.8 |
| 4''' | 3.18* | 3.29* | 3.69 | 73.4 | 74.3 | 72.5 |
| 5''' | 3.38* | 3.65* | 3.6 | 68.8 | 77.3 | 77.3 |
| 6''' | 1.09 *d* (6.18) | 1.21 *d* (6.24) | 1.21 *d* (6.24) | 18.3 | 18.0 | 18.1 |
| 3`-$OCH_3$ | 3.78 s | - | - | 56.2 | - | - |

* Overlapped peaks – confirmed from COSY, HSQC and HMBC experiments

Compound **111** showed an extraordinary effect on the growth of *S. aureus*, *E. coli*, *M. luteus* and *C. albicans* with highest MIC $6.25\times10^{-2}$ mg/mL. However, compound **50** failed to have any effect against the tested organisms. The modified microtitre assay was the biological test used in this study to examine the antimicrobial activity of the compounds and determine their MIC values. Various antibiotics outlined on Table 3.3 were used as a positive control and the negative controls were water, nutrient broth and normal saline.

**Table 3.27**: The MIC (mg/mL) of isolated compounds from *Citrus*

| **Compounds** | **All concentrations in (mg/mL)** | | | | |
|---|---|---|---|---|---|
| | *S. aureus* | *E. coli* | *P. aeruginosa* | *M. luteus* | *C. albicans* |
| **50** | N/A | N/A | N/A | N/A | N/A |
| **57** | N/A | N/A | $2.5\times10^{-1}$ | $5x10^{-1}$ | $2.5\times10^{-1}$ |
| **110** | $2.5\times10^{-1}$ | N/A | $5x10^{-1}$ | $5x10^{-1}$ | $2.5\times10^{-1}$ |
| **111** | $2.5\times10^{-1}$ | $5x10^{-1}$ | $2.5\times10^{-1}$ | $2.5\times10^{-1}$ | $6.25\times10^{-2}$ |
| **112** | N/A | N/A | $5\times10^{-1}$ | $2.5\times10^{-1}$ | $2.5\times10^{-1}$ |
| **113** | N/A | N/A | $5x10^{-1}$ | $2.5\times10^{-1}$ | $2.5\times10^{-1}$ |
| **114** | N/A | N/A | $5x10^{-1}$ | $2.5\times10^{-1}$ | $5\times10^{-1}$ |
| **115** | N/A | N/A | N/A | $5x10^{-1}$ | N/A |
| **116** | N/A | N/A | $5\times10^{-1}$ | $1.25\times10^{-1}$ | $2.5\times10^{-1}$ |
| **117** | N/A | N/A | N/A | $5x10^{-1}$ | $5x10^{-1}$ |
| **118** | N/A | N/A | N/A | $2.5\times10^{-1}$ | $5\times10^{-1}$ |
| **119** | N/A | N/A | N/A | $1.25\times10^{-1}$ | $2.5x10^{-1}$ |

*N/A: No Activity

### 3.2.11 Discussion

*Citrus* is one of the most interesting pharmaceutical genera of the Rutaceae family. Many studies have documented this genus to contain different groups of secondary metabolites (Benavente-Garcia *et al.,* 1997; Nijveldt *et al.,* 2000; Encyclopedia Britannica, 2019).

One of the largest classes of natural products found in *Citrus* is flavonoids, which are considered as polyphenolic compounds with structural skeletons of flavanone, flavone, and/or flavonol (Široká *et al.,* 2013). Flavonoids have been studied and reported for many

healthf be refiling properties such as, antimicrobial, anti-inflammatory, antioxidant, cardiovascular and anticarcinogenic (Nijveldt *et al.*, 2001).

The present work focuses on two important species of this genus *C. grandis* and *C. sinensis* using different parts for phytochemical study and screening of their antimicrobial properties on two Gram-positive bacterial strains *Micrococcus luteus* (NCTC 7508) and *Staphylococcus aureus* (NCTC 12981), and two Gram-negative strains *Escherichia coli* (NCTC 12241) and *Pseudomonas aeruginosa* (NCTC 12903) and the only fungal strain *Candida albicans* (ATCC 90028), which is considered one of the most common pathogenic fungi.

The result of preliminary antimicrobial screening of *C. grandis* leaves extracts showed the most potent activity with an MIC value of $3.125\times10^{-1}$ mg/mL against *P. aeruginosa* and *M. luteus*. Bioassay-guided chemical investigation led to the isolation of six compounds, **50**, **57**, **111**, **112**, **114** and **115**. Compounds **111** showed significant antimicrobial activity against the microbes tested. To the best of our knowledge, this is the first report on antimicrobial activity of Iraqi *C. grandis* leaves.

The primarily antimicrobial screening for the peel and leaves of *C. sinensis* extracts against the microbes used in this work revealed that the DCM extract of *C. sinensis* peel showed the strongest higher level of activity with MIC $4.88\times10^{-3}$ mg/mL against the bacterium *M. luteus*. Moreover, the most active extract in *C. sinensis* leaves was the DCM extract, which presented a significant MIC $3.12\times10^{-1}$ against *M. luteus* and *C. albicans*. Both chromatographic and spectroscopic techniques led to isolation and identification of compounds **50**, **57**, **112**, **114**,**115** from the DCM extract of *C. sinensis* leaves and **48**, **50**, **51**, **57**, **102**, **110**, **111**, **113**, **116**, **117**, **119** from DCM and methanolic extracts of *C. sinensis* peels.

The analysis of the antimicrobial results for the isolated compounds revealed that the most effective compound was **111,** which is a flavonoid substituted with five oxygenated

methyls. According to Tian-Yang Wang *et al*. (2018), the most active antimicrobial flavonoids have double bond on C2=C3 and are substituted on position 5 and 7 by OH. Seemingly, occupation of positions 5, 6, 7 by $OCH_3$ could offer notable inhibitory activity. Compound **50** was not active with the maximum concentration was used in this assay. However, this compound was reported to possess major antiviral effect, anti-inflammatory and analgesic activity (Kumar and Pandey, 2013).

The number of the hydroxyl group results is another influencing factor. Increasing hydroxyl group numbers led to reducing polarity of the compound, which explained inactivity on biological membranes.

The primary testing to determine the mechanism of action for the tested compounds revealed all compounds tested were bacteriostatic.

# *Chapter 4*

# The Anti-MRSA Activity of Isolated Compounds

## 4.1 Methicillin-resistant *Staphylococcus aureus* (MRSA)

Methicillin-resistant *Staphylococcus aureus* (MRSA) is a human pathogen, which is resistant to several types of antibiotics. The organism can be isolated from around a third of the population without significant symptoms (Otto, 2013). The infection levels with MRSA vary from moderate to serious and sometimes leads to death (Lowy, 2003; Moellering Jr, 2011; Otto, 2013).

*Staphylococci* have been found on earth for more than a billion years depending on many historical indicators (Moellering Jr, 2011). In the 19$^{th}$ century, it was recorded as pathogenic, because it was identified as the main reason for wound infections. Most civilisations successfully treated infections caused by this bacterium using different agents such as honey, copper salts and myrrh. The discovery of penicillin from *Penicillium notatum* in 1928 provided a good new way to inhibit *S. aureus* especially in the 1940s, when penicillin was introduced presented as medication from *S. aureus*. Unfortunately, in 1942s *S. aureus* developed penicillin resistance.

The basic molecular structure of penicillin is a *β*-lactam ring, which inhibits the synthesis of the bacterial peptidoglycan cell wall. On the other hand, *S. aureus* produces the enzyme *β*-lactamase, which is considered as the main reason of inactivation of penicillin by attacking the *β*-lactam ring and changing it to open chain (Figure 4.1) (Palavecino, 2007; Moellering Jr, 2011; Kuriyama *et al.*, 2014; Elhassan *et al.*, 2015).

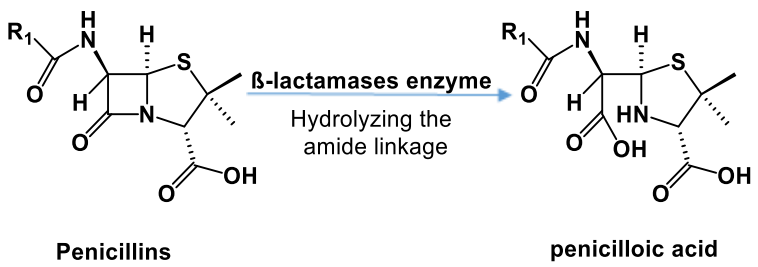


***Figure 4.1**: Inactivation of penicillin by β-lactamase enzymes*

In 1959, methicillin (Figure 4.2) became available as an alternative to penicillin. This antibiotic initially showed significant inhibitory activity against penicillin-resistant *Staphylococcus aureus*. After two years of clinical use, however, the first MRSA strain was detected in the United Kingdom (Jevons, 1961). A short time later, the resistant strain was isolated from other European countries and subsequently from Japan, Australia, and the United States of America (Enright *et al.*, 2002; Moellering Jr, 2011). Methicillin resistance is due to the presence of the *mecA* gene in conjunction with other genetic factors. The *mecA* gene encodes a unique penicillin-binding protein, designated 2' (PB2') or 2a (PBP2a), that has reduced affinity to β-lactam antibiotics (Tsubakishita *et al.*, 2010).

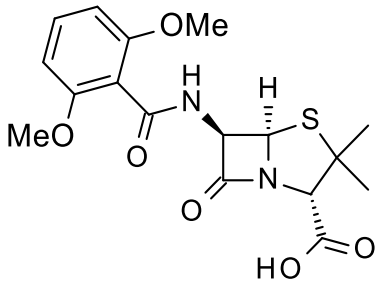


***Figure 4.2**: Structure of methicillin*

In the 1970s, North America, some European countries and two hospitals (East Anglia and Kettering) in England suffered from outbreaks of MRSA. The Kettering outbreak affected most hospitals in the UK by an epidemic of MRSA (Cox *et al.*, 1995; Newsom, 2004). In the 1980s, the MRSA had spread globally. Between 1999 to 2000, in the USA, around 125,969 incidences of hospitalisations were identified with MRSA infections. Furthermore, between January 1998 and June 2003, the annual average percentage of *S. aureus* isolates that were MRSA increased further to 51.6% of ICU and 42% of inpatient non-ICU *S. aureus* isolates (System, 2004; David and Daum, 2010).

It has been reported that the percentage of MRSA infections in children under 15 years of age in England was 0.9% in 1990 and 13% in 2000 (Khairulddin *et al.*, 2004). In Sweden, the general infections were 325 in 2000 and raised in 2003 to 544 (Stenhem *et al.*, 2006). The Data of National Statistics in England and Wales recorded that MRSA infections caused the death of 364 individuals in 2011 compared to 485 in 2010 (Kyte, 2011). The number of infections decreased from 2013 to 2016 (CDC, 2019). A total of 12,784 *Staphylococcus aureus* infections were reported through both the MRSA bacteraemia and methicillin-susceptible *S. aureus* (MSSA) bacteraemia surveillance schemes (Public Health England, 2018). The figure represents a 3.7% increase in the numbers of bacteraemias caused by *S. aureus* from 2016-17 (total number 12,324) and a staggering 29.4% increase from 2011-12 (total number 9,883) when MSSA reporting was made mandatory. However, of the *S. aureus* infections reported during 2017-18, only about 6.6% were MRSA cases, which was a 41.4% decrease from 2011/12, in which 11.3% of all reported cases of *S. aureus* infections were caused by MRSA, and a 1.1% decrease from 2016/17 in which the figure was 6.7%. Whilst the actual reasons behind this continuous decline in MRSA cases are not absolutely clear, it can be assumed that there may be many factors that are behind this decline in MRSA infection ratio such as developed hospital practices including preferred cleaning and expanded regard for the significance of sterile medications for open injuries. Nevertheless, it is necessary to develop new antibiotics to tackle against the issues of antibiotic resistance including MRSA.

### 4.2 Types of MRSA

Two main types of MRSA have been identified. These are community-associated MRSA (CA-MRSA**)** and health care-associated MRSA (HA-MRSA)**.**

### 4.2.1 Community-associated MRSA (CA-MRSA)

Healthy people who have never attended hospitals can become infected with MRSA. It has been reported that the cause of such infections was by coming in contact with people suffering from MRSA especially when sharing household facilities. CA-MRSA is the main cause of skin infections and septicemia.

### 4.2.2 Healthcare-associated MRSA (HA-MRSA)

Healthcare-associated infections**,** also known as a nosocomial infections, are infections that are acquired in a hospital or other healthcare facility. The HA-MRSA is caused mainly because of lack of nosocomial factors in hospital facilities or as a result for medical or surgical treatments. This type of MRSA infection poses a serious risk to patients, staff and visitors. Moreover, the treatment requires significant costs and long time to heal (Miller *et al.*, 2011; NHS, 2017).

## 4.3 Treatment of MRSA infections

It is a big challenge to treat MRSA infections due to resistance factors. Many antibiotics have been used for the treatment of MRSA infections. These include trimethoprim-sulfamethoxazole, clindamycin, minocycline, fluoroquinolones, linezolid, daptomycin, tigecycline, ceftaroline and doxycycline. Recovery time, drug dosage, location of the infection and course of treatment depend on a patient's condition and the severity of the infection (Gould *et al.*, 2012).

## 4.4 Natural products with potent anti-MRSA activity

Natural products are considered potential sources for novel medications, including remedies for MRSA infections. Many studies documented the use of different plants with potential activity against MRSA. One study, for example, demonstrated a significant inhibitory

effect of an essential oil from *Thymus vulgaris* against MRSA ATCC33592 (Tohidpour *et al.*, 2010). Brazilian plants have been shown to have inhibitory activity against MRSA ATCC 33591 (Machado *et al.*, 2003). *Althaea officinalis*, *Melissa officinalis*, *Mentha longifolia* and *Rosa damascene* identified from the Palestinian flora showed remarkable anti-MRSA effects (Abu-Shanab *et al.*, 2007). Traditional Ghana medicinal plants have been used successfully as anti-MRSA agents (Pesewu *et al.*, 2008). Seven Nigerian plants, *Acalypha wilkesiana, Ageratum conyzoides, Bridella ferruginea, Terminalia avicennioides, Phyllanthus discoideus* and *Ocimum gratissimum*, proved to have inhibitory effects on *S. aureus* strain (MRSA-NCIB8588) (Akinyemi *et al.*, 2005). Many compounds derived from *Desmodium caudatum* had notable anti-MRSA activity (Sasaki *et al.*, 2012). Xanthones, anthraquinones, quinones, calcarides, aflatoxins and comazaphilones were shown to have significant anti-MRSA effects (Xu *et al.*, 2015). Many compounds isolated from marine bacteria and fungi are also effective anti-MRSA agents (Debbab *et al.*, 2010). Compounds derived from a marine isolate of the fungus, *Pseudallescheria* showed potent anti-MRSA activity (Li *et al.*, 2006).

## 4.5 Materials and methods

### 4.5.1 Tested materials

A total of twenty compounds have been tested for anti MRSA activity in this study. These include thirteen compounds from *Ruta chalepensis*, namely, arborinine (**107**), bergapten (**43**), chalepin (**45**), chalepensin (**46**), γ-fagarine (**42**), graveoline (**105**), 6-hydroxy-rutin 3′-7-dimethyl ether (**103**), imperatorin (**104**), isopimpinellin (**44**), kokusaginine (**99**), rutamarin (**47**), rutin (**48**) and rutin 3′-methyl ether (**101**) (Figure 3.5). The compounds isolated from the *Citrus* species, which were tested for anti-MRSA activity, include demethylnobiletin (**113**), hesperidin (**50**), 3-methoxynobiletin (**110**), nobiletin (**57**), salvigenin (**118**), sinensetin (**111**) and tangeritin (**116**) (Figure 3.80). The isolation procedures for these compounds have been described in

*Chapter 2* (2.3.3).

### 4.5.2 Resistant strains of *Staphylococcus aureus*

Five methicillin-resistant *S. aureus* strains (SA1199B, XU212, MRSA340702, EMRSA-15MRSA274819) and standard strain (ATCC25923) were used in this study. All the bacterial strains were obtained from the UCL School of Pharmacy and the experiments were performed in the University of East London.

### 4.5.3 Materials used for the MRSA assay

A summary of all of the materials, which were used in the anti-MRSA assay is presented in Table 4.1

**Table 4.1**: Materials used in MRSA assay

| Chemical and regents | Supplier |
|---|---|
| $Ca^{2+}$, $Mg^{2+}$ | Sigma-Aldrich Gillingham, UK |
| Mueller-Hinton broth | Oxoid |
| Normal saline | Sigma-Aldrich Company Ltd., UK |
| 3-[4,5-dimethylthiazol-2-yl]-2,5-diphenyltetrazolium bromide | Sigma-Aldrich Company Ltd., UK |
| DMSO | Sigma-Aldrich Company Ltd., UK |
| Norfloxacin | Sigma |

### 4.5.4 The anti-MRSA assay

*Preparation of culture medium:* Mueller-Hinton broth (MHB) was prepared according to the instruction given by the supplier. The MHB was adjusted to contain cations- 20 mg/L $Ca^{2+}$ and 10 mg/L of $Mg^{2+}$.

*Preparation of tested compounds*: Compounds and antibiotics were dissolved in predetermined amounts of DMSO (less than 1% concentration in the final well), which was further diluted with MHB to obtain the targeted starting concentration (128 μg/mL).

*Preparation of MTT:* It was achieved by dissolving the required amount of 3-(4,5-dimethylthiazol-2-yl)-2,5-diphenyltetrazolium bromide in methanol to obtain a concentration of 5 μg/mL.

*Supension of subculture of the bacteria:* All bacterial strains were subcultured one day before the experiment. Bacterial strains were subcultured in nutrient agar slopes by streaking the bacteria with a loop followed by incubation at 37º for 12-18 h.

*Anti-MRSA assay:* This experiment was performed using 96-well plates. The first step on this assay was to add (100 μL) of MHB to all wells except those in column 12. To the first row of the plate, 100 μL of test compounds or antibiotic were added. Using a multi-channel pipette, the materials of the first well were mixed properly, followed by the transfer of 100 μL of the well contents to the wells of the second column and so on until column 10. Finally, 100 μL content from the wells of column 10 were transferred to the wells of column 12.

An inoculum density of $5 \times 10^5$ cfu of each of the test organisms was prepared in normal saline (9 g/L) by comparison with a 0.5 MacFarland standard. MHB (125 μL) was dispensed into 10 wells of a 96 well microtitre plate (Nunc, 0.3 mL volume per well). Then microtitre plates were incubated at 37°C for 18 h. To determine the minimum inhibitory concentrations (MICs), 20 μL of MTT was add to the microtitre plate and incubated for 20 min. It is colourimetric method, bacterial growth was indicated by the colour changing from yellow to dark blue and the MIC was recorded as the lowest concentration at which no growth was observed. As a positive control norfloxacin, a well-known antibiotic was used.

The method was used to determine the MIC considered as a broth microdilution method according to National Committee for Clinical Laboratory Standards with modification using nutrient broth as the medium (Rahman *et al.*, 2008; Shiu *et al.*, 2011; Ioannou *et al.*, 2012; Nurunnabi *et al.*, 2018; Rahman *et al.*, 2018; Tareq *et al.*, 2018).

## 4.6 Results and discussion

Twenty isolated compounds from *R. chalepensis*, *Citrus grandis* and *C. sinensis* were tested for activity against six MRSA strains (Table 4.2). The results revealed that fifteen of them inhibited the MRSA strains with different MIC values. Arborinine (**107**), chalepensin (**46**), 6-hydroxy-rutin 3′-7-dimethyl ether (**103**) and sinensetin (**111**) were the most active against all MRSA strains tested.

In spite of the fact that chalepin (**45**), chalepensin (**46**) and rutamarin (**47**) (Figure 4.3) are all furanocoumarin derivatives, they caused different levels of inhibitions because of structural differences. The order of anti-MRSA potency in these compounds was **46** > **47** > **45** (Table 4.2). Functional groups were the main differences among these three compounds contributing to their differences in lipophilicity. All three compounds are 3-substituted furanocoumarins, among which, except for **46**, the other two compounds are dihydrofuranocoumarins. Rutamarin (**47**), which is simply the acetylated product of chalepin (**45**) was more active than **45**, presumably because of more lipophilicity caused by acetylation.

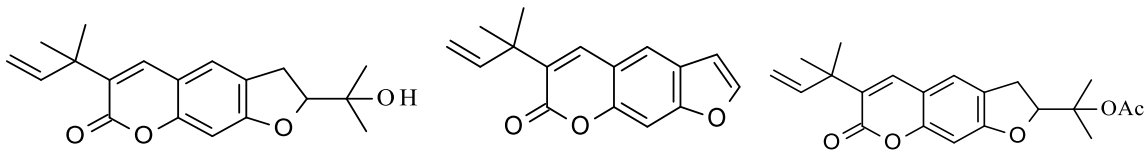


Chalepin (**45**) Chalepensin (**46**) Rutamarin (**47**)

***Figure 4.3****: Structural similarities and differences in anti-MRSA furanocoumarins* ***45-47***

6-Hydroxy-rutin 3′-7-dimethyl ether (**103**), rutin (**48**) and rutin 3′-methyl ether (**101**) are flavonoid glycosides, having only differences in the presence/absence and in the number of methyl ether groups in them, giving them varying degrees of lipophilicity (Figure 4.4). Rutin (**48**) does not contain an OMe group, while compound **101** has an OMe group on 3′ position, and **103** has two OMe groups in positions 3′ and 7. In addition, in **103**, position 6 is occupied

by a hydroxyl group. The highest anti-MRSA potency of compound **103** may be because of the different functional groups and their unique positions that make this compound as the most liphophilic among these three compounds. The order of anti-MRSA selectivity in these compounds was **103** > **101** > **48** (Table 4.2).

**Table 4.2**: Anti-MRSA activity of selected compounds isolated in this study

| **Compounds** | **MIC values in μg/mL** | | | | | |
|---|---|---|---|---|---|---|
| | **XU212** | **ATCC 25923** | **SA1199B** | **EMRSA-15** | **MRSA340702** | **MRSA274819** |
| **42** | - | - | - | - | - | - |
| **44** | - | - | - | - | - | - |
| **43** | - | - | - | - | - | - |
| **45** | 256 | - | 256 | - | 256 | 256 |
| **46** | 64 | 128 | - | - | 64 | 64 |
| **47** | 128 | - | 128 | - | 128 | 128 |
| **48** | - | - | - | - | - | 256 |
| **50** | - | - | - | - | - | - |
| **57** | - | 256 | - | - | - | - |
| **99** | - | - | - | - | - | 256 |
| **101** | 256 | 128 | - | - | 256 | 256 |
| **103** | 32 | 64 | - | - | 128 | 256 |
| **104** | - | 256 | 256 | - | - | 128 |
| **105** | - | - | - | - | - | - |
| **107** | - | 256 | - | 128 | 64 | 256 |
| **110** | - | 256 | - | 256 | - | - |
| **111** | - | 128 | - | 256 | 128 | 256 |
| **113** | - | 256 | - | 256 | - | - |
| **116** | - | - | - | - | - | - |
| **118** | - | - | - | - | - | - |
| Norfloxacin | 16 | 2 | 32 | 1 | 64 | 64 |

Compound **107** is an acridone alkaloid containing three methyl groups, two of which are oxygenated. This compound has been reported to have many pharmaceutical applications as antimicrobial, antiviral, antiplasmodial, antimalarial and anticancer agents and,

not surprisingly, as anti-MRSA agent (Sohrab *et al.*, 2004; Réthy *et al.*, 2007; Oliveira *et al.*, 2009; Amoa Onguéné *et al.*, 2013; Fouotsa *et al.*, 2013).

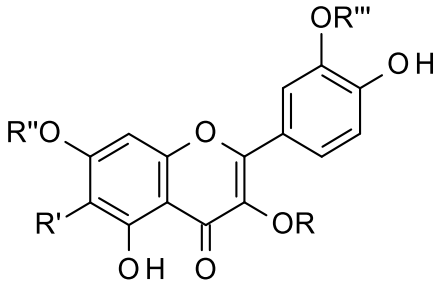


| Compounds | R | R’ | R’’ | R’’’ |
|---|---|---|---|---|
| **48** | Rutinosyl | H | H | H |
| **101** | Rutinosyl | H | H | Me |
| **103** | Rutinosyl | OH | Me | Me |

***Figure 4.4****: Structural similarities and differences in anti-MRSA flavonoids* ***48****,* ***101*** *and* ***103***

Compounds **110**, **111**, **113**, **116** and **118** are flavonoids. Compounds **110** and **111** exhibited three aromatic protons as ABX pattern in positions 2′, 5′ and 6′. Compound **110** has six oxygenated methyl groups and one free proton in position 6 while, compound **111** contains five oxygenated methyl groups with no substituent at positions 3 and 8. Compounds **116** and **118** are known as a symmetrical ring because it has only one methoxy group in position 4′. Compound **116** consists of five methoxy groups and position 3 is free while, compound **118** contains three methoxy groups, a hydroxyl group in position 5 and two free protons in positions 3 and 8. Among these tested flavonoids, compound **111** showed a distinct effect on the MRSA strains tested. Compounds **42**, **44**, **43**, **50**, **105**, **116** and **118** did not possess any anti-MRSA activity against the strain at the highest concentration used in this assay.

This seems to be the first report on the evaluation of the anti-MRSA effect of the isolated compounds, from *R. chalepensis*, *C. grandis* and *C. sinensis* against a number of MRSA strains.

# *Chapter 5*

# Scanning Electron Microscopic Analysis

## 5.1 What is scanning electron microscope (SEM)

A scanning electron microscope (SEM), a surfaceimaging tool, is an electron microscope that can generate images of a sample by scanning the surface with a focused beam of accelerated electrons. SEM was introduced to study the topography and composition of solid material, and was first commercially made available in 1965. This microscope consists of an electron optical column, a vacuum system, electronics, and software. The specimen chamber is large and there are lenses above the specimen to focus the beam of electrons onto the specimen surface. At the top of the column an electron gun is located, which produces the electron beam. This beam is scanned in a rectangular area on the specimen. The interaction between the beam of electrons and the specimen generates different signals, which are detected and produce the image. A secondary electron signal is the most commonly used signal and provides topographic information of the specimen surface (Hearle *et al.*, 1972; Lawes, 1987; Goldstein *et al.*, 2017).

## 5.2 Applications of scanning electron microscope

SEM is used in a number of industrial, commercial, research and forensic applications, some of which are outlined below.

### 5.2.1 Industrial uses

SEM is a useful instrument used to examine the surface structure of components and products in different industrial sectors such as microelectronics, semiconductors, medical devices and food processing. Moreover, SEM is considered as an important tool in the paper industry to study the paper strength which is generally affected by fibre quality, fibre bonding and network factors (Li, 2002). One of the new trends in applications of SEM is in the cosmetics industry, where it can provide information about the shape and size of tiny particles in cosmetic products before any product reaches the consumer. For instance, the small and round particles

give better impact on the consistency and performance of the product in mixing and flowing, than the overlarge or serrated particles (ATA, 2018)

### 5.2.2 Commercial

The industrialization or development of products required to study the composition and topography of products. For example, for optimal performance, stainless steel equally coated with specific chemicals. The SEM is considered as a helpful tool to detect any cracks, imperfections or contaminants on the surfaces of such coated products (ATA, 2018).

### 5.2.3 Research

The SEM has helped scientific research in universities in different fields. For example, biologists use SEM to gain an increased level of information on various biological specimens, and geologists apply this technique to learn more about crystalline structures, soil and rock**.** Moreover, SEM is considered as one of the fundamental instruments to study the nanoparticles in pharmaceutical research, e.g., in drug delivery, in dental studies, and in biomedical research. Additionally, the SEM has been used in food science, environmental studies, and forensic research (Carr, 1971; ATA, 2018).

## 5.3 The use of the scanning electron microscopy (SEM) in microbiology

This instrument can provide information about the micromorphology of microorganisms (Kaláb *et al.*, 2008) in spite of the fact that, very limited research has been conducted to study the microorganisms using the SEM (Carr, 1971; Marrie *et al.*, 1983; Franson *et al.*, 1984; Arroyo *et al.*, 2014). One of the earliest SEM research studies on bacteria (Williams and Davies, 1967) was performed at theUniversity of Liverpool where they recommended the use of the SEM to study the morphological features of microorganisms. Greenwood and O'Grady (1969) studied the effect of ampicillin on the surface of bacteria *Staplylococcus aureus* and *Streptococcus*

*pyogenes*. They found that the antibiotics had an effect on cell division of the bacteria and caused significant damage to the cell wall.

In the present study, the effect of many pure compounds, which had shown significant antimicrobial activity, was investigated by scanning electron microscopy.

## 5.4 Materials and methods

The isolation and antimicrobial activity of the purified compounds are described in *Chapters 2* and *3*. Six compounds, chalepensin (**46**), nobiletin (**57**), 6-hydroxy-rutin-3'-7-dimethyl ether (**103**), imperatorin (**104**), sinensetin (**111**) and arborinine (**107**) were tested. The effect of the pure compounds on the morphology of two Gram-positive bacteria, *Micrococcus luteus* and *Staphylococcus aureus*, two Gram-negative bacteria, *Escherichia coli* and *Pseudomonas aeruginosa*, and the fungus, *Candida albicans* was investigated.

The test samples were selected from microtitre plates at the MIC concentrations. 100 µL of 5% v/v unbuffered glutaraldehyde (Agar Scientific, UK) was added to the target well and fixed at 4$^{o}$C. After 24 hours fixation in glutaraldehyde, the samples were removed and passed through isopore membrane filters (0.4 micron filters from Merk), washed three times with distilled water and then air dried at room temperature. The filters were attached to aluminium specimen stubs with sticky carbon tabs (Agar Scientific, UK). All samples were sputter-coated with gold. They were then examined with an FEI InspectS scanning electron microscope using a range of operating voltages and working distances.

## 5.5 Results and discussion

In this study, the SEM was chosen because it is one of the useful tools, which has been used to study the morphological features of microorganisms for viewing the coated samples and detecting any surface damage or change. This study was designed to capture images of untreated

(control) and treated strains of *Escherichia coli*, *Candida albicans*, *Micrococcus luteus*, *Staphylococcus aureus* and *Pseudomonas aeruginosa*.

*Candida albicans* is one of the important opportunist pathogenic fungi that can cause serious systemic infections. The treatment of this microbe is considered as a big challenge because it is eukaryotic like the host cell (Endo *et al.*, 2010). *C. albicans* is a dimorphic yeast *i.e.* it can grow either as typical budding yeast cells or as hyphae depending on the environmental conditions (Sudbery *et al.*, 2004; Mayer *et al.*, 2013). In reality, it can produce a variety of cell forms and therefore it really should be described as polymorphic. Untreated *C. albicans* under the SEM showed budding cells and hyphae (Figure 5.1). The compounds **46**, **57**, **103**, **111** and **107** caused apparent damage to the surface of *C. albicans* (Figure 5.1), which was clear to detect under the SEM. Compounds **46**, **103** and **111** showed the same action against the surface of *C. albicans.* Some cells, following treatment with compound **57,** possessed particles or small swellings on the surface of the cell wall. Moreover, compound **107** generated a mucous layer around the cells and changed their shape.

The Gram-positive bacterial species, *Micrococcus luteus* has a primary coccoid shape. This organism can cause 'simple' infections particularly in individuals with suppressed immune systems (Bonjar, 2004). In the present study, a sample of the untreated strain of *M. luteus* was examined with the SEM (Figure 5.2). The growth of *M. luteus* was significantly inhibited by compounds **46**, **103**, **104**, **107** and **111.** The treated samples were all examined with the SEM (Figure 5.2). The compounds caused changes to the shape of the cells, increased the agglutinability of the cell walls and affected the progress of cell division (Figure 5.2). These effects could explain the possible mechanism of action of the compounds. There have been very few studies on the effects of antibacterial compounds on the cell surface of *M. luteus*

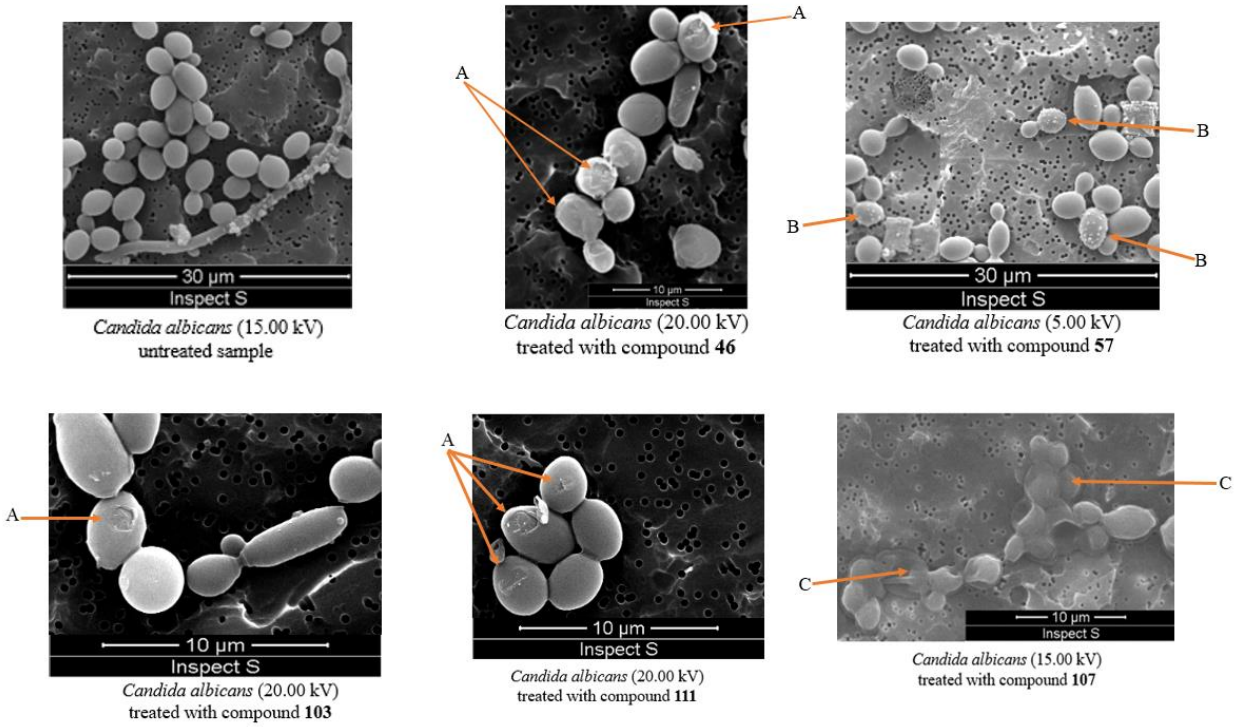


***Figure 5.1**: Untrated and treated samples of Candida albicans strain*

A: surface damage; B: surface particles/small swellings; C: mucous layer

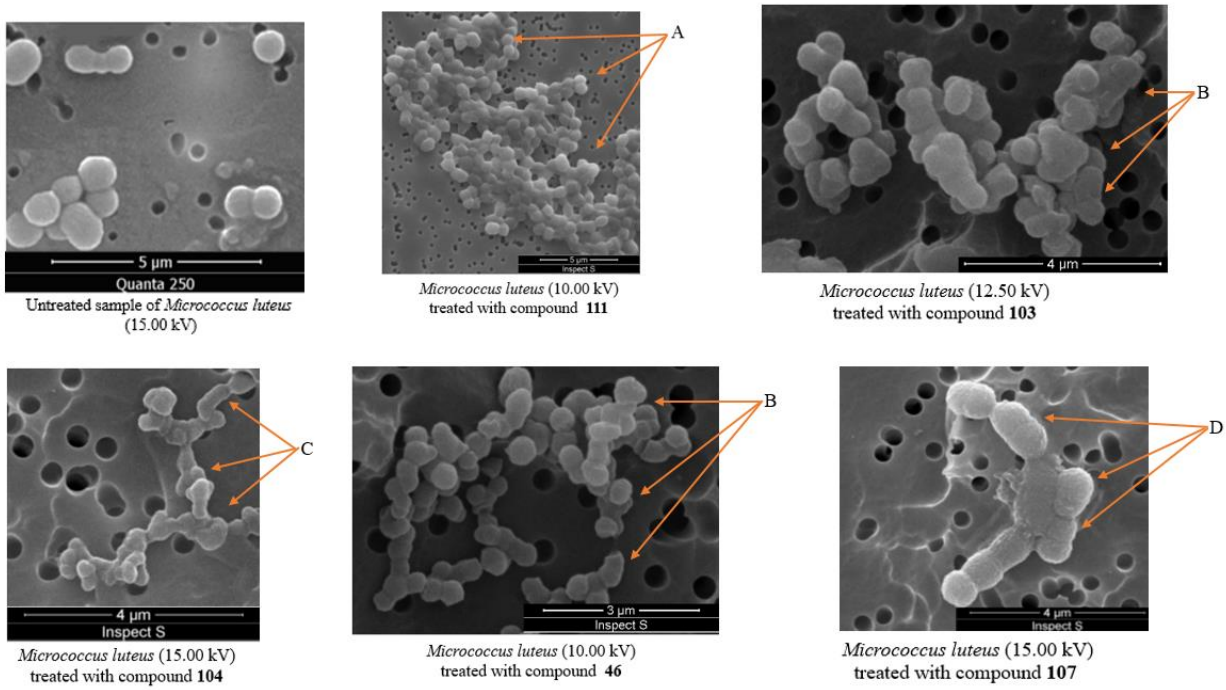


***Figure 5.2**: Untrated and treated samples of Micrococcus luteus*

A: shrinking cells; B: changing shape; C: elongated cells; D: swelling cells

(Greenwood and O'Grady, 1969a; Greenwood and O'Grady, 1972; Greenwood and O'Grady, 1973a; Greenwood and O'Grady, 1973b; Monodane *et al*., 1989; De Lillo *et al*., 1997).

*Staphylococcus aureus* is widely found on the skin or in the nose. In general, these bacteria cause simple skin infections. This bacterial infection can be fatal, however, if the infection is transferred to blood, bones, lungs or heart (Wertheim *et al.*, 2005; Taylor and Unakal, 2017). *S. aureus* cells are cocci and, following cell division, produce clusters of cells (Lowy, 1998; Taylor and Unakal, 2017). The untreated cells of *S. aureus* (Figure 5.3) and the treated samples (Figure 5.4) were examined with the SEM. Compound **46** inhibited the growth of *S. aureus* by producing cells of a variable and reduced size. Compound **111** affected cell division and cell shape. Compound **107** caused damage to the cell wall of some cells (Figure 5.3). The *S. aureus* cell wall consists of 80-90% of peptidoglycan, teichoic acids, and proteins (Umeda, 1988; Dmitriev *et al.*, 2004).

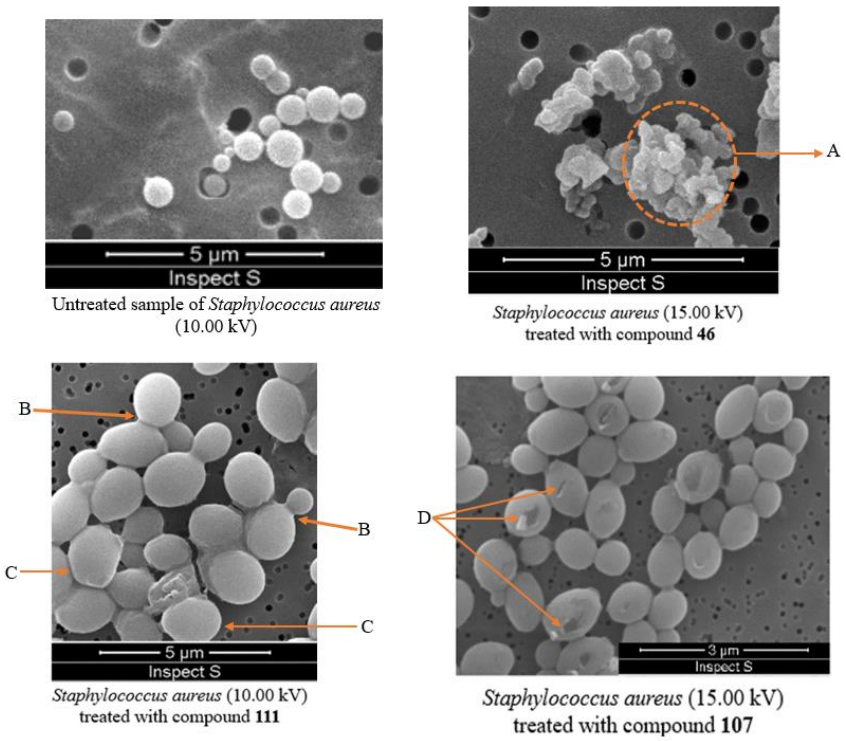


***Figure 5.3**: Untreated and treated samples of Staphylococcus aureus*
A: reduced size cells; B: cell division; C: variable shape; D: surface damage

*Pseudomonas aeruginosa* is a common environmental bacterial species and is classified as Gram-negative with a rod shape (0.5-0.8 × 1.5-8 μm) (Bennik, 1999). These bacteria can be isolated from soil, water, plants and animals (Stover *et al.*, 2000). It was first isolated from infections by Gessard in 1882 and identified as a pathogenic organism in 1890 by Charrin (Bodey *et al.*, 1983; Lyczak *et al.*, 2000) and in the meantime, research proved it to be responsible for community-acquired and hospital-acquired infections (Driscoll *et al.*, 2007). Both untreated and treated samples *P. aeruginosa* (Figure 5.4) were investigated using the SEM to observe the morphological effects of the selected compounds . Compounds **107** and **111** caused pronounced morphological damage, while the effect of compound **103** was simply on the bacterial surface or no fundamental difference could be detected between the untreated and treated samples.

Gram-negative bacterium *Escherichia coli* resides in the normal microflora in the human intestine, while some modified strains are pathogenic and cause health hazards. This rod-shaped bacterium is able to cause many infections such as in the central nervous system, urinary and gastrointestinal system (Nataro and Kaper, 1998; Dho-Moulin and Fairbrother, 1999). The normal strain of *E. coli* and the treated specimen (Figure 5.5) were analysed and compared under SEM to detect any surface damage. Compound (**107**) caused significant modifications on the surface of bacteria while compound **111** caused simple damage (Figure 5.5).

There are only a handful of preliminary studies available where SEM was used to study the effect of phytochemicals on the morphological aspects of microorganisms. To the best of our knowledge, this assay and the possible mechanism of action of selected compounds are reported here for the first time.

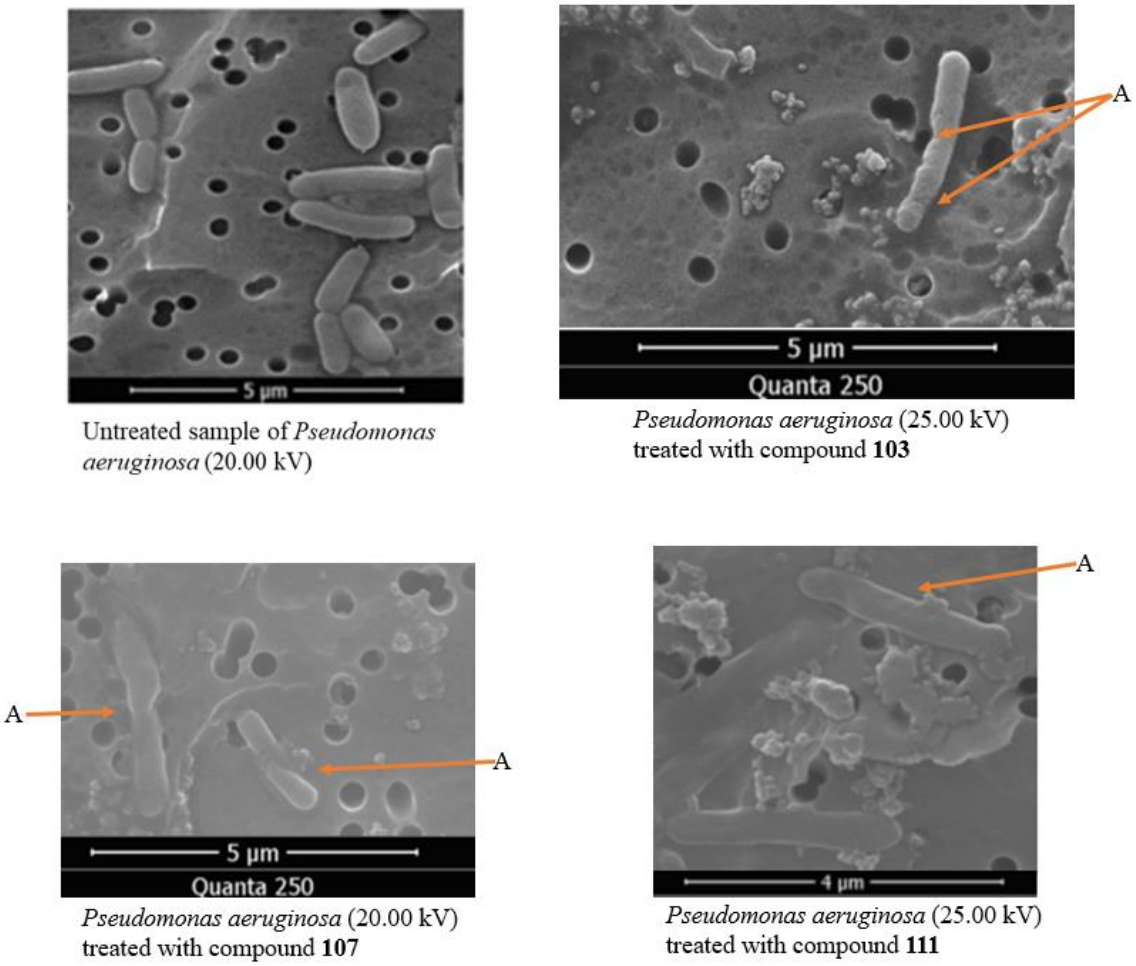


Untreated sample of *Pseudomonas aeruginosa* (20.00 kV)

*Pseudomonas aeruginosa* (25.00 kV) treated with compound **103**

*Pseudomonas aeruginosa* (20.00 kV) treated with compound **107**

*Pseudomonas aeruginosa* (25.00 kV) treated with compound **111**

***Figure 5.4**: Untrated and treated samples of Pseudomonas aeruginosa*

A: A: degradation of the cell wall

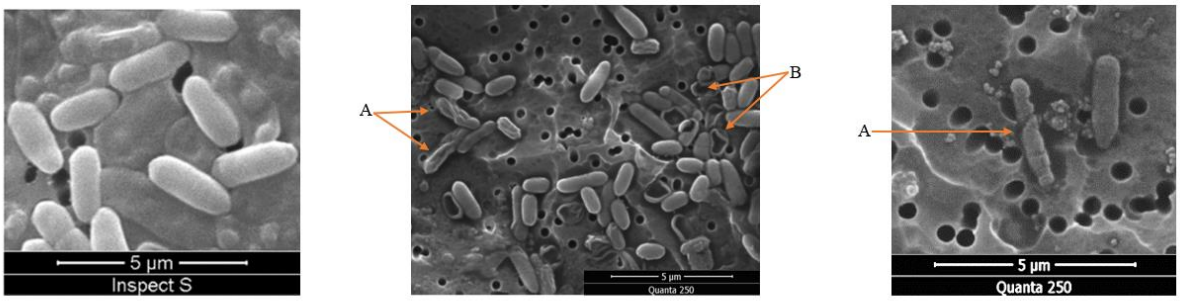


*Untreated Escherichia coli* (10.00 kV)

*Escherichia coli* (25.00 kV) treated with compound **111**

*Escherichia coli* (25.00 kV) treated with compound **107**

***Figure 5.5**: Untrated and treated samples of Escherichia coli*

A: A: degradation of the cell wall; B: Cell lysis

## 5.6 Conclusion

This new SEM assay was carried out in conjunction with the resazurin assay and in the presence of standard samples to detect any morphological changes. There was evidence of the cell wall degradation in the treated samples when compared with untreated samples, for example the effect of compound **107** on *P. aeruginosa* (Figure 5.4). This indicates that this compound could be damaging the cytoplasmic membrane proteins or it could be binding with the proteins. Moreover, the treated sample of *C. albicans* with compound **107** (Figure 5.1) created a mucilage layer around the cells, which may be a protective response. Some compounds caused shrinkage of cells or example compound **46** against *S. aureus* (Figure 5.3). On the other hand, some compounds caused swelling of the cells, for example compound **107** against *M. luteus* (Figure 5.2). This suggests that these particular compounds may have the ability to affect the osmotic concentration of the cells. . Moreover, compound **111** affected cell division of *S. aureus*, which could be a possible effect of the compounds on the cell-cycle phases.

One of the main benefits of this assay could potentially be a better understanding of structure-activity relationships among the tested phytochemicals based on their effects on the morphology of microbial cells.

# *Chapter 6*

# Conclusion and Recommendations

In the present study, three Iraqi medicinal plants from the Rutaceae family *viz*: *Citrus grandis* (leaves), *Citrus sinensis* (leaves and peel) and *Ruta chalepensis* (fruits, stems, leaves and roots) have been investigated for their phytochemical and antimicrobial properties following a bioassay-guided approach.

The antimicrobial activity of the selected plants was evaluated using the microtitre resazurin assay, and performed using two Gram-positive bacterial strains, *Micrococcus luteus* and *Staphylococcus aureus*, two Gram-negative bacterial strains *Escherichia coli* and *Pseudomonas aeruginosa* and one fungal strain *Candida albicans.*

The DCM extracts of *C. grandius* and *C. sinensis* leaves gave strong inhibitory activity against all of the bacterial strains used in this study. While, both of the DCM and the MeOH extracts of *C. sinensis* peel exhibited significant activity, the DCM extract was particularly potent against *M. luteus* (MIC $4.88 \times 10^{-3}$ mg/mL). The phytochemical studies on the active extracts/fractions of *C. grandis* and *C. sinensis* revealed fourteen flavonoids (Figure 3.80) including hesperidin (**50**), rutin (**48**), narirutin (**51**), rutin 3`-methyl ether (**101**), 3-methoxynobiletin (**110**), nobiletin (**57**), sinensetin (**111**), 6,7,8,3',4'-pentamethoxyl-flavone (**112**), demethylnobiletin (**113**), 5-desmethylsinensetin (**114**), cirsilineol (**115**), tangeritin (**116**), tetramethylscutellarein (**117**), salvigenin (**118**) and Marcitrus (**119)**, which is reported for the first time from the Iraqi species of *C. grandis.* Compound **119** is also reported for the first time as a natural product.

*Ruta chalepensis*, which is well known as a good source of a variety of secondary metabolites, e.g., alkaloids, coumarins, flavonoids and terpenes, has been investigated in the current project for the antimicrobial activity of its fruits, leaves, stems and roots. The *n*-hexane, DCM and MeOH extracts of the fruits, leaves, and stems showed notable antimicrobial activity, particularly, the leaf methanolic extracts against C. *albicans* (MIC $1.95 \times 10^{-2}$ mg/mL). While,

the root MeOH extract exhibited a low level of antimicrobial activity, both the *n*-hexane and the DCM extracts did not display any effect with the maximum concentration 10 mg/mL. The phytochemical studies carried out on *R. chalepensis* active parts/extracts/fractions led to the isolation of nineteen compounds (Figure 3.5) including bergapten (**43**), kokusaginine (**99**), isokokusaginine (**100**), skimmianine (**41**), rutin (**48**), rutin 3'-methyl ether (**101**), rutin 7,4'-dimethyl ether (**102**), 6-hydroxy-rutin-3'-7-dimethyl ether (**103**), chalepin (**45**), chalepensin (**46**), rutamarin (**47**), isopimpinellin (**44**), γ-fagarine (**42**), imperatorin (**104**), graveoline (**105**), ribalinium (**106**), arborinine (**107**), 3`,6-disinapoylsucrose (**108**) and hexadecane (**109**). To the best of our knowledge, this is the first report on the phytochemical studies on the fruits of the Iraqi species of *R. chalepensis*. Compounds **100-102** and **108** are reported here for the first time from *R. chalepensis*. Moreover, compound 6-hydroxy-rutin-3'-7-dimethyl ether (**103**) is a new natural product.

The compounds isolated from *C. grandis*, *C. sinensis* and *R. chalepensis* extracts exhibited potent antimicrobial activity. Compounds **42**, **43**, **44**, **45**, **46**, **47**, **48**, **50**, **57**, **99**, **101**, **103**, **104**, **105**, **107**, **109**, **110**, **111**, **112**, **113**, **114**, **115**, **116**, **117**, **118** and **119** were screened to evaluate their antimicrobial proprieties against the microbial strains mentioned earlier, and 1 mg/mL concentration was selected as the maximum dosage (stock concentration).

Compounds **42**, **43**, **44**, **45**, **46**, **47**, **48**, **50**, **57**, **99**, **101**, **103**, **104**, **105**, **107**, **110**, **111**, **113**, **116** and **118** were assessed for their anti-MRSA activity against five methicillin-resistant *Staphylococcus aureus* strains (SA1199B, XU212, MRSA340702, EMRSA-15MRSA274819) and standard strain (ATCC25923). Compounds **45**, **46**, **47**, **57**, **101**, **103**, **104**, **107**, **110**, **111** and **113** showed anti-MRSA efficacy.

It is important to understand the mechanism of action of any medication or bioactive compound including antimicrobials. This may help to determine how the tested compounds

inhibit the growth of microorganisms. Compounds **46**, **57**, **103**, **104**, **111** and **107** were investigated using the scanning election microscope (SEM) to understand the mechanism of action of these compounds. The results revealed how some of these compounds affected the morphological features of the microorganisms by damaging the cell wall, shrinking cells, dilating cells or affecting the cell division progress.

This seems to be the first report of a study on antimicrobial the mechanism of action of compounds directly from resazurin microtitre assay plates using the SEM and looking for morphological changes connected with the compound

Future studies:

- Investigation of the antimalarial activity and antioxidant properties of the isolated compounds. The previous studies on both of *R. chalepensis* and *Citrus* extracts were indicated their antimalarial and antioxidant activities but most of the isolated compounds need to be studied.
- Assessment of the performance of isolated compounds from *Citrus* in the cosmetics industry. As the *Citus* extracts are an important components in cosmetics and they contain different secondary metabolites, there is a need to identify the responsible compounds responsible for the activity.
- Synthesis of structural analogues of active antimicrobial compounds identified in this study. Plants extraxcts provided unique compounds, which is difficuilt to obtain and maybe with a simple synthesis these compounds can be produced in larger quantities to carry out more extensive antimicrobial studies toward there mechasims of action and structure activity realashionships.

## Refrencess:


Abu-Gharbieh, E. & Shehab, N. G. 2017. Therapeutic potentials of *Crataegus azarolus* var. eu-azarolus Maire leaves and its isolated compounds. *BMC Complementary and Alternative Medicine,* **17**, 218.

Abu-Shanab, B., Adwan, G. M., Jarrar, N., Abu-Hijleh, A. & Adwan, K. 2007. Antibacterial activity of four plant extracts used in Palestine in folkloric medicine against methicillin-resistant *Staphylococcus aureus*. *Turkish Journal of Biology,* **30,** 195-198.

Acquaviva, R., Iauk, L., Sorrenti, V., Lanteri, R., Santangelo, R., Licata, A., Licata, F., Vanella, A., Malaguarnera, M. & Ragusa, S. 2011. Oxidative profile in patients with colon cancer: effects of *Ruta chalepensis L*. *Eur Rev Med Pharmacol Sci,* **15,** 181-191.

Adamska-Szewczyk, A., Glowniak, K. & Baj, T. 2016. Furochinoline alkaloids in plants from Rutaceae family–a review. *Current Issues in Pharmacy and Medical Sciences,* **29,** 33-38.

Adjanohoun, J., Ahyi, M., Ake Assi, L., Alia, A., Amai, C., Gbile, Z., Johnson, C., Kakooko, Z., Lutakome, H. & Morakinyo, O. 1993.Traditional medicine and pharmacopoeia: contribution to ethnobotanical and floristic studies in Uganda. *Scientific, Technical and Research Commission of the Organization of the African Unity (OAU/STRC),* **433**.

Agyare, C., Obiri, D. D., Boakye, Y. D. & Osafo, N. 2013. Anti-inflammatory and analgesic activities of African medicinal plants. *Medicinal Plant Research in Africa.* Elsevier.

Akinyemi, K. O., Oladapo, O., Okwara, C. E., Ibe, C. C. & Fasure, K. A. 2005. Screening of crude extracts of six medicinal plants used in South-West Nigerian unorthodox medicine for anti-methicillin resistant *Staphylococcus aureus* activity. *BMC Complementary and Alternative Medicine,* **5,** 6.

Akowuah, G., Zhari, I., Norhayati, I., Sadikun, A. & Khamsah, S. 2004. Sinensetin, eupatorin, 3′-hydroxy-5, 6, 7, 4′-tetramethoxyflavone and rosmarinic acid contents and antioxidative effect of *Orthosiphon stamineus* from Malaysia. *Food Chemistry,* **87,** 559-566.

Alanis, A., Calzada, F., Cervantes, J., Torres, J. & Ceballos, G. 2005. Antibacterial properties of some plants used in Mexican traditional medicine for the treatment of gastrointestinal disorders. *Journal of Ethnopharmacology,* **100,** 153-157.

Alarif, W. M., Abdel-Lateff, A., Al-Abd, A. M., Basaif, S. A., Badria, F. A., Shams, M. & Ayyad, S.-E. N. 2013. Selective cytotoxic effects on human breast carcinoma of new

methoxylated flavonoids from *Euryops arabicus* grown in Saudi Arabia. *European Journal of Medicinal Chemistry*, **66,** 204.

Albach, R., Juarez, A. & Lime, B. 1969. Time of naringin production in grapefruit. *Journal of the American Society for Horticultural Science.*

Al-Bakri, A. G. & Afifi, F. U. 2007. Evaluation of antimicrobial activity of selected plant extracts by rapid XTT colorimetry and bacterial enumeration. *Journal of Microbiological Methods,* **68,** 19-25.

Al–Douri, N. A. 2014. Some important medicinal plants in Iraq. *ASJ International Journal of Advances in Herbal and Alternative Medicine,* **2,** 10-20.

Ali, A. A., Al-Rahwi, K. & Lindequist, U. 2004. Some medicinal plants used in Yemeni herbal medicine to treat malaria. *African Journal of Traditional, Complementary and Alternative Medicines,* **1,** 72-76.

Ali, A., Demirci, B., Kiyan, H. T., Bernier, U. R., Tsikolia, M., Wedge, D. E., Khan, I. A., Can Başer, K. H. & Tabanca, N. 2013. Biting deterrence, repellency, and larvicidal activity of *Ruta chalepensis* (Sapindales: Rutaceae) essential oil and its major individual constituents against mosquitoes. *Journal of Medical Entomology,* **50,** 1267-1274.

Ali-Shtayeh, M. & Abu Ghdeib, S. I. 1999. Antifungal activity of plant extracts against dermatophytes. *Mycoses,* **42,** 665-672.

Al-Said, M. S., Tariq, M., Al-Yahya, M., Rafatullah, S., Ginnawi, O. & Ageel, A. 1990. Studies on *Ruta chalepensis*, an ancient medicinal herb still used in traditional medicine. *Journal of Ethnopharmacology,* **28,** 305-312.

Al-Snafi, A. 2018. Traditional uses of Iraqi medicinal plants. *IOSR Journal Of Pharmacy,* **8**, 32-95. ISSN: 2319-4219.

Alzoreky, N. & Nakahara, K. 2003. Antibacterial activity of extracts from some edible plants commonly consumed in Asia. *International Journal of Food Microbiology,* **80,** 223-230.

Amoa Onguéné, P., Ntie-Kang, F., Lifongo, L. L., Ndom, J. C., Sippl, W. & Mbaze, L. M. A. 2013. The potential of anti-malarial compounds derived from African medicinal plants. Part I: A pharmacological evaluation of alkaloids and terpenoids. *Malaria Journal,* **12,** 449.

Arbab, I. A., Abdul, A. B., Aspollah, M., Abdelwahab, S. I., Ibrahim, M. Y. & Ali, Z. 2012. A review of traditional uses, phytochemical and pharmacological aspects of selected

members of *Clausena* genus (Rutaceae). *Journal of Medicinal Plants Research,* **6,** 5107-5118.

Arias, B. A. & Ramón-Laca, L. 2005. Pharmacological properties of citrus and their ancient and medieval uses in the Mediterranean region. *Journal of Ethnopharmacology,* **97,** 89-95.

Arooj, N., Dar, N. & Samra, Z. Q. 2014. Stable silver nanoparticles synthesis by *Citrus sinensis* (orange) and assessing activity against food poisoning microbes. *Biomedical and Environmental Sciences,* **10,** 815-818.

Arroyo, E., Enríquez, L., Sánchez, A., Ovalle, M. & Olivas, A. 2014. Scanning electron microscopy of bacteria *Tetrasphaera duodecadis*. *Scanning: The Journal of Scanning Microscopies,* **36,** 547-550.

Aschoff, J. K., Kaufmann, S., Kalkan, O., Neidhart, S., Carle, R. & Schweiggert, R. M. 2015. In vitro bioaccessibility of carotenoids, flavonoids, and vitamin C from differently processed oranges and orange juices [*Citrus sinensis* (L.) Osbeck]. *Journal of Agricultural and Food Chemistry,* **63,** 578-587.

Asgary, S. & Keshvari, M. 2013. Effects of *Citrus sinensis* juice on blood pressure. *ARYA Atherosclerosis,* **9,** 98.

Ata 2018. SEM & Imaging: The Applications and Practical Uses of Scanning Electron Microscopes. *ATA Scientific Instirument*. https://www.atascientific.com.au/sem-imaging-applications-practical-uses-scanning-electron-microscopes/.

Atrooz, O. M. 2009. The antioxidant activity and polyphenolic contents of different plant seeds extracts. *Pakistan Journal of Biological Sciences,* **12,** 1063.

Ayukekbong, J. A., Ntemgwa, M. & Atabe, A. N. 2017. The threat of antimicrobial resistance in developing countries: causes and control strategies. *Antimicrobial Resistance & Infection Control,* **6,** 47.

Babu-Kasimala, M., Tukue, M. & Ermias, R. 2014. Phytochemical screening and antibacterial activity of two common terrestrial medicinal plants *Ruta chalepensis* and *Rumex nervosus*. *Bali Medical Journal,* **3,** 116-121.

Balouiri, M., Sadiki, M. & Ibnsouda, S. K. 2016. Methods for in vitro evaluating antimicrobial activity: A review. *Journal of Pharmaceutical Analysis,* **6,** 71-79.

Bandatmakuru, S. & Arava, V. 2018. Novel synthesis of graveoline and graveolinine. *Synthetic Communications,* **48**, 20, 2635–2641.Taylor & Francis.

Barreca, D., Bellocco, E., Leuzzi, U. & Gattuso, G. 2014. First evidence of C-and O-glycosyl flavone in blood orange (*Citrus sinensis* (L.) Osbeck) juice and their influence on antioxidant properties. *Food Chemistry,* **149,** 244-252.

Bas, E., Recio, M. C., Giner, R. M., Máñez, S., López-Ginés, C., Gil-Benso, R. & Ríos, J. L. 2007. Demethylnobiletin inhibits delayed-type hypersensitivity reactions, human lymphocyte proliferation and cytokine production. *British Journal of Pharmacology,* **152,** 1272-1282.

Bay, D. C. & Turner, R. J. 2016. Small multidrug resistance efflux pumps. *Efflux-Mediated Antimicrobial Resistance in Bacteria.* 45-71. Springer. Adis, Cham.

Beer, M. F., Frank, F. M., Germán Elso, O., Ernesto Bivona, A., Cerny, N., Giberti, G., Luis Malchiodi, E., Susana Martino, V., Alonso, M. R., Patricia Sülsen, V. & Cazorla, S. I. 2016. Trypanocidal and leishmanicidal activities of flavonoids isolated from *Stevia satureiifolia* var. *satureiifolia. Pharmaceutical Biology,* **54,** 2188-2195.

Béjar, E., Bussmann, R., Roa, C. & Sharon, D. 2001. *Herbs of Southern Ecuador: a field guide to the medicinal plants of Vilcabamba*. Latino Herbal Press. ISBN : 0971520402.

Ben Sghaier, M., Pagano, A., Mousslim, M., Youssef, A., Kovacic, H. & Luis, J. 2016. Rutin inhibits proliferation, attenuates superoxide production and decreases adhesion and migration of human cancerous cells. *Biomedicine & Pharmacotherapy, **84***, 1972-1978.

Benavente-Garcia, O., Castillo, J., Marin, F., Ortuno, A. & Del Rio, J. 1997. Uses and properties of *Citrus* flavonoids. *Journal of Agricultural and Food Chemistry,* **45,** 4505-4515.

Bennaoum, Z. & Benhassaini, H. 2017. Autoécologie et place des espèces du genre Ruta dans les formations végétales en Algérie nord-occidentale. *ecologia Mediterranea,* **43,** 1.

Bennik, M. H. J. 1999. Pseudomonas/*Pseudomonas aeruginosa*. *In:* Robinson, R. K. (ed.) *Encyclopedia of Food Microbiology.* Oxford: Elsevier. eBook ISBN: 9780123847331.

Bhat, G. P. & Surolia, N. 2001. In vitro antimalarial activity of extracts of three plants used in the traditional medicine of India. *The American Journal of Tropical Medicine and Hygiene,* **65,** 304-308.

Bocco, A., Cuvelier, M.-E., Richard, H. & Berset, C. 1998. Antioxidant activity and phenolic composition of *Citrus* peel and seed extracts. *Journal of Agricultural and Food Chemistry,* **46,** 2123-2129.

Bodey, G. P., Bolivar, R., Fainstein, V. & Jadeja, L. 1983. Infections caused *by Pseudomonas aeruginosa. Reviews of Infectious Diseases,* **5,** 279-313.

Bonjar, G. S. 2004. Evaluation of antibacterial properties of Iranian medicinal-plants against *Micrococcus luteus*, *Serratia marcescens*, *Klebsiella pneumoniae* and *Bordetella bronchoseptica*. *Asian Journal of Plant Sciences*, **3,** 82-86.

Boo, K.-H., Kim, H.-N., Riu, K.-Z., Kim, Y.-W., Cho, M.-J. & Kim, S.-M. 2007. Analysis of the limonoid contents of dangyuja (*Citrus* spp.) by liquid chromatography-mass spectrometry (LC-MS). *Applied Biological Chemistry*, **50,** 238-243.

Bouabidi, W., Hanana, M., Gargouri, S., Amri, I., Fezzani, T., Ksontini, M., Jamoussi, B. & Hamrouni, L. 2015. Chemical composition, phytotoxic and antifungal properties of *Ruta chalepensis L*. essential oils. *Natural Product Research,* 29**,** 864-868.

Boyd, D. R., Sharma, N. D., Carroll, J. G., Loke, P. L., O'dowd, C. R. & Allen, C. C. R. 2013. Biphenyl dioxygenase-catalysed cis -dihydroxylation of tricyclic azaarenes: chemoenzymatic synthesis of arene oxide metabolites and furoquinoline alkaloids. *RSC Advances*, **3,** 10944-10955.

Breitmaier, E. & Sinnema, A. 1993. *Structure elucidation by NMR in organic chemistry: A practical guide*. First edition, Wiley and Sons Ltd. West Sussex, England.

Burroughs, T., Najafi, M., Lemon, S. M. & Knobler, S. L. 2003. *The resistance phenomenon in microbes and infectious disease vectors: implications for human health and strategies for containment: workshop summary*. National Academies Press. ISBN: 0-309-50746-4.

Caengprasath, N., Ngamukote, S., Mäkynen, K. & Adisakwattana, S. 2013. The protective effects of pomelo extract (*Citrus grandis* L. Osbeck) against fructose-mediated protein oxidation and glycation. *Experimental and Clinical Sciences journal*, **12,** 491.

Cardile, V., Graziano, A. C. E. & Venditti, A. 2015. Clinical evaluation of Moro (*Citrus sinensis* (L.) Osbeck) orange juice supplementation for the weight management. *Natural Product Research*, **29,** 2256-2260.

Carr, K.E., 1971. Applications of scanning electron microscopy in biology. In *International review of cytology*, **30**, 183-255. Academic Press.

Carson, C.F., Mee, B.J. and Riley, T.V., 2002. Mechanism of action of Melaleuca alternifolia (tea tree) oil on Staphylococcus aureus determined by time-kill, lysis, leakage, and salt tolerance assays and electron microscopy. Antimicrobial agents and chemotherapy, 46(6),1914-1920.

CDC 2019. Methicillin-resistant *Staphylococcus aureus* (MRSA). *Centers for Disease Control and Prevention.* U.S. Department of Health & Human Services.

Chakravarty, H. L. 1976. *Plant wealth of Iraq: A dictionary of economic plants.* Baghdad: Ministry of Agriculture & Agrarian *Reform,* **1**.

Chase, M. W., Morton, C. M. & Kallunki, J. A. 1999. Phylogenetic relationships of Rutaceae: a cladistic analysis of the subfamilies using evidence from RBC and ATP sequence variation. *American Journal of Botany,* **86,** 1191-1199.

Chen, C., Huang, Y., Huang, F., Wang, C. W. & Ou, J. 2001. Water-soluble glycosides from *Ruta graveolens*. *Journal of Natural Products,* **64,** 990-992.

Chen, X.-M., Tait, A. R. & Kitts, D. D. 2017. Flavonoid composition of orange peel and its association with antioxidant and anti-inflammatory activities. *Food Chemistry,* **218,** 15-21.

Chen, Y., Liu, X., Pan, R., Zhu, X., Steinmetz, A., Liao, Y.-H., Wang, N., Peng, B. & Chang, Q. 2013. Intestinal transport of 3,6 '-disinapoylsucrose, A major active component of *Polygala tenuifolia*, using Caco-2 cell monolayer and *in situ* rat intestinal perfusion models. *Planta medica,* ***79*** (15), 1434-1439.

Chiba, H., Uehara, M., Wu, J., Wang, X., Masuyama, R., Suzuki, K., Kanazawa, K. & Ishimi, Y. 2003. Hesperidin, a *Citrus* flavonoid, inhibits bone loss and decreases serum and hepatic lipids in ovariectomized mice. *The Journal of Nutrition,* **133**, 1892-1897.

Chinou, I. 2008. Primary and secondary metabolites and their biological activity. *Chromatographic Science Series,* **99,** 59.

Cirmi, S., Maugeri, A., Ferlazzo, N., Gangemi, S., Calapai, G., Schumacher, U. & Navarra, M. 2017. Anticancer potential of *Citrus* juices and their extracts: A systematic review of both preclinical and clinical studies. *Frontiers in Pharmacology,* **8,** 420.

Connell, J. 2008. *The global health care chain: from the Pacific to the world*. Routledge. Taylorfrancis.

Correa, M. C., Palero, F., Dubreuil, N., Etienne, L., Hulak, M., Tison, G., Warot, S., Crochard, D., Ris, N. & Kreiter, P. 2016. Molecular characterization of parasitoids from armored scales infesting *Citrus* orchards in Corsica, France. *BioControl,* **61,** 639-647. Springer.

Cosgrove, S. E. 2006. The relationship between antimicrobial resistance and patient outcomes: mortality, length of hospital stay, and health care costs. *Clinical Infectious Diseases,* **42,** S82-S89.

Cowan, M. M. 1999. Plant products as antimicrobial agents. *Clinical Microbiology Reviews,* **12,** 564-582.

Cox, R., Conquest, C., Mallaghan, C. & Marples, R. 1995. A major outbreak of methicillin-resistant *Staphylococcus aureus* caused by a new phage-type (EMRSA-16). *Journal of Hospital Infection,* **29,** 87-106.

Cox, S., Gustafson, J., Mann, C., Markham, J., Liew, Y. C., Hartland, R., Bell, H. C., Warmington, J. & Wyllie, S. G. 1998. Tea tree oil causes K+ leakage and inhibits respiration in Escherichia coli. *Letters in Applied Microbiology,* **26,** 355-358.

Cushnie, T. T. & Lamb, A. J. 2005. Antimicrobial activity of flavonoids. *International Journal of Antimicrobial Agents,* **26,** 343-356.

Damsud, T., Grace, M., Adisakwattana, S. & Phuwapraisirisan, P. 2014. Orthosiphol A from the aerial parts of *Orthosiphon aristatus* is putatively responsible for hypoglycemic effect via α-glucosidase inhibition. *Natural product communications,* **9** (5), 1934578X1400900512.

Davenport, T. 1990. *Citrus* flowering. *Horticultural Reviews,* 12**,** 349-408.

David, M. Z. & Daum, R. S. 2010. Community-associated methicillin-resistant *Staphylococcus aureus*: epidemiology and clinical consequences of an emerging epidemic. *Clinical Microbiology Reviews,* **23,** 616-687.

Davidson, P. M., Taylor, T. M. & Schmidt, S. E. 2013. Chemical preservatives and natural antimicrobial compounds. *Food microbiology,* 765-801. American Society of Microbiology.

De Amicis, F., Aquila, S., Morelli, C., Guido, C., Santoro, M., Perrotta, I., Mauro, L., Giordano, F., Nigro, A., Andò, S. And Panno, M.L. 2015. Bergapten drives autophagy through the up-regulation of PTEN expression in breast cancer cells. *Molecular Cancer,* **14,** 130.

De Castro, M. L. & Priego-Capote, F. 2010. Soxhlet extraction: Past and present panacea. *Journal of Chromatography A,* 1217, 2383-2389.

De Feo, V., De Simone, F. & Senatore, F. 2002. Potential allelochemicals from the essential oil of *Ruta graveolens*. *Phytochemistry,* **61,** 573-578.

De La Torre, B. G. & Albericio, F. 2018. The pharmaceutical industry in 2017. An analysis of fda drug approvals from the perspective of molecules. *Molecules,* **23,** 533.

De Lillo, A., Quirós, L. M. & Fierro, J. F. 1997. Relationship between antibacterial activity and cell surface binding of lactoferrin in species of genus *Micrococcus*. *FEMS Microbiology Letters*, **150,** 89-94.

De Lima Procópio, R.E., da Silva, I.R., Martins, M.K., de Azevedo, J.L. and de Araújo, J.M., 2012. Antibiotics produced by Streptomyces. *The Brazilian Journal of infectious diseases*, *16*(5), 466-471.

De Sa, R. Z., Rey, A., Argañaraz, E. & Bindstein, E. 2000. Perinatal toxicology of *Ruta chalepensis* (Rutaceae) in mice. *Journal of Ethnopharmacology*, **69,** 93-98.

Debbab, A., Aly, A. H., Lin, W. H. & Proksch, P. 2010. Bioactive compounds from marine bacteria and fungi. *Microbial Biotechnology,* **3,** 544-563.

Dehghan, H., Sarrafi, Y., Salehi, P. & Nejad Ebrahimi, S. 2017. α- Glucosidase inhibitory and antioxidant activity of furanocoumarins from *Heracleum persicum*. *Medicinal Chemistry Research*, **26,** 849-855.

Dhale, D., K. Markandeya, S. & Niturkar, Y. D. 2010. Standardization of homoeopathic drug *Ruta graveolens* L. *Journal of Phytology*, **2**, 3.

Dho-Moulin, M. & Fairbrother, J. M. 1999. Avian pathogenic *Escherichia coli* (APEC). *Veterinary Research,* **30,** 299-316.

Dias, D. A., Urban, S. & Roessner, U. 2012. A historical overview of natural products in drug discovery. *Metabolites,* **2,** 303-336.

Diwan, R. and Malpathak, N., 2011. *Ruta graveolens* cultures as screening resources for phyto-pharmaceuticals: bio-prospecting, metabolic phenotyping and multivariate analysis. *Jaime A. Teixeira da Silva, Bioremediation (eds) Biodiversity and bioavailability. Global Science Books*, **5**, 1-9.

Dmitriev, B. A., Toukach, F. V., Holst, O., Rietschel, E. & Ehlers, S. 2004. Tertiary structure of *Staphylococcus aureus* cell wall murein. *Journal of Bacteriology,* **186,** 7141-7148.

Dreyer, D. L. 1966. *Citrus* bitter principles—V.: Botanical distribution and chemotaxonomy in the Rutaceae. *Phytochemistry,* **5,** 367-378.

Driscoll, J. A., Brody, S. L. & Kollef, M. H. 2007. The epidemiology, pathogenesis and treatment of *Pseudomonas aeruginosa* infections. *Drugs,* **67,** 351-368.

Drummond, A. J. & Waigh, R. D. 2000. The development of microbiological methods for phytochemical screening. *Recent Research Developments in Phytochemistry,* **4**, 143-152.

Dugo, G. & Di Giacomo, A. 2002. *Citrus*: the genus *Citrus*, medicinal and aromatic plants industrial profiles. *Taylor & Francis, New York,* **26**, 195-201.

Dugrand-Judek, A., Olry, A., Hehn, A., Costantino, G., Ollitrault, P., Froelicher, Y. & Bourgaud, F. 2015. The distribution of coumarins and furanocoumarins in *Citrus* species closely matches *Citrus* phylogeny and reflects the organization of biosynthetic pathways. *PLOS one,* **10,** 0142757.

Duraipandiyan, V., Ayyanar, M. & Ignacimuthu, S. 2006. Antimicrobial activity of some ethnomedicinal plants used by Paliyar tribe from Tamil Nadu, India. *BMC Complementary and Alternative Medicine,* **6,** 35.

Ecocrop 2018. *Citrus grandis*. http://ecocrop.fao.org/ecocrop/srv/en/cropView?id=712.

El Sayed, K., Al-Said, M. S., El-Feraly, F. S. & Ross, S. A. 2000. New quinoline alkaloids from *Ruta chalepensis*. *Journal of Natural Products,* **63,** 995-997.

Elaine Monteiro, C.-L., James Andreas, M., Marcelo Rogério Da, S., Luis Octávio, R., Simone Yasue, S., Norberto Peporine, L., Maria Cláudia Marx, Y., José Rubens, P. & Vanderlan Da Silva, B. 2010. Alkaloids from stems of *Esenbeckia leiocarpa* Engl. (Rutaceae) as potential treatment for Alzheimer Disease. *Molecules,* **15,** 9205-9213.

Elhassan, M. M., Ozbak, H. A., Hemeg, H. A., Elmekki, M. A. & Ahmed, L. M. 2015. Absence of the mecA gene in methicillin resistant *Staphylococcus aureus* isolated from different clinical specimens in shendi city, Sudan. *BioMed Research International,* 2015.

Elumalai, K. & Id, K. 2016. Antioxidant activity and phytochemical screening of different solvent extracts Cluasena excavata burm F. *Rutaceae*. *MOJ Ecology & Environmental Sciences,* **1,** 1.

Encyclopedia Britannica. 2019. *Citrus*. https://www.britannica.com/plant/Citrus.

Endo, E. H., Cortez, D. a. G., Ueda-Nakamura, T., Nakamura, C. V. & Dias Filho, B. P. 2010. Potent antifungal activity of extracts and pure compound isolated from pomegranate peels and synergism with fluconazole against *Candida albicans*. *Research in Microbiology,* **161,** 534-540.

Enright, M. C., Robinson, D. A., Randle, G., Feil, E. J., Grundmann, H. & Spratt, B. G. 2002. The evolutionary history of methicillin-resistant *Staphylococcus aureus* (MRSA). *Proceedings of the National Academy of Sciences,* **99,** 7687-7692.

Espina, L., Somolinos, M., Lorán, S., Conchello, P., García, D. & Pagán, R. 2011. Chemical composition of commercial *Citrus* fruit essential oils and evaluation of their

antimicrobial activity acting alone or in combined processes. *Food Control,* **22,** 896-902.

Etebu, E. & Nwauzoma, A. 2014. A review on sweet orange (*Citrus sinensis* L Osbeck): health, diseases and management. *American Journal of Research Communication,* **2**, 33-70.

Fatima, A., Khanam, S., Rahul, J.S., Naz, F., Ali, F. & Siddique, Y.H., 2017. Protective effect of tangeritin in transgenic Drosophila model of Parkinson's disease. *Front Biosci,* **9**, 44-53.

Favela-Hernández, J. M. J., González-Santiago, O., Ramírez-Cabrera, M. A., Esquivel-Ferriño, P. C. & Camacho-Corona, M. D. R. 2016. Chemistry and Pharmacology of *Citrus sinensis*. *Molecules,* **21,** 247.

Fejzić, A. & Ćavar, S. 2014. Phenolic Compounds and Antioxidant Activity of Some Citruses. *Bulletin of the Chemists and Technologists of Bosnia and Herzegovina,* **42,** 1-4.

Fernandez-Lopez, R., Machon, C., Longshaw, C. M., Martin, S., Molin, S., Zechner, E. L., Espinosa, M., Lanka, E. & De La Cruz, F. 2005. Unsaturated fatty acids are inhibitors of bacterial conjugation. *Microbiology,* **151,** 3517-3526.

Flamini, G., Cioni, P. L. & Morelli, I. 2003. Use of solid-phase micro-extraction as a sampling technique in the determination of volatiles emitted by flowers, isolated flower parts and pollen. *Journal of Chromatography a,* **998,** 229-233.

Fouotsa, H., Mbaveng, A., Mbazoa Djama, C., Nkengfack, A., Farzana, S., M Iqbal, C., Meyer, J., Lall, N. & Kuete, V. 2013. *Antibacterial constituents of three Cameroonian medicinal plants: Garcinia nobilis, Oricia suaveolens and Balsamocitrus camerunensis*. *BMC complementary and alternative medicine*, **13**, 1, 81.

Franson, T. R., Sheth, N. K., Rose, H. D. & Sohnle, P. G. 1984. Scanning electron microscopy of bacteria adherent to intravascular catheters. *Journal of Clinical Microbiology,* **20,** 500-505.

Funaguchi, N., Ohno, Y., La, B. L. B., Asai, T., Yuhgetsu, H., Sawada, M., Takemura, G., Minatoguchi, S., Fujiwara, T. & Fujiwara, H. 2007. Narirutin inhibits airway inflammation in an allergic model. *Clinical and Experimental Pharmacology and Physiology,* **34,** 766-770.

Gancel, A.-L., Ollitrault, P., Froelicher, Y., Tomi, F., Jacquemond, C., Luro, F. & Brillouet, J.-M. 2005. Leaf volatile compounds of six *Citrus* somatic allotetraploid hybrids

originating from various combinations of lime, lemon, citron, sweet orange, and grapefruit. *Journal of Agricultural and Food Chemistry,* **53,** 2224-2230.

Garcia, A. R., Amaral, A. C. F., Azevedo, M. M., Corte-Real, S., Lopes, R. C., Alviano, C. S., Pinheiro, A. S., Vermelho, A. B. & Rodrigues, I. A. 2017. Cytotoxicity and anti-Leishmania amazonensis activity of *Citrus sinensis* leaf extracts. *Pharmaceutical Biology,* **55,** 1780-1786.

Garg, A., Garg, S., Zaneveld, L. J. D. & Singla, A. K. 2001. Chemistry and pharmacology of the *Citrus* bioflavonoid hesperidin. Chichester, UK. *Phytotherapy research*, **15**, 8, 655-669.

Gaston, J. L., Grundon, M. F. & James, K. J. 1980. Quinoline alkaloids. Part 19. Synthesis of O -methylptelefolonium iodide and (±)-dubinidine. *Journal of the Chemical Society, Perkin Transactions 1***,** 1136-1138.

Gattuso, G., Barreca, D., Gargiulli, C., Leuzzi, U. & Caristi, C. 2007. Flavonoid composition of *Citrus* juices. *Molecules,* **12,** 1641-1673.

Ghazanfar, S. A. 1994. *Handbook of Arabian medicinal plants*, CRC press.

Ghosh, S., Bishayee, K. & Khuda-Bukhsh, A. 2014. Graveoline Isolated from Ethanolic Extract of *Ruta graveolens* Triggers Apoptosis and Autophagy in Skin Melanoma Cells: A Novel Apoptosis-Independent Autophagic Signaling Pathway. *Phytotherapy research*, **28**, 8, 1153-1162.

Gibbons, S., 2012. An introduction to planar chromatography and its application to natural products isolation. *In Natural Products Isolation* (117-153). Humana Press.

Gil-Izquierdo, A., Gil, M. I., Ferreres, F. & Tomás-Barberán, F. A. 2001. In vitro availability of flavonoids and other phenolics in orange juice. *Journal of Agricultural and Food Chemistry*, **49,** 1035-1041.

Giovanni, D. & Angelo, D. G. 2002. *Citrus*, The genus *Citrus Book*.

Goes, T. C., Antunes, F. D., Alves, P. B. & Teixeira-Silva, F. 2012. Effect of sweet orange aroma on experimental anxiety in humans. *The Journal of Alternative and Complementary Medicine,* **18,** 798-804.

Goldstein, F., Chumpitaz, J., Guevara, J., Papadopoulou, B., Acar, J. & Vieu, J. 1986. Plasmid-mediated resistance to multiple antibiotics in Salmonella typhi. *Journal of Infectious Diseases,* **153,** 261-265.

Goldstein, J. I., Newbury, D. E., Michael, J. R., Ritchie, N. W., Scott, J. H. J. & Joy, D. C. 2017. *Scanning Electron Microscopy and X-ray Microanalysis*, Springer. ISBN978-1-4939-6676-9. DOI: 10.1007/978-1-4939-6676-9.

Gómez-Ariza, J., Garcia-Barrera, T. & Lorenzo, F. 2004. Determination of flavour and off-flavour compounds in orange juice by on-line coupling of a pervaporation unit to gas chromatography–mass spectrometry. *Journal of Chromatography A,* **1047,** 313-317.

Gómez-Ariza, J., Villegas-Portero, M. & Bernal-Daza, V. 2005. Characterization and analysis of amino acids in orange juice by HPLC–MS/MS for authenticity assessment. *Analytica Chimica Acta,* **540,** 221-230.

Gomez-Flores, R., Gloria-Garza, M. A., De La Garza-Ramos, M. A., Quintanilla-Licea, R. & Tamez-Guerra, P. 2016. Antimicrobial effect of chalepensin against *Streptococcus mutans*. *Journal of Medicinal Plants Research,* **10,** 631-634.

Gonzalez, A., Darias, V., Alonso, G., Boada, J. & Rodriguez–Luis, F. 1977. Cytostatic activity of some Canary Islands species of Rutaceae. *Planta Medica,* **31,** 351-356.

Gonzalez-Trujano, M., Carrera, D., Ventura-Martinez, R., Cedillo-Portugal, E. & Navarrete, A. 2006. Neuropharmacological profile of an ethanol extract of *Ruta chalepensis* L. in mice. *Journal of Ethnopharmacology,* **106,** 129-135.

Gootz, T. D. 1990. Discovery and development of new antimicrobial agents. *Clinical Microbiology Reviews,* **3,** 13-31.

Goudeau, D., Uratsu, S. L., Inoue, K., Goes Dasilva, F., Leslie, A., Cook, D., Reagan, R. L. & Dandekar, A. M. 2008. Tuning the orchestra: Selective gene regulation and orange fruit quality. *Plant Science,* **174,** 310-320.

Goulas, V. & Manganaris, G. A. 2012. Exploring the phytochemical content and the antioxidant potential of *Citrus* fruits grown in Cyprus. *Food Chemistry,* **131,** 39-47.

Gould, I. M., David, M. Z., Esposito, S., Garau, J., Lina, G., Mazzei, T. & Peters, G. 2012. New insights into meticillin-resistant *Staphylococcus aureus* (MRSA) pathogenesis, treatment and resistance. *International Journal of Antimicrobial Agents,* **39,** 96-104.

Gray, A. I. & Waterman, P. G. 1978. Coumarins in the Rutaceae. *Phytochemistry,* **17,** 845-864.

Graziola, F., Marcílio Candido, T., Oliveira, C., D'almeida Peres, D., Issa, M., Mota, J., Rosado, C., Consiglieri, V., Kaneko, T., Velasco, M. & Baby, A. R. 2016. Gelatin-based microspheres crosslinked with glutaraldehyde and rutin oriented to cosmetics. *Brazilian Journal of Pharmaceutical Sciences, **52***, 4, 603-612.

Groppo, M., Pirani, J. R., Salatino, M. L., Blanco, S. R. & Kallunki, J. A. 2008. Phylogeny of Rutaceae based on twononcoding regions from cpDNA. *American Journal of Botany*, 95**,** 985-1005.

Greenwood, D. & O'grady, F. 1969a. A comparison of the effects of ampicillin on *Escherichia coli* and *Proteus mirabilis*. Journal of medical microbiology, **2**, 435-441.

Greenwood, D. & O'grady, F. 1969b. Antibiotic-induced surface changes in microorganisms demonstrated by scanning electron microscopy. Science, **163**, 1076-1078.

Greenwood, D. & O'grady, F. 1972. Scanning electron microscopy of *Staphylococcus aureus* exposed to some common anti-staphylococcal agents. Microbiology, **70**, 263-270.

Greenwood, D. & O'grady, F. 1973a. The two sites of penicillin action in *Escherichia coli*. Journal of Infectious Diseases, **128**, 791-794.

Greenwood, D. & O'grady, F. 1973b. Comparison of the responses of *Escherichia coli* and Proteus Hearle, J., Sparrow, J. & Cross, P. 1972. The use of the scanning electron microscope'; 1972. Pergamon Press Ltd, United-Kingdom.

Guardia, T., Rotelli, A. E., Juarez, A. O. & Pelzer, L. E. 2001. Anti-inflammatory properties of plant flavonoids. Effects of rutin, quercetin and hesperidin on adjuvant arthritis in rat. *Il Farmaco,* **56,** 683-687.

Gunatilaka, A. L. 2006. Natural products from plant-associated microorganisms: distribution, structural diversity, bioactivity, and implications of their occurrence. *Journal of Natural Products,* **69,** 509-526.

Gunatilaka, A. L., Kingston, D. G., Wijeratne, E. K., Bandara, B. R., Hofmann, G. A. & Johnson, R. K. 1994. Biological activity of some coumarins from Sri Lankan Rutaceae. *Journal of Natural Products,* **57,** 518-520.

Günaydin A, K. & Savci B, S. 2005. Phytochemical studies on *Ruta chalepensis* (LAM.) lamarck. *Natural Product Research,* **19,** 203-210.

Günther, H. 2013. *NMR spectroscopy: basic principles, concepts and applications in chemistry*, John Wiley & Sons. ISBN: 978-3-527-33004-1.

Gyawali, R. & Ibrahim, S. A. 2014. Natural products as antimicrobial agents. *Food Control,* **46,** 412-429.

Gyawali, R., Hayek, S. & Ibrahim, S. 2014. Plant extracts as antimicrobials in food products: Mechanisms of action, extraction methods, and applications. *Handbook of natural antimicrobials for food safety and quality*, 49-68. Woodhead Publishing: Sawston, UK.

Hamdan, D., El-Readi, M. Z., Tahrani, A., Herrmann, F., Kaufmann, D., Farrag, N., El-Shazly, A. & Wink, M. 2011. Chemical composition and biological activity of *Citrus jambhiri* Lush. *Food Chemistry,* **127,** 394-403.

Hammoud, L., Seghiri, R., Benayache, S., Mosset, P., Lobstein, A., Chaabi, M., León, F., Brouard, I., Bermejo, J. & Benayache, F. 2012. A new flavonoid and other constituents from *Centaurea nicaeensis* All. var. *walliana* M. *Natural Product Research,* **26,** 203-208.

Han, S., Kim, H. M., Lee, J. M., Mok, S.-Y. & Lee, S. 2010. Isolation and identification of polymethoxyflavones from the hybrid *Citrus*, Hallabong. *Journal of Agricultural and Food Chemistry,* **58,** 9488-9491.

Harborne, J. B. 2013. The flavonoids: advances in research since 1980, Springer.

Havsteen, B. H. 2002. The biochemistry and medical significance of the flavonoids. *Pharmacology & Therapeutics*, **96,** 67-202.

He, H., Cai, X., Guan, X., Hu, F. & Xie, L. 2003. Antifungal protein from endophytic bacteria BS-2 and its control effect against anthracnose. *Acta Phytopathol Sin,* **33,** 373-378.

Heggers, J. P., Velanovich, V., Robson, M. C., Zoellner, S. M., Schileru, R., Boertman, J. & Niu, X. 1987. Control of burn wound sepsis: a comparison of in vitro topical antimicrobial assays. *The Journal of Trauma,* **27,** 176-179.

Heywood, V. H., Brummitt, R. K., Culham, A. & Seberg, O. 2007. Flowering plant families of the world. ISBN: 1554072069, 9781554072064. Firefly Books.

Hillebrand, S., Schwarz, M. & Winterhalter, P. 2004. Characterization of anthocyanins and pyranoanthocyanins from blood orange [*Citrus sinensis* (L.) Osbeck] juice. *Journal of Agricultural and Food Chemistry,* **52,** 7331-7338.

Hostettmann, K., Marston, A. & Hostettmann, M. 1986. *Preparative chromatography techniques*. Berlin: Springer. DOI: https://doi.org/10.1007/978-3-662-03631-0.

Hostettmann, K., Marston, A., Ndjoko, K. & Wolfender, J. L. 2000. The potential of African plants as a source of drugs. *Current Organic Chemistry,* **4**, 973-1010.

Houghton, P. J. & Mukherjee, P. K. 2009. *Evaluation of herbal medicinal products: perspectives on quality, safety and efficacy*. ISBN: 0853697515, 9780853697510. Pharmaceutical Press London.

Iauk, L., Mangano, K., Rapisarda, A., Ragusa, S., Maiolino, L., Musumeci, R., Costanzo, R., Serra, A. & Speciale, A. 2004. Protection against murine endotoxemia by treatment with

*Ruta chalepensis* L., a plant with anti-inflammatory properties. *Journal of Ethnopharmacology,* **90,** 267-272.

Ioannou, E., Quesada, A., Rahman, M. M., Gibbons, S., Vagias, C. & Roussis, V. 2012. Structures and antibacterial activities of minor dolabellanes from the brown alga *Dilophus spiralis*. *European Journal of Organic Chemistry,* **2012,** 5177-5186.

Jandacek, R. J. 2017. Linoleic acid: a nutritional quandary. *In Healthcare,* **5**. Multidisciplinary Digital Publishing Institute.

Jin, H.-G., Ko, H. J., Chowdhury, M. A., Lee, D.-S. & Woo, E.-R. 2016. A new indole glycoside from the seeds of *Raphanus sativus*. *Archives of Pharmacal Research,* **39,** 755-761.

Jourdan, P. S., Mcintosh, C. A. & Mansell, R. L. 1985. Naringin levels in *Citrus* tissues: II. quantitative distribution of naringin in *Citrus paradisi* MacFad. *Plant Physiology,* **77,** 903-908.

Kaláb, M., Yang, A.-F. & Chabot, D. 2008. Conventional scanning electron microscopy of bacteria. *Infocus Magazine,* **10,** 42-61.

Kalemba, D. & Kunicka, A. 2003. Antibacterial and antifungal properties of essential oils. *Current Medicinal Chemistry,* **10,** 813-829.

Kamal, L.Z.M, Mohd Hassan, N., Taib, N. M. & Soe, M.K. 2018. Graveoline from *Ruta angustifolia* (L.) Pers. and Its Antimicrobial Synergistic Potential in Erythromycin or Vancomycin Combinations. *Sains Malaysiana*, **47**, 10, 2429-2435.

Kamel, K. M., Abd El-Raouf, O. M., Metwally, S. A., Abd El-Latif, H. A. & El-Sayed, M. E. 2014. Hesperidin and rutin, antioxidant *Citrus* flavonoids, attenuate cisplatin-induced nephrotoxicity in rats. *Journal of Biochemical and Molecular Toxicology*, **28**, 312-319.

Kamsu-Foguem, B. & Foguem, C. 2014. Adverse drug reactions in some African herbal medicine: literature review and stakeholders' interview. *Integrative Medicine Research*, **3**, 126-132.

Kanes, K., Tisserat, B., Berhow, M. & Vandercook, C. 1993. Phenolic composition of various tissues of Rutaceae species. *Phytochemistry,* **32**, 967-974.

Kaviya, S., Santhanalakshmi, J., Viswanathan, B., Muthumary, J. & Srinivasan, K. 2011. Biosynthesis of silver nanoparticles using *Citrus sinensis* peel extract and its antibacterial activity. *Spectrochimica Acta Part A: Molecular and Biomolecular Spectroscopy,* **79**, 594-598.

Kawaii, S., Tomono, Y., Katase, E., Ogawa, K. & Yano, M. 1999. Quantitation of flavonoid constituents in *Citrus* fruits. *Journal of Agricultural and Food Chemistry,* **47**, 3565-3571.

Khairulddin, N., Bishop, L., Lamagni, T., Sharland, M. & Duckworth, G. 2004. Emergence of methicillin resistant *Staphylococcus aureus* (MRSA) bacteraemia among children in England and Wales, 1990–2001. *Archives of Disease in Childhood,* **89**, 378-379.

Khlifi, D., Sghaier, R. M., Amouri, S., Laouini, D., Hamdi, M. & Bouajila, J. 2013. Composition and anti-oxidant, anti-cancer and anti-inflammatory activities of *Artemisia herba-alba*, *Ruta chalpensis* L. and *Peganum harmala* L. *Food and Chemical Toxicology,* **55**, 202-208.

Khoury, M., Stien, D., Ouaini, N., Eparvier, V., Arnold Apostolides, N. & El Beyrouthy, M. 2014. Chemical composition and antimicrobial activity of the essential oil of *Ruta chalepensis* L. growing wild in Lebanon. *Chemistry & Biodiversity,* **11**, 1990-1997.

Kikuchi, H., Sekiya, M., Katou, Y., Ueda, K., Kabeya, T., Kurata, S. and Oshima, Y., 2009. Revised structure and synthesis of celastramycin a, a potent innate immune suppressor. *Organic letters*, *11*(8), 1693-1695.

Kim, G.-N., Shin, J.-G. & Jang, H.-D. 2009. Antioxidant and antidiabetic activity of Dangyuja (*Citrus grandis* Osbeck) extract treated with Aspergillus saitoi. *Food Chemistry,* **117,** 35-41.

Kim, H., Moon, J. Y., Mosaddik, A. & Cho, S. K. 2010. Induction of apoptosis in human cervical carcinoma HeLa cells by polymethoxylated flavone-rich *Citrus grandis* Osbeck (Dangyuja) leaf extract. *Food and Chemical Toxicology,* **48**, 2435-2442.

Klainer, A. S. & Betsch, C. J. 1970. Scanning-beam electron microscopy of selected microorganisms. *The Journal of infectious diseases,* **121,** 339-343.

KnöLker, H. J. 2017. The Alkaloids: Chemistry and Biology, **78**. Academic Press.

Koblovská, R., Macková, Z., Vítková, M., Kokoška, L., Klejdus, B. & Lapčík, O. 2008. Isoflavones in the Rutaceae family: twenty selected representatives of the genera *Citrus*, Fortunella, Poncirus, Ruta and Severinia. *Phytochemical Analysis: An International Journal of Plant Chemical and Biochemical Techniques*, **19**, 64-70.

Kokwaro, J.O., 2009. Medicinal plants of east Africa. University of Nairobi press. ISBN: 9966-846-84-0.

Krayni, H., Fakhfakh, N., Aloui, L., Zouari, N., Kossentini, M. & Zouari, S. 2015. Chemical composition and chelating activity of *Ruta chalepensis* L.(Rutaceae) essential oil as influenced by phenological stages and plant organs. *Journal of Essential Oil Research*, **27**, 514-520.

Kubena, K. S. & Mcmurray, D. N. 1996. Nutrition and the immune system: a review of nutrient–nutrient interactions. *Journal of the American Dietetic Association,* **96**, 1156-1164.

Kumar, A., Banerjee, N., Singamaneni, V., K Dokuparthi, S., Chakrabarti, T. & Mukhopadhyay, S. 2018. Phytochemical investigations and evaluation of antimutagenic activity of the alcoholic extract of *Glycosmis pentaphylla* and *Tabernaemontana coronaria* by Ames test. *Natural Product Research,* **32,** 582-587.

Kumar, K., Ganesh, M., Baskar, S., Srinivasan, K., Kanagasabai, R., Sambathkumar, R., Kumar, S. S. & Sivakumar, T. 2006. Evaluation of Anti-inflammatory activity and toxicity studies of *Chloroxylon swietenia* in Rats. *Ancient science of life,* **25**, 33.

Kumar, S. & Pandey, A. K. 2013. Chemistry and biological activities of flavonoids: an overview. *The Scientific World Journal,* 2013.

Kuo, P. C., Liao, Y. R., Hung, H. Y., Chuang, C.-W., Hwang, T. L., Huang, S. C., Shiao, Y. J., Kuo, D. H. & Wu, T. S. 2017. Anti-inflammatory and neuroprotective constituents from the peels of *Citrus grandis*. *Molecules,* **22**, 967.

Kurita, O., Fujiwara, T. & Yamazaki, E. 2008. Characterization of the pectin extracted from *Citrus* peel in the presence of citric acid. *Carbohydrate Polymers,* **74**, 725-730.

Kuriyama, T., Karasawa, T. & Williams, D. W. 2014. Antimicrobial chemotherapy: Significance to healthcare. In *Biofilms in Infection Prevention and Control.* 209-244. Elsevier. Academic Press.

Kwon, Y. S., Choi, W. G., Kim, W. J., Kyung Ckim, W., Kim, M. J., Kang, W. H. & Kim, C. M. 2002. Antimicrobial constituents of *Foeniculum vulgare*. *Archives of Pharmacal Research,* **25**, 154-157.

Kyte, L. 2011. Deaths involving MRSA: England and Wales, 2006 to 2010.

Ladanyia, M. & Ladaniya, M. 2010. *Citrus fruit: biology, technology and evaluation*, Academic press. Elsevier. ISBN: 978-0-12-374130-1.

Lam, I. K., Alex, D., Wang, Y. H., Liu, P., Liu, A. L., Du, G. H. & Yuen Lee, S. M. 2012. *In vitro* and *in vivo* structure and activity relationship analysis of polymethoxylated

flavonoids: identifying sinensetin as a novel antiangiogenesis agent. *Molecular Nutrition & Food Research,* **56**, 945-956.

Lawes, G. 1987. Scanning electron microscopy and X-ray microanalysis.

Laport, M., Santos, O. & Muricy, G. 2009. Marine sponges: potential sources of new antimicrobial drugs. *Current Pharmaceutical Biotechnology,* **10**, 86-105.

Lee, C. H., Jeong, T. S., Choi, Y. K., Hyun, B. H., Oh, G. T., Kim, E. H., Kim, J. R., Han, J. I. & Bok, S. H. 2001. Anti-atherogenic effect of *Citrus* flavonoids, naringin and naringenin, associated with hepatic ACAT and aortic VCAM-1 and MCP-1 in high cholesterol-fed rabbits. *Biochemical and Biophysical Research Communications,* **284**, 681-688.

Lehrner, J., Eckersberger, C., Walla, P., Pötsch, G. & Deecke, L. 2000. Ambient odor of orange in a dental office reduces anxiety and improves mood in female patients. *Physiology & Behavior,* **71**, 83-86.

Levy, S. B. & Marshall, B. 2004. Antibacterial resistance worldwide: causes, challenges and responses. *Nature Medicine,* **10**, S122.

Levy, S. B. 1982. Microbial resistance to antibiotics. An evolving and persistent problem. *The Lancet,* **2**, 83-88.

Li, S., Lo, C.-Y. & Ho, C.-T. 2006. Hydroxylated polymethoxyflavones and methylated flavonoids in sweet orange (*Citrus sinensis*) peel. *Journal of Agricultural and Food Chemistry*, **54**, 4176-4185.

Li, S., Sang, S., Pan, M.-H., Lai, C.-S., Lo, C.-Y., Yang, C. S. & Ho, C.-T. 2007. Anti-inflammatory property of the urinary metabolites of nobiletin in mouse. *Bioorganic & Medicinal Chemistry Letters,* **17**, 5177-5181.

Li, S., Zhao, M., Li, Y., Sui, Y., Yao, H., Huang, L. & Lin, X. 2014a. *Preparative Isolation of six Anti-Tumour Biflavonoids from Selaginella Doederleinii Hieron by High-Speed Counter-Current Chromatography*. *Phytochemical analysis*, **25**, 127-133.

Li, X., Kim, S.-K., Nam, K. W., Kang, J. S., Choi, H. D. & Son, B. W. 2006. A New Antibacterial dioxopiperazine alkaloid related to gliotoxin from a marine isolate of the fungus *Pseudallescheria*. *The Journal of Antibiotics,* **59**, 248.

Li, Y., Cai, S., He, K. & Wang, Q. 2014b. Semisynthesis of polymethoxyflavonoids from naringin and hesperidin. *Journal of Chemical Research,* **38**, 287-290.

Li, Z., Zhao, Z. & Zhou, Z. 2018. Simultaneous Separation and Purification of Five polymethoxylated flavones from "Dahongpao" Tangerine (*Citrus tangerina* Tanaka) using macroporous adsorptive resins combined with prep-HPLC. *Molecules,* **23**, 2660.

Li, Z. 2002. *Industrial applications of electron microscopy,* CRC Press. ISBN: 9780824708283

Lim, H.-K., Moon, J. Y., Kim, H., Cho, M. & Cho, S. K. 2009. Induction of apoptosis in U937 human leukaemia cells by the hexane fraction of an extract of immature *Citrus grandis* Osbeck fruits. *Food Chemistry,* **114**, 1245-1250.

Lim, H.-K., Yoo, E.-S., Moon, J.-Y., Jeon, Y.-J. & Cho, S. K. 2006. Antioxidant Activity of Extracts from Dangyuja (*Cirus grandis* Osbeck) Fruits Produced in Jeju Island. *Food Science and Biotechnology,* **15**, 312-316.

Lima, L. M., Perazzo, F. F., Carvalho, J. C. T. & Bastos, J. K. 2007. Anti-inflammatory and analgesic activities of the ethanolic extracts from *Zanthoxylum riedelianum* (Rutaceae) leaves and stem bark. *Journal of Pharmacy and Pharmacology,* **59**, 1151-1158.

Lin, L. T., Hsu, W. C. & Lin, C. C. 2014. Antiviral natural products and herbal medicines. *Journal of Traditional and Complementary Medicine,* **4**, 24-35.

Livermore, D. M. 2003. Bacterial resistance: origins, epidemiology, and impact. *Clinical Infectious Diseases,* **36**, S11-S23.

Llor, C. & Bjerrum, L. 2014. Antimicrobial resistance: risk associated with antibiotic overuse and initiatives to reduce the problem. *Therapeutic Advances in Drug Safety,* **5**, 229-241.

Lo, W.-S., Lim, Y.-P., Chen, C.-C., Hsu, C.-C., Souček, P., Yun, C.-H., Xie, W. & Ueng, Y.-F. 2012. A dual function of the furanocoumarin chalepensin in inhibiting Cyp2a and inducing Cyp2b in mice: the protein stabilization and receptor-mediated activation. *Archives of Toxicology,* **86**, 1927-1938.

Lowy, F. D. 1998. *Staphylococcus aureus* infections. *New England Journal of Medicine,* **339,** 520-532.

Lowy, F. D. 2003. Antimicrobial resistance: the example of *Staphylococcus aureus*. *The Journal of Clinical Investigation,* **111**, 1265-1273.

Lu, X., Cao, X., Liu, X. & Jiao, B. 2010. Marine microbes-derived anti-bacterial agents. *Mini Reviews in Medicinal Chemistry,* **10**, 1077-1090.

Lyczak, J. B., Cannon, C. L. & Pier, G. B. 2000. Establishment of *Pseudomonas aeruginosa* infection: lessons from a versatile opportunist1*Address for correspondence: Channing

Laboratory, 181 Longwood Avenue, Boston, MA 02115, USA. *Microbes and Infection*, **2,** 1051-1060.

Ma, G., Zhang, L., Matsuta, A., Matsutani, K., Yamawaki, K., Yahata, M., Wahyudi, A., Motohashi, R. & Kato, M. 2013. Enzymatic formation of β-citraurin from β-cryptoxanthin and zeaxanthin by carotenoid cleavage dioxygenase4 in the flavedo of *Citrus* fruit. *Plant Physiology***, 163**, 682-695.

Mabry, T., Markham, K. R. & Thomas, M. B. 2012. *The systematic identification of flavonoids*, Springer Science & Business Media. Springer. ISBN: 978-3-642-88460-3. DOI: 10.1007/978-3-642-88458-0.

Machado, T., Pinto, A., Pinto, M., Leal, I., Silva, M., Amaral, A., Kuster, R. & Netto-Dossantos, K. 2003. *In vitro* activity of Brazilian medicinal plants, naturally occurring naphthoquinones and their analogues, against methicillin-resistant *Staphylococcus aureus*. *International Journal of Antimicrobial Agents,* **21**, 279-284.

Mancuso, G., Borgonovo, G., Scaglioni, L. & Bassoli, A. 2015. Phytochemicals from *Ruta graveolens* activate TAS2R bitter taste receptors and TRP channels involved in gustation and nociception. *Molecules,* **20**, 18907-18922.

Mansourabadi, A. H., Sadeghi, H. M., Razavi, N. & Rezvani, E. 2015. Anti-inflammatory and Analgesic Properties of Salvigenin, *Salvia officinalis* Flavonoid Extracted. *Advanced Herbal Medicine*, **1**, 31-41.

Manthey, J. A. & Guthrie, N. 2002. Antiproliferative activities of *Citrus* flavonoids against six human cancer cell lines. *Journal of Agricultural and Food Chemistry*, **50**, 5837-5843.

Markham, K. R., Sheppard, C. & Geiger, H. 1987. 13C-NMR studies of some naturally occurring *amentoflavone* and *hinokifavone biflavonoids*. *Phytochemistry*, **26**, 3335-3337.

Marrie, T., Noble, M. & Costerton, J. 1983. Examination of the morphology of bacteria adhering to peritoneal dialysis catheters by scanning and transmission electron microscopy. *Journal of Clinical Microbiology*, **18,** 1388-1398.

Martín, C. M. C., Gaitén, Y. I. G. & Amado, E. R. 2011. Acercamiento al género Murraya (Rutaceae) ya la especie *Murraya paniculata* (L.) Jack. *Revista Cubana de Plantas Medicinales,* **16,** 408-418.

Martínez-Pérez, E. F., Hernández-Terán, F. & Serrano-Gallardo, L. B. 2017. In vivo effect of *Ruta chalepensis* extract on hepatic cytochrome 3A1 in rats. *African Journal of Traditional, Complementary, and Alternative Medicines*, **14**, 62.

Matsubara, Y., Yusa, T., Sawabe, A., Iizuka, Y., Takekuma, S.-I. & Yoshida, Y. 1991. Structures of new cyclic peptides in young unshiu (*Citrus unshiu* Marcov.), orange (*Citrus sinensis* Osbeck.) and amanatsu (*Citrus natsudaidai*) peelings. *Agricultural and Biological Chemistry*, **55**, 2923-2929.

Matsuda, H., Morikawa, T., Toguchida, I. & Yoshikawa, M. 2002. Structural requirements of flavonoids and related compounds for aldose reductase inhibitory activity. *Chemical and Pharmaceutical Bulletin*, **50**, 788-795.

Maundu, P. M. 2001. *Ethnobotany of the Loita Maasai: towards community management of the Forest of the Lost Child: experiences from the Loita Ethnobotany Project*, Unesco.

Mayer, F. L., Wilson, D. & Hube, B. 2013. *Candida albicans* pathogenicity mechanisms. *Virulence*, **4,** 119-128.

Mejri, J., Abderrabba, M. & Mejri, M. 2010. Chemical composition of the essential oil of *Ruta chalepensis* L: Influence of drying, hydro-distillation duration and plant parts. *Industrial Crops and Products*, **32**, 671-673.

Meléndez, P. & Capriles, V. 2006. Antibacterial properties of tropical plants from Puerto Rico. *Phytomedicine*, **13**, 272-276.

Menichini, F., Loizzo, M. R., Bonesi, M., Conforti, F., De Luca, D., Statti, G. A., De Cindio, B., Menichini, F. & Tundis, R. 2011. Phytochemical profile, antioxidant, anti-inflammatory and hypoglycemic potential of hydroalcoholic extracts from *Citrus medica* L. cv Diamante flowers, leaves and fruits at two maturity stages. *Food and Chemical Toxicology*, **49**, 1549-1555.

Meyer, J. 2005. *Toddalia asiatica* (L.) Lam. National Herbarium, Pretoria and South African National Biodiversity Institute, South Africa.

Milind, P. & Dev, C. 2012. Orange: range of benefits. *International Research Journal of Pharmacy*, **3**, 59-63.

Miller, B. A., Chen, L. F., Sexton, D. J. & Anderson, D. J. 2011. Comparison of the burdens of hospital-onset, healthcare facility-associated *Clostridium difficile* infection and of healthcare-associated infection due to methicillin-resistant *Staphylococcus aureus* in community hospitals. *Infection Control & Hospital Epidemiology*, **32**, 387-390.

Mills, E., Cooper, C., Seely, D. & Kanfer, I. 2005. African herbal medicines in the treatment of HIV: Hypoxis and Sutherlandia. An overview of evidence and pharmacology. *Nutrition Journal,* **4**, 19.

Moellering Jr, R. C. 2011. MRSA: the first half century. *Journal of Antimicrobial Chemotherapy,* **67**, 4-11.

Mohammed, K., Agarwal, M., Newman, J. & Ren, Y. 2017. Optimization of headspace solid-phase microextraction conditions for the identification of volatiles compounds from the whole fruit of lemon, lime, mandarin and orange. *Journal of Biosciences and Medicines,* **5**, 176-186.

Mohanty, I., Joshi, S., Trivedi, D., Srivastava, S. & Gupta, S. 2002. Lycopene prevents sugar-induced morphological changes and modulates antioxidant status of human lens epithelial cells. *British Journal of Nutrition,* **88**, 347-354.

Mokbel, M. S. & Hashinaga, F. 2006. Evaluation of the antioxidant activity of extracts from buntan (*Citrus grandis* Osbeck) fruit tissues. *Food Chemistry,* **94**, 529-534.

Mokbel, M. S. & Suganuma, T. 2006. Antioxidant and antimicrobial activities of the methanol extracts from pummelo (*Citrus grandis* Osbeck) fruit albedo tissues. *European Food Research and Technology,* **224**, 39-47.

Molan, A.-L., Faraj, A. M. & Mahdy, A. S. 2012. Antioxidant activity and phenolic content of some medicinal plants traditionally used in Northern Iraq. *Phytopharmacology*, **2**, 224-233.

Mondol, M. a. M. & Shin, H. J. 2014. Antibacterial and antiyeast compounds from marine-derived bacteria. *Marine Drugs,* **12**, 2913-2921.

Monodane, T., Kusamichi, M., Tokunaga, M. & Torii, M. 1989. Cell Surface of *Micrococcus luteus*. *Microbiology and Immunology,* **33,** 165-174.

Moran, M. 2005. A breakthrough in R&D for neglected diseases: new ways to get the drugs we need. *Plos Medicine,* **2**, 302.

Morocho, V., Valle, A., Garcia, J., Gilardoni, G., Cartuche, L. & Suarez, A. I. 2018. -Glucosidase inhibition and antibacterial activity of secondary metabolites from the Ecuadorian species *Clinopodium taxifolium* (Kunth) Govaerts. *Molecules,* **23**.

Morrow, R., Deyhim, F., Patil, B. S. & Stoecker, B. J. 2009. Feeding orange pulp improved bone quality in a rat model of male osteoporosis. *Journal of Medicinal Food,* **12**, 298-303.

Murakami, A., Nakamura, Y., Torikai, K., Tanaka, T., Koshiba, T., Koshimizu, K., Kuwahara, S., Takahashi, Y., Ogawa, K. & Yano, M. 2000. Inhibitory effect of *Citrus nobiletin* on phorbol ester-induced skin inflammation, oxidative stress, and tumor promotion in mice. *Cancer Research,* **60**, 5059-5066.

Nakano, D., Ishitsuka, K., Matsuda, N., Kouguchi, A., Tsuchihashi, R., Okawa, M., Okabe, H., Tamura, K. & Kinjo, J. 2017. Screening of promising chemotherapeutic candidates from plants against human adult T-cell leukemia/lymphoma (V): coumarins and alkaloids from *Boenninghausenia japonica* and *Ruta graveolens*. *Journal of Natural Medicines*, **71**, 170-180.

Naqishbandi, A. 2014. Plants used in Iraqi traditional medicine in Erbil-Kurdistan region. *Zanco Journal of Medical Sciences,* **18**, 811-815.

Narang, N. & Jiraungkoorskul, W. 2016. Anticancer activity of key lime, *Citrus aurantifolia*. *Pharmacognosy Reviews,* **10**, 118.

Nataro, J. P. & Kaper, J. B. 1998. Diarrheagenic escherichia coli. *Clinical Microbiology reviews,* **11,** 142-201.

Newman, D. J. & Cragg, G. M. 2007. Natural products as sources of new drugs over the last 25 years. *Journal of Natural Products,* **70**, 461-477.

Newman, D. J. & Cragg, G. M. 2016. Natural products as sources of new drugs from 1981 to 2014. *Journal of Natural Products,* **79**, 629-661.

Newsom, S. 2004. MRSA—past, present, future. SAGE Publications Sage UK: London, England.

Ngunde Ngwendson, J., Bedir, E., Efange, S., Okunji, C., Iwu, M., Schuster, B. & Khan, I. 2003. Constituents of *Peucedanum zenkeri* seeds and their antimicrobial effects. *Die Pharmazie-An International Journal of Pharmaceutical Sciences,* **58**, 587-589.

NHS 2017. Healthcare associated infections. https://www.nhs.uk/conditions/mrsa. https://improvement.nhs.uk/resources/healthcare-associated-infections.

Nieto, J. & Gutierrez, A. 1986. $^{1}$H NMR spectra at 360 MHz of diosmin and hesperidin in DMSO solution. *Spectroscopy Letters,* **19**, 427-434.

Nijveldt, R.J., Van Nood, E.L.S., Van Hoorn, D.E., Boelens, P.G., Van Norren, K. & Van Leeuwen, P.A., 2001. Flavonoids: a review of probable mechanisms of action and potential applications. *The American journal of clinical nutrition*, **74**, 418-425.

Niu, G. & Tan, H. 2013. Biosynthesis and regulation of secondary metabolites in microorganisms. *Science China Life Sciences,* **56**, 581-583.

Njoroge, S. M., Koaze, H., Karanja, P. N. & Sawamura, M. 2005. Volatile constituents of redblush grapefruit (*Citrus paradisi*) and pummelo (*Citrus grandis*) peel essential oils from Kenya. *Journal of Agricultural and Food Chemistry,* **53**, 9790-9794.

Noori, S., Hassan, Z. M., Yaghmaei, B. & Dolatkhah, M. 2013. Antitumor and immunomodulatory effects of salvigenin on tumor bearing mice. *Cellular Immunology,* **286**, 16-21.

Nurunnabi, T. R., Nahar, L., Al-Majmaie, S., Rahman, S. M., Sohrab, M. H., Billah, M. M., Ismail, F. M., Rahman, M. M., Sharples, G. P. & Sarker, S. D. 2018. Anti-MRSA activity of oxysporone and xylitol from the endophytic fungus *Pestalotia* sp. growing on the Sundarbans mangrove plant *Heritiera fomes*. *Phytotherapy Research,* **32**, 348-354.

O′Neill, T., Johnson, J. A., Webster, D. & Gray, C. A. 2013. The Canadian medicinal plant *Heracleum maximum* contains antimycobacterial diynes and furanocoumarins. *Journal of Ethnopharmacology,* **147**, 232-237.

Obanla, T. O., Hayek, S. A., Gyawali, R. & Ibrahim, S. A. Interaction Between Bifidobacterium and Medical Drugs. Proceedings of the 2013 National Conference on Advances in Environmental Science and Technology, 2016. Springer, 171-178.

O'brien, J., Wilson, I., Orton, T. & Pognan, F. 2000. Investigation of the Alamar Blue (resazurin) fluorescent dye for the assessment of mammalian cell cytotoxicity. *European Journal of Biochemistry,* **267**, 5421-5426.

Oliveira, A. B., Dolabela, M. F., Braga, F. C., Jácome, R. L., Varotti, F. P. & Póvoa, M. M. 2009. Plant-derived antimalarial agents: new leads and efficient phythomedicines. Part I. Alkaloids. *Anais da Academia Brasileira de Ciencias,* **81**, 715-740.

Openshaw, H. 1967. Quinoline alkaloids, other than those of Cinchona. *The Alkaloids: Chemistry and Physiology.* Elsevier.

Orwa, J., Jondiko, I., Minja, R. & Bekunda, M. 2008. The use of *Toddalia asiatica* (L) Lam.(Rutaceae) in traditional medicine practice in East Africa. *Journal of Ethnopharmacology,* **115**, 257-262.

Otto, M. 2013. Community-associated MRSA: what makes them special? *International Journal of Medical Microbiology,* **303**, 324-330.

Owis, A. I. 2019. *Citrus* Polymethoxyflavones: Biofunctional Molecules of Therapeutic Interest. *Studies in Natural Products Chemistry.* Elsevier.

Pal, C., Kundu, M. K., Bandyopadhyay, U. & Adhikari, S. 2011. Synthesis of novel heme-interacting acridone derivatives to prevent free heme-mediated protein oxidation and degradation. *Bioorganic & Medicinal Chemistry Letters,* **21**, 3563-3567.

Palavecino, E. 2007. Clinical, epidemiological, and laboratory aspects of methicillin-resistant *Staphylococcus aureus* (MRSA) infections. *Methicillin-Resistant Staphylococcus aureus (MRSA) Protocols.* Springer. 1-19. Humana Press.

Park, H.-Y., Ha, S. K., Eom, H. & Choi, I. 2013. Narirutin fraction from *Citrus* peels attenuates alcoholic liver disease in mice. *Food and Chemical Toxicology,* **55**, 637-644.

Park, J. B. 2015. Antimicrobial effects of natural products. . *Book chapter(The Battle Against Microbial Pathogens: Basic Science, Technological Advances and Educational Programs (A. Méndez-Vilas, Ed.)).* Printed in Spain. ISBN: 978-84-942134-6-5.

Patil, R. H., Patil, M. P. & Maheshwari, V. L. 2016. Bioactive secondary metabolites from endophytic fungi: a review of biotechnological production and their potential applications. *Studies in Natural Products Chemistry,* **49**, 189-205. Elsevier.

Pelaez, F. 2006. The historical delivery of antibiotics from microbial natural products-can history repeat? *Biochemical Pharmacology,* **71**, 981-990.

Pelletier, S. W., Chokshi, H. P. & Desai, H. K. 1986. Separation of diterpenoid alkaloid mixtures using vacuum liquid chromatography. *Journal of Natural Products*, **49**, 892-900.

Perez, C. & Anesini, C. 1994. In vitro antibacterial activity of Argentine folk medicinal plants against Salmonella typhi. *Journal of Ethnopharmacology*, **44**, 41-46.

Pesewu, G. A., Cutler, R. R. & Humber, D. P. 2008. Antibacterial activity of plants used in traditional medicines of Ghana with particular reference to MRSA. *Journal of Ethnopharmacology,* **116**, 102-111.

Petrovska, B. B. 2012. Historical review of medicinal plants' usage. *Pharmacognosy Reviews*, **6**, 1.

Pietta, P.-G. 2000. Flavonoids as antioxidants. *Journal of Natural Products,* **63**, 1035-1042.

Pigili, R. & Runja, C. 2014. Medicinal plants used in dengue treatment: an overview. *International Journal of Chemical and Natural Science* **2**, 70-6.

Pollio, A., De Natale, A., Appetiti, E., Aliotta, G. & Touwaide, A. 2008. Continuity and change in the Mediterranean medical tradition: Ruta spp.(rutaceae) in Hippocratic medicine and present practices. *Journal of Ethnopharmacology,* **116**, 469-482.

Priya, P. S., Sasikumar, J. & Gowsigan, G. 2009. Antibacterial activity of methanol extract of *Ruta chalapensis* (L), *Quercus infectoria* (Oliver) and *Canthium parviflorum* (Lam). *Ancient Science of Life,* **29**, 28.

Public Health England. 2018. *Staphylococcus auresis* (MRSA and MSSA) bacteraemia: mandatory surveillance 2017/18. Summary of the Mandatory Surveillance Annual Epidemiological Commentary 2017/18, London.

Pullen, C., Schmitz, P., Meurer, K., Bamberg, D.D.V., Lohmann, S., Franca, S.D.C., Groth, I., Schlegel, B., Möllmann, U., Gollmick, F. and Gräfe, U., 2002. New and bioactive compounds from Streptomyces strains residing in the wood of Celastraceae. *Planta*, *216*(1), pp.162-167.

Quent, V. M., Loessner, D., Friis, T., Reichert, J. C. & Hutmacher, D. W. 2010. Discrepancies between metabolic activity and DNA content as tool to assess cell proliferation in cancer research. *Journal of Cellular and Molecular Medicine,* **14**, 1003-1013.

Quintanilla-Licea, R., Mata-Cárdenas, B., Vargas-Villarreal, J., Bazaldúa-Rodríguez, A., Kavimngeles-Hernández, I., Garza-González, J. & Hernández-García, M. 2014. Antiprotozoal activity against *Entamoeba histolytica* of plants used in northeast Mexican traditional medicine. Bioactive compounds from *Lippia graveolens* and *Ruta chalepensis*. *Molecules,* **19,** 21044-21065.

Rahman, H., Austin, B., Mitchell, W. J., Morris, P. C., Jamieson, D. J., Adams, D. R., Spragg, A. M. & Schweizer, M. 2010. Novel anti-infective compounds from marine bacteria. *Marine Drugs,* **8**, 498-518.

Rahman, M. M., Garvey, M., Piddock, L. J. & Gibbons, S. 2008. Antibacterial terpenes from the oleo-resin of *Commiphora molmol* (Engl.). *Phytotherapy Research,* **22**, 1356-1360.

Rahman, M. M., Shiu, W. K., Gibbons, S. & Malkinson, J. P. 2018. Total synthesis of acylphloroglucinols and their antibacterial activities against clinical isolates of multi-drug resistant (MDR) and methicillin-resistant strains of *Staphylococcus aureus*. *European Journal of Medicinal Chemistry,* **155**, 255-262.

Rahmatullah, M., Ishika, T., Rahman, M., Swarna, A., Khan, T., Monalisa, M. N., Seraj, S., Mou, S. M., Mahal, M. J. & Biswas, K. R. 2011. Plants prescribed for both preventive

and therapeutic purposes by the traditional healers of the Bede community residing by the Turag River, Dhaka district. *American Eurasian Journal of Sustainable Agriculture*, **5**, 325-331.

Ramawat, K. G., Dass, S. & Mathur, M. 2009. *Herbal drugs: ethnomedicine to modern medicine*. New york, Springer. DOI: 10.1007/978-3-540-79116-42.

Rani, G., Yadav, L. & Kalidhar, S. 2009. Chemical examination of *Citrus sinensis* flavedo variety pineapple. *Indian journal of pharmaceutical sciences,* **71**, 677.

Ratheesh, M., Sindhu, G. & Helen, A. 2013. Anti-inflammatory effect of quinoline alkaloid skimmianine isolated from *Ruta graveolens* L. *Inflammation Research,* **62**, 367-376.

Reid, R. G. & Sarker, S. D. 2012. Isolation of natural products by low-pressure column chromatography. In *Natural Products Isolation*, 3rd Edition, Springer.

Réthy, B., Zupkó, I., Minorics, R., Hohmann, J., Ocsovszki, I. & Falkay, G. 2007. Investigation of cytotoxic activity on human cancer cell lines of arborinine and furanoacridones isolated from *Ruta graveolens*. *Planta Medica,* **73**, 41-48.

Ribeiro, A. B., Abdelnur, P. C. V., Garcia, C. F., Belini, A., Severino, V. G. P., Da Silva, M. F. T. D. G., Fernandes, J. B., Vieira, P. C., De Carvalho, S. A. & De Souza, A. A. 2008. Chemical characterization of *Citrus sinensis* grafted on *C. limonia* and the effect of some isolated compounds on the growth of *Xylella fastidiosa*. *Journal of Agricultural and Food Chemistry,* **56**, 7815-7822.

Rice-Evans, C. A., Miller, N. J. & Paganga, G. 1996. Structure-antioxidant activity relationships of flavonoids and phenolic acids. *Free Radical Biology and Medicine,* **20**, 933-956.

Richardson, J. S. M., Sethi, G., Lee, G. S. & Malek, S. N. A. 2016b. Chalepin: isolated from *Ruta angustifolia* L. Pers induces mitochondrial mediated apoptosis in lung carcinoma cells. *BMC Complementary and Alternative Medicine,* **16**, 389.

Ricke, S. 2003. Perspectives on the use of organic acids and short chain fatty acids as antimicrobials. *Poultry Science,* **82**, 632-639.

Rimbara, E. 2012. hugo and Russell's Pharmaceutical Microbiology. *Helicobacter,* **17**, 240-240.

Riss, T. L. & Moravec, R. A. 2006. Cell proliferation assays: improved homogeneous methods used to measure the number of cells in culture. *Cell Biology (Third Edition).* Elsevier.

Rossi, Y. E. & Palacios, S. M. 2013. Fumigant toxicity of *Citrus sinensis* essential oil on *Musca domestica* L. adults in the absence and presence of a P450 inhibitor. *Acta Tropica,* **127**, 33-37.

Rostagno, M. A. & Prado, J. M. 2013. Natural product extraction: principles and applications, Royal Society of Chemistry.

Roy, D., Kundu, S., Ghosh, B., Dutta, P. & Pal, R. 2014. Performance of pummelo germplasm in new alluvial zone of West Bengal. *Journal of Crop and Weed,* **10**, 179-182.

Russo, M., Rigano, F., Arigò, A., Sciarrone, D., Calabrò, M. L., Farnetti, S., Dugo, P. & Mondello, L. 2016. Rapid isolation, reliable characterization, and water solubility improvement of polymethoxyflavones from cold-pressed mandarin essential oil. *Journal of Separation Science,* **39**, 2018-2027.

Saduf, N., Neelofar, M., Aabid, M. R., Irshad, A. N. & Gg, M. U. D. 2018. Rather., *et al*."A Detailed Review on Morphotaxonomy and Chemoprofiling of Skimmia anquetilia NP Taylor and Airy Shaw. *Acta Scientific Microbiology,* **1**, 56-60.

Sahai, A. & Manocha, M. 1993. Chitinases of fungi and plants: their involvement in morphogenesis and host-parasite interaction. *FEMS Microbiology Reviews,* **11**, 317-338.

Saleem, M., Nazir, M., Ali, M. S., Hussain, H., Lee, Y. S., Riaz, N. & Jabbar, A. 2010. Antimicrobial natural products: an update on future antibiotic drug candidates. *Natural Product Reports,* **27**, 238-254.

Sampaio, O., Vieira, L., Bellete, B., King-Diaz, B., Lotina-Hennsen, B., Da Silva, M. & Veiga, T. 2018. Evaluation of alkaloids isolated from *Ruta graveolens* as photosynthesis inhibitors. *Molecules,* **23**, 2693.

San Miguel, E. 2003. Rue (*Ruta* L., Rutaceae) in traditional Spain: Frequency and distribution of its medicinal and symbolic applicationsLa Ruda (*Ruta* L., Rutaceae) en la españa tradicional: Frecuencia y distribución de sus aplicaciones medicinales y simbólicas. *Economic Botany,* **57**, 231-244.

Sánchez, F., Quintero, A., Usubillaga, A. & González, C.N. 2001. Chemotaxonomic value of essential oil compounds in *Citrus* species. In *International Conference on Medicinal and Aromatic Plants. Possibilities and Limitations of Medicinal and Aromatic Plant,* **576**, 49-51.

Sandjo, L. P., Kuete, V., Tchangna, R. S., Efferth, T. & Ngadjui, B. T. 2014. Cytotoxic benzophenanthridine and furoquinoline alkaloids from *Zanthoxylum buesgenii* (Rutaceae). *Chemistry Central Journal,* **8**, 61.

Santoro, M., Guido, C., De Amicis, F., Sisci, D., Cione, E., Dolce, V., Donà, A., Panno, M. L. & Aquila, S. 2016. Bergapten induces metabolic reprogramming in breast cancer cells. *Oncology Reports,* **35**, 568-576.

Sarker, S. D. & Nahar, L. 2012. Natural Product Isolation. Third edition. *Natural Products Isolation.* 3rd Edition, Springer. New York: Humana Press.

Sarker, S. D., Latif, Z. & Gray, A. I. 2006. Natural Products Isolation, 2nd Edition, Springer Science & Business Media.

Sarker, S. D., Nahar, L. & Kumarasamy, Y. 2007. Microtitre plate-based antibacterial assay incorporating resazurin as an indicator of cell growth, and its application in the in vitro antibacterial screening of phytochemicals. *Methods*, **42**, 321-324.

Sasaki, H., Kashiwada, Y., Shibata, H. & Takaishi, Y. 2012. Prenylated flavonoids from *Desmodium caudatum* and evaluation of their anti-MRSA activity. *Phytochemistry,* **82**, 136-142.

Sawadogo, W. R., Schumacher, M., Teiten, M.-H., Cerella, C., Dicato, M. & Diederich, M. 2013. A survey of marine natural compounds and their derivatives with anti-cancer activity reported in 2011. *Molecules,* **18**, 3641-3673.

Selli, S. & Kelebek, H. 2011. Aromatic profile and odour-activity value of blood orange juices obtained from Moro and Sanguinello (*Citrus sinensis* L. Osbeck). *Industrial Crops and Products,* **33**, 727-733.

Selli, S., Canbas, A., Varlet, V., Kelebek, H., Prost, C. & Serot, T. 2007. Characterization of the most odor-active volatiles of orange wine made from a Turkish cv. Kozan (*Citrus sinensis* L. Osbeck). *Journal of Agricultural and Food Chemistry,* **56**, 227-234.

Shallcross, L. J., Howard, S. J., Fowler, T. & Davies, S. C. 2015. Tackling the threat of antimicrobial resistance: from policy to sustainable action. *Philosophical Transactions of the Royal Society B,* **370**, 20140082.

Sharon-Asa, L., Shalit, M., Frydman, A., Bar, E., Holland, D., Or, E., Lavi, U., Lewinsohn, E. & Eyal, Y. 2003. *Citrus* fruit flavor and aroma biosynthesis: isolation, functional characterization, and developmental regulation of Cstps1, a key gene in the production of the sesquiterpene aroma compound valencene. *The Plant Journal,* **36**, 664-674.

Sheehan, M. & Atherton, D. 1994. One-year follow up of children treated with Chinese medicinal herbs for atopic eczema. *British Journal of Dermatology*, **130**, 488-493.

Shen, B. 2015. A new golden age of natural products drug discovery. *Cell,* **163**, 1297-1300.

Sheng, X., Sun, Y., Yin, Y., Chen, T. & Xu, Q. 2008. Cirsilineol inhibits proliferation of cancer cells by inducing apoptosis via mitochondrial pathway. *Journal of Pharmacy and Pharmacology*, **60**, 1523-1529.

Shiu, W. K., Rahman, M. M., Curry, J., Stapleton, P., Zloh, M., Malkinson, J. P. & Gibbons, S. 2011. Antibacterial acylphloroglucinols from *Hypericum olympicum*. *Journal of Natural Products*, **75**, 336-343.

Shobana, N., Yeshoda, P. & Shanmugam, P. 1989. A convenient approach to the synthesis of prenyl-, furo-and pyrano-quinoline alkaloids of the rutaceae. *Tetrahedron*, **45**, 757-762.

Shu Shan, D., Zhi Wei, D., Jing, X., Zhu Feng, G., Jiang Bin, F., Kai, Y., Li, F., Cheng Fang, W., Hai Yan, J. & Hai Bo, Y. 2013. Cytotoxic Constituents from the Stems of *Clausena lansium* (Lour.) Skeels. *Molecules*, **18**, 10768-10775.

Silverstein, R. M. & Bassler, G. C. 1962. Spectrometric identification of organic compounds. *Journal of Chemical Education,* **39**, 546.

Široká, J., Martincová, A., Pospíšilová, M. & Polášek, M. 2013. Assay of *Citrus* flavonoids, troxerutin, and ascorbic acid in food supplements and pharmaceuticals by capillary zone electrophoresis. *Food Analytical Methods*, **6**, 1561-1567.

Skariyachan, S., G. Rao, A., Patil, M., Saikia, B., Bharadwaj Kn, V. & Rao Gs, J. 2014. Antimicrobial potential of metabolites extracted from bacterial symbionts associated with marine sponges in coastal area of Gulf of Mannar Biosphere, India. *Letters in Applied Microbiology,* **58**, 231-241.

Smith, P. A. & Romesberg, F. E. 2007. Combating bacteria and drug resistance by inhibiting mechanisms of persistence and adaptation. *Nature Chemical Biology,* **3,** 549.

Sohrab, M., Chowdhury, R., Rahman, K., Hasan, C. & Rashid, M. A. 2004. Antibacterial activity and cytotoxicity of extractives from *Ravenia spectabilis*. *Fitoterapia*, **75**, 510-513.

Sohrab, M.H., Chowdhury, R., Rahman, K.M., Hasan, C.M. & Rashid, M.A., 2004. Antibacterial activity and cytotoxicity of extractives from *Ravenia spectabilis*. *Fitoterapia*, **75**, 510-513.

Souravh Bais & Abrol, N. 2016. Review on chemistry and pharmacological potential of amentoflavone. *Current Research in Neuroscience*, **6**.

Spiegel-Roy, P. & Goldschmidt, E. E. 1996. *The biology of Citrus*, Cambridge University Press.

Steduto, P., Hsiao, T., Fereres, E. & Raes, D. 2012. Respuesta del rendimiento de los cultivos al agua. *Estudio Fao: Riego Y Drenaje (Fao) Spa*, **66**.

Stenhem, M., Örtqvist, Å., Ringberg, H., Larsson, L., Olsson-Liljequist, B., Hæggman, S. & Ekdahl, K. 2006. Epidemiology of methicillin-resistant *Staphylococcus aureus* (MRSA) in Sweden 2000–2003, increasing incidence and regional differences. *BMC Infectious Diseases*, **6**, 30.

Stover, C., Pham, X., Erwin, A., Mizoguchi, S., Warrener, P., Hickey, M., Brinkman, F., Hufnagle, W., Kowalik, D. & Lagrou, M. 2000. Complete genome sequence of *Pseudomonas aeruginosa* PAO1, an opportunistic pathogen. *Nature*, 406**,** 959.

Strobel, G. A. 2003. Endophytes as sources of bioactive products. *Microbes and Infection*, **5**, 535-544.

Sudbery, P., Gow, N. & Berman, J. 2004. The distinct morphogenic states of *Candida albicans*. *Trends in Microbiology*, **12,** 317-324.

Suhaimi, S. A., Hong, S. L. & Malek, S. N. A. 2017. Rutamarin, an active constituent from *Ruta angustifolia* Pers., induced apoptotic cell death in the HT29 colon adenocarcinoma cell line. *Pharmacognosy Magazine*, **13**, S179.

Suliman, M. B. 2018. Preliminary phytochemical screening and thin layer chromatography analysis of *Swietenia macrophylla* King methanol extracts. *Chemistry of Advanced Materials*, **3**.

Sultanbawa, Y. 2011. Science against microbial pathogens: communicating current research and technological advances. *Formatex Research Center, Spain***,** 1084-1093.

Sun, Y. L., Kang, H. M., Han, S. H., Park, Y. C. & Hong, S. K. 2015. Taxonomy and phylogeny of the genus *Citrus* based on the nuclear ribosomal DNA its region sequence. *Pakistan Journal of Botany*, **47**, 95-101.

Supabphol, R. & Tangjitjareonkun, J. 2014. Chemical constituents and biological activities of *Zanthoxylum limonella* (Rutaceae): A review. *Tropical Journal of Pharmaceutical Research*, **13**, 2119-2130.

Swingle, W. T. 1943. The botany of *Citrus* and its wild relatives in the orange subfamily. *The Citrus Industry*, **1**, 128-474.

Swingle, W. T. 1967. The botany of *Citrus* and its wild relations. *The Citrus Industry*, **1**, 190-422.

System, N. N. I. S. 2004. National Nosocomial Infections Surveillance (NNIS) system report, data summary from January 1992 through June 2004, issued October 2004. *American Journal of Infection Control*, **32**, 470-485.

Taiping, Z. & Shaolin, P. 2000. Introduction to the Origin and Evolution of Pomelo and Its Distribution in China [J]. *Chinese Journal of Ecology*, **5**, 010.

Tamene, D. & Endale, M. 2019. Antibacterial activity of coumarins and carbazole alkaloid from roots of *Clausena anisata*. *Advances in Pharmacological Sciences*, 2019.

Tamokou, J., Mbaveng, A. & Kuete, V. 2017. Antimicrobial activities of African medicinal spices and vegetables. *Medicinal Spices and Vegetables from Africa*, 207-237. Academic press. Elsevier.

Tang, J.-L., Zhan, S.-Y. & Ernst, E. 1999. Review of randomised controlled trials of traditional Chinese medicine. *Bmj*, **319**, 160-161.

Tareq, F. S., Hasan, C. M., Rahman, M. M., Hanafi, M. M. M., Colombi Ciacchi, L., Michaelis, M., Harder, T., Tebben, J., Islam, M. T. & Spiteller, P. 2018. Anti-*Staphylococcal* calopins from fruiting bodies of *Caloboletus radicans*. *Journal of Natural Products*, **81**, 400-404.

Tavares, L. D. C., Zanon, G., Weber, A. D., Neto, A. T., Mostardeiro, C. P., Da Cruz, I. B., Oliveira, R. M., Ilha, V., Dalcol, I. I. & Morel, A. F. 2014. Structure-activity relationship of benzophenanthridine alkaloids from *Zanthoxylum rhoifolium* having antimicrobial activity. *Plos One*, **9**, 97000.

Taylor, T. A. & Unakal, C. G. 2017. *Staphylococcus aureus*. *StatPearls [Internet]*. StatPearls Publishing. https://www.ncbi.nlm.nih.gov/books/NBK441868/.

Tedone, L., Costa, R., De Grazia, S., Ragusa, S. & Mondello, L. 2014. Monodimensional (GC–FID and GC–MS) and Comprehensive Two-dimensional Gas Chromatography for the Assessment of Volatiles and Fatty Acids from *Ruta chalepensis* Aerial Parts. *Phytochemical Analysis*, **25**, 468-475.

Terashima, M., Kakuno, Y., Kitano, N., Matsuoka, C., Murase, M., Togo, N., Watanabe, R. & Matsumura, S. 2012. Antioxidant activity of flavonoids evaluated with myoglobin method. *Plant cell reports*, **31**, 291-298.

The *Citrus* and Date Crop Germplasm Committee, U. C. 2004. *Citrus* and Date Germplasm: Crop Vulnerability, Germplasm Activities, Germplasm Needs. *Citrus and Date Crop Germplasm Committee, USA.*

Thomson, P., Taddonio, T., Tait, M. & Prasad, J. 1989. Susceptibility of *Pseudomonas* and *Staphylococcus* wound isolates to topical antimicrobial agents: a 10-year review and clinical evaluation. *Burns*, **15**, 190-192.

Tian-Shung, W., Chang-Sheng, K. & Furukawa, H. 1983. Acridone alkaloids and a coumarin from *Citrus grandis*. *Phytochemistry*, **22**, 1493-1497.

Tohidpour, A., Sattari, M., Omidbaigi, R., Yadegar, A. & Nazemi, J. 2010. Antibacterial effect of essential oils from two medicinal plants against methicillin-resistant *Staphylococcus aureus* (MRSA). *Phytomedicine*, **17**, 142-145.

Trovato, A., Monforte, M., Barbera, R., Rossitto, A., Galati, E. & Forestieri, A. 1996. Effects of fruit juices of *Citrus sinensis* L. and *Citrus limon* L. on experimental hypercholesterolemia in the rat. *Phytomedicine*, **2**, 221-227.

Ueng, Y. F., Chen, C. C., Chung, Y. T., Liu, T. Y., Chang, Y. P., Lo, W. S., Murayama, N., Yamazaki, H., Souček, P. & Chau, G. Y. 2011. Mechanism-based inhibition of cytochrome P450 (CYP) 2A6 by chalepensin in recombinant systems, in human liver microsomes and in mice *in vivo*. *British Journal of Pharmacology*, **163**, 1250-1262.

Ulubelen, A., Terem, B., Tuzlaci, E., Cheng, K. & Kong, Y. 1986. Alkaloids and coumarins from *Ruta chalepensis*. *Phytochemistry*, **25**, 2692-2693.

Um, Y. R., Kong, C.-S., Lee, J. I., Kim, Y. A., Nam, T. J. & Seo, Y. 2010. Evaluation of chemical constituents from *Glehnia littoralis* for antiproliferative activity against HT-29 human colon cancer cells. *Process Biochemistry*, **45**, 114-119.

Umeda, A. 1988. Structure of *Staphylococcus aureus* cell wall determined by the freeze-substitution method. *Nihon Saikingaku Zasshi. Japanese Journal of Bacteriology*, **43,** 961-969.

Vats, M., Singh, H. & Sardana, S. 2011. Phytochemical screening and antimicrobial activity of roots of *Murraya koenigii* (Linn.) Spreng.(Rutaceae). *Brazilian Journal of Microbiology*, **42**, 1569-1573.

Ventura, U., Salgado, G., Castelán, E., Palma, L., Rivera, C. & Sánchez, G. 2012. Interpretation methods of nutrient diagnosis in orange cv. Valencia (*citrus sinensis* L. Osbeck). *Terra Latinoamericana,* **30**, 139-145.

Verma, S. & Singh, S. 2008. Current and future status of herbal medicines. *Veterinary World,* **1**, 347.

Véronique Zech-Matterne (Éditeur), G. F. É. 2018. Livre numérique AGRUMED: Archaeology and history of *Citrus* fruit in the Mediterranean.

Verpoorte, R. 2009. Medicinal Plants: A Renewable Resource for Novel Leads and Drugs. In: Ramawat K. (eds) Herbal Drugs: Ethnomedicine to Modern Medicine. Springer, Berlin, Heidelberg. DOI: https://doi.org/10.1007/978-3-540-79116-4_1Viljoen, A. M., Moolla, A., Van Vuuren, S. F., Van Zyl, R. L., Hüsnü, K., Başer, C., Demirci, B., Özek, T. & Trinder-Smith, T. H. 2006. The biological activity and essential oil composition of 17 Agathosma (Rutaceae) species. *Journal of Essential Oil Research,* **18**.

Wang, J., Dong, M. & Guo, Y. 2009. Limonoids from Rutaceae and their biological activities: research advances. *Journal of International Pharmaceutical Research,* **36**, 321-365.

Wang, X., Li, F., Zhang, H., Geng, Y., Yuan, J. & Jiang, T. 2005. Preparative isolation and purification of polymethoxylated flavones from Tangerine peel using high-speed counter-current chromatography. *Journal of Chromatography A,* **1090**, 188-192.

Wang, Y. C., Chuang, Y.-C. & Ku, Y.-H. 2007. Quantitation of bioactive compounds in *Citrus* fruits cultivated in Taiwan. *Food chemistry,* **102**, 1163-1171.

Wannes, W. A., Tounsi, M. S. & Marzouk, B. 2017. A review of Tunisian medicinal plants with anticancer activity. *Journal of Complementary and Integrative Medicine,* **15**.

Waterman, P. G. 1975. Alkaloids of the Rutaceae: their distribution and systematic significance. *Biochemical Systematics and Ecology,* **3,** 149-180.

Watson, E. F. G. a. D. G. 1993. *Citrus* app. *Citrus*. *Southern Group of State Foresters*.

Wertheim, H. F., Melles, D. C., Vos, M. C., Van Leeuwen, W., Van Belkum, A., Verbrugh, H. A. & Nouwen, J. L. 2005. The role of nasal carriage in *Staphylococcus aureus* infections. *The Lancet Infectious Diseases,* 5**,** 751-762.

WHO, World Health Organization.2008. *Global tuberculosis control: surveillance, planning, financing: WHO report 2008*.

WHO, World Health Organization. 2014. *Antimicrobial resistance: global report on surveillance*, World Health Organization.

Williams, S. & Davies, F. 1967. Use of a scanning electron microscope for the examination of actinomycetes. *Microbiology,* **48,** 171-177.

Wu, G. 2010. Assays based on integrated cell system properties. *Assay Development: Fundamentals and Practices***,** 289-306.

Wu, M., Zhang, H., Zhou, C., Jia, H., Ma, Z. & Zou, Z. 2015. Identification of the chemical constituents in aqueous extract of Zhi-Qiao and evaluation of its antidepressant effect. *Molecules*, **20,** 6925-6940.

Wu, P. P., Zhang, K., Lu, Y. J., He, P. & Zhao, S. Q. 2014. *In vitro* and *in vivo* evaluation of the antidiabetic activity of ursolic acid derivatives. *European Journal of Medicinal Chemistry*, **80**, 502-508.

Wu, T. S., Shi, L. S., Wang, J. J., Iou, S. C., Chang, H. C., Chen, Y. P., Kuo, Y. H., Chang, Y. L. & Tenge, C. M. 2003. Cytotoxic and antiplatelet aggregation principles of *Ruta graveolens*. *Journal of the Chinese Chemical Society*, **50**, 171-178.

Wu, T.-S., Li, C.-Y., Leu, Y.-L. & Hu, C.-Q. 1999. Limonoids and alkaloids of the root bark of Dictamnus angustifolius. *Phytochemistry,* **50**, 509-512.

Wu, V. C.-H., Qiu, X., Bushway, A. & Harper, L. 2008. Antibacterial effects of American cranberry (*Vaccinium macrocarpon*) concentrate on foodborne pathogens. *LWT-Food Science and Technology,* **41**, 1834-1841.

Xi, W., Fang, B., Zhao, Q., Jiao, B. & Zhou, Z. 2014. Flavonoid composition and antioxidant activities of Chinese local pummelo (*Citrus grandis* Osbeck.) varieties. *Food chemistry,* **161**, 230-238.

Xiao, H., Yang, C. S., Li, S., Jin, H., Ho, C. T. & Patel, T. 2009. Monodemethylated polymethoxyflavones from sweet orange (*Citrus sinensis*) peel inhibit growth of human lung cancer cells by apoptosis. *Molecular Nutrition & Food Research,* **53**, 398-406.

Xu, B., Wang, L., González-Molleda, L., Wang, Y., Xu, J. & Yuan, Y. 2014. Antiviral activity of (+)-rutamarin against Kaposi's sarcoma-associated herpesvirus by inhibition of the catalytic activity of human topoisomerase II. *Antimicrobial Agents and Chemotherapy,* **58**, 563-573.

Xu, C. J., Fraser, P. D., Wang, W.-J. & Bramley, P. M. 2006. Differences in the carotenoid content of ordinary *Citrus* and lycopene-accumulating mutants. *Journal of Agricultural and Food Chemistry,* **54**, 5474-5481.

Xu, L., Meng, W., Cao, C., Wang, J., Shan, W. & Wang, Q. 2015. Antibacterial and antifungal compounds from marine fungi. *Marine Drugs,* **13**, 3479-3513.

Yeşilada, E., Honda, G., Sezik, E., Tabata, M., Goto, K. & Ikeshiro, Y. 1993. Traditional medicine in Turkey IV. Folk medicine in the Mediterranean subdivision. *Journal of Ethnopharmacology,* **39**, 31-38.

Yong Moon, J., Kim, H., Cho, M., Chang, W. Y., Kim, C.-T. & Cho, S. K. 2009. Induction of Apoptosis in SNU-16 Human Gastric Cancer Cells by the Chloroform Fraction of an Extract of Dangyuja (*Citrus grandis* Leaves. *Journal of the Korean Society for Applied Biological Chemistry,* **52**, 168-175.

Zhang, H. W., Song, Y. C. & Tan, R. X. 2006. Biology and chemistry of endophytes. *Natural Product Reports,* **23**, 753-771.

Zhang, M., Duan, C., Zang, Y., Huang, Z. & Liu, G. 2011. The flavonoid composition of flavedo and juice from the pummelo cultivar (*Citrus grandis* (L.) Osbeck) and the grapefruit cultivar (*Citrus paradisi*) from China. *Food Chemistry,* **129**, 1530-1536.

Zhao, L. 2009. The characteristic analysis of several mineral contents in Chinese orange juice. *Spectroscopy and Spectral Analysis,* **29**, 259-262.

Zheng, Y. M., Lu, A. X., Shen, J. Z., Kwok, A. H. Y. & Ho, W. S. 2016. Imperatorin exhibits anticancer activities in human colon cancer cells via the caspase cascade. *Oncology Reports,* **35**, 1995-2002.

**Appendix 1**: The numbers and names of the isolated compounds from *Ruta chalepensis* and *Citrus species*

| Compound number | Compound name | Compound number | Compound name |
|---|---|---|---|
| **41** | Skimmianine | **110** | 3-methoxynobiletin |
| **42** | γ-fagarine | **111** | Sinensetin |
| **43** | Bergapten | **112** | 6,7,8,3',4'-pentamethoxyl-flavone |
| **44** | Isopimpinellin | **113** | Demethylnobiletin |
| **45** | Chalepin | **114** | 5-desmethylsinensetin |
| **46** | Chalepensin | **115** | Cirsilineol |
| **47** | Rutamarin | **116** | Tangeritin |
| **48** | Rutin | **117** | Tetramethylscutellarein |
| **50** | Hesperidin | **118** | Salvigenin |
| **51** | Narirutin | **119** | Marcitrus |
| **57** | Nobiletin | | |
| **99** | Kokusaginine | | |
| **100** | Isokokusaginine | | |
| **101** | Rutin 3'-methyl ether | | |
| **102** | Rutin 7,4'-dimethyl ether | | |
| **103** | 6-hydroxy-rutin-3'-7-dimethyl ether | | |
| **104** | Imperatorin | | |
| **105** | Graveoline | | |
| **106** | Ribalinium | | |
| **107** | Arborinine | | |
| **108** | 3`,6-disinapoylsucrose | | |
| **109** | Hexadecane | | |

**Appendix 2:** HMBC for compound **47**

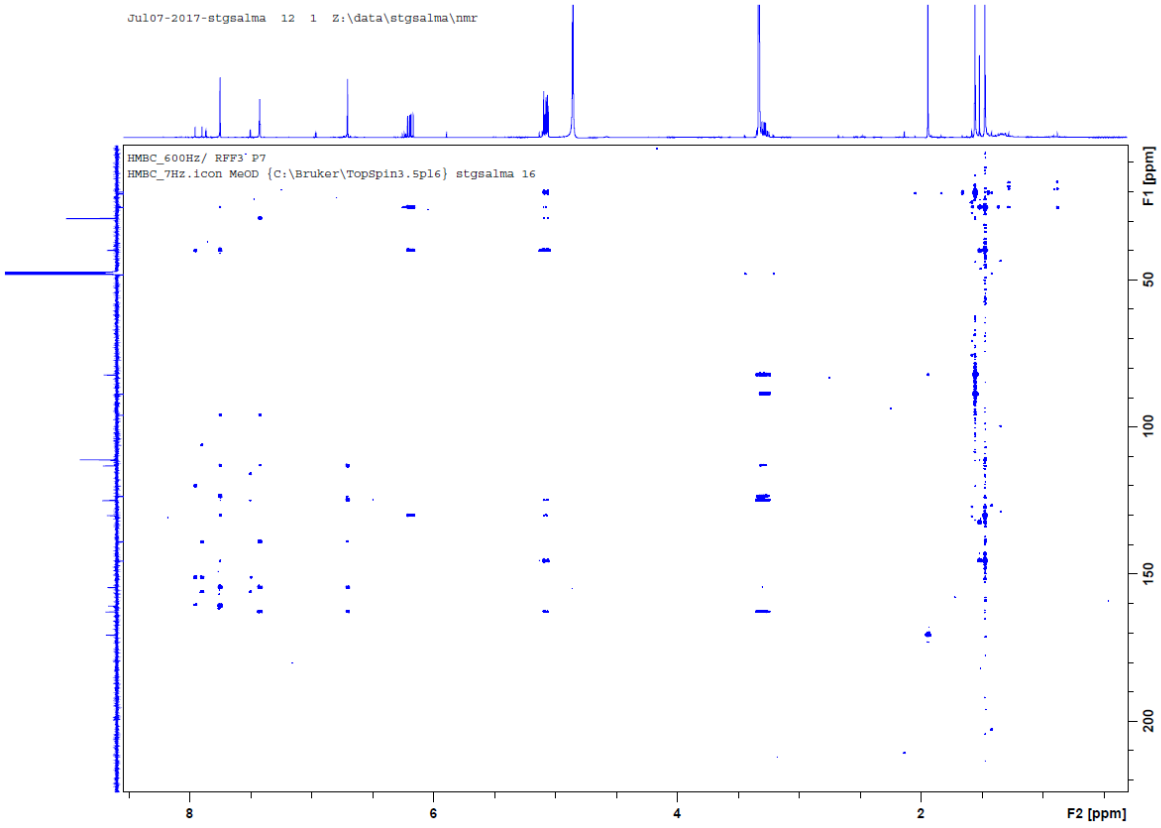

**Appendix 3:** HMBC for compound **106**

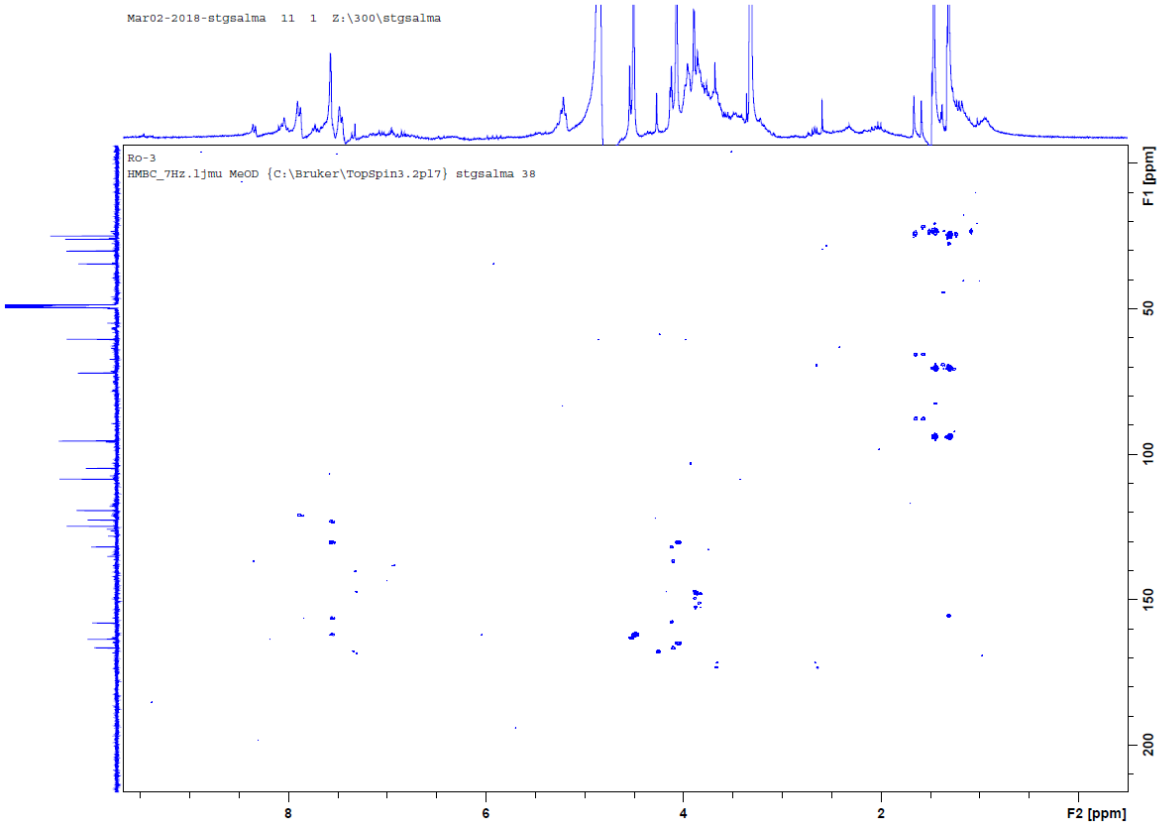

**Appendix 4:** HMBC for compound **105**

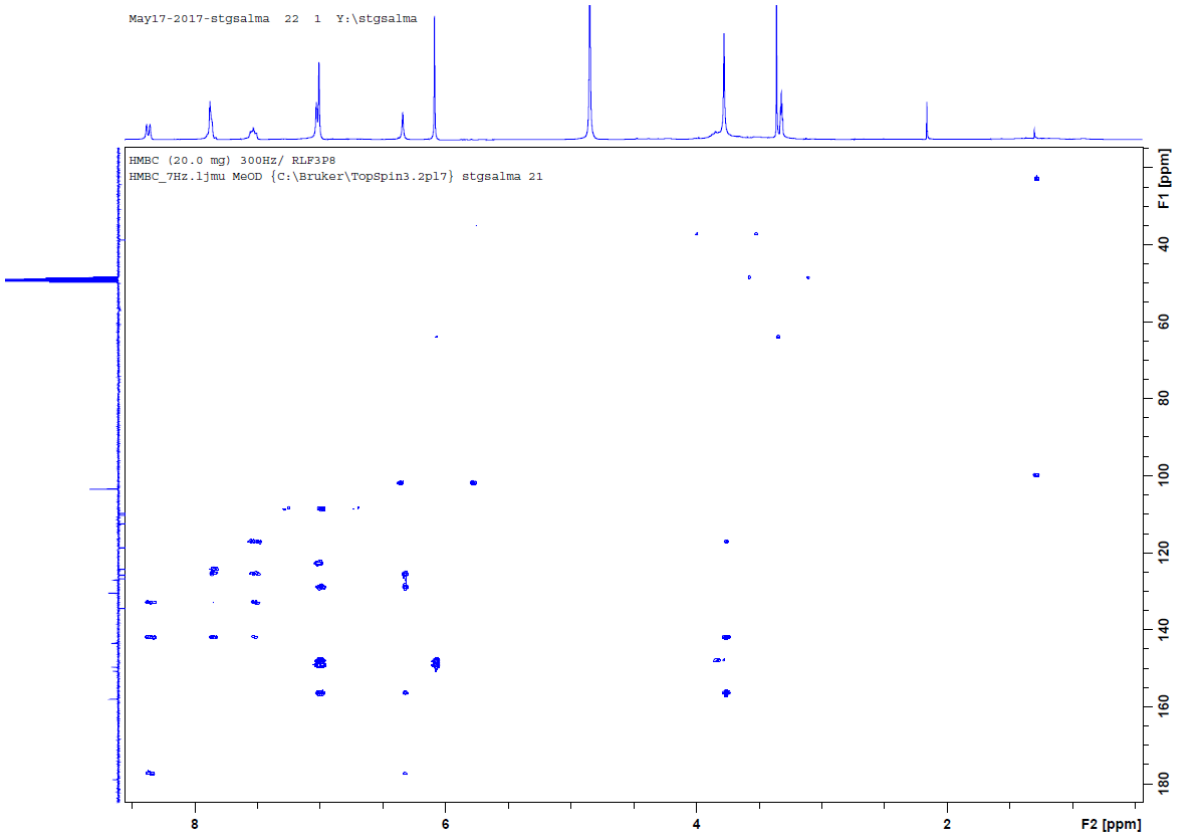

**Appendix 5:** $^{13}C$ for compound **48**

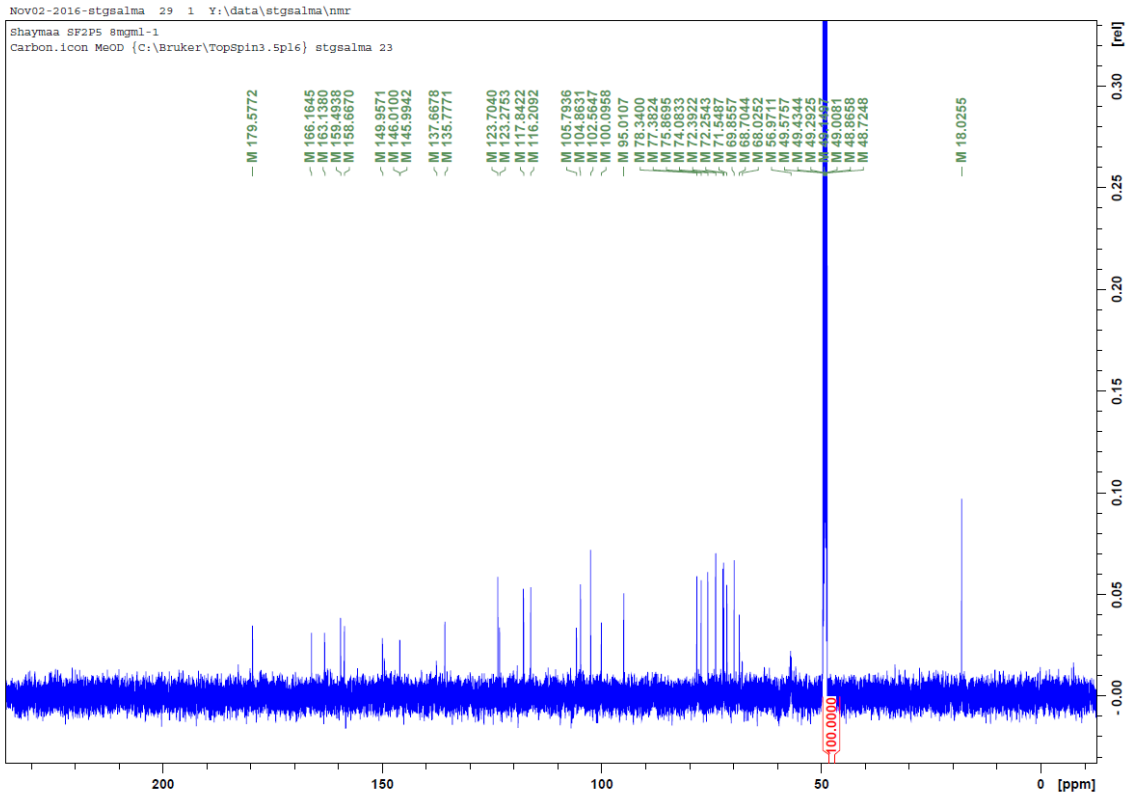

**Appendix 6:** HMBC for compound **101**

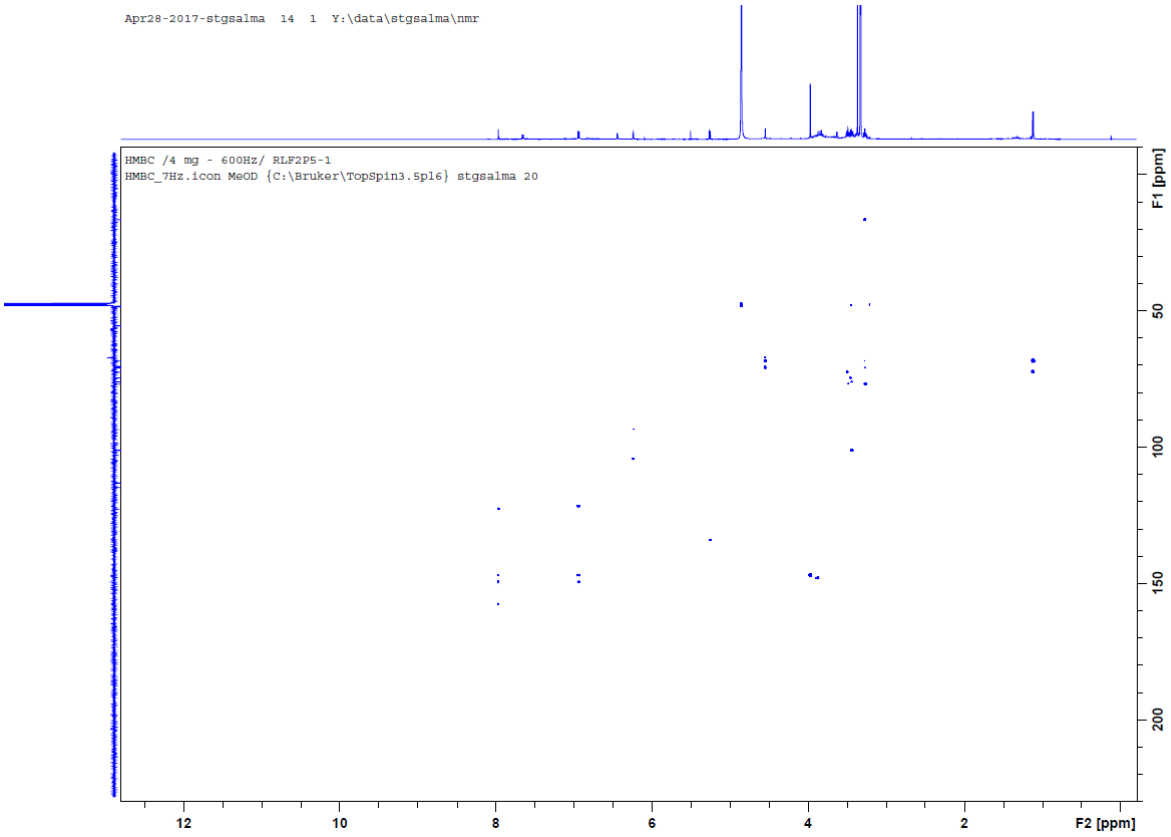

**Appendix 7:** List of presentations

- Al-Majmaie, S., Nahar, L., Sharples, G. P. and Sarker, S. D. (2016). Phytochemical and Antimicrobial Studies on Selected Medicinal Plants from the Iraqi Flora. Poster presentation- UK, Liverpool John Moores University, June 2016.
- Al-Majmaie, S., Nahar, L., Sharples, G. P. and Sarker, S. D. (2017). Phytochemical and Antimicrobial Studies on Selected Medicinal Plants from the Iraqi Flora. Poster presentation- UK, The 9th MMU Postgraduate Research Conference.
- Al-Majmaie, S., Nahar, L., Sharples, G. P. and Sarker, S. D. (2018). Screening for Phytochemical and Antimicrobial Activity on Some Iraqi Traditional Herbal Medicine. Poster presentation- PHYTOPHARM 2018, Horgen, Switzerland, 25-27 June 2018.
- Al-Majmaie, S., Nahar, L., Sharples, G. P. and Sarker, S. D. (2018). Screening for Phytochemical and Antimicrobial Activity for *Citrus sinensis* and *Citrus grandis* on Iraqi Flora. Poster presentation- PSE-YSM 2018, Liverpool, UK, 02-05 July 2018.
- Al-Majmaie, S., Nahar, L., Sharples, G. P. and Sarker, S. D. (2017). Phytochemical and Antimicrobial Studies on *Ruta chalepensis* L. (Rutaceae). Oral presentation- UK, Liverpool John Moores University, Monday 19$^{th}$ June 2017.
- Al-Majmaie, S., Nahar, L., Sharples, G. P. and Sarker, S. D. (2018). HPLC-PDA Based Chemical Profiling and Antimicrobial Activity Studies on *Citrus grandis* and *C. sinensis* from the Iraqi Flora. Oral presentation- ISCNP30 and ICOB10, Athens, Greece, 25-29 November 2018.
- Al-Majmaie, S., Nahar, L., Sharples, G. P. and Sarker, S. D. (2018). *In vitro* antimicrobial activity of *Ruta chalepensis* L. growing in Iraq. Oral presentation- PSE-YSM 2018, Liverpool, UK, 02-05 July 2018.
- Al-Majmaie, S., Sharples, G. P., Nahar, L., Wadi, K., Nath, S., Dempster, N., Jasim, H., Al-Groshi., A. and Sarker, S. D. (2019). Antimicrobial activity and mechanisms of action of selected flavonoids from the Rutaceae. Oral presentation- Trends in Natural Product Research – PSE Young Scientists' Meeting, 19-22 June, Budapest, Hungary.

**Appendix 8:** List of papers during the PhD project

**Al-Majmaie**, S., Nahar, L., Sharples, G. P., Wadi, K. and Sarker, S. D. (2019) Isolation and antimicrobial activity of rutin and its derivatives from *Ruta chalepensis* (Rutaceae) growing in Iraq, *Records of Natural Products* **13**, 64-70.

Nurunnabi, T. R., Nahar, L., **Al-Majmaie**, S., Rahman, S. M. M., Sohrab, M. H., Billah, M. M., Ismail, F. M. D., Rahman, M. M., Sharples, G. P. and Sarker, S. D. (2018) Anti-MRSA activity of oxysporone and xylitol from the endophytic fungus *Pestalotia* sp. growing on the Sundarbans mangrove plant *Heritiera fomes*, *Phytotherapy Research* **32**, 348-354.

Nurunnabi, T. R., **Al-Majmaie**, S., Nakouti I., Nahar, L., Rahman, S. M. M., Sohrab, M. H., Billah, M. M., Ismail, F. M. D., Sharples, G. P. and Sarker, S. D**.** (2018) Antimicrobial activity of the ethyl acetate extract and its major metabolite, kojic acid, from endophytic fungus *Colletotrichum gloeosporioides* isolated from *Sonneratia apetala*, a mangrove plant of the Sundarbans, *Asian Pacific Journal of Tropical Medicine* **11**, 350-354.

Uddin, S., Alnsour, L., Segun, P., Servi, H., Celik, S., Gokturk, R. S., Al Groshi, A., **Al-Majmaie**, S., Guetchueng, S. T., Nahar, L., Dempster, N. M., Ismail, F. M. D., Ritchie, K. J. and Sarker, S. D. (2017). Flavonoids from two Turkish *Centaurea* species and their chemotaxonomic implications, *Trends in Phytochemical Research* **1**, 243-248.

Nurunnabi, T. R., **Al-Majmaie**, S., Nahar, L., Nakouti, I., Rahman, S. M. M., Sohrab, M. H., Billah, M. M., Ismail, F. M. D., Sharples, G. P. and Sarker, S. D. (2019) Sonneratinone: A new antimicrobial benzofuranone derivative from the endophytic fungus *Aspergillus niger* isolated from the Mangrove plant *Sonneratia apetala* Buch.-Ham., *Trends in Phytochemical Analysis* (submitted).